

The activity of the plant defensin NaD1 against human fungal pathogens

Submitted by

Brigitte Maria Elizabeth Hayes, B.Sc. (Hons)

A thesis submitted in total fulfilment
of the requirements for the degree of
Doctor of Philosophy

Department of Biochemistry
School of Molecular Sciences
Faculty of Science, Technology and Engineering



La Trobe University
Bundoora, Victoria, 3086
Australia

September 2014

Table of Contents

Table of Contents	I
List of Figures	VI
List of Tables	IX
List of Publications	X
Abbreviations	XI
Abstract	XV
Statement of Authorship	XVI
Acknowledgements	XVII

Introduction	1
---------------------------	----------

<u>Chapter 1</u> Literature Review	10
---	-----------

<u>Chapter 2</u> Activity of NaD1 against human fungal pathogens	27
---	-----------

2.1 Introduction	28
-------------------------------	-----------

2.2 Materials and Methods	36
--	-----------

2.2.1 NaD1 extraction from <i>N. alata</i> flowers.....	36
---	----

2.2.1.1 Acid extraction and heat treatment.....	36
---	----

2.2.1.2 Cation exchange chromatography on SP-Sepharose.....	36
---	----

2.2.1.3 Reversed-phase high performance liquid chromatography.....	37
--	----

2.2.2 Expression of histatin 5 in <i>Rosetta gami</i> cells.....	37
--	----

2.2.2.1 Incorporation of DNA encoding histatin 5 into pHUE plasmid.....	37
---	----

2.2.2.2 Transformation of pHUE-histatin 5 into <i>Rosetta gami B cells</i>	39
--	----

2.2.2.3 Expression of histatin 5.....	39
---------------------------------------	----

2.2.3 Source of the other antimicrobial peptide stocks.....	40
---	----

2.2.3.1 Protein expression in <i>Pichia pastoris</i>	41
--	----

2.2.4 Fungal strains.....	42
---------------------------	----

2.2.4.1 Filamentous fungi.....	42
--------------------------------	----

2.2.4.2 Yeast.....	42
--------------------	----

2.2.5 Fungal growth inhibition assays.....	42
--	----

2.2.6 <i>C. albicans</i> growth curve in half-strength PDB.....	44
---	----

2.2.7 <i>C. albicans</i> survival assays.....	44
---	----

2.2.8 Permeabilisation kinetics (SYTOX) assay.....	44
--	----

2.2.9 Synergy assays.....	45
---------------------------	----

2.3	Results	47
2.3.1	NaD1 activity against <i>C. albicans</i>	47
2.3.2	Effect of antimicrobial peptides on the growth of <i>C. albicans</i> DAY185	50
2.3.3	Effect of temperature on the activity of NaD1 against <i>C. albicans</i>	51
2.3.4	Effect of Mg ²⁺ and Ca ²⁺ on NaD1's activity against <i>C. albicans</i>	52
2.3.5	Kinetics of <i>C. albicans</i> permeabilisation by NaD1	53
2.3.6	The effect of serum on the activity of antifungal peptides against <i>C. albicans</i>	54
2.3.7	Activity of antifungal peptides against a range of human fungal pathogens	57
2.3.7.1	<i>Cryptococcus species</i>	57
2.3.7.2	<i>Aspergillus species</i>	60
2.3.7.3	Summary of AMP inhibitory activity against <i>Cryptococcus</i> and <i>Aspergillus strains</i>	64
2.3.8	Synergistic activity of NaD1 with protease inhibitors and AMPs against human fungal pathogens	64
2.3.8.1	<i>NaD1 activity in combination with the antimicrobial peptides batenecin and Bac2a, and the protease inhibitors BPTI and NaCys2 against various fungal pathogens</i>	65
2.3.8.1.1	<i>Synergy assays with C. gattii R265</i>	65
2.3.8.1.2	<i>Synergy assays with A. niger and A. flavus 5310</i>	68
2.3.8.1.3	<i>Synergy assays with C. albicans</i>	74
2.3.8.2	<i>Synergy of NaD1 and two other plant defensins against C. albicans</i>	77
2.3.8.3	<i>Synergy of NaD1 with two human antifungal peptides against C. albicans</i>	79
2.3.8.4	<i>Synergy between NaD1 and the chemical fungicide amphotericin B against C. albicans</i>	81
2.4	Discussion	82
 Chapter 3 Uptake of NaD1 into fungal cells		90
3.1	Introduction	91
3.1.1	Endocytosis	91
3.1.2	Polyamine transporters	95
3.1.3	Passive transport	96
3.2	Materials and Methods	98
3.2.1	BODIPY-labelling of NaD1	98
3.2.2	Fungal growth inhibition assays	98
3.2.3	Confocal microscopy of <i>C. albicans</i> and Fov hyphae	100
3.2.4	Monitoring of BODIPY-NaD1 uptake into <i>C. albicans</i> by flow cytometry	101
3.2.5	Confirmation of correct gene deletions in <i>S. cerevisiae</i> mutants	101

3.3	Results	103
3.3.1	Antifungal activity of BODIPY-labelled NaD1	103
3.3.2	Uptake of NaD1 into <i>Fusarium oxysporum f. sp. vasinfectum</i> hyphae	104
3.3.3	Uptake of NaD1 into <i>C. albicans</i>	105
3.3.4	Determination of the mechanism of NaD1 uptake into yeast cells.....	110
3.3.4.1	<i>Latrunculin A</i>	111
3.3.4.2	<i>CCCP</i>	112
3.3.4.3	<i>Endocytosis mutants</i>	114
3.3.5	Investigation of the involvement of protein transport in NaD1's activity.....	116
3.3.5.1	<i>Brefeldin A and nocodazole</i>	117
3.3.5.2	<i>ESCRT deletion mutants</i>	118
3.4	Discussion	119

Chapter 4 Mechanism of action of NaD1 against *Candida albicans* 125

4.1	Introduction	126
4.2	Materials and Methods	131
4.2.1	<i>C. albicans</i> deletion library screen.....	131
4.2.2	Complementation of <i>C. albicans HOG1</i> and <i>PBS2</i> genes.....	133
4.2.2.1	<i>Genomic DNA extraction from C. albicans</i>	133
4.2.2.2	<i>Cloning of PBS2 and HOG1 genes from C. albicans</i>	133
4.2.2.3	<i>Preparation of linearised pDDB78 vector for insertion of HOG1 and PBS2 PCR products</i>	134
4.2.2.4	<i>Transformation of PCR product and digested pDDB78 into S. cerevisiae BY4741Δtrp</i>	135
4.2.2.5	<i>Miniprep to isolate pDDB78-PBS2 and pDDB79-HOG1 plasmids from BY4741Δtrp</i>	135
4.2.2.6	<i>Transformation of E. coli with pDDB78-PBS2 and pDDB78-HOG1</i> ...	135
4.2.2.7	<i>Plasmid purification from E. coli</i>	136
4.2.2.8	<i>Screening of pDDB78-PBS2 and pDDB78-HOG1</i>	136
4.2.2.9	<i>Linearising plasmids for transformation into C. albicans</i>	137
4.2.2.10	<i>Transformation of C. albicans deletion mutants</i>	137
4.2.3	Fungal growth inhibition assays	137
4.2.4	Detection of Hog1 activation by Western blot.....	138
4.2.5	Microscopy with ROS probe DHR 123	139
4.2.6	Flow cytometry with DHR 123 and DAF-FM.....	139
4.2.7	Survival assays.....	139

4.3	Results	140
4.3.1	NaD1 sensitive and resistant mutants identified in the screen of the <i>C. albicans</i> deletion libraries	140
4.3.2	Complementation of <i>HOG1</i> and <i>PBS2</i> genes	146
4.3.3	Detection of Hog1 phosphorylation in response to NaD1	149
4.3.4	Production of reactive oxygen species.....	150
4.3.5	Fungal inhibition of <i>C. albicans</i> by NaD1 in the presence of ascorbate ...	153
4.3.6	Survival of <i>C. albicans</i> by NaD1 in the presence of sorbitol	154
4.4	Discussion	155

Chapter 5 The impact of stress signalling pathways on the potency of plant defensins on fungal pathogens 159

5.1	Introduction	160
5.2	Materials & Methods	167
5.2.1	Fungal growth inhibition assays	167
5.2.2	Confirmation of correct gene deletions in <i>C. albicans</i> mutants.....	169
5.2.2.1	Extraction of genomic DNA from <i>C. albicans</i> cells	169
5.2.2.2	PCR screen using ARG4 detect primers.....	169
5.2.3	Confirmation of correct deletions in <i>S. cerevisiae</i> mutants	171
5.2.4	BODIPY-NaD1 uptake into <i>C. albicans</i> monitored by flow cytometry....	171
5.2.5	Detection of Hog1 phosphorylation in response to NaD2	172
5.2.6	Synergy with FK506 and cercosporamide	173
5.3	Results	174
5.3.1	NaD1's effect on calcineurin signalling, the Cap1 oxidative stress response and the cell wall integrity and mating pathways in <i>C. albicans</i>	174
5.3.2	The effect of NaD1 on the growth of <i>S. cerevisiae</i> <i>hog1</i> , <i>mpk1</i> , <i>cnal</i> , <i>yap1</i> and <i>fus3</i> deletion mutants	178
5.3.3	<i>S. cerevisiae</i> deletions in genes which function upstream of Hog1	182
5.3.4	G-protein coupled receptors.....	185
5.3.5	The effect of other plant defensins on the growth of <i>C. albicans</i> signalling mutants	192
5.3.6	Detection of <i>C. albicans</i> Hog1 phosphorylation in response to NaD2.....	194
5.3.7	The effect of inhibitors of the calcineurin and cell wall integrity pathways on the antifungal activity of NaD1 and NaD2	195
5.4	Discussion	198

Chapter 6 Concluding remarks	210
6.1 Introduction	211
6.2 Findings of this study	211
6.2.1 NaD1 inhibits the growth of human fungal pathogens	211
6.2.2 NaD1 acts in synergy with protease inhibitors and other antimicrobial peptides	213
6.2.3 The three step mechanism of NaD1 is conserved in <i>C. albicans</i>	213
6.2.4 NaD1 may be internalised by endocytosis, but does not appear to require internal protein transport.....	214
6.2.5 <i>C. albicans</i> tolerates low NaD1 concentrations by activating Hog1	215
6.2.6 NaD1 induces ROS, but not osmotic stress	215
6.2.7 NaD1 activates Hog1 through different upstream signalling cascades in <i>C. albicans</i> and <i>S. cerevisiae</i>	216
6.2.8 <i>C. albicans</i> tolerates plant defensins with different stress response pathways	216
6.2.9 A GPCR may contribute to NaD1 activity	217
6.2.10 NaD1 and NaD2 act in synergy in <i>C. albicans</i> growth assays with stress signalling inhibitors.....	217
6.3 Future directions	218
6.3.1 What is NaD1's primary target?	218
6.3.2 How does synergy occur?	218
6.3.3 NaD1 uptake by endocytosis	219
6.3.4 GPCRs and NaD1	220
6.3.5 Fus3 and Hog1 activation in <i>S. cerevisiae</i>	221
6.3.6 Hog1 activation by NaD1 in other pathogens.....	221
6.3.7 Stress pathway activation by other AMPs	222
6.3.8 NaD2's mechanism of action.....	222
6.3.9 Inhibitors of stress signalling pathways.....	224
6.4 In summary	225
 Appendix	 226
AI Hayes et al. (2013).....	226
AII Amino acid dropout media recipes.....	236
AIII Sequencing of pDDB78- <i>HOG1</i> and pDDB78- <i>PBS2</i>	237
 References	 240

List of Figures

Figure 0.1	The secondary and tertiary structure of plant defensins.....	3
Figure 0.2	Loop regions of the plant defensin NaD1	6
Figure 2.1	NaD1, NaD2 and HXP4	30
Figure 2.2	Cathelicidin processing and structure.....	33
Figure 2.3	The structure of h β D2	34
Figure 2.4	The amino acid sequences of histatin 3 and histatin 5	35
Figure 2.5	Primer design for incorporation of the histatin 5 coding sequence into the pHUE plasmid.....	38
Figure 2.6	Protein dilutions for synergy assays.....	45
Figure 2.7	The growth of <i>C. albicans</i> DAY185 in different media.....	47
Figure 2.8	The growth of <i>C. albicans</i> DAY185 over six hours in half-strength PDB.....	48
Figure 2.9	The survival of <i>C. albicans</i> DAY185 after treatment with NaD1.....	49
Figure 2.10	The effect of NaD1, HXP4, bactenecin, Bac2a, BMAP-28 and CP29 on the growth of <i>C. albicans</i>	50
Figure 2.11	The activity of NaD1 against <i>C. albicans</i> DAY185 at 30°C and 37°C ...	51
Figure 2.12	The effect of Mg ²⁺ and Ca ²⁺ on the activity of NaD1 against <i>C. albicans</i>	52
Figure 2.13	The rate of permeabilisation of the plasma membrane of <i>C. albicans</i> by NaD1, CP29 and BMAP-28.....	53
Figure 2.14	The effect of serum on the activity of NaD1, CP29 and Bac2a against <i>C. albicans</i>	55
Figure 2.15	The effect of bovine serum albumin on the growth inhibitory activity of CP29.....	56
Figure 2.16	The effect of various antimicrobial peptides on the growth of three <i>C. neoformans</i> isolates	58
Figure 2.17	The effect of various antimicrobial peptides on the growth of three <i>C. gattii</i> isolates.....	59
Figure 2.18	The effect of various antimicrobial peptides on the growth of <i>A. niger</i>	60
Figure 2.19	The effect of various antimicrobial peptides on the growth of three <i>A. flavus</i> isolates.....	62
Figure 2.20	The effect of various antimicrobial peptides on the growth of three <i>A. paraciticus</i> isolates	63
Figure 2.21	Synergy between NaD1 and two AMPs against <i>C. gattii</i> R265.....	66
Figure 2.22	Synergy between NaD1 and two protease inhibitors against <i>C. gattii</i> R265	67
Figure 2.23	Synergy between NaD1 and two AMPs against <i>A. niger</i> 5181	69
Figure 2.24	Synergy of NaD1 with two AMPs against <i>A. flavus</i> 5310	70
Figure 2.25	Synergy between NaD1 and two protease inhibitors against <i>A. niger</i> 5181	72
Figure 2.26	Synergy between NaD1 and two protease inhibitors against <i>A. flavus</i> 5310	73
Figure 2.27	Synergy between NaD1 and two AMPs against <i>C. albicans</i> DAY185 ...	75
Figure 2.28	Synergy between NaD1 and two protease inhibitors against <i>C. albicans</i>	76
Figure 2.29	Synergy between NaD1 and two plant defensins against <i>C. albicans</i>	78
Figure 2.30	Synergy between NaD1 and two human AFPs against <i>C. albicans</i>	80
Figure 2.31	Synergy between NaD1 and amphotericin B against <i>C. albicans</i>	81

Figure 3.1	Inhibitors of endocytosis and protein trafficking	94
Figure 3.2	PCR with kanB primer	102
Figure 3.3	The effect of BODIPY-labelled NaD1 on fungal growth	103
Figure 3.4	NaD1 binds to the cell surface and is internalised into Fov hyphae	104
Figure 3.5	BODIPY-NaD1 accumulated on the cell surface of <i>C. albicans</i> cells ...	105
Figure 3.6	NaD1 uptake into <i>C. albicans</i> cells	106
Figure 3.7	BODIPY-NaD1 uptake occurs prior to PI fluorescence	107
Figure 3.8	Uptake of HPLC purified BODIPY-NaD1 into <i>C. albicans</i>	108
Figure 3.9	BODIPY-NaD1 uptake monitored by flow cytometry.....	109
Figure 3.10	Uptake inhibitors and endocytosis deletion mutants.....	110
Figure 3.11	Latrunculin A reduces the effect of NaD1 against <i>C. albicans</i>	111
Figure 3.12	Flow cytometry monitoring BODIPY-NaD1 uptake after treatment with CCCP	112
Figure 3.13	Confocal microscopy monitoring BODIPY-NaD1 and PI uptake after CCCP treatment.....	113
Figure 3.14	The effect of NaD1 on growth of <i>S. cerevisiae</i> endocytosis mutants ...	114
Figure 3.15	PCR check of <i>S. cerevisiae</i> <i>clc1Δ</i> , <i>ede1Δ</i> and <i>bzz1Δ</i> mutants	115
Figure 3.16	Protein transport inhibitors and ESCRT machinery deletion mutants ...	116
Figure 3.17	Brefeldin A and nocodazole do not affect the activity of NaD1 against <i>C. albicans</i>	117
Figure 3.18	The effect of NaD1 on the growth of <i>C. albicans</i> ESCRT mutants.....	118
Figure 3.19	Yeast components essential for NaD1 internalisation.....	124
Figure 4.1	Transposon insertion method of gene deletion used to construct <i>C. albicans</i> homozygous deletion mutants	128
Figure 4.2	Homologous recombination method of gene deletion used to construct <i>C. albicans</i> homozygous deletion mutants.....	129
Figure 4.3	Sample preparation for <i>C. albicans</i> library screens	132
Figure 4.4	The distribution of deletion mutants from the 2 μM NaD1 sensitivity screen	140
Figure 4.5	The distribution of deletion mutants from the 5 μM NaD1 resistance screen.....	141
Figure 4.6	The effect of NaD1 on the growth of <i>C. albicans</i> cell wall deletion mutants	142
Figure 4.7	The effect of NaD1 on the growth of <i>C. albicans</i> kinase deletion mutants	143
Figure 4.8	The effect of NaD1 on the growth of <i>C. albicans</i> transcription factor deletion mutants.....	144
Figure 4.9	The amplification of <i>PBS2</i> and <i>HOG1</i> genes.....	146
Figure 4.10	Amplified DNA from the <i>PBS2</i> and <i>HOG1</i> transformants.....	147
Figure 4.11	The effect of NaD1 to growth of <i>hog1Δ</i> and <i>pbs2Δ</i> mutants and complements.....	148
Figure 4.12	Hog1 is activated by NaD1 treatment	149
Figure 4.13	ROS production in <i>C. albicans</i> cells after NaD1 treatment	150
Figure 4.14	Flow cytometry monitoring DHR 123 and DAF-FM fluorescence after treatment with NaD1	151
Figure 4.15	The survival of <i>C. albicans</i> in the presence of various concentrations of NaD1	152
Figure 4.16	The effect of ascorbate on NaD1 activity against <i>C. albicans</i>	153
Figure 4.17	The effect of sorbitol on NaD1 activity against <i>C. albicans</i>	154
Figure 4.18	Overview of NaD1's mechanism against <i>C. albicans</i>	158
Figure 5.1	Oxidative, osmotic and cell wall stress response pathways in <i>C. albicans</i> and <i>S. cerevisiae</i>	161
Figure 5.2	The <i>S. cerevisiae</i> Fus3 and Kss1 signalling pathways	163

Figure 5.3	Two GPCRs exist in <i>S. cerevisiae</i>	164
Figure 5.4	PCR with <i>ARG4</i> detect primers.....	170
Figure 5.5	The effect of NaD1 on the growth of CWI, Cap1 oxidative stress response, calcineurin and mating pathway deletion mutants.....	175
Figure 5.6	PCR screen of <i>cap1</i> ^{-/-} , <i>cek2</i> ^{-/-} and <i>crz1</i> ^{-/-} mutants.....	177
Figure 5.7	The effect of NaD1 on the growth of <i>S. cerevisiae</i> with mutations in the HOG, CWI, calcineurin and Yap1 transcription factor pathways.....	178
Figure 5.8	PCR screen to confirm gene deletions in <i>S. cerevisiae hog1Δ</i> , <i>mpk1Δ</i> , <i>cna1Δ</i> , <i>yap1Δ</i> and <i>fus3Δ</i>	180
Figure 5.9	The effect of hydrogen peroxide on the growth of <i>C. albicans</i> and <i>S. cerevisiae</i>	181
Figure 5.10	The effect of NaD1 on the growth of <i>S. cerevisiae</i> mutants from the two alternative osmosensing pathways of Hog1 activation.....	183
Figure 5.11	PCR screen to confirm gene deletions in the <i>S. cerevisiae hog1Δ</i> , <i>msb2Δ</i> , <i>sho1Δ</i> and <i>SLN1/sln1Δ</i> mutants.....	184
Figure 5.12	Pertussis toxin reduces the effect of NaD1 against <i>C. albicans</i> and <i>S. cerevisiae</i>	185
Figure 5.13	Flow cytometry monitoring BODIPY-NaD1 uptake after treatment with cellular inhibitors.....	186
Figure 5.14	Addition of brefeldin A reduces rescue of NaD1 growth inhibition of <i>C. albicans</i> by pertussis toxin.....	187
Figure 5.15	The growth inhibitory activity of NaD1 against <i>S. cerevisiae</i> GPCR and Fus3 mating pathway mutants.....	189
Figure 5.16	PCR screen to confirm gene deletions in the <i>S. cerevisiae fus3Δ</i> , <i>ste3Δ</i> , <i>ste2Δ</i> and <i>gpr1Δ</i> mutants.....	190
Figure 5.17	The effect of additional dextrose on the activity of NaD1 against <i>C. albicans</i> and <i>S. cerevisiae</i> in half-strength PDB.....	191
Figure 5.18	The effect of the plant defensins NaD1, NaD2 and DmAMP1 on the growth of <i>C. albicans</i> wildtype and <i>hog1Δ</i> and <i>mkc1Δ</i> mutants.....	193
Figure 5.19	The Hog1 pathway is activated in <i>C. albicans</i> by NaD2 treatment.....	194
Figure 5.20	Synergy of NaD1 with FK506 and cercosporamide against <i>C. albicans</i>	196
Figure 5.21	Synergy of NaD2 with FK506 and cercosporamide against <i>C. albicans</i>	197
Figure 5.22	<i>C. albicans</i> stress signalling in response to NaD1.....	199
Figure 5.23	MAP kinase signalling in <i>S. cerevisiae</i>	202
Figure 5.24	MAP kinase signalling in <i>C. albicans</i>	204
Figure 6.1	Reporter system for Hog1 activation.....	223
Figure A.1	Sequencing of pDDB78- <i>HOG1</i> (HOG1-1).....	237
Figure A.2	Sequencing of pDDB78- <i>PBS2</i> (PBS2-3).....	239

List of Tables

Table 0.1	Identified mechanisms of plant defensins	5
Table 2.1	Antimicrobial peptides used in antifungal assays against human pathogens.....	31
Table 2.2	Levels of synergy	46
Table 4.1	The mutant hits identified in the NaD1 screen of <i>C. albicans</i> deletion libraries.....	141
Table 4.2	Growth inhibition of mutants from the <i>C. albicans</i> library screens by NaD1	145
Table 5.1	The effect of NaD1 on the growth of <i>C. albicans</i> wildtype and mutants in various stress signalling pathways.....	176
Table 5.2	The effect of NaD1 on growth of <i>S. cerevisiae</i> wildtype and mutants in various stress signalling pathways.....	179
Table A.1	Amino acid dropout mix recipes	236

List of Publications

Hayes BME, Bleackley MR, Wiltshire JL, Anderson MA, Traven A, van der Weerden NL (2013) Identification and mechanism of action of the plant defensin NaD1 as a new member of the antifungal drug arsenal against *Candida albicans*. *Antimicrob Agents Chemother* **57**: 3667-3675

Hayes BME, Anderson MA, Traven A, van der Weerden NL, Bleackley MR (2014) Activation of stress signalling pathways enhances tolerance of fungi to chemical fungicides and antifungal proteins. *Cell Mol Life Sci* **71**: 2651-2666

Bleackley MR, **Hayes BM**, Parisi K, Saiyed T, Traven A, Potter ID, van der Weerden NL, Anderson MA (2014) Bovine pancreatic trypsin inhibitor is a new antifungal peptide that inhibits cellular magnesium uptake. *Mol Microbiol* **92**: 1188-1197

Abbreviations

°C	degrees Celsius
× g	times gravity
Abs (595)	absorbance at 595 nm
AFP	antifungal peptide
AMP	antimicrobial peptide
ATP	adenosine triphosphate
BCA	bicinchoninic acid assay
BODIPY	4,4-difluoro-5,7-dimethyl-4-bora-3a,4a-diaza-s-indacene-3-propionyl ethylenediamine
BMAP-28	bovine myeloid antimicrobial protein 28
BMG	buffered minimal glycerol
BMM	buffered minimal methanol
bp	base pair(s)
BPTI	bovine pancreatic trypsin inhibitor
BSA	bovine serum albumin
bZIP	basic leucine zipper domain
Ca	<i>Candida albicans</i>
CCCP	carbonyl cyanide m-chlorophenyl hydrazone
CME	clathrin-mediated endocytosis
CP29	cecropin-melittin hybrid 29
CPP	cell-penetrating peptide
CTPP	C-terminal pro-peptide
CWI	cell wall integrity pathway
DAF-FM	4-amino-5-methylamino-2',7'-difluorofluorescein
DAPI	4',6-diamidino-2-phenylindole
DHR 123	dihydrorhodamine 123
DmAMP1	<i>Dahlia merckii</i> antimicrobial protein 1
DMSO	dimethylsulfoxide
DNA	deoxyribonucleic acid
dNTP	deoxyribonucleotide triphosphate
DPSS	diode-pumped solid-state laser
DTT	dithiothreitol
EDC	1-ethyl-3-(3-dimethylaminopropyl)carbodiimide

EDTA	ethylenediaminetetraacetic acid
ESCRT	Endosomal sorting complexes required for transport
ER	endoplasmic reticulum
FCS	fetal calf serum
FITC	fluorescein isothiocyanate
Fov	<i>Fusarium oxysporum f. sp. vasinfectum</i>
Fw	forward primer
g	gram(s)
GPCR	G-protein coupled receptor
GTP	guanosine triphosphate
h	hour(s)
h β D2	human beta-defensin 2
HeNe	helium-neon laser
HOG	high-osmolarity glycerol pathway
HPLC	high performance liquid chromatography
HsAFP1	<i>Heuchera sanguinea</i> antifungal protein 1
HXP4	Hexima protein 4
IC ₅₀	concentration to inhibit 50% of growth
ID	inhibition difference
IPTG	isopropyl-1-thio- β -D-galactosidase
kb	kilobase(s)
kDa	kilodalton(s)
L	litre(s)
LB broth	Luria Bertani broth
M	molar
MCS	multiple cloning site
MES	2-(<i>N</i> -morpholino)ethanesulfonic acid
min	minute(s)
mL	millilitre(s)
mm	millimetre(s)
mM	millimolar
MVB	multivesicular body
MWCO	molecular weight cut off
NaCys2	<i>Nicotiana alata</i> cystatin 2
NaD1	<i>Nicotiana alata</i> defensin 1

NaD2	<i>Nicotiana alata</i> defensin 2
nm	nanometre(s)
NO	nitric oxide
OD ₅₉₅	optical density at 595 nm
OD ₆₀₀	optical density at 600 nm
ORF	open reading frame
PBS	phosphate buffered saline
PCR	polymerase chain reaction
PDB	potato dextrose broth
PDA	potato dextrose agar
PEG	polyethylene glycol
PI	propidium iodide
PLATE	PEG, LiOAc, TE buffer
PVDF	polyvinylidene fluoride membrane
RNA	ribonucleic acid
ROS	reactive oxygen species
RP-HPLC	reverse phase high performance liquid chromatography
rpm	revolutions per minute
RsAFP2	<i>Raphanus sativus</i> antifungal protein 2
RT	room temperature
Rv	reverse primer
s	second(s)
Sc	<i>Saccharomyces cerevisiae</i>
SDA	Sabouraud's dextrose agar
SDS	sodium dodecyl sulphate
SDS-PAGE	sodium dodecyl sulphate polyacrylamide gel electrophoresis
TBS	Tris-buffered saline
TBST	Tris-buffered saline with 0.05% (v/v) Tween 20
TCA	trichloroacetic acid
TE	Tris, EDTA buffer
TF	transcription factor
TGN	<i>trans</i> -Golgi network
Tris	tris(hydroxymethyl)aminomethane
μL	microlitre(s)
μM	micromolar

UTR	untranslated region
VPS	vacuolar protein sorting
WT	wildtype
w/v	weight per volume
YNB	yeast nitrogen base
YPD	yeast peptone dextrose medium

Abstract

The plant defensin NaD1 is a small cysteine-rich peptide that has potent antifungal activity against pathogens of plants. Its mechanism of action has been partially defined against the plant pathogen *Fusarium oxysporum f. sp. vasinfectum* (Fov). It has a three step mechanism which involves binding to the hyphal cell wall, disruption of the plasma membrane and entry into the cytoplasm, where reactive oxygen species are produced.

The primary aim of this thesis was to evaluate whether NaD1 has potential for the treatment of human fungal diseases and to shed more light on the mechanism of action. This study revealed that NaD1 inhibits the growth of a number of fungal pathogens which affect human health, including *Candida albicans*, which can cause invasive infections of mucosal tissues, and species of *Cryptococcus* and *Aspergillus*, which can cause meningitis and infect the lungs. NaD1's activity against yeast allowed the use of several experimental techniques to which yeast cells are more amenable than filamentous fungi, including time-lapse microscopy and flow cytometry. Furthermore, libraries of mutants and advanced genomic data are available. This led to the discovery that NaD1's three step mechanism of action initially observed in Fov is conserved in *C. albicans*, so findings in yeast are also likely to apply to filamentous fungal species.

Using confocal microscopy, cellular inhibitors and deletion mutants it was revealed that NaD1 enters the cytoplasm of *C. albicans*, and most likely does so by endocytosis. After entering the cytoplasm, retrograde transport is not required for NaD1's antifungal activity. Screening of a partial *C. albicans* deletion mutant library revealed that the high-osmolarity glycerol stress response pathway protects the yeast from the deleterious effects of NaD1. The role of various stress pathways in enhancing tolerance to antifungal peptides and fungicides was reviewed and led to the hypothesis that manipulation of these stress response pathways could be used to enhance the activity of antifungal molecules.

Statement of Authorship

Except where reference is made in the text of the thesis, this thesis contains no material published elsewhere or extracted in whole or in part from a thesis submitted for the award of any other degree or diploma. No other person's work has been used without due acknowledgment in the main text of the thesis. This thesis has not been submitted for the award of any degree or diploma in any other tertiary institution.

Brigitte Hayes

29/09/2014

Acknowledgements

Firstly, I would like to thank my supervisors Professor Marilyn Anderson and Dr Nicole van der Weerden for their support and guidance throughout my PhD. I am extremely grateful to have had the opportunity to work on such an interesting project and to learn from such knowledgeable people.

A big thankyou to Dr Mark Bleackley for all his help with project planning, thesis editing and general yeast discussions. Thankyou to all the members of the lab, especially my fellow PhD students, for making it enjoyable to come to work every day.

I would also like to thank Dr Ana Traven at Monash University, for allowing me to spend time in her lab and for her help with all things *Candida albicans*. Her expertise has been invaluable.

Lastly, thankyou to my family for the encouragement and for putting up with any stress induced grumpiness.

Introduction

With the appearance of fungicide and drug resistance, fungal disease is an ever increasing burden in agriculture and human health. Fungal pathogens are responsible for significant damage and loss of many important agricultural crops (Fisher et al., 2012; Gao et al., 2000).

A number of fungal pathogens are also responsible for human illness, particularly in immunocompromised individuals. With an increase in HIV/AIDS, diabetes, chemotherapy, transplantation and immune suppressive therapy, the incidence of fatal fungal infections is on the rise (Brown et al., 2012; Koselj-Kajtina et al., 2001; Latge & Calderone, 2002; Wanke et al., 2000). Human pathogens that are particularly common and dangerous to immunocompromised hosts are *Candida*, *Aspergillus* and *Cryptococcus* species (Brown et al., 2012; Latge & Calderone, 2002). Unfortunately, there are limitations to the use of the current therapeutics, with issues of resistance (Eliopoulos et al., 2002; Sanglard, 2002), toxicity and cost (Wong-Beringer & Kriengkauykiat, 2003).

The need for novel approaches to treat and prevent fungal disease in both plant and mammalian systems, has led to evaluation of the potential of antimicrobial peptides as therapeutic agents. Mammals and plants naturally express a number of antimicrobial peptides (AMPs) as part of their innate immune system. These peptides can display antifungal, antibacterial and insecticidal activities (Brandenburg et al., 2012; Peters et al., 2010; Theis & Stahl, 2004). Several antimicrobial peptides are currently in clinical trial for treatment of human disease. Examples include the frog skin antimicrobial peptide Magainin, which is in clinical trial for the treatment of diabetic foot ulcers, and Novexatin, a cationic antimicrobial peptide being trialed for the treatment of fungal infections of toenails (Fox, 2013).

Human AMPs include α - and β -defensins, histatins and cathelicidins (Pasupuleti et al., 2012; Smet & Contreras, 2005; van der Weerden et al., 2013; Wiesner & Vilcinskas, 2010; Zasloff, 2002). Plants express many families of antimicrobial peptides including thionins, heveins, knottins, lipid transfer proteins, chitinases, glucanases, snakins, protease inhibitors and defensins (Garcia-Olmedo et al., 1998; Theis & Stahl, 2004; van der Weerden et al., 2013). The plant defensins, in particular, have significant activity against fungal pathogens, and are being trialed in the protection of transgenic crops (Gao et al., 2000; Gaspar et al., 2014; Kaur et al., 2011; Terras et al., 1995).

This thesis will focus on a plant defensin and its mechanism of action in inhibition of fungal growth. Plant defensins are a particularly interesting subset of peptides, as they display a wide range of biological activities and mechanisms. These peptides are small (~5 kDa), basic proteins, that are produced by many plant tissues, including seeds, leaves, flowers and fruit (Lay & Anderson, 2005). They share a common tertiary structure, with a triple-stranded anti-parallel β -sheet and an α -helix stabilised by four disulphide bonds (Figure 0.1A). This structure, a cysteine-stabilised $\alpha\beta$ motif, is highly stable to extremes in pH and temperature (Figure 0.1B) (Janssen et al., 2003; Lay et al., 2003a). However, the secondary structures are highly variable, with only eight cysteine residues, an aromatic residue at position 11, two glycine residues at positions 13 and 34 and a glutamic acid at position 29 (relative to RsAFP2 from *Raphanus sativa*) being conserved (Figure 0.1B) (Lay et al., 2003b; van der Weerden & Anderson, 2012b).

The plant defensins can be divided into two classes based on their precursor structure (Lay & Anderson, 2005). The class I defensins consist of a mature defensin domain, as well as an endoplasmic reticulum (ER) signal sequence (Lay et al., 2003a) (Figure 0.1C). Well characterised examples of this class are the *R. sativus* defensins RsAFP1 and RsAFP2, the *Medicago sativa* defensin MsDef1 (also known as alfAFP) and the *Dahlia merckii* defensin DmAMP1 (Gao et al., 2000; Terras et al., 1992; Thevissen et al., 1996). Class II defensins contain an ER signal sequence, a mature defensin domain and an additional C-terminal pro-peptide (CTPP) of 27-33 amino acids (Lay et al., 2003a) (Figure 0.1C). This class includes defensins from several solanaceous plants, including NaD1 from *Nicotiana glauca*, PhD1 and PhD2 from *Petunia hybrida* and TPP3 from *Lycopersicon esculentum* (Lay et al., 2003a; Milligan & Gasser, 1995). To date, only two class II defensins from species outside the solanaceous family have been found; HaDef1 from sunflower *Helianthus annuus* roots and ZmESR6 from *Zea mays* (Balandin et al., 2005; de Zélicourt et al., 2007). The CTPP functions as a vacuolar targeting signal and also has a role in detoxification of the peptide in the plant cells (Lay et al., 2014; Lay et al., 2003a).

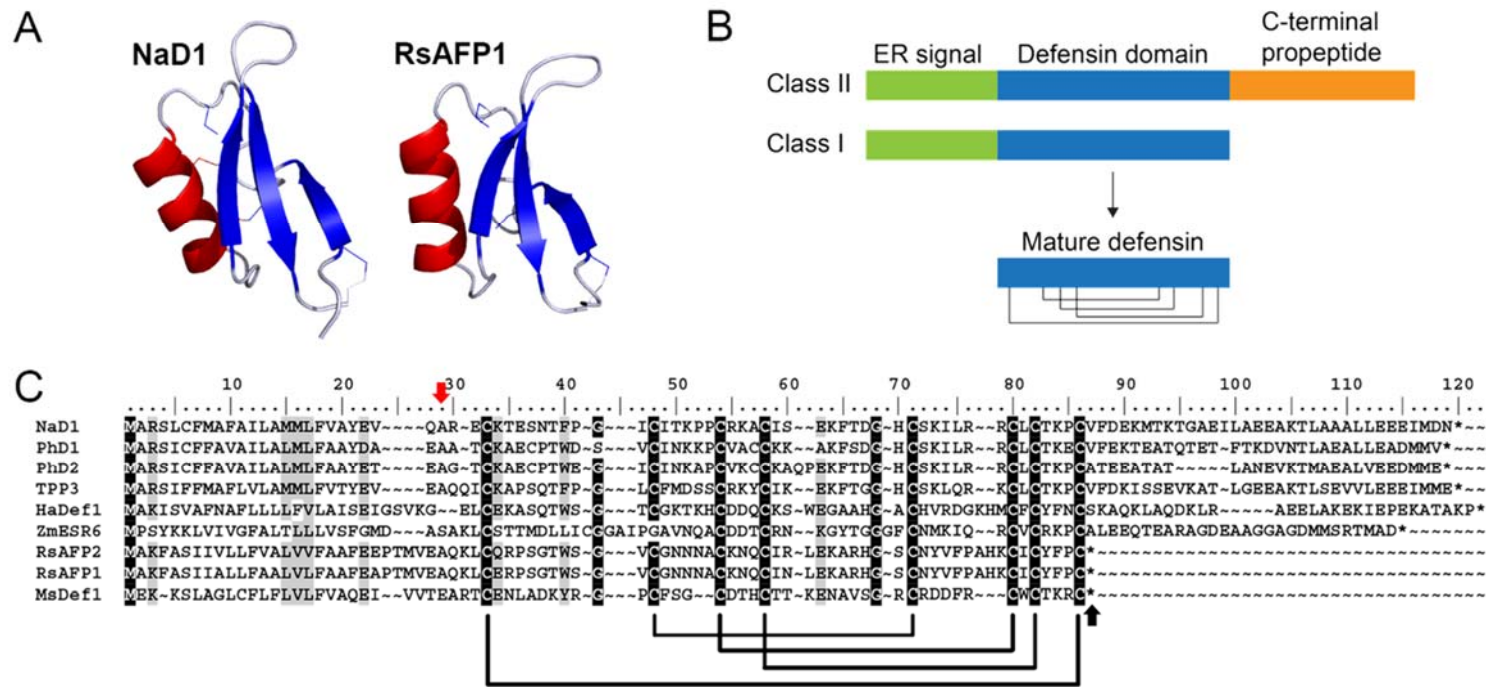


Figure 0.1 The secondary and tertiary structure of plant defensins

(A) The three-dimensional structure of the plant defensins NaD1 (PDB: 1MR4) and RsAFP1 (PDB: 1AYJ). Each contain an α -helix, shown in red. The three β -strands are shown in blue. Both structures also contain four disulphide bonds. (B) Class I defensins have an ER signal and a defensin domain. Class II defensins also have an additional CTPP. Both classes are processed to leave only the mature defensin domain. Disulphide bond connectivity is also shown for the mature defensin. (C) An alignment of the amino acid sequence of several plant defensins. A red arrow denotes the end of the ER signal sequence. The mature defensin domain begins at residues 30 and ends at position 86, which is represented by a black arrow. The C-terminal propeptide (CTPP) is shown from position 87 onwards. Disulphide bond connectivity of the mature defensin domain is also shown below. The top six sequences represent class II defensins, which contain a CTPP. The remainder are class I defensins.

Plant defensins are generally antimicrobial. The best characterised have antifungal activity, although some target bacteria or insects (Lay & Anderson, 2005; van der Weerden et al., 2013). The level of antifungal activity can differ greatly between defensins, and also varies depending on the test pathogen (Spelbrink et al., 2004). Plant defensins also have different targets and mechanisms of actions (van der Weerden et al., 2013; Vriens et al., 2014). However, the mechanisms of action has only been studied for a small number of plant defensins and those that have been studied have not had their mechanisms fully defined. The most well characterised plant defensins and their identified mechanisms are shown in Table 0.1.

Table 0.1 Identified mechanisms of plant defensins

Defensin	Source	Mechanism	References
RsAFP2	<i>Raphanus sativus</i>	Induces K ⁺ efflux and Ca ²⁺ influx in <i>Neurospora crassa</i> , stimulates Ca ²⁺ uptake in <i>Fusarium culmorum</i> , permeabilises <i>N. crassa</i> plasma membranes, binds glucosylceramide in <i>Pichia pastoris</i> membranes, induces reactive oxygen species in <i>Candida albicans</i> , activates caspases and induces apoptosis in <i>C. albicans</i> , induces accumulation of ceramides in <i>C. albicans</i> , impairs yeast to hyphal transition and induces septin mislocalisation in <i>C. albicans</i>	Thevissen et al. (1996) De Samblanx et al. (1997) Thevissen et al. (1999) Thevissen et al. (2004) Aerts et al. (2007) Aerts et al. (2009) Thevissen et al. (2012)
DmAMP1	<i>Dahlia merckii</i>	Induces K ⁺ efflux and Ca ²⁺ influx in <i>N. crassa</i> , permeabilises <i>N. crassa</i> plasma membranes, binds mannosyldiinositolphosphoryl-ceramide in <i>Saccharomyces cerevisiae</i> membranes	Thevissen et al. (1996) Thevissen et al. (1999) Thevissen et al. (2003)
Psd1	<i>Pisum sativum</i>	Localises to the nucleus of <i>Fusarium solani</i> cells, binds to cyclin F and halts the cell cycle in <i>N. crassa</i> , likely to interact with ergosterol and/or glucosylceramide in membranes, likely to initially be adsorbed or inserted into membranes	Lobo et al. (2007) Gonçalves et al. (2012)
MsDef1	<i>Medicago sativa</i>	Blocks mammalian L-type Ca ²⁺ channels, antifungal activity requires glucosylceramide in <i>Fusarium graminearum</i> plasma membranes, causes hyperbranching of <i>F. graminearum</i> , permeabilises <i>F. graminearum</i> plasma membranes, disrupts Ca ²⁺ homeostasis in <i>N. crassa</i> , partially inhibits conidial germination of <i>N. crassa</i>	Spelbrink et al. (2004) Ramamoorthy et al. (2007) Sagaram et al. (2011) Muñoz et al. (2014)
MtDef4	<i>Medicago truncatula</i>	Permeabilises <i>F. graminearum</i> plasma membranes, interacts with phosphatidic acid, is internalised into <i>F. graminearum</i> cells, disrupts Ca ²⁺ homeostasis in <i>N. crassa</i> , inhibition of conidial germination and cell fusion in <i>N. crassa</i>	Sagaram et al. (2011) Sagaram et al. (2013) Muñoz et al. (2014)
HsAFP1	<i>Heuchera sanguinea</i>	Induces reactive oxygen species and apoptosis in <i>C. albicans</i>	Aerts et al. (2011)
NaD1	<i>Nicotiana glauca</i>	Internalised into <i>Fusarium oxysporum</i> cells, induces production of reactive oxygen species in <i>F. oxysporum</i> , permeabilises <i>F. oxysporum</i> plasma membranes, requires the <i>F. oxysporum</i> cell wall for antifungal activity, binds phosphatidylinositol 4,5-bisphosphate	van der Weerden et al. (2008) van der Weerden et al. (2010) Poon et al. (2014)

The functional residues of the plant defensins lie (at least in part) in the exposed loop regions of their three-dimensional structure. De Samblanx and co-workers (1997) reported that the activity of the defensin RsAFP2 is dependent on the residues Phe40, Tyr38 (corresponding to Loop 5 of NaD1, Figure 0.2) and Thr10, all of which lie within exposed loops of the protein. A substitution at these positions with the corresponding residues from a defensin which lacks antifungal activity, sI α 2, reduced the antifungal activity of RsAFP2 against the pathogen *Fusarium culmorum*. This was confirmed by substitutions at these positions with alanine residues, which also reduced activity (De Samblanx et al., 1997). The importance of exposed loops was also studied by Lin and co-workers (2007) who swapped the functional loop of the α -amylase inhibitor VrD1 with the equivalent loop of the protein VrD2. Native VrD2 had no α -amylase inhibitory activity. However chimeric VrD2, containing the VrD1 loop, did have inhibitory activity against α -amylase from the insect species *Tenebrio molitor* (Lin et al., 2007). Although the loop is essential for antifungal activity the interacting partner in the fungal cell has not been defined for most defensins. The exceptions are MtDef4 and NaD1. MtDef4 binding to phosphatidic acid (PA) and entry into *Fusarium graminearum* cells is dependent on the β 2- β 3 loop (Loop 5 of NaD1, Figure 0.2) of the protein (Sagaram et al., 2013). This loop (or more specifically residue R40 within this loop) is also essential for NaD1 induced growth inhibition of *Fusarium oxysporum f. sp. vasinfectum* (Fov) and binding to phosphoinositides (Poon et al., 2014).

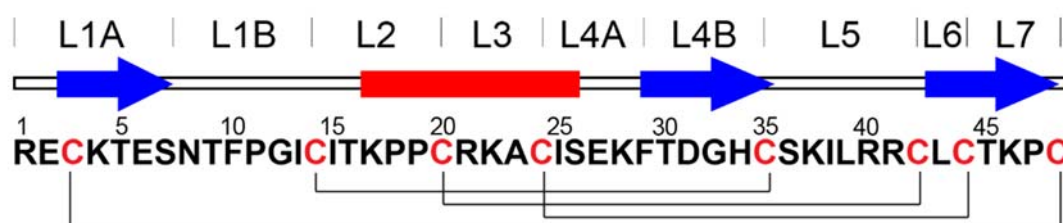


Figure 0.2 Loop regions of the plant defensin NaD1

NaD1's amino acid sequence is shown with the cysteines in red and the disulphide bond connectivity below. Blue arrows show the section of NaD1's sequence which form β -strands in the tertiary structure. The red rectangle represents the α -helix. The areas corresponding to the loop regions of NaD1 (Loop 1A to Loop 7) are shown above (van der Weerden & Anderson, 2012a).

The aim of this thesis was to determine whether the plant defensin NaD1 has the potential to be used as a therapeutic for treatment of fungal disease in humans. All of the work on its spectrum of antifungal activity and mechanism of action has been conducted with plant pathogens. The known mechanisms of NaD1's action against plant pathogens is described below.

The action of NaD1 on fungal pathogens involves binding to the fungal cell wall, permeabilisation of the plasma membrane and accumulation in the cytoplasm (van der Weerden et al., 2008). The fluorescent dye SYTOX green, which is unable to enter intact hyphae, has been used to confirm the involvement of the cell wall and plasma membrane in the action of NaD1. SYTOX green enters the cytoplasm of Fov hyphae after NaD1 treatment, indicating that membrane permeabilisation has occurred (van der Weerden et al., 2008).

Removal of the hyphal cell wall abolishes NaD1's ability to permeabilise the plasma membrane. Treatment of Fov hyphae with β -glucanase or proteinase K prior to NaD1 treatment blocks SYTOX green uptake (van der Weerden et al., 2010). Furthermore, analysis of solubilised cell wall fractions with α -NaD1 antibody indicated that NaD1 binds to the cell wall of Fov hyphae (van der Weerden et al., 2008).

At the plasma membrane, NaD1 is hypothesised to bind to phosphatidylinositol 4,5-bisphosphate (PI(4,5)P₂). NaD1 binds to PI(4,5)P₂ on lipid strips and also binds to PI(4,5)P₂ in a bilayer (based on binding to PI(4,5)P₂ containing liposomes) (Poon et al., 2014). This confirms that plant defensins act through different mechanisms, as three plant defensins have been found to bind to different lipids (PI(4,5)P₂ for NaD1, M(IP)₂C for DmAMP1 and GlcCer for RsAFP2).

NaD1 induced cell death does not simply involve leakage of cytoplasmic contents. Imaging of fluorescently labelled NaD1 revealed that NaD1 enters the cytoplasm of Fov hyphae, before the cytoplasm develops a granular appearance (van der Weerden, 2007). Immunogold labelling was also used to confirm that NaD1 enters the cytoplasm of Fov hyphae (van der Weerden et al., 2008). In Chapter 3 of this thesis, I also describe uptake of fluorescently labelled NaD1 into *C. albicans*. Permeabilisation kinetic assays give further evidence supporting the hypothesis that NaD1 does not act simply through membrane permeabilisation. The rate of membrane permeabilisation by NaD1 is delayed when compared to the peptides CP29 and BMAP-28, which are considered to be pore forming peptides. CP29 and BMAP-28 cause rapid uptake of SYTOX green into Fov hyphae, whereas there is a 15 min delay between NaD1 treatment and detection of SYTOX green uptake (van der Weerden et al., 2010). Together this data indicates that the action of NaD1 is not due to permeabilisation of the plasma membrane alone, but requires action within the cell.

Many of the details regarding the mechanism of action of the plant defensin NaD1 still remain unknown. NaD1's ability to inhibit human pathogens has not been investigated. Nor has NaD1's primary target or the method of uptake into fungal cells been identified. The likelihood of fungal resistance to NaD1 has also not been studied. To answer these unknowns, *C. albicans* was used as model organism, because it is a major pathogen in humans and there are extensive genetic resources available to assist in the identification of NaD1's targets.

Investigation revealed that NaD1 inhibits several important human fungal pathogens, including *C. albicans* and species of *Aspergillus* and *Cryptococcus* (Chapter 2 of this thesis). In Chapter 3 of this thesis, I show that NaD1's mechanism of action against human fungal pathogens involves binding to the fungal cell wall, permeabilisation of the plasma membrane and accumulation in the cytoplasm. I also show that uptake of NaD1 into the fungal cytoplasm is likely to be through endocytosis. Screening of a partial *C. albicans* deletion library led to the discovery that *C. albicans* requires the high-osmolarity glycerol (HOG) stress response pathway for tolerance of NaD1 (This work is described in Chapter 4 of this thesis and has been published) (Hayes et al., 2013) (Appendix AI). In contrast, NaD2 (another defensin isolated from *N. alata*) and DmAMP1 (from *D. merckii*) activate both the HOG pathway and the CWI pathway in *C. albicans* (Chapter 5 of this thesis).

Tolerance of *C. albicans* to the radish defensin RsAFP2 also requires the CWI pathway (Thevissen et al., 2012).

Upon further search of the literature it became apparent that stress signalling pathways have an essential role in protecting pathogens against the deleterious effects of antifungal agents. Along with NaD1, NAD2, RsAFP2 and DmAMP1, many antimicrobial peptides and chemical fungicides activate different stress response pathways, leading to the production of molecules that protect cells against osmotic, oxidative and cell wall stress. Most interestingly, the pathways activated differ according to the antifungal therapy and may hint at the mechanism of antifungal activity. Thus the literature review for this thesis is focused on fungal stress response pathways and their involvement in tolerance to antifungal peptides and chemical fungicides. This review has been published in Cellular and Molecular Life Sciences (Hayes et al., 2014) and incorporates data from later sections of this thesis (particularly Chapter 4 and Chapter 5). I have written all of this literature review with mentoring by my supervisors.

Chapter 1

Literature Review

This literature review has been published in Cellular and Molecular Life Sciences:

Hayes BME, Anderson MA, Traven A, van der Weerden NL, Bleackley MR (2014)
Activation of stress signalling pathways enhances tolerance of fungi to chemical fungicides
and antifungal proteins. *Cell Mol Life Sci* **71**: 2651-2666

Due to copyright, the review has been excluded from this version of the thesis.

Chapter 2

Activity of NaD1 against human fungal pathogens

2.1 Introduction

The innate immune system in eukaryotes is the first line of defence against potential pathogens, such as bacteria and fungi. Innate immune molecules, also known as antimicrobial peptides (AMPs), are an important part of this defence. To date, the APD2 antimicrobial peptide database contains 2400 peptides that have been identified from numerous sources, such as from plants, animals and fungi (Wang et al., 2009a). Most plant peptides are active against fungal pathogens, which is understandable given that fungal species are major pathogens of plants (Strange & Scott, 2005). In contrast, most mammalian peptides have been reported to have antibacterial activity and little is known about their role in preventing fungal infections. The best characterised antifungal peptides from humans are the salivary histatins (Oppenheirn et al., 1988). Human defensins HNP1, HNP2, h β D2 and h β D3 have also been reported to be active against the pathogen *C. albicans* (Lupetti et al., 2002). It is likely that humans have other innate immunity molecules involved in protection from fungal disease that have not been characterised. Despite the existence of human peptides with antifungal activity, fungal disease is becoming increasingly problematic to human health. This has arisen from the exponential increase in the number of patients who have become immunocompromised due to cancer treatments, organ transplantation or HIV (Brown et al., 2012; Koselj-Kajtina et al., 2001; Latge & Calderone, 2002; Wanke et al., 2000). Invasive fungal infections contribute significantly to mortality rates among these patients (Brown et al., 2012; Menzin et al., 2009). The mortality rate of infection with species of *Aspergillus* can reach as high as 95%. For infection by *Cryptococcus* or *Candida* species mortality rates can be as high as 70-75% (Brown et al., 2012). The aim of this Chapter is to examine the antifungal activity of AMPs, of both plant and animal origin, against human fungal pathogens to assess their potential application in treatment of fungal infections in humans (particularly the immunocompromised).

Three fungal genera, *Aspergillus*, *Cryptococcus* and *Candida*, were chosen for this work because they are of particular concern to humans. Each genus is described briefly below.

The yeast *Candida albicans* is the most common cause of fungal infection in humans. *C. albicans* is a dimorphic fungus, with both a yeast and hyphal form. It is part of the normal flora of the skin, gastrointestinal and urinary tracts, but can become pathogenic in immunocompromised individuals. While mucosal infections are rarely fatal, systemic infections are life threatening (Berman & Sudbery, 2002) with mortality rates as high as 75% reported for *Candida* infections (Brown et al., 2012).

The most troublesome member of the *Cryptococcus* species is *Cryptococcus neoformans*. The incidence of infection by this pathogen has surged with the increase in HIV/AIDS and immunosuppressive therapies (Brown et al., 2012; Idnurm et al., 2005). Among immunosuppressed patients, *C. neoformans* mortality rates can be up to 70% (Brown et al., 2012; Butts & Krysan, 2012). *C. neoformans* has specific virulence factors which differ from most fungi. These include the ability to produce melanin and the formation of a polysaccharide capsule. The capsule is a protective barrier that can also impede phagocytosis, as well as inhibiting the production of cytokines and complement (Bose et al., 2003; Idnurm et al., 2005).

Aspergillus species are filamentous fungi which also cause severe infections in immunosuppressed patients. The overall mortality rate from invasive infection is up to 58% and can reach 90% when the central nervous system is infected. The most common *Aspergillus* infections are caused by *Aspergillus fumigatus*, *Aspergillus flavus*, *Aspergillus niger* and *Aspergillus terreus* (Patterson, 2005).

In this Chapter I examined the activity of a number of antimicrobial peptides of both plant and animal origin against *C. albicans*, *Cryptococcus* and *Aspergillus* species. The antimicrobial peptides tested and their origin are listed in Table 2.1. They are also described in detail in the following section.

NaD1 is a class II plant defensin isolated from the flowers of *N. alata*. Defensins were described in detail in the Introduction of this thesis. Plant defensins are small, basic proteins, which are present in most plant tissues. They have a highly stable structure, due to the presence of four disulphide bonds (Lay & Anderson, 2005). HXP4 is a variant of NaD1 that has improved antifungal activity against several plant pathogens. HXP4 was created by incorporating Loop 1B of NaD2 (a class I defensin also isolated from the flowers of *N. alata*) into the NaD1 sequence (van der Weerden & Anderson, 2012a) (Figure 2.1). Refer to Figure 0.2 for the location of all loops in the NaD1 sequence.

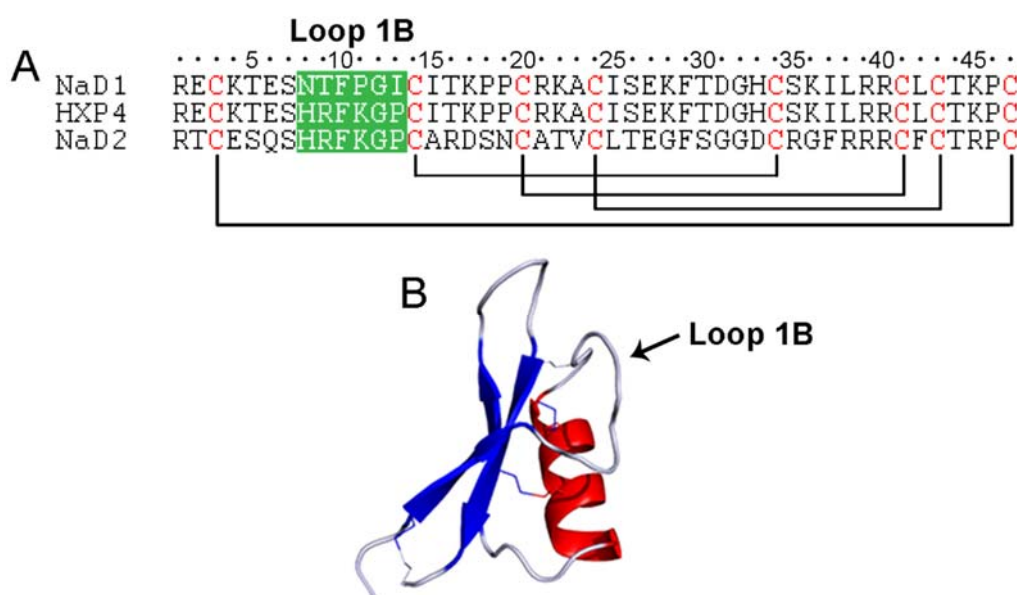


Figure 2.1 NaD1, NaD2 and HXP4

(A) Alignment of the mature defensin sequence of NaD1, NaD2 and HXP4. HXP4 was generated by swapping Loop 1B of NaD2 into NaD1. Loop 1B is highlighted in green and cysteine are red. Disulphide bond connectivity is also shown. (B) The three-dimensional structure of NaD1 (PDB: 1MR4), with Loop 1B shown with an arrow.

Table 2.1 Antimicrobial peptides used in antifungal assays against human pathogens

Protein sequences of antimicrobial peptides. Cysteine residues are shown in red.

AMP	Type	Source	Sequence	Reference
NaD1	Defensin	Plant	<p>RE⁵CKTESNTFFPGI¹⁰CITKPP¹⁵CRKA²⁰CISEKFTDGH²⁵CSKILRR³⁰CLCTKPC³⁵</p>	Lay et al. (2003a)
HXP4	Defensin	Plant	<p>RE⁵CKTESHRFKGP¹⁰CITKPP¹⁵CRKA²⁰CISEKFTDGH²⁵CSKILRR³⁰CLCTKPC³⁵</p>	van der Weerden & Anderson (2012a)
Bactenecin	Cathelicidin	Bovine	<p>RL⁵CRIVVIRV¹⁰CR</p>	Wu & Hancock (1999b)
Bac2a	Cathelicidin	Bovine	<p>RLARIVVIRVAR</p>	Wu & Hancock (1999a)
BMAP-28	Cathelicidin	Bovine	<p>GGLRSLGRKILRAWKKYGP⁵IIPIIRIG¹⁰</p>	Skervlavaj et al. (1996)
CP29	Cecropin/ Melittin hybrid	Synthetic	<p>KWKSFIK⁵LLTTAVKKV¹⁰LTGLPALIS¹⁵</p>	Friedrich et al. (2000)
HβD2	β-defensin	Human	<p>GIGDPVT⁵CLKSGAI¹⁰CHPVF¹⁵CPRRYKQIGT²⁰CGLPGTK²⁵CC³⁰CKK³⁵P⁴⁰</p>	Schröder & Harder (1999)
Histatin 5	Salivary histatin	Human	<p>DSHAKRHHGYK⁵RRKFHEKHH¹⁰SHRGY¹⁵</p>	Troxler et al. (1990)

The second class of peptides, the cathelicidins, are mammalian antimicrobial peptides. They were originally grouped based on the presence of an N-terminal prosequence which has high homology to the bovine peptide cathelin. The precursor protein is expressed with the cathelin-like domain, which is then cleaved off leaving a mature, cationic antimicrobial peptide (Figure 2.2A) (Zanetti, 2004). The precursor of the cathelicidin peptide Bac5 is stored in bovine neutrophil granules and is released and processed to the mature peptide upon infection or inflammation (Scocchi et al., 1992; Zanetti, 2004; Zanetti et al., 1991). Mature cathelicidin peptides are highly variable in length and structure (Figure 2.2B and C) (Ramanathan et al., 2002; Zanetti, 2004). Three cathelicidin peptides were tested in this study, the bovine peptides BMAP-28 and bactenecin and a synthetic variant of bactenecin called Bac2a. Bactenecin is a 12 amino acid cathelicidin with a loop structure held in place by a single disulphide bond. It is produced by bovine neutrophils and is primarily active against gram-negative bacteria including: *Escherichia coli*, *Pseudomonas aeruginosa* and *Salmonella typhimurium* (Wu & Hancock, 1999b). A derivative of bactenecin, called Bac2a, is a synthetic linearised form of bactenecin which has acquired activity against gram-positive bacteria (Wu & Hancock, 1999a). The antifungal activity of these two peptides has not been reported apart from the observation that Bac2a permeabilises membranes of *Fov in vitro* (van der Weerden et al., 2010). BMAP-28 is another cathelicidin from cows which forms an amphipathic α -helical structure. It is active against several gram-positive and gram-negative bacteria, as well as *C. albicans*, *C. neoformans* and *Fov* (Skerlavaj et al., 1996; van der Weerden et al., 2010).

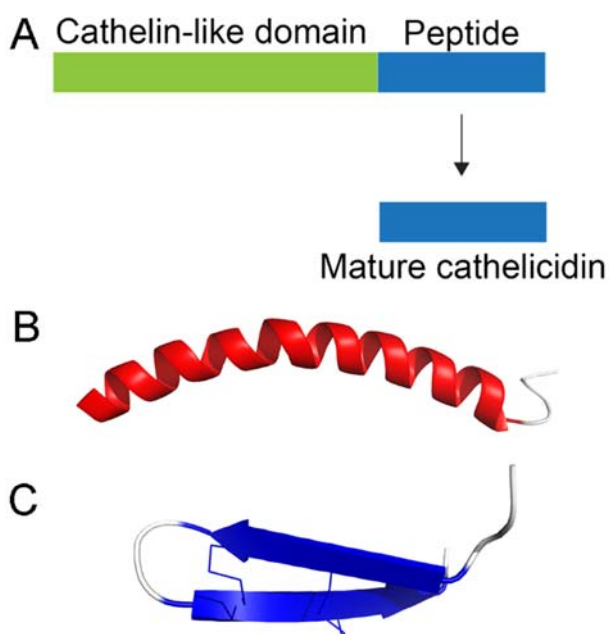


Figure 2.2 Cathelicidin processing and structure

(A) The cathelicidin precursor protein consists of a cathelin-like domain and a cathelicidin peptide sequence. This precursor protein is processed to the mature cathelicidin peptide. The three-dimensional solution structure of (B) the human cathelicidin LL-37 (PDB: 2K60) (Wang, 2008) and (C) the pig cathelicidin protegrin 1 (PDB: 1PG1) (Fahrner et al., 1996) are also shown.

The peptide CP29 is a synthetic 26 amino acid α -helical peptide produced by combining the N-terminal region of the silkworm antibacterial peptide cecropin A with the N-terminal α -helix of the bee venom peptide, melittin. This peptide permeabilises bacterial membranes (Friedrich et al., 2000). It also inhibits the growth of the fungal plant pathogen *Fov* and rapidly permeabilises the fungal membrane (van der Weerden et al., 2010). Its activity on human pathogens has not been investigated.

Human beta-defensin 2 (hβD2) is produced by human epithelial cells (Ganz, 2003). It consists of a triple-stranded anti-parallel β-sheet and three disulphide bonds (Figure 2.3). Human defensins are primarily antibacterial and are part of the human innate immune response (Ganz, 2003; Schröder & Harder, 1999). However, antifungal activity has been reported for hβD2 against several *Candida* species and *A. fumigatus* (Feng et al., 2005; Okamoto et al., 2004). Up-regulation of hβD2 mRNA has also been observed in response to treatment of a human keratinocyte cell line with *T. rubrum* or *C. albicans* and cultured human bronchial epithelial cells with *A. fumigatus* (Alekseeva et al., 2009; Ishikawa et al., 2009).

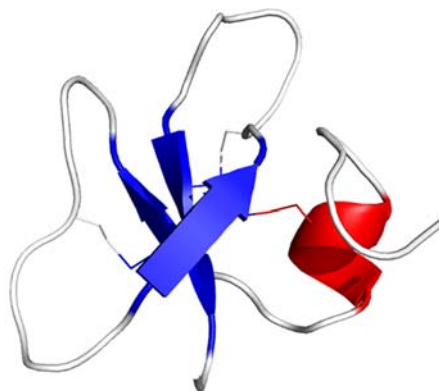


Figure 2.3 The structure of hβD2

The three-dimensional structure of human β-defensin 2 (PDB: 1FQQ) (Sawai et al., 2001).

The last peptide, histatin 5, is a cationic, histidine-rich protein which is present in human saliva. It is 24 amino acids long (3 kDa) and is produced after cleavage of the 4 kDa histatin 3 protein (Figure 2.4) (Oppenheirn et al., 1988; Perinpanayagam et al., 1995; Sabatini & Azen, 1989; Troxler et al., 1990). Histatin 5 kills the yeast *C. albicans* and does so with a lower lethal dose concentration than histatin 3 (LD₅₀'s of 1.8 μM and 9.2 μM, respectively) (Edgerton et al., 1998; Xu et al., 1991). Histatin 5's mechanism of action has been well studied in *C. albicans* (Edgerton et al., 1998; Helmerhorst et al., 1999; Koshlukova et al., 1999; Vylkova et al., 2007).



Figure 2.4 The amino acid sequences of histatin 3 and histatin 5

The 24 amino acid peptide histatin 5 is produced from histatin 3. The amino acid sequence corresponding to histatin 5 is in blue. The cleavage site is represented by an arrow.

As part of the research for this Chapter, I also determined whether NaD1 can act synergistically with other antimicrobial peptides and proteinase inhibitors against human pathogens. This was initiated due to observations of synergy between NaD1 and several proteinase inhibitors and chemical fungicides against plant fungal pathogens (Anderson et al., 2009; McKenna, 2012). Synergy describes the phenomena where the combined effect of two molecules is greater than the expected effect if their individual activities are simply added. For example, the combination of 0.5 μM NaD1 and 3 μM of the protease inhibitor bovine pancreatic trypsin inhibitor (BPTI) resulted in much greater growth inhibition of *F. graminearum* than was expected by adding the growth inhibition observed by those concentrations of each peptide alone (McKenna, 2012). Synergy values (or inhibition differences) were calculated using Limpel's Formula, which is described in Section 2.2.9.

NaD1 synergy with human and mammalian AMPs has not been investigated and may prove to be a viable method to increase killing of human fungal pathogens. Synergy may also reduce the development of resistance through utilisation of antifungal peptides with differing mechanisms of action.

2.2 Materials and Methods

2.2.1 NaD1 extraction from *N. alata* flowers

2.2.1.1 Acid extraction and heat treatment

N. alata flowers were collected and subjected to acid extraction, essentially as described by van der Weerden et al, (2008). The flowers were ground to a fine powder using liquid nitrogen and a mortar and pestle before sulphuric acid (50 mM, 4 mL/ g of fresh flowers) was added. The mixture was then homogenised further in an Ultra-Turrax homogenizer for 5 min, before it was stirred for 1 h at 4°C. The mixture was filtered through Miracloth (Merck Millipore) and clarified by centrifugation at 25,000 × g (15 min, 4°C). The supernatant was adjusted to pH 7.0 with 5 M NaOH and was stirred overnight at 4°C. Insoluble material was then removed by centrifugation at 25,000 × g for 15 min (4°C). The supernatant was boiled for 10 min, allowed to cool to room temperature and centrifuged (25,000 × g, 15 min, 4°C). The supernatant was adjusted to pH 6.0 with 1 M HCl and buffered with 1 M potassium phosphate buffer (pH 6.0) to a final concentration of 10 mM before ion exchange chromatography on SP-Sepharose.

2.2.1.2 Cation exchange chromatography on SP-Sepharose

The extract from the *N. alata* flowers was applied to an SP-Sepharose cation exchange column (approximately 5 mL bead volume/ L of extract, GE healthcare) that had been equilibrated with 10 mM phosphate buffer (pH 6.0, 20 column volumes). Unbound proteins were removed by washing with the same buffer. Bound proteins were eluted with 10 mM potassium phosphate buffer (pH 6.0) containing 500 mM NaCl. Ten fractions of approximately 8 mL were collected. The presence of protein in the elution fractions was confirmed using Coomassie Blue. Fractions (30 µL) were spotted onto blotting paper (Whatman, 3 mm), which was immersed in Coomassie Blue (0.2% w/v Coomassie Brilliant Blue R-250 in 20% ethanol and 7% acetic acid, Sigma). The blotting paper was destained in water.

2.2.1.3 Reversed-phase high performance liquid chromatography

RP-HPLC was performed using a 1200 series HPLC (Agilent Technologies) fitted with a semi-prep column (Zorbax 300SB-C8, 4.6 × 150 mm, flow rate of 1 mL/min, Agilent Technologies). The sample was loaded in 100% buffer A (0.1% trifluoroacetic acid) and proteins were eluted using a 40 min linear gradient from 0–100% buffer B (60% acetonitrile, 0.089% trifluoroacetic acid). Proteins were detected by monitoring absorbance at 215 nm. The collected proteins were lyophilised (Dynamac FD5 freeze dryer) and dissolved in 200 µL of sterile milliQ water. Protein concentration was determined using a bicinchoninic acid (BCA) protein assay (Pierce) with BSA as the standard protein.

2.2.2 Expression of histatin 5 in *Rosetta gami* cells

2.2.2.1 Incorporation of DNA encoding histatin 5 into pHUE plasmid

Primers were designed for amplification of DNA encoding histatin 5 and insertion into the pHUE plasmid (Catanzariti et al., 2004) using a modified site-directed mutagenesis by inverse PCR protocol (originally described in Hemsley et al. (1989)). As the histatin 5 coding sequence is relatively short, primers were designed that included the histatin 5 sequence, so that the entire pHUE plasmid could be amplified and the histatin 5 coding sequence could be incorporated into the vector in a single PCR (Figure 2.5). Each primer consisted of 15 bases homologous to the pHUE plasmid (either side of the MCS) and half of the histatin 5 sequence (37 bases in primer 1, 38 bases in primer 2). Care was taken to ensure that the histatin 5 coding sequence was in frame with the DNA encoding ubiquitin and the *SacI* cleavage site. Each primer also contained a 5' phosphate for ligation of the linear plasmid into a circular plasmid after PCR (Figure 2.5).

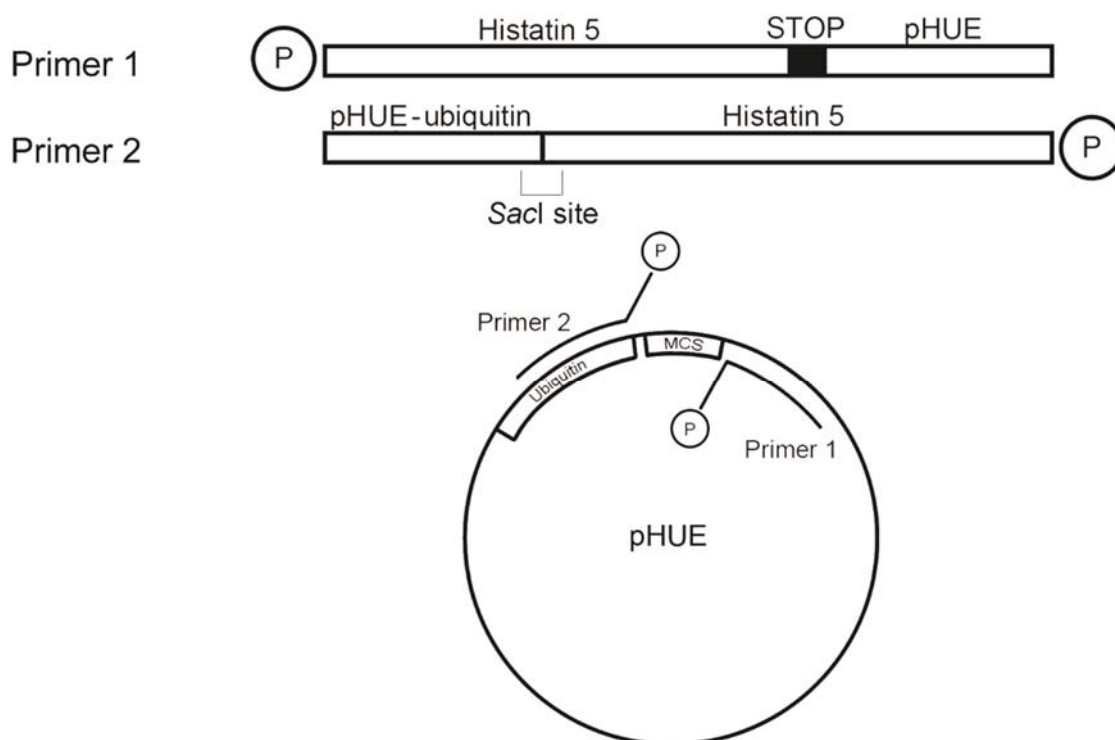


Figure 2.5 Primer design for incorporation of the histatin 5 coding sequence into the pHUE plasmid

Each primer was designed to contain 15 bases homologous to the pHUE plasmid and half the sequence encoding histatin 5 (37 or 38 bases). Five prime phosphates were included in the primers to facilitate cyclisation of the linear pHUE plasmid after PCR.

The primer sequences were as follows:

Primer 1 ATTCCATGAAAAGCATCATTACATCGAGGCTATTGAGAGCTCGGTACCGTC

Primer 2 TTTCTTTTATACCCATGATGTCTCTTTGCATGTGAATCTCCACCGCGGAGGGCG

Underlined sections are homologous to the pHUE multiple cloning site. The section in bold represents the *SacI* restriction enzyme site.

PCR was performed with Phusion polymerase. Reactions contained 2× Phusion master mix (Thermo Fisher), 2 µL of 10 µM primers (1 and 2), 10 ng of pHUE plasmid template (purified from *E. coli* XL1-Blue cells using the Wizard Plus SV miniprep DNA Purification kit, Promega) and water to a total volume of 50 µL. The PCR conditions were 98°C for 5 min, 30 cycles of 98°C for 30 sec, 66°C for 1 min and 72°C for 3 min, and then 72°C for 10 min. Amplified DNA was separated on a 1% agarose gel and DNA of the appropriate size was excised and purified using a Wizard SV PCR purification kit (Promega) according

to the manufacturer's instructions. Amplified linear product (12 μ L) was circularised by incubating at 4°C overnight with 3 μ L of T4 ligase (New England Biolabs) and 3 μ L of T4 ligase buffer (New England Biolabs). This ligation mix was used for transformation of *Rosetta gami* cells.

2.2.2.2 Transformation of pHUE-histatin 5 into Rosetta gami B cells

The plasmid was transformed into *Rosetta gami* cells by adding 4 μ L of the ligation mixture (Section 2.2.2.1) to 20 μ L cells in a 1.5 mL Eppendorf tube and incubating on ice for 30 min. The cells were heat shocked at 42°C for 30 sec and then immediately placed on ice. Luria Bertani (LB) broth (250 μ L) was then added and the cells were allowed to recover during shaking for 1 h at 37°C. Cells (approximately 100 μ L) were plated onto agar containing kanamycin (15 μ g/mL), chloramphenicol (34 μ g/mL), ampicillin (50 μ g/mL) and tetracycline (10 μ g/mL) and incubated overnight at 37°C.

Colonies with the correct insert were identified by PCR. A scraping from each colony was placed in a reaction mix containing 12.5 μ L 2 \times GoTaq master mix (Promega), 4 μ L of 10 μ M Fw (5' GGCCGCACTCTCTCAGACTAC) and Rv (5' CTCAAGACCCGTTTAG AGG) primers and water to 25 μ L. The PCR conditions were 94°C for 5 min, 20 cycles of 94°C for 30 sec, 46°C for 30sec and 72°C for 1 min, followed by 72°C for 5 min. Amplified DNA was separated on a 1.2% agarose gel. Plasmid DNA from colonies which were PCR positive was also sent for sequencing. Plasmids were purified from overnight cultures (5 mL LB with 50 μ g/mL ampicillin, 37°C) using the Wizard Plus SV miniprep DNA Purification kit (Promega) and were sequenced by the Australian Genomic Research Facility (AGRF, Melbourne, Australia) using the Fw and Rv primers from above.

2.2.2.3 Expression of histatin 5

Histatin 5 was expressed in *Rosetta gami* B cells essentially as described in the QIAexpressionest manual (Qiagen, 2003). A *Rosetta gami* B colony transformed with pHUE-histatin 5 was used to inoculate 5 mL of 2 \times yeast tryptone (2YT) broth containing kanamycin, chloramphenicol, ampicillin and tetracycline (concentrations as in Section 2.2.2.2). Cultures were incubated at 37°C, overnight with constant shaking (180 rpm) and were then used to inoculate 2 \times 500 mL 2YT (with antibiotics) in 2 L baffled flasks. Cultures were grown at 37°C with constant shaking (180 rpm) until they reached an OD₆₀₀

of 0.6-0.8. Cells were then induced with 0.5 mM IPTG and were grown for a further 3 h. Cells were collected by centrifugation (13,000 rpm, 10 min, 4°C) and the pellet was resuspended in lysis buffer (50 mM Tris-HCl pH 8.0, 300 mM NaCl and 10 mM imidazole, 25 mL/L) before being frozen at -80°C overnight. Cells were thawed and sonicated on ice (3× 1 min, with 2 min intervals). The sample was then centrifuged at 12,000 rpm for 15 min and the supernatant was transferred to a new tube. The supernatant was added to 4 mL of pre-equilibrated Ni-NTA beads (Amintra) in a 50 mL tube and placed on a circular mixer at room temperature for 30 min. The beads were then transferred to a column and were washed with 10 column volumes of lysis buffer followed by 10 column volumes of wash buffer (100 mM Tris-HCl pH 8.0, 600 mM NaCl and 40 mM imidazole). Proteins were eluted at room temperature in four column volumes of elution buffer over 20 min (100 mM Tris-HCl pH 8.0, 600 mM NaCl and 500 mM imidazole). The eluate was collected in 1 mL aliquots and checked for protein using Coomassie Blue (See Section 2.2.1.2). Fractions with protein were pooled and dialysed against dialysis buffer (50 mM Tris-HCl pH 8.0, 300 mM NaCl, 500 mL) for 20 h at 4°C with 3,500 MWCO tubing (Spectrum laboratories). Fresh dialysis buffer was added after 16 h. The protein was cleaved from the His-Ubiquitin tag by addition of 1 mM DTT together with 100 µg of Usp2-cc enzyme (Baker et al., 2005) followed by incubation on a circular mixer for 3 h at RT. The histatin 5 was purified away from His-Ubiquitin using a RP-HPLC (1200 series HPLC, ZORBAX 300SB-C8 column, flow rate 3 ml/min, Agilent Technologies) with a 40 min linear gradient of 0–100% buffer B (60% acetonitrile, 0.089% trifluoroacetic acid). The collected proteins were lyophilised (Dynavac FD5 freeze dryer) and dissolved in sterile milliQ water. Protein concentration was determined using a bicinchoninic acid (BCA) protein assay (Pierce) with BSA as the standard protein.

2.2.3 Source of the other antimicrobial peptide stocks

The peptides bactenecin, Bac2a, CP29 and BMAP-28 were synthesised by GL Biochem (Shanghai) or GenScript (USA). Their sequences are as follows:

Bactenecin (RLCRIVVIRVCR)	(Wu & Hancock, 1999b)
Bac2a (RLARIVVIRVAR)	(Wu & Hancock, 1999a)
CP29 (KWKSFIKKLTTAVKKVLTGLPALIS)	(Friedrich et al., 2000)
BMAP-28 (GGLRSLGRKILRAWKKYGPIIVPIIRI)	(Skerlavaj et al., 1996)

NaD2 was purified from *N. alata* flowers as described in Section 2.2.1. NaCys2 was expressed using the pHUE system by Dr Simon Poon (La Trobe University). BPTI was purchased from Amresco. HXP4 was created by Dr Nicole van der Weerden (La Trobe University) using mutagenesis and was expressed in *Pichia pastoris* GS115 (Life Technologies). The human β -defensin 2 and DmAMP1 coding sequences were ordered from GenScript and were also expressed in the *Pichia* system.

2.2.3.1 Protein expression in *Pichia pastoris*

DNA fragments encoding HXP4 and DmAMP1 were purchased from GenScript (Piscataway, NJ, USA) for insertion into the pPIC9 vector (Life Technologies) via *NotI* and *XhoI* restriction sites. The ligated pPIC9 vector was transformed into electrocompetent *P. pastoris* GS115 cells (Life Technologies). The pPIC9 vector, *Pichia* transformation and expression are described in the *Pichia* expression kit user manual (Invitrogen, 2010).

For expression of protein, 25 mL of buffered minimal glycerol (BMG, 100 mM potassium phosphate pH 6.0, 1.34% yeast nitrogen base, 5% biotin and 1% glycerol) in a 250 mL flask was inoculated with a scraping of cells from a glycerol stock and incubated overnight at 30°C. This 25 mL culture was then used to inoculate 200 mL of BMG in a 1 L baffled flask, prior to another overnight incubation at 30°C. Cells were collected by centrifugation at 1500 \times g (10 min) and were resuspended in 800 mL of buffered minimal methanol (BMM, 100 mM potassium phosphate pH 6.0, 1.34% yeast nitrogen base, 5% biotin and 0.5% methanol). The culture was divided into two 2 L baffled flasks and the incubation was continued for 48 h at 28°C, with the addition of 2 mL of 100% methanol after 24 h. After 48 h, the culture was centrifuged for 15 min at 10,000 rpm and the supernatant was collected. The supernatant (~ 800 mL) was diluted two-fold with milliQ water and adjusted to pH 6.0 with 5 M KOH, before all the diluted supernatant was subjected to cation exchange chromatography on an SP-Sepharose column (10 mL bead volume, GE Healthcare). For the cation exchange chromatography method see Section 2.2.1.2. Following cation exchange chromatography, fractions containing protein were subjected to analysis by SDS-PAGE and RP-HPLC (see Section 2.2.1.3). Protein concentration was determined using a BCA protein assay (Pierce).

2.2.4 Fungal strains

2.2.4.1 Filamentous fungi

A. niger (5181), *A. flavus* (2001, 5310, and 5311) and *Aspergillus paraciticus* (4467, 4469, 4470) spores (kind gift from Associate Professor Dee Carter, University of Sydney) were grown on half-strength potato dextrose agar plates (PDA, Becton Dickson) for 14 days.

2.2.4.2 Yeast

Cryptococcus gattii (WM276, R265 and Bal 11) and *C. neoformans* (JEC20, JEC21 and H99) strains (kind gift from Associate Professor Dee Carter, University of Sydney) were obtained from glycerol stocks and were grown in yeast peptone dextrose (YPD) medium for 24 h at 30°C. *C. albicans* DAY185 (kind gift from Dr Ana Traven, Monash University) (Davis et al., 2000) was streaked onto YPD agar from a glycerol stock. A scraping was then taken from plates and added to YPD broth. Overnight cultures were incubated at 30°C (250 rpm).

2.2.5 Fungal growth inhibition assays

Growth inhibition assays were performed essentially as described in Broekaert et al. (1990).

For *Aspergillus* assays, spores were collected by flooding plates with 20 mL of half-strength potato dextrose broth (PDB, Becton Dickinson). This spore suspension was removed from the plate and centrifuged at 14,000 rpm for 15 min to collect the spores. The spores were resuspended in approximately 1 mL of half-strength PDB and counted using a haemocytometer. Spores were then diluted to a final concentration of 5×10^4 spores/mL in half-strength PDB. For *Cryptococcus* growth inhibition assays, cells (20 μ L) were counted with a haemocytometer and diluted to 1.5×10^6 cells/mL in half-strength PDB. For *C. albicans* inhibition assays, cells (20 μ L) were counted with a haemocytometer and diluted to 5×10^3 cells/mL in half-strength PDB.

Test proteins were serially diluted, to a final volume of 20 μL and added to the wells of a 96 well microtitre plate (Greiner) by a TECAN Evo100 liquid handling robot in triplicate (three wells on one plate) before diluted spores or cells (80 μL) were added to the wells. Growth was monitored by measuring absorbance at 595 nm, in a SpectraMAX M5e plate reader (Molecular Devices), using the 9 well-scan. Measurements were taken before and after 24 h incubation at 25°C for *Aspergillus* and 30°C for *Candida* and *Cryptococcus*. For NaD1 activity against *C. albicans* at 37°C, plates were prepared as above, but were incubated at 37°C for 24 h before absorbance at 595 nm was measured. The *C. albicans* DAY185 strain was used when testing the activity of NaD1 in serum. Protein (10 μL) was added to 10 μL of fetal calf serum (FCS, 50 % in half-strength PDB) and added to 80 μL of cells (5×10^3 cells/mL in half-strength PDB) to give a final concentration of 5 % serum. The *C. albicans* DAY185 strain was also used when testing NaD1's activity in different media. The cells were grown overnight in YPD (5 mL, 30°C) and then diluted to 5×10^3 cells/mL in half-strength PDB, full-strength PDB or YPD media. Cells (80 μL) were then added to 20 μL of the test protein in a microtitre plate and incubated overnight at 30°C before measuring the optical density at 595 nm.

The effect of bovine serum albumin (BSA) on the activity of CP29 was tested by serial dilution of 10 μL of CP29 down a 96 well microtitre plate, with a top final concentration of 10 μM CP29. BSA (10 mg/mL, Promega) was added to give final concentrations of 0, 0.25, 0.5 or 1 $\mu\text{g}/\mu\text{L}$ (10 μL added per well). *C. albicans* DAY185 (80 μL , 5000 cells/mL) was then added and plates were incubated overnight at 30°C.

The effect of Mg^{2+} and Ca^{2+} on the activity of NaD1 was tested by adding 10 μL of magnesium chloride (MgCl_2) or calcium chloride (CaCl_2) to a microtitre plate (Greiner) to a top final concentration of 1 mM or 10 mM. NaD1 (50 μM , 10 μL) and 80 μL of *C. albicans* (5×10^3 cells/mL) were added. The plate was incubated overnight at 30°C before absorbance was measured at 595 nm.

2.2.6 *C. albicans* growth curve in half-strength PDB

For the *C. albicans* growth curve, an overnight culture of DAY185 was diluted to an OD₆₀₀ of 0.2 with half-strength PDB. Cells were then incubated at 30°C (250 rpm) and OD₆₀₀ was measured every hour. The doubling time of the DAY185 cells was calculated using the formula:

$$\frac{\ln 2 \times t}{\ln b - \ln a}$$

t = time (hours)

a = optical density at beginning of time period

b = optical density at end of time period

(Rieg et al., 1999)

2.2.7 *C. albicans* survival assays

C. albicans DAY185 overnight cultures were diluted to an OD₆₀₀ of 0.3 in half-strength PDB and incubated for 5 h (30°C, 250 rpm). After incubation the cells were diluted to an OD₆₀₀ of 1.0. Cells were then treated with NaD1 (2, 3.5, 5, 10, 20 or 50 µM) for 15 min, 30 min or 1 h (30°C, 250 rpm). Each treatment was diluted 1/1000 and 1/10,000 in sterile milliQ water and 20 µL of each dilution was placed on YPD agar (four treatments per plate). Plates were then tilted to allow the drop to spread down the plate. Colonies were counted after incubation overnight at 30°C. Each count was multiplied by the dilution factor and compared to a no-treatment control.

2.2.8 Permeabilisation kinetics (SYTOX) assay

Permeabilisation assays were performed essentially as described in van der Weerden et al. (2010). *C. albicans* DAY185 cells were grown overnight in 5 mL of YPD (250 rpm, 30°C). Cells were then diluted to an OD₆₀₀ of 0.4 with half-strength PDB. SYTOX green (2 µL of a 5 mM stock, Life Technologies) was added to 10 mL of the diluted *C. albicans* cells. The test proteins (10 µL of 20 µM or 0 µM) were added to the wells of a black, flat-bottomed, 96 well microtitre plate (Nunc) in triplicate. The cell and SYTOX mixture (90 µL) was added to the plate just prior to measurement of fluorescence every 2 min for 3 h with excitation at 488 nm and emission at 538 nm. The kinetics run was performed in a SpectraMAX M5e plate reader (Molecular Devices).

2.2.9 Synergy assays

Antifungal assays were used to determine if there was synergistic action between NaD1 and various antimicrobial peptides, protease inhibitors and amphotericin B (Sigma). The assay was performed as described by Anderson et al. (2009). Spores and yeast cells were prepared as in Section 2.2.5. Assays were performed in 96 well microtitre plates (Greiner) and dilutions were prepared using a TECAN Evo100 liquid handling robot. NaD1 (10 μ L of a 10 \times stock) was serially diluted four times down a microtitre plate. A second test protein (10 μ L of a 10 \times stock) was serially diluted six times across the plate (Figure 2.6). The final protein volume after addition of both NaD1 and the test protein was 20 μ L. The top concentration of NaD1 and the protein of interest that was used differed depending on the pathogen, and were chosen based on the IC₅₀ of the individual proteins against each pathogen.

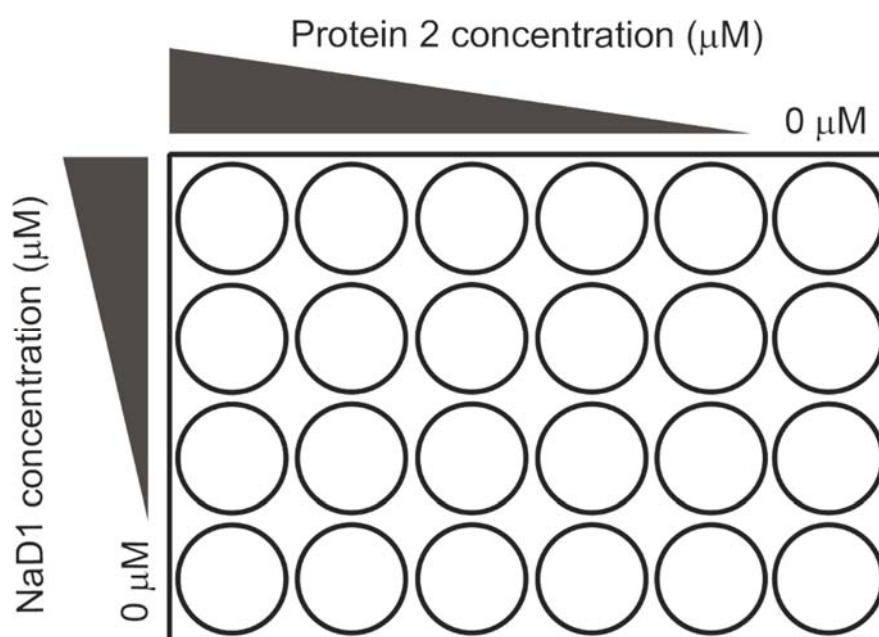


Figure 2.6 Protein dilutions for synergy assays

Synergy assays were performed in 96 well microtitre plates. NaD1 was serially diluted down the plate and a test protein was diluted across the plate. Each well contained the two proteins, protein and water or water only.

Fungi (80 μ L in half-strength PDB) were added to the plates. The following cell concentrations were used: *Aspergillus* spores (5×10^4 spores/mL), *Cryptococcus* cells (1.5×10^6 cells/mL) or *C. albicans* cells (5000 cells/mL). The plates were incubated for 24 h at 25°C for *Aspergillus* and at 30°C for yeast and fungal growth was determined by measuring absorbance at 595 nm (SpectraMAX M5e plate reader, Molecular Devices). Synergy was calculated using Limpel's formula (Richer, 1987).

Limpel's Formula:

$$Ee = x + y - \left(\frac{xy}{100}\right)$$

Ee = expected inhibition

x = inhibition by protein 1

y = inhibition by protein 2

Synergy is defined as the difference between the expected (*Ee*) and observed (*Io*) inhibitions.

$$\text{Inhibition difference (ID)} = Io - Ee$$

Synergy has occurred when the observed inhibition of fungal growth is greater than the expected growth if the antifungal activities of individual proteins were working additively.

The level of synergy observed was further divided into no synergy, low, medium, high and very high synergy categories as a method of comparison (Table 2.2).

Table 2.2 Levels of synergy

Inhibition difference (*Io*-*Ee*) and the corresponding levels of synergy (McKenna, 2012).

Inhibition difference (ID)	Level of synergy
0-14	No synergy or very low synergy
15-30	Low synergy
31-45	Medium synergy
46-80	High synergy
80-100	Very high synergy

2.3 Results

2.3.1 NaD1 activity against *C. albicans*

NaD1 was tested against *C. albicans* in a range of media to determine whether it inhibits growth. NaD1 had substantial antifungal activity against the pathogen in half-strength PDB and PDB, but was not active in YPD, a high nutrient medium (Figure 2.7).

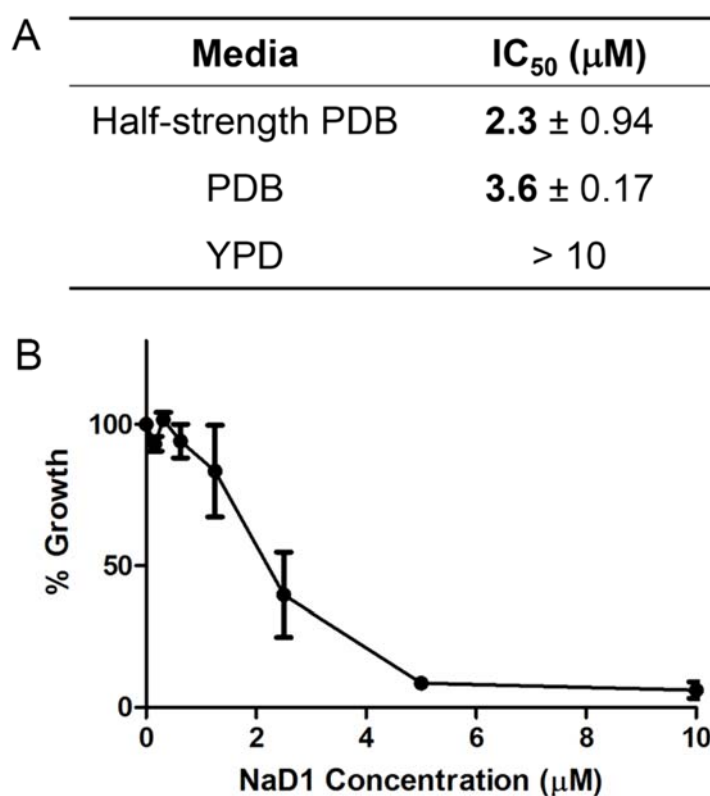


Figure 2.7 The growth of *C. albicans* DAY185 in different media

(A) IC₅₀ values ± SD (from at least three biological replicates) for the activity of NaD1 against *C. albicans* DAY185 after fungal inhibition assays were performed in half-strength PDB, full-strength PDB and YPD. (B) Growth inhibition of DAY185 by NaD1 in half-strength PDB. Data is relative to a no-protein control. Error bars represent SEM (n=6).

C. albicans had a doubling time of 2.13 hours (SEM 0.66, n=3) in half-strength PDB. A growth curve of DAY185 in half-strength PDB is shown in Figure 2.8. All subsequent growth inhibition assays were performed with half-strength PDB.

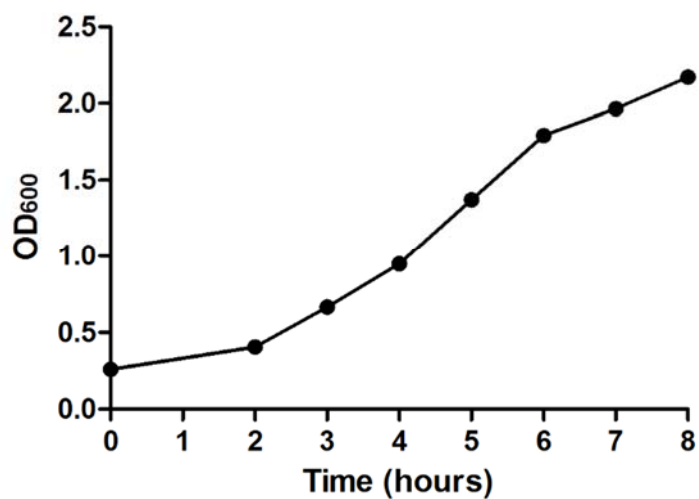


Figure 2.8 The growth of *C. albicans* DAY185 over six hours in half-strength PDB

DAY185 has a doubling time of approximately 2 h when grown in half-strength PDB. Data is a representative example from three independent experiments.

Yeast cell survival assays were conducted to determine whether NaD1 is fungicidal or fungistatic. *C. albicans* DAY185 cells were incubated with varying concentrations of NaD1 for 15 min, 30 min or 60 min before plating onto YPD agar. There was a significant reduction in the number of viable cells at all three time points, indicating that NaD1 is fungicidal. The level of cell death was dependent on NaD1 concentration. The length of incubation had no significant effect on the amount of cell death (Figure 2.9).

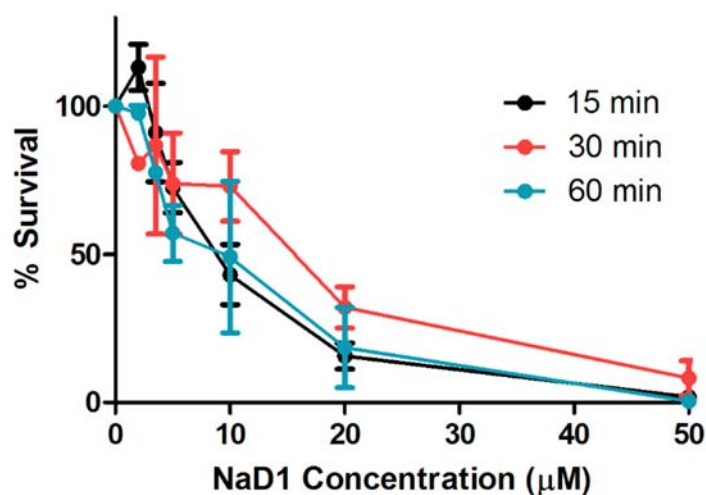


Figure 2.9 The survival of *C. albicans* DAY185 after treatment with NaD1

Percentage of *C. albicans* DAY185 cells surviving after exposure to various concentrations of NaD1 for 15 min, 30 min or 60 min. Data is relative to a no-protein control. Error bars represent SEM (n=3).

2.3.2 Effect of antimicrobial peptides on the growth of *C. albicans* DAY185

Five additional antimicrobial peptides were screened for activity against *C. albicans* DAY185 cells. NaD1, HXP4 and Bac2a were the most effective at inhibiting the growth of *C. albicans* DAY185, with IC_{50} 's of 2 μ M for all three peptides. CP29 and bactenecin had less activity, with IC_{50} values of 3.9 μ M and 3.2 μ M, respectively. BMAP-28 was the least effective peptide with an IC_{50} value of 8.8 μ M.

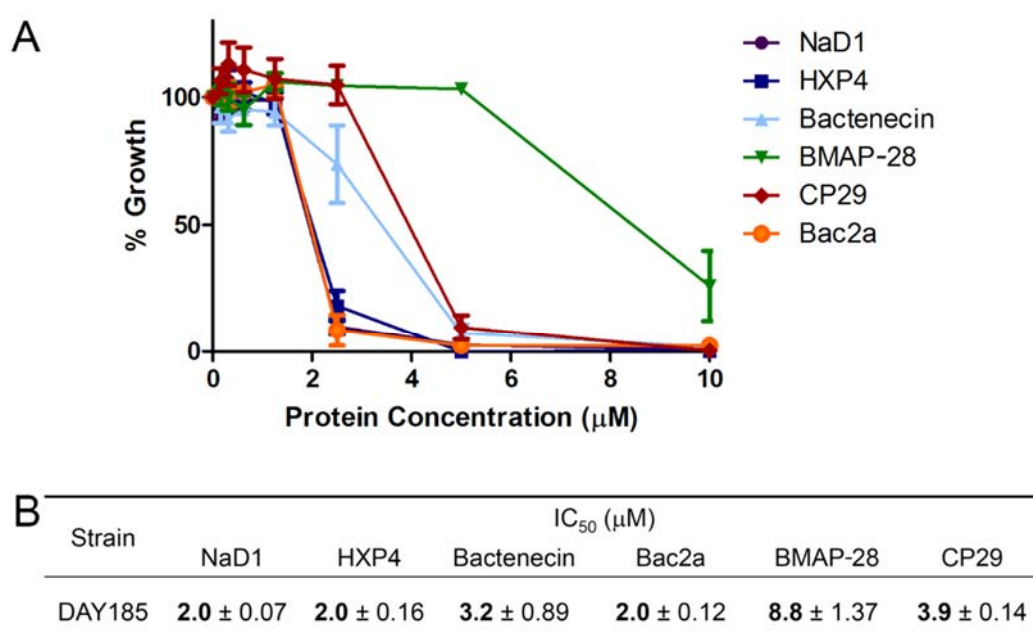


Figure 2.10 The effect of NaD1, HXP4, bactenecin, Bac2a, BMAP-28 and CP29 on the growth of *C. albicans*

(A) Growth inhibition of DAY185 cells in the presence of various concentrations of the antimicrobial peptides NaD1 (—●—), HXP4 (—■—), bactenecin (—▲—), Bac2a (—▼—), BMAP-28 (—◆—) and CP29 (—◇—). Data is shown relative to a no-protein control. Error bars represent SEM (n=4). (B) The IC_{50} for each peptide is in bold ± standard deviation (n=4).

2.3.3 Effect of temperature on the activity of NaD1 against *C. albicans*

The growth inhibitory activity of NaD1 against *C. albicans* DAY185 at 37°C was compared to growth at 30°C. NaD1 had a similar effect on growth at both these temperatures (Figure 2.11).

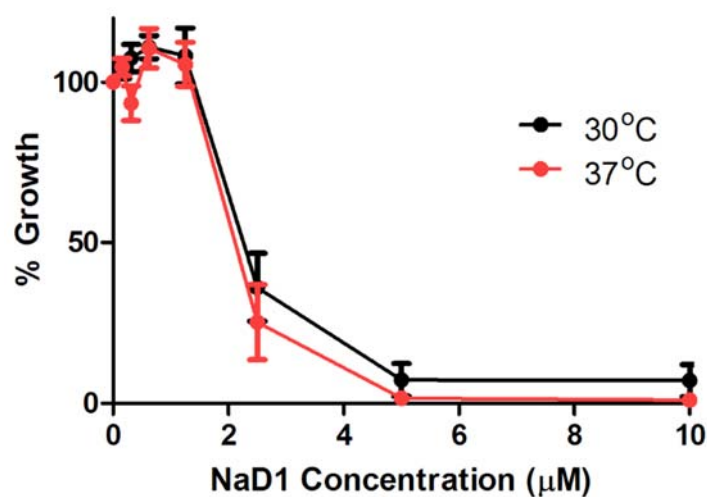


Figure 2.11 The activity of NaD1 against *C. albicans* DAY185 at 30°C and 37°C

NaD1 was added to DAY185 in half-strength PDB and the cells were grown at 30°C or 37°C. NaD1 was equally effective at both temperatures. Data is relative to a no-protein control. Error bars represent SEM (n=3).

2.3.4 Effect of Mg^{2+} and Ca^{2+} on NaD1's activity against *C. albicans*

The growth inhibitory activity of NaD1 against plant pathogens is negatively impacted by divalent cations, with Ca^{2+} being more effective at blocking growth inhibition than Mg^{2+} (van der Weerden, 2007). This led to the question of whether divalent cations also diminish the activity of NaD1 against *C. albicans*. The complete growth inhibition obtained with 5 μ M NaD1 in the absence of divalent cations was abolished by 1 mM Ca^{2+} and 10 mM Mg^{2+} (Figure 2.12).

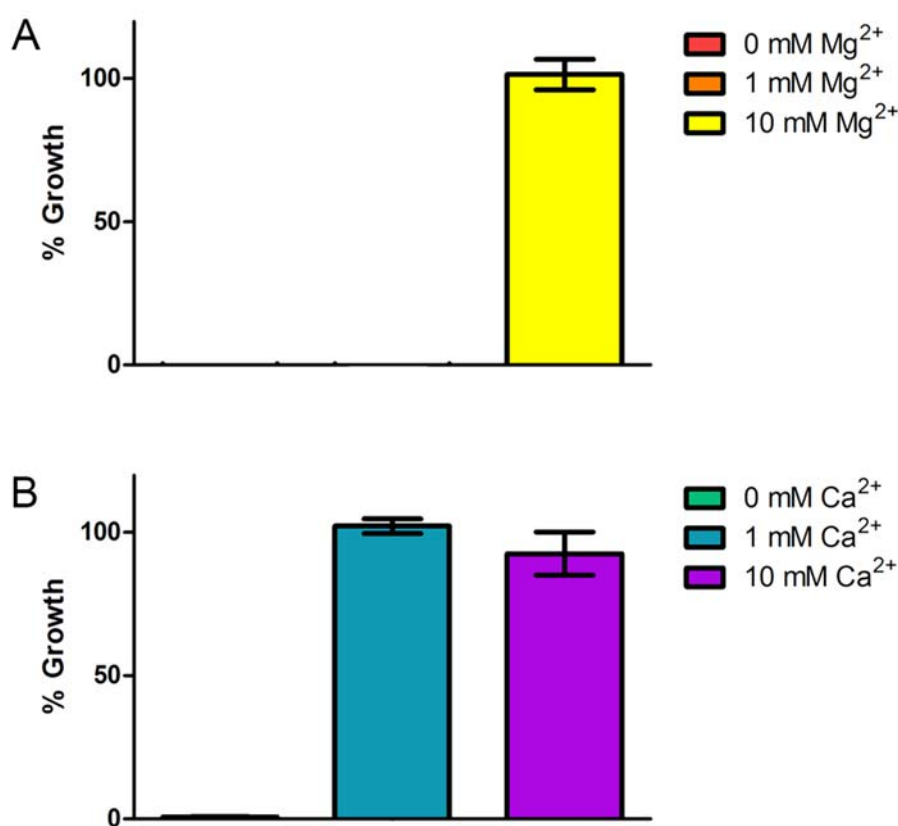


Figure 2.12 The effect of Mg^{2+} and Ca^{2+} on the activity of NaD1 against *C. albicans*

C. albicans DAY185 was treated with 5 μ M NaD1 in the presence and absence of (A) Mg^{2+} or (B) Ca^{2+} .

Data are shown as percentage growth relative to no-NaD1 controls. Error bars represent SEM (n=3).

2.3.5 Kinetics of *C. albicans* permeabilisation by NaD1

The rate at which NaD1 permeabilises the plasma membrane of *C. albicans* was observed using SYTOX green, which fluoresces in the presence of nucleic acids. Thus, it only fluoresces when it has entered cells when the plasma membrane has been compromised. The fluorescence emission from SYTOX green was monitored over a 3 h time period after addition of the fluorophore and the test proteins to *C. albicans* cells. The peptides CP29 and BMAP-28 were included as positive controls as they rapidly permeabilise the plasma membrane. Addition of these peptides to the cells led to a rapid increase in SYTOX green fluorescence (Figure 2.13). In contrast, NaD1 induced membrane permeabilisation was slower, and only began after a 40 min delay (Figure 2.13).

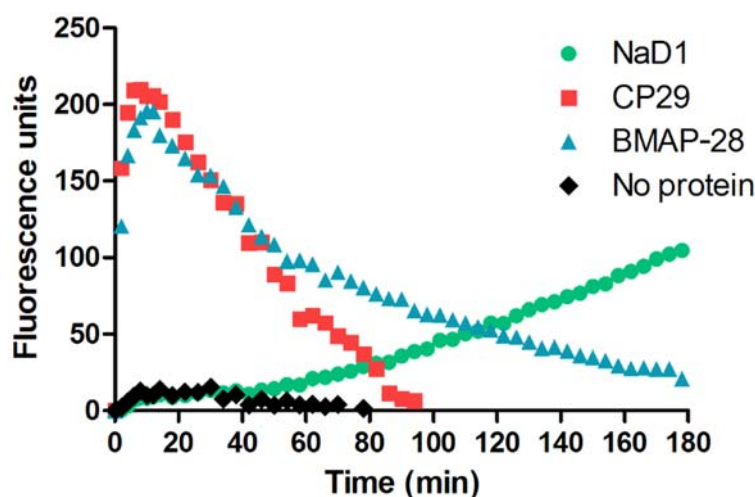


Figure 2.13 The rate of permeabilisation of the plasma membrane of *C. albicans* by NaD1, CP29 and BMAP-28

C. albicans DAY185 cells were treated with 20 μ M NaD1, CP29 or BMAP-28 in the presence of the nucleic acid binding dye SYTOX green. The increase in fluorescence is related to membrane permeabilisation and SYTOX green entry into the cell. A no-protein control was included for comparison. Fluorescence was monitored over 3 h with reads every 2 min. Data are shown relative to the $t=0$ reading. Data are a representative example of three independent experiments.

2.3.6 The effect of serum on the activity of antifungal peptides against *C. albicans*

The inhibitory activity of some antimicrobial peptides is reduced in the presence of serum (Johansson et al., 1998; Maisetta et al., 2008). Thus, the activity of NaD1, CP29 and Bac2a on *C. albicans* was tested in the presence of serum.

NaD1 was active in the presence of 5% fetal calf serum. However, the activity was about two-fold lower than the serum free control (an IC_{50} of about 4.5 μ M in serum compared to 2.5 μ M of the no-serum control) (Figure 2.14A). NaD1's activity was reduced further when the serum was heat inactivated (IC_{50} of about 10 μ M) (Figure 2.14D).

In contrast, the activity of CP29 increased in the presence of 5% fetal calf serum, with an IC_{50} of 2.5 μ M compared to 4 μ M for the no-serum control (Figure 2.14B). Furthermore the activity of CP29 was the same in heat-inactivated or untreated serum (IC_{50} of about 2.5 μ M) (Figure 2.14E). An increase in antifungal activity also occurred when bovine serum albumin (BSA) was added to the CP29 antifungal assay (Figure 2.15).

The activity of Bac2a was not affected by 5% serum. The IC_{50} was about 2 μ M in both 5% serum and the serum free control (Figure 2.14C) but was two-fold lower in heat-inactivated serum compared to the untreated serum control (IC_{50} of about 4 μ M) (Figure 2.14F).

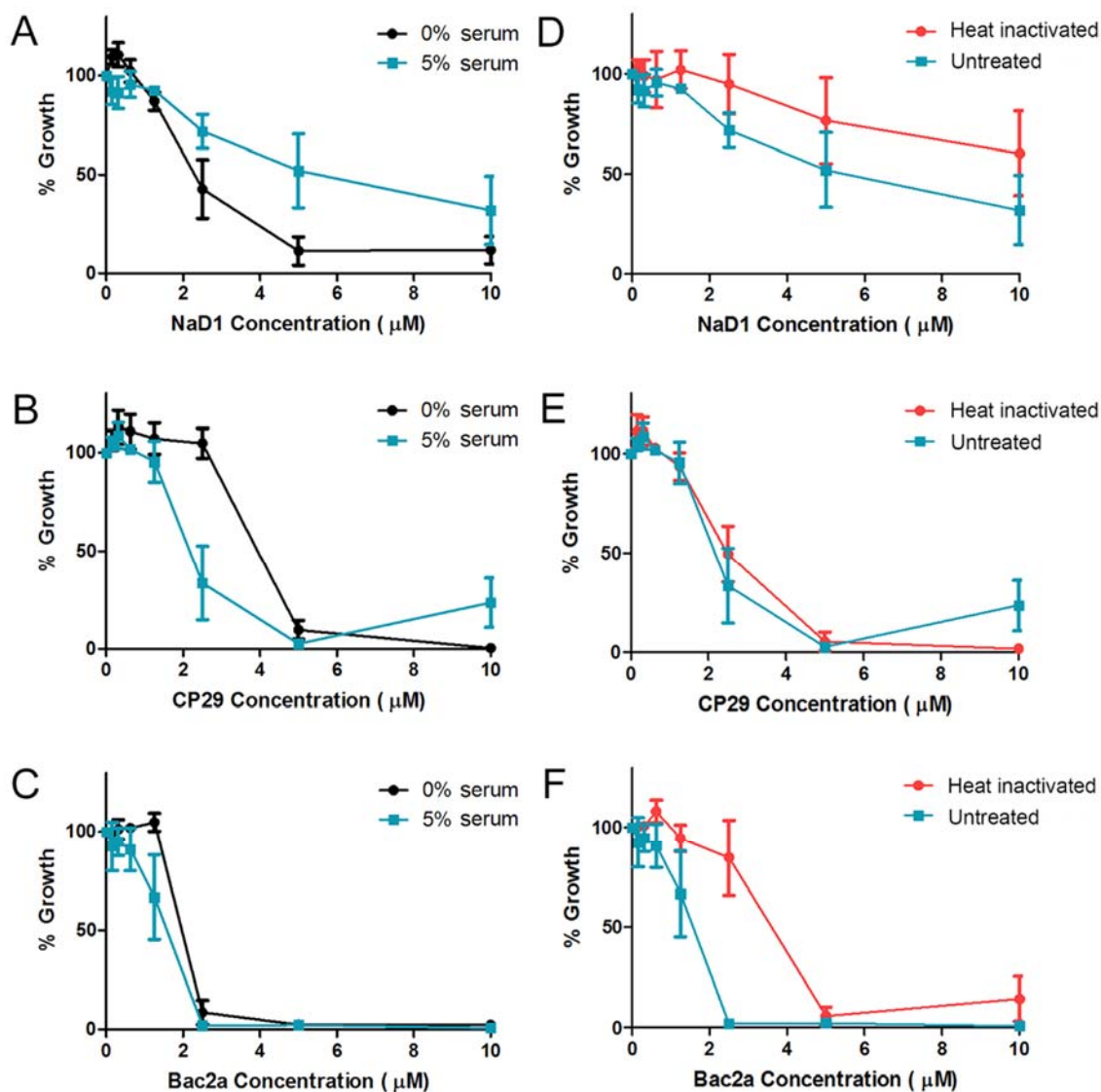


Figure 2.14 The effect of serum on the activity of NaD1, CP29 and Bac2a against *C. albicans*

C. albicans DAY185 was incubated with various concentrations of (A) NaD1, (B) CP29 or (C) Bac2a in the presence or of 5% fetal calf serum or a serum free control (0% serum). The activity of NaD1 in 5% serum was reduced compared to the serum free control, whereas the activity of CP29 and Bac2a was higher or unaffected by 5% serum. DAY185 was also incubated with (D) NaD1, (E) CP29 or (F) Bac2a in the presence of 5% fetal calf serum that had or had not been heat inactivated. NaD1 and Bac2a were more active in untreated serum. The IC_{50} of CP29 was about 2.5 μ M in both heat inactivated and untreated serum. Data are relative to a no-protein control. Error bars represent SEM (n=4).

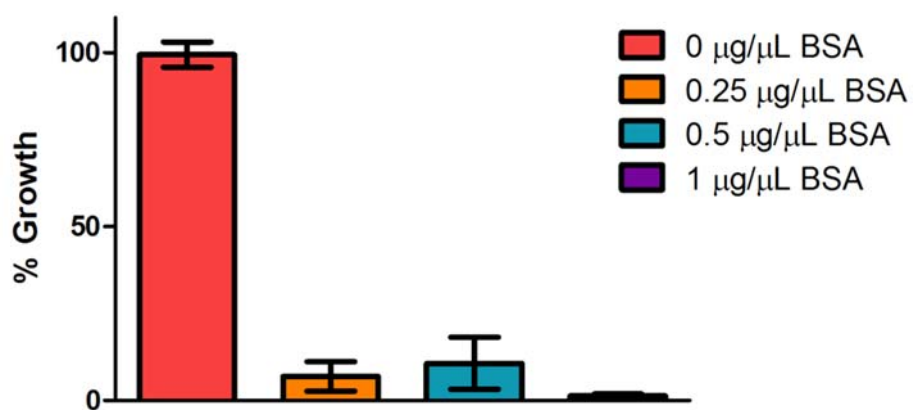


Figure 2.15 The effect of bovine serum albumin on the growth inhibitory activity of CP29

DAY185 cells were incubated with 5 μM CP29 in the presence of various concentrations of bovine serum albumin (BSA). The antifungal activity of CP29 was significantly higher at all BSA concentrations tested. Data are relative to a no-protein control. Error bars represent SEM (n=3).

2.3.7 Activity of antifungal peptides against a range of human fungal pathogens

Six antimicrobial peptides were tested for antifungal activity against human pathogens. The pathogens included three strains of *C. neoformans* (JEC20, JEC21 and H99), three strains of *C. gattii* (WM276, R265 and Bal 11), one strain of *A. niger* (5181), three strains of *A. flavus* (5310, 5311 and 2001), and three strains of *A. paraciticus* (4470, 4467 and 4469).

2.3.7.1 *Cryptococcus species*

The activity of six peptides against *C. neoformans* is presented in Figure 2.16. Bac2a was the most effective peptide against JEC20 (IC₅₀ 0.3µM) and JEC21 (IC₅₀ 0.8 µM), but had less activity against H99 (IC₅₀ 2.2 µM). NaD1 and its variant HXP4 had similar activity against JEC20 (IC₅₀'s of 0.9 and 1.1 µM respectively) but HXP4 was more effective against JEC21 and H99. Bactenecin, BMAP-28 and CP29 were the least effective at inhibiting the growth of all three *C. neoformans* isolates. *C. neoformans* JEC20 was the most sensitive isolate, with the lowest IC₅₀ values with all antimicrobial peptides.

All three *C. gattii* strains were similar in their susceptibility to AFPs (Figure 2.17). NaD1, HXP4 and Bac2a were the most active peptides, and had similar IC₅₀ values across all the three pathogens (IC₅₀'s of 1.3 to 2.5 µM). Bactenecin was the next most effective peptide with IC₅₀'s of between 3.7 and 3.8 µM. NaD1 was more effective than HXP4 against all three *C. gattii* strains. BMAP-28 and CP29 were particularly ineffective against these strains, with IC₅₀ values higher than 5 µM (the highest concentration tested) apart from CP29 against strain Bal 11 with an IC₅₀ of 3.6 µM.

Overall, the *C. neoformans* strains were more sensitive to the AFPs than the *C. gattii* strains.

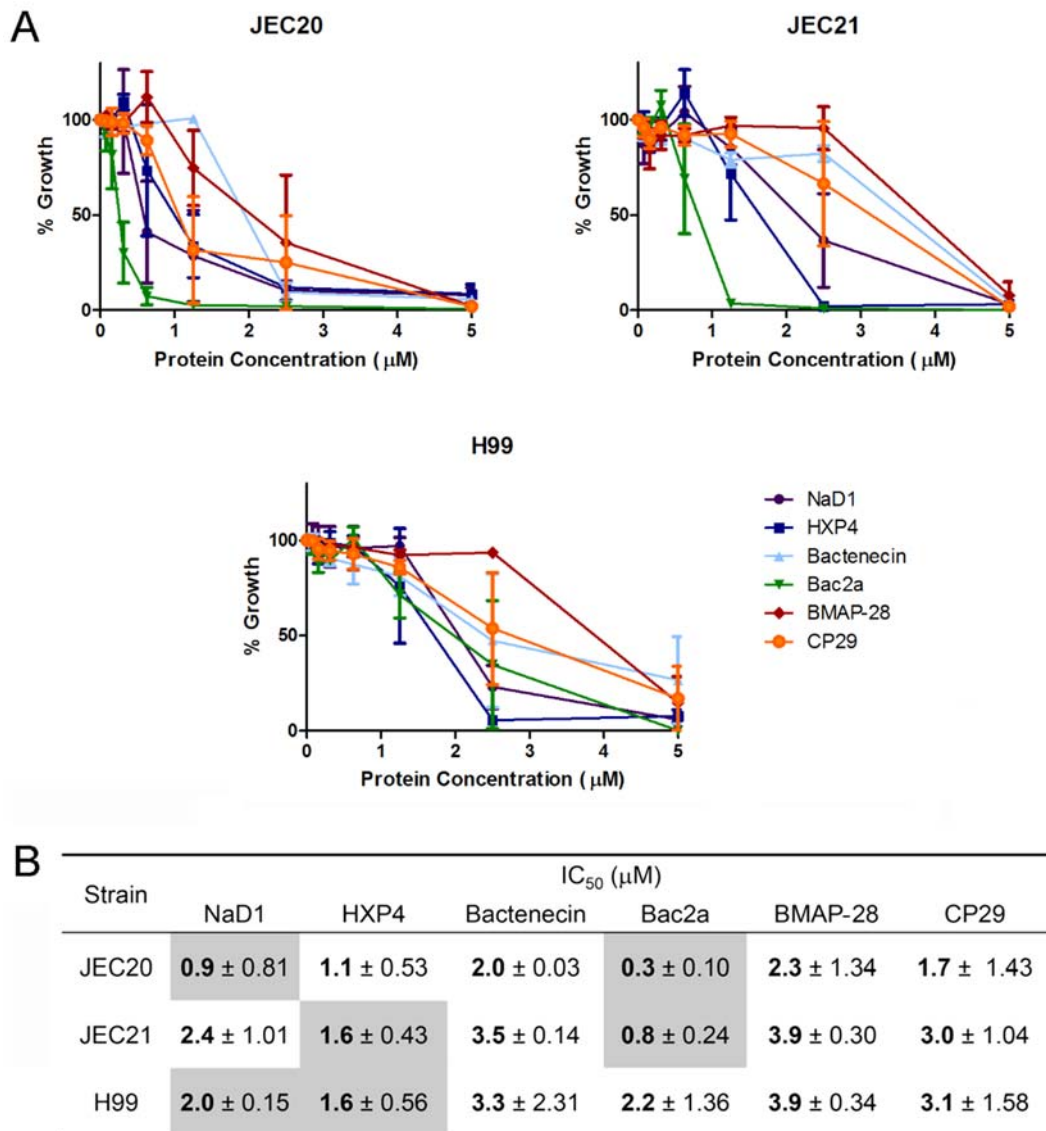


Figure 2.16 The effect of various antimicrobial peptides on the growth of three *C. neoformans* isolates

(A) Growth inhibition of *C. neoformans* JEC20, JEC21 and H99 in the presence of various concentrations of the antimicrobial peptides NaD1 (—●—), HXP4 (—■—), bactenecin (—▲—), Bac2a (—▼—), BMAP-28 (—◆—) and CP29 (—◇—). The two most effective peptides for each strain are highlighted in grey. Data are shown relative to a no-protein control. Error bars represent SEM (n=3). (B) The IC₅₀ for each peptide is shown in bold ± standard deviation (n=3).

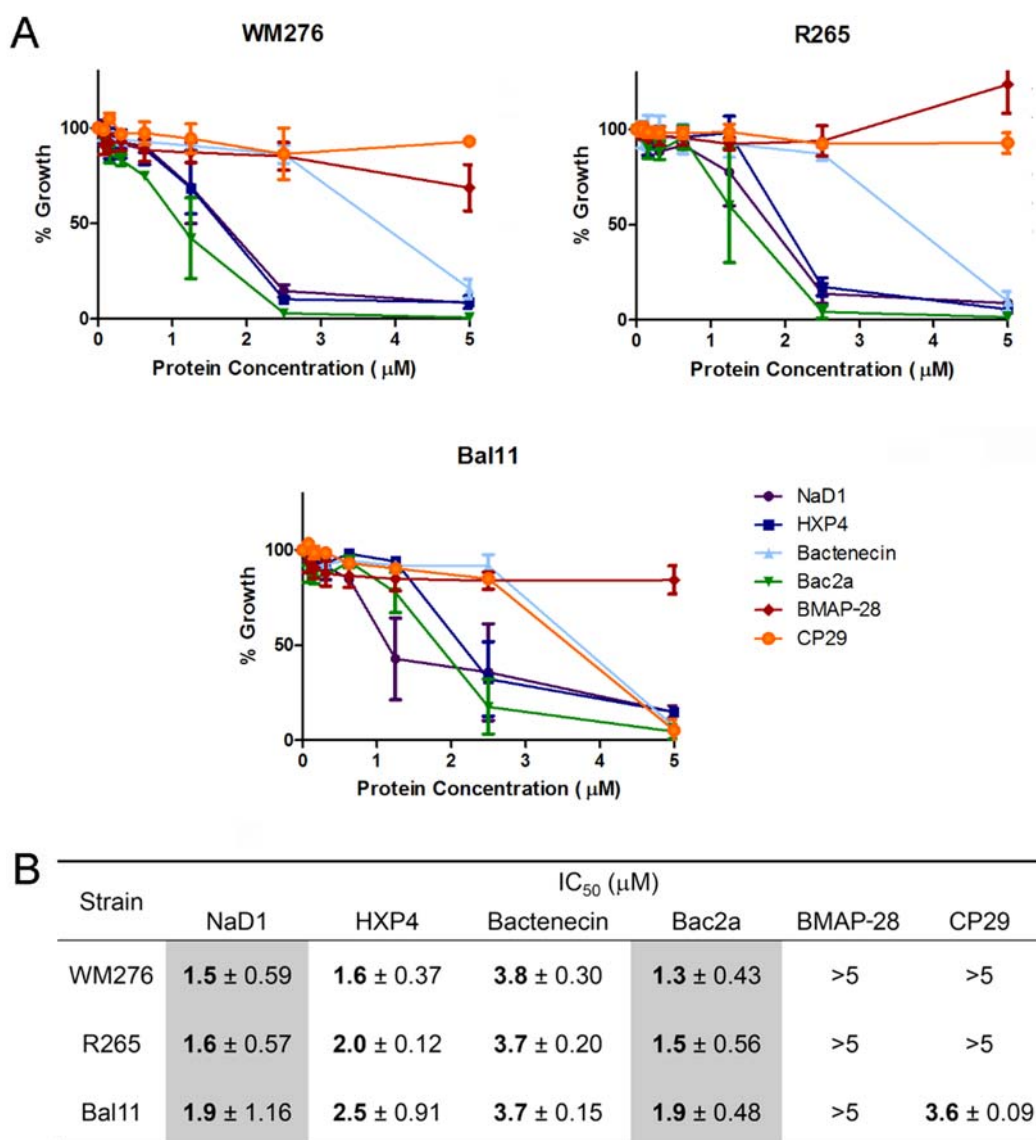


Figure 2.17 The effect of various antimicrobial peptides on the growth of three *C. gattii* isolates

(A) Growth inhibition of *C. gattii* WM276, R265 and Bal11 in the presence of various concentrations of the antimicrobial peptides NaD1 (—●—), HXP4 (—■—), bactenecin (—▲—), Bac2a (—▼—), BMAP-28 (—◆—) and CP29 (—○—). The two most effective peptides for each strain are highlighted in grey. Data are shown relative to a no-protein control. Error bars represent SEM (n=3). (B) The IC₅₀ for each peptide is shown in bold ± standard deviation (n=3).

2.3.7.2 *Aspergillus species*

The activity of the peptides against *A. niger* is presented in Figure 2.18. Bac2a was the most active peptide, with an IC_{50} of 0.8 μ M, followed by NaD1 and its variant HXP4 which had IC_{50} values of 2.1 and 2.2 μ M, respectively. CP29 and bactenecin were the least effective, with IC_{50} values greater than 10 μ M.

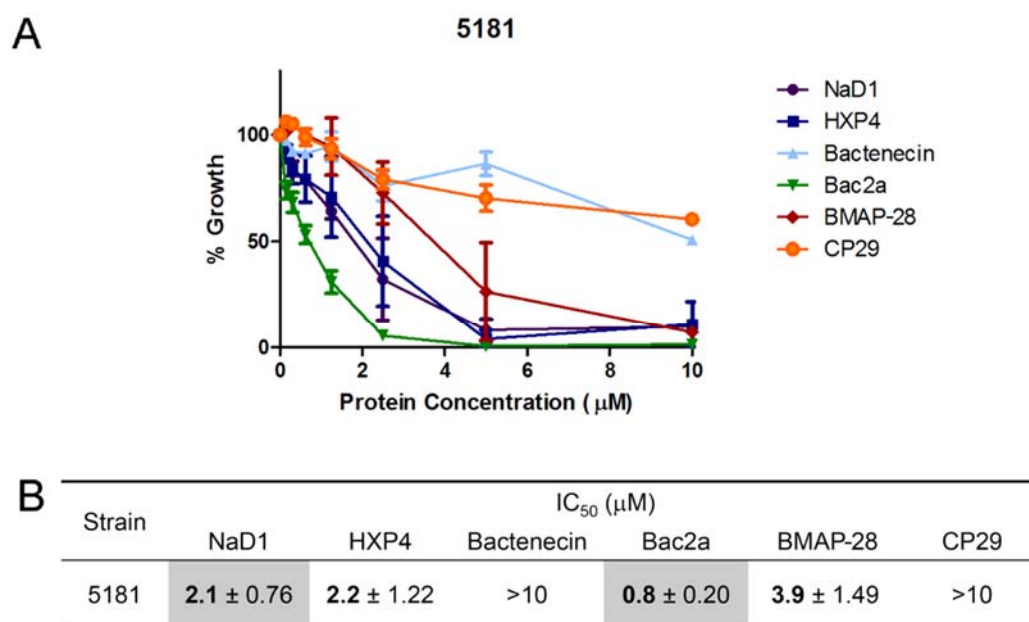


Figure 2.18 The effect of various antimicrobial peptides on the growth of *A. niger*

(A) Growth inhibition of *A. niger* 5181 in the presence of various concentrations of the antimicrobial peptides NaD1 (—●—), HXP4 (—■—), bactenecin (—▲—), Bac2a (—▼—), BMAP-28 (—◆—) and CP29 (—○—). The two most effective peptides are highlighted in grey. Data are shown relative to a no-protein control. Error bars represent SEM (n=3). (B) The IC_{50} for each peptide is shown in bold \pm standard deviation (n=3).

Figure 2.19 has the relative activity of the six peptides against three *A. flavus* strains. *A. flavus* was not as susceptible to AMPs as the other fungal species. Bac2a was the most effective at inhibiting the growth of these pathogens with IC₅₀'s between 1.6 and 2.1 μM. HXP4, the variant of NaD1, was the next best performer with IC₅₀'s between 2.8 and 3.5 μM. In contrast, NaD1 had low activity against the three *A. flavus* strains tested, with IC₅₀ values greater than 10 μM. Like NaD1, batenecin, CP29 and BMAP-28 were relatively ineffective in inhibiting the growth of all three pathogens.

Activity against the three *A. paraciticus* strains is presented in Figure 2.20. Bac2a had the highest inhibitory activity, followed by NaD1 and HXP4, with IC₅₀ values below 5 μM in all cases. Strain 4469 was significantly more sensitive to all the peptides compared to the other two isolates. For example, batenecin, BMAP-28 and CP29 had no activity below 10 μM against strains 4470 and 4467, whereas they had IC₅₀ values below 2 μM against strain 4469.

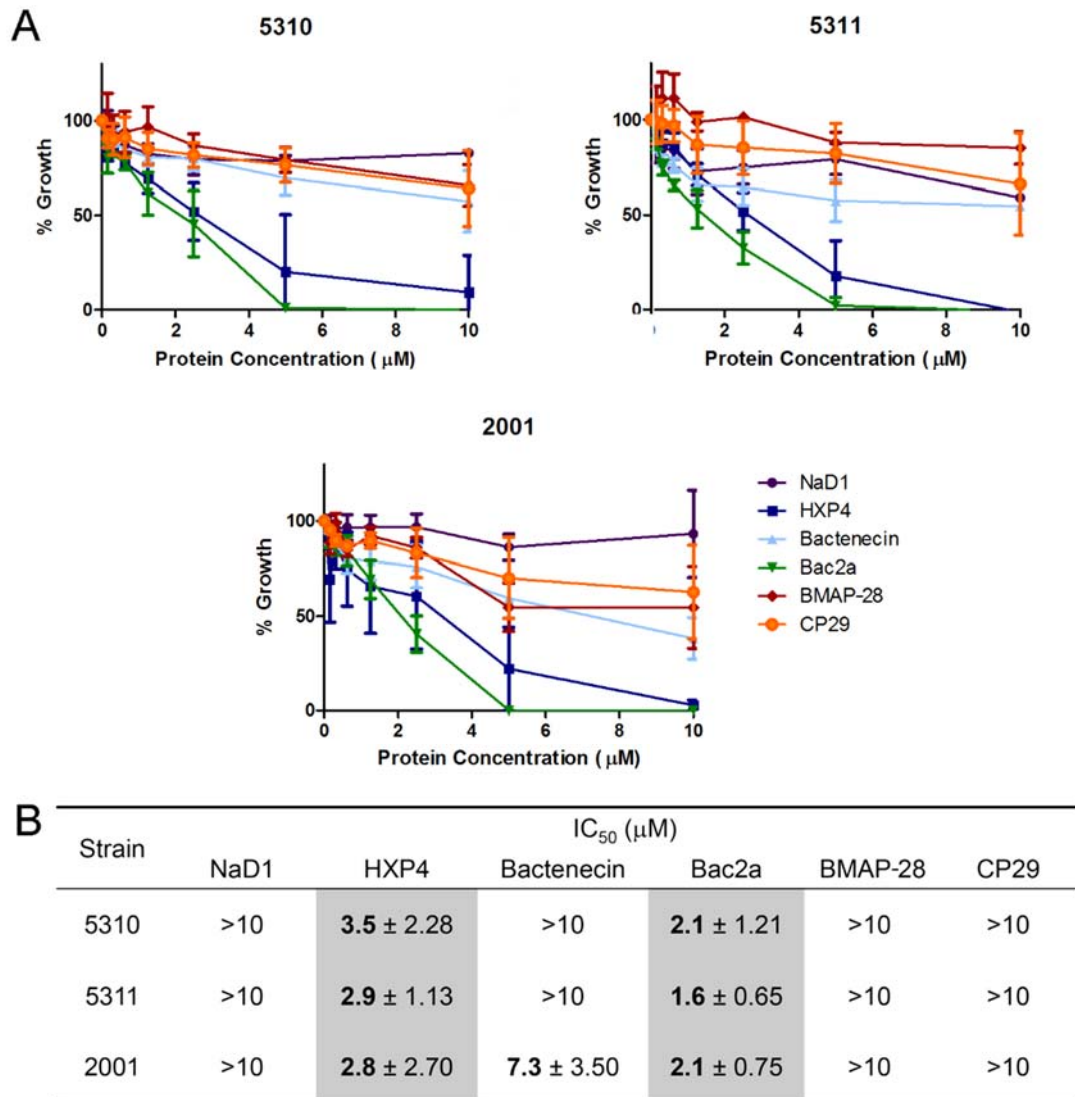


Figure 2.19 The effect of various antimicrobial peptides on the growth of three *A. flavus* isolates

(A) Growth inhibition of *A. flavus* 5310, 5311 and 2001 in the presence of various concentrations of the antimicrobial peptides NaD1 (—●—), HXP4 (—■—), bactenecin (—▲—), Bac2a (—▼—), BMAP-28 (—◆—) and CP29 (—●—). The two most effective peptides for each strain are highlighted in grey. Data are shown relative to a no-protein control. Error bars represent SEM (n=3). (B) The IC₅₀ for each peptide is shown in bold ± standard deviation (n=3).

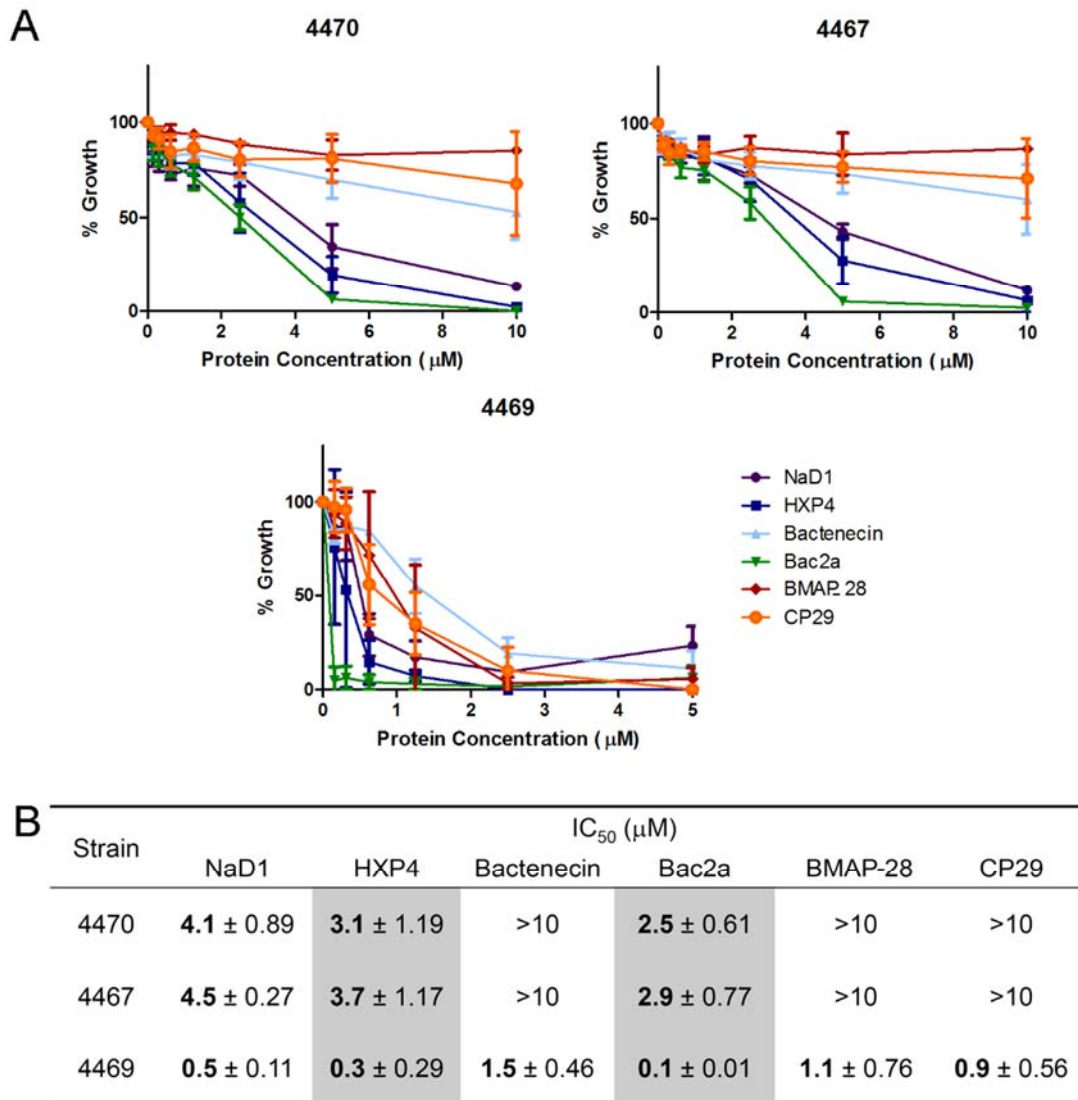


Figure 2.20 The effect of various antimicrobial peptides on the growth of three *A. paraciticus* isolates

(A) Growth inhibition of *A. paraciticus* 4470, 4467 and 4469 in the presence of various concentrations of the antimicrobial peptides NaD1 (—●—), HXP4 (—■—), bactenecin (—▲—), Bac2a (—▼—), BMAP-28 (—◆—) and CP29 (—○—). The two most effective peptides for each strain are highlighted in grey. Data are shown relative to a no-protein control. Error bars represent SEM (n=3). (B) The IC₅₀ for each peptide is shown in bold ± standard deviation (n=3).

2.3.7.3 Summary of AMP inhibitory activity against *Cryptococcus* and *Aspergillus* strains

Overall, the most sensitive of the *Aspergillus* strains tested was *A. parviticus* 4469. This isolate was the only pathogen that was inhibited by all peptides tested with IC₅₀ values less than 10 µM. Bac2a was consistently the most active peptide against all pathogens. Overall, bactenecin, BMAP-28 and CP29 were the least active peptides with IC₅₀ values of greater than 10 µM in most cases. NaD1 had significant activity, with IC₅₀ values less than 5 µM, against *A. niger* and *A. parviticus*. However, *A. flavus* was more resistant to NaD1, despite retaining its sensitivity to the NaD1 variant HXP4 (Figure 2.18 - Figure 2.20).

2.3.8 Synergistic activity of NaD1 with protease inhibitors and AMPs against human fungal pathogens

Certain proteinase inhibitors and defensins significantly enhance the activity of NaD1 and HXP4 against a range of plant pathogens (Anderson et al., 2009; McKenna, 2012). The aim of the following section was to identify molecules that act in synergy with NaD1 against human pathogens. NaD1 was tested in combination with a series of other antifungal molecules against the human fungal pathogens *C. gattii* R265, *A. niger* 5181, *A. flavus* 5310 and *C. albicans* DAY185. *C. gattii* R265 was chosen to represent the *Cryptococcus* species because it had intermediate sensitivity to NaD1 (see Figure 2.16, Figure 2.17). The sensitivity of the *Aspergillus* species to NaD1 ranged from sensitive (*A. niger* 5181) to resistant (three *A. flavus* species), so a representative of each of these species was chosen for synergy assays. The levels of synergy were classified (as low, medium, high or very high) as described in Table 2.2. Occasionally low concentrations of peptides result in negative percentage inhibition values, possibly due to the peptides promoting growth by acting as a protein source. In these cases, negative values were adjusted to 0% growth inhibition before expected inhibition values (Ee) and inhibition differences (ID) were calculated. Also note that some assays were performed on different days and with different NaD1 stocks, so the IC₅₀ values for NaD1 alone can vary. However, the overall patterns of synergy were consistent across three independent experiments.

2.3.8.1 NaD1 activity in combination with the antimicrobial peptides bactenecin and Bac2a, and the protease inhibitors BPTI and NaCys2 against various fungal pathogens

2.3.8.1.1 Synergy assays with *C. gattii* R265

When combined with a sub-inhibitory concentration of NaD1 (1 μ M), bactenecin inhibited growth of *C. gattii* R265 at a concentration that was much lower than the concentration required for the same level of inhibition when NaD1 was not present (Figure 2.21). For example, when used on its own, bactenecin did not inhibit the growth of *C. gattii* at 1 μ M. However, when combined with NaD1 (1 μ M) growth was inhibited by 76.2%. According to Limpel's formula, the bactenecin and NaD1 combination produced high levels of synergy, with inhibition difference (ID) values of 65.4 and 53.3 at 1 μ M and 0.5 μ M bactenecin, respectively (Figure 2.21A and B).

Bac2a also acted in synergy with NaD1 against *C. gattii* R265. For example, 1 μ M Bac2a did not inhibit the growth of *C. gattii* R265, but in the presence of 1 μ M NaD1, growth inhibition rose to 83%. The Bac2a and NaD1 combination against *C. gattii* R265 resulted high levels of synergy at 0.25 μ M, 0.5 μ M and 1 μ M Bac2a (Figure 2.21C and D).

Bovine pancreatic trypsin inhibitor (BPTI) also displayed synergy with NaD1 at low concentrations. BPTI alone at 0.313 μ M did not inhibit growth but in combination with 1 μ M NaD1 the observed growth inhibition was 76.5%. The combination of BPTI and NaD1 resulted in high levels of synergy at 0.313 μ M and 0.625 μ M BPTI (Figure 2.22A and B)

The protease inhibitor NaCys2, a cystatin from *N. alata*, also acted in synergy with NaD1. NaCys2 alone at 5 μ M did not inhibit growth but in combination with 1 μ M NaD1 the observed growth inhibition of 83.1%. The combination of NaCys2 and NaD1 resulted in high levels of synergy at 2.5 μ M and 5 μ M NaCys2 (Figure 2.22C and D).

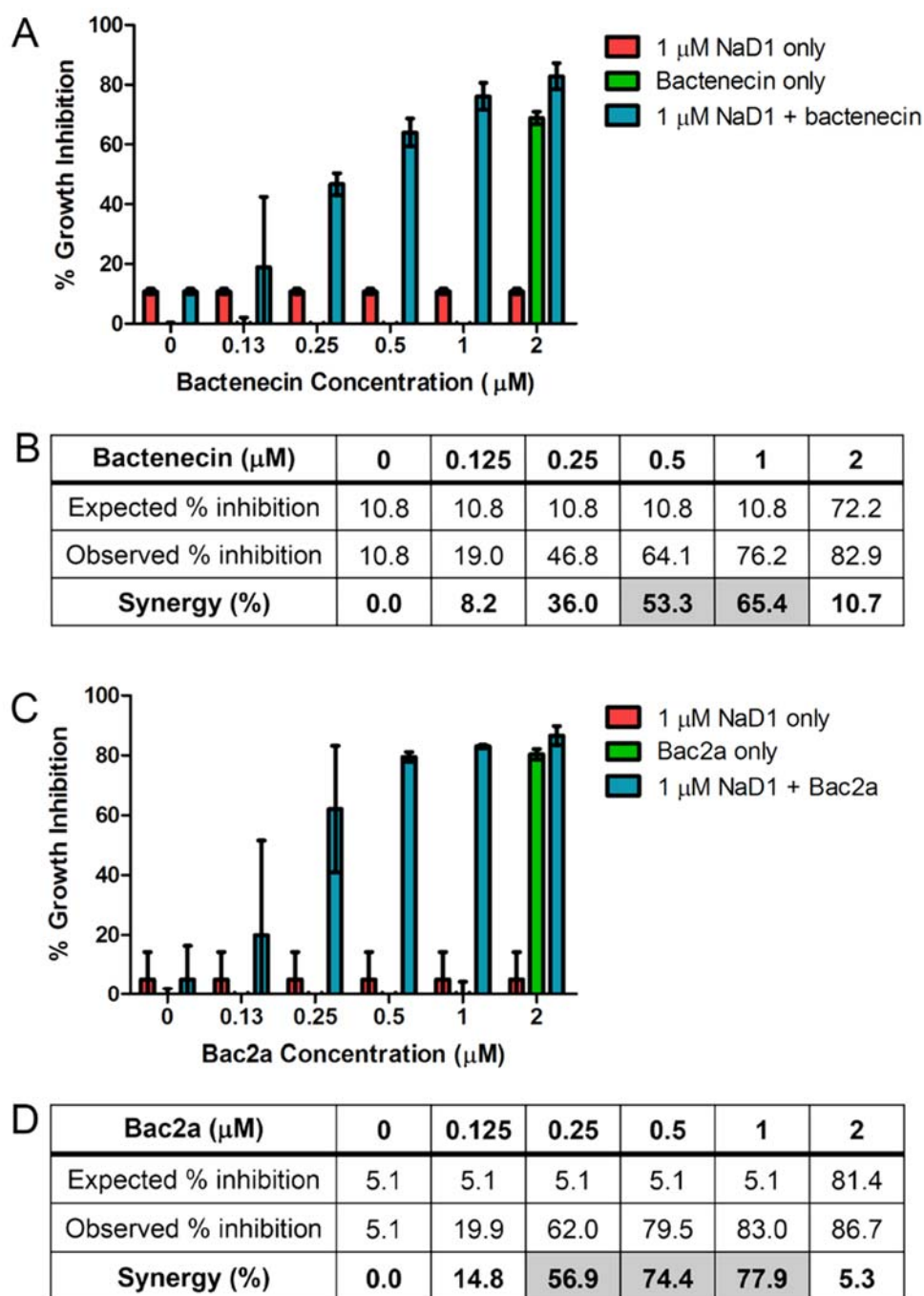


Figure 2.21 Synergy between NaD1 and two AMPs against *C. gattii* R265

Growth inhibition of *C. gattii* R265 in the presence of 1 μM NaD1 only, peptide only and NaD1 and peptide combined for (A) bactenecin and (C) Bac2a at multiple concentrations. Data are relative to a no-protein control. Data are a representative example from three independent experiments. Error bars represent standard deviation from two replicates. Synergy between the peptides and NaD1 was calculated using Limpel's formula and is shown for various concentrations of (B) bactenecin and (D) Bac2a. Concentrations of peptide that produced high or very high synergy with NaD1 are shaded in grey. The expected and observed inhibitions are also shown.

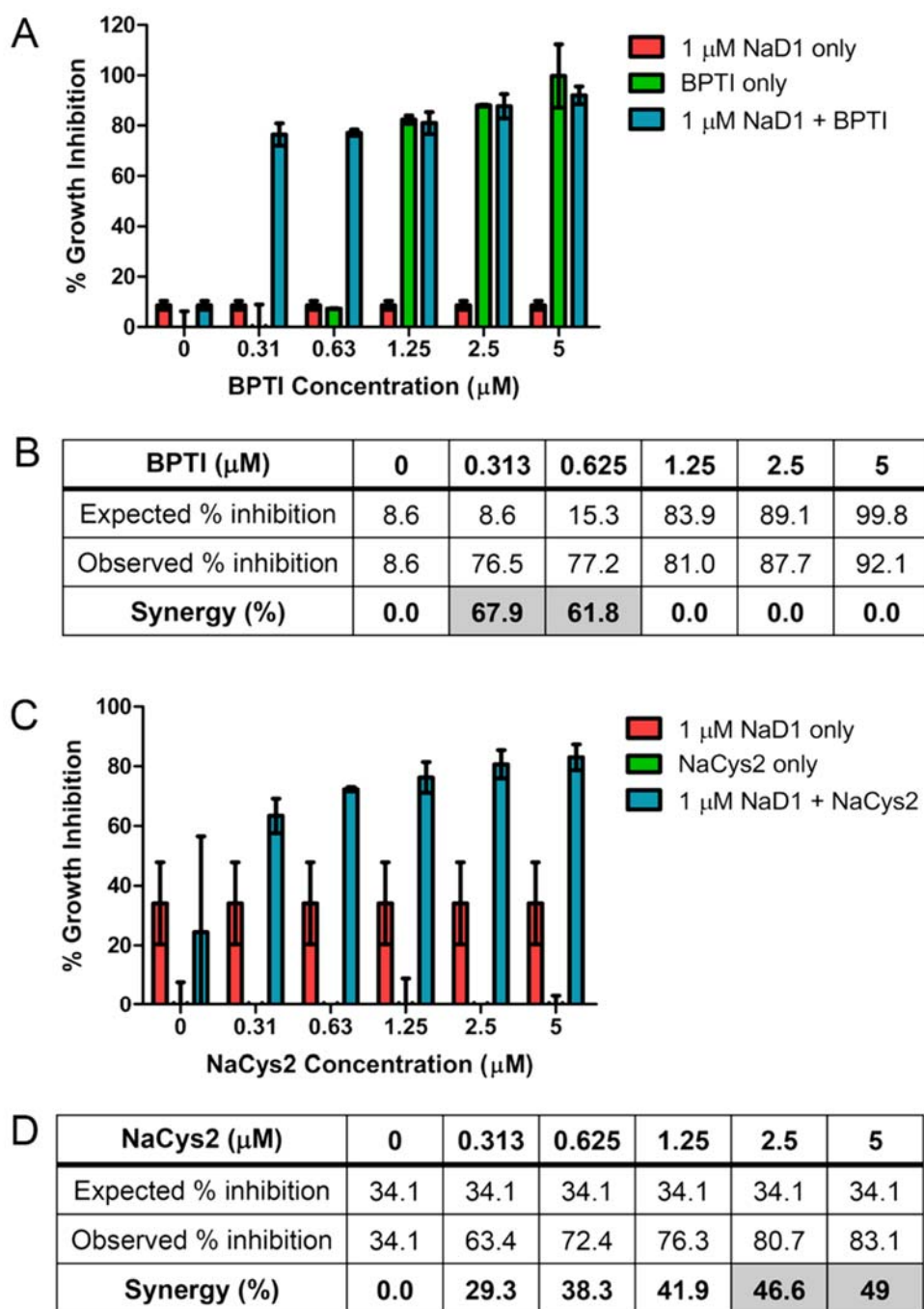


Figure 2.22 Synergy between NaD1 and two protease inhibitors against *C. gattii* R265

Growth inhibition of *C. gattii* R265 in the presence of 1 μM NaD1 only, peptide only and NaD1 and peptide combined for (A) BPTI and (C) NaCys2 at multiple concentrations. Data are relative to a no-protein control. Data are a representative example from three independent experiments. Error bars represent standard deviation from two replicates. Synergy between the peptides and NaD1 was calculated using Limpel's formula and is shown for various concentrations of (B) BPTI and (D) NaCys2. Concentrations of peptide that produced high or very high synergy with NaD1 are shaded in grey. The expected and observed inhibitions are also shown.

2.3.8.1.2 Synergy assays with *A. niger* and *A. flavus* 5310

Bactenecin alone had low activity against the filamentous fungus *A. niger* 5181 ($IC_{50} > 10 \mu\text{M}$, Figure 2.18). However, bactenecin acted in synergy with NaD1 against this pathogen. For example, the combination of $2.5 \mu\text{M}$ bactenecin and $2.5 \mu\text{M}$ NaD1, led to 49.5% growth inhibition, compared to an expected inhibition of 22.1% if their activity was additive. According to Limpel's formula, the combination of bactenecin and NaD1 resulted in low (at $2.5 \mu\text{M}$ bactenecin) and medium (at $5 \mu\text{M}$ bactenecin) levels of synergy (Figure 2.23A and B). There was no synergy between bactenecin and NaD1 against *A. flavus* 5310 at the concentrations tested (Figure 2.24A and B). Synergy was also not observed when the concentration of NaD1 was increased to $5 \mu\text{M}$ (data not shown).

The Bac2a and NaD1 combination was synergistic against both *A. niger* 5181 and *A. flavus* 5310. For example, at $1.25 \mu\text{M}$ Bac2a there was no growth inhibition of *A. niger* 5181. Yet, in the presence of $2.5 \mu\text{M}$ NaD1 the observed growth inhibition was 79.3%. The combination of Bac2a and NaD1 resulted in high synergy values (at $0.625 \mu\text{M}$, $1.25 \mu\text{M}$ and $2.5 \mu\text{M}$) (Figure 2.23C and D). Bac2a also displayed synergy with $2.5 \mu\text{M}$ NaD1 against the more resistant *Aspergillus* strain *A. flavus* 5310. According to Limpel's formula the combination of NaD1 and Bac2a resulted in high synergy values at $1.25 \mu\text{M}$ and $2.5 \mu\text{M}$ Bac2a (Figure 2.24C and D).

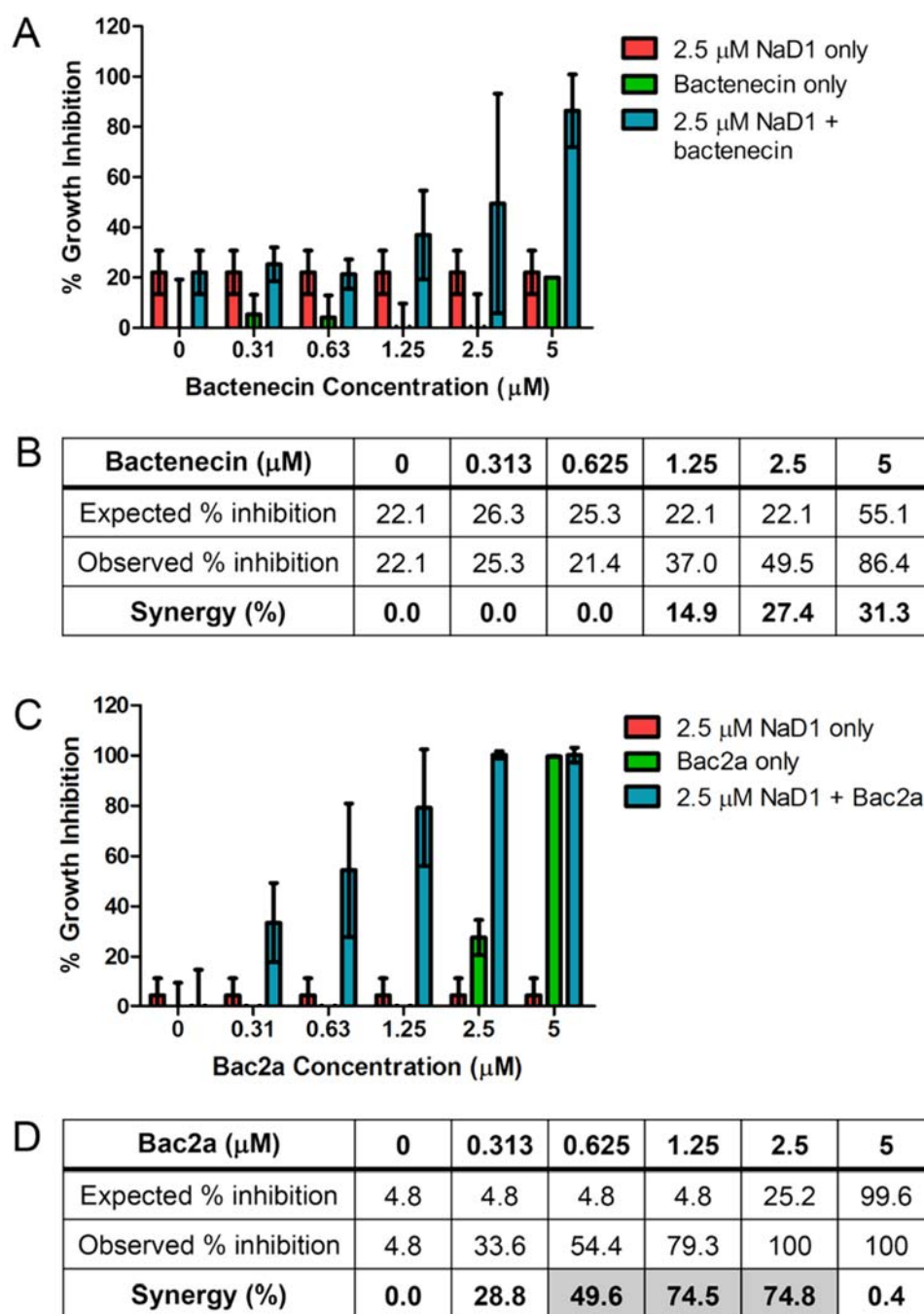


Figure 2.23 Synergy between NaD1 and two AMPs against *A. niger* 5181

Growth inhibition of *A. niger* 5181 in the presence of 2.5 μM NaD1 only, peptide only and NaD1 and peptide combined for (A) bactenecin and (C) Bac2a at multiple concentrations. Data are relative to a no-protein control. Data are a representative example from three independent experiments. Error bars represent standard deviation from two replicates. Synergy between the peptides and NaD1 was calculated using Limpel's formula and is shown for various concentrations of (B) bactenecin and (D) Bac2a. Concentrations of peptide that produced high or very high synergy with NaD1 are shaded in grey. The expected and observed inhibitions are also shown.

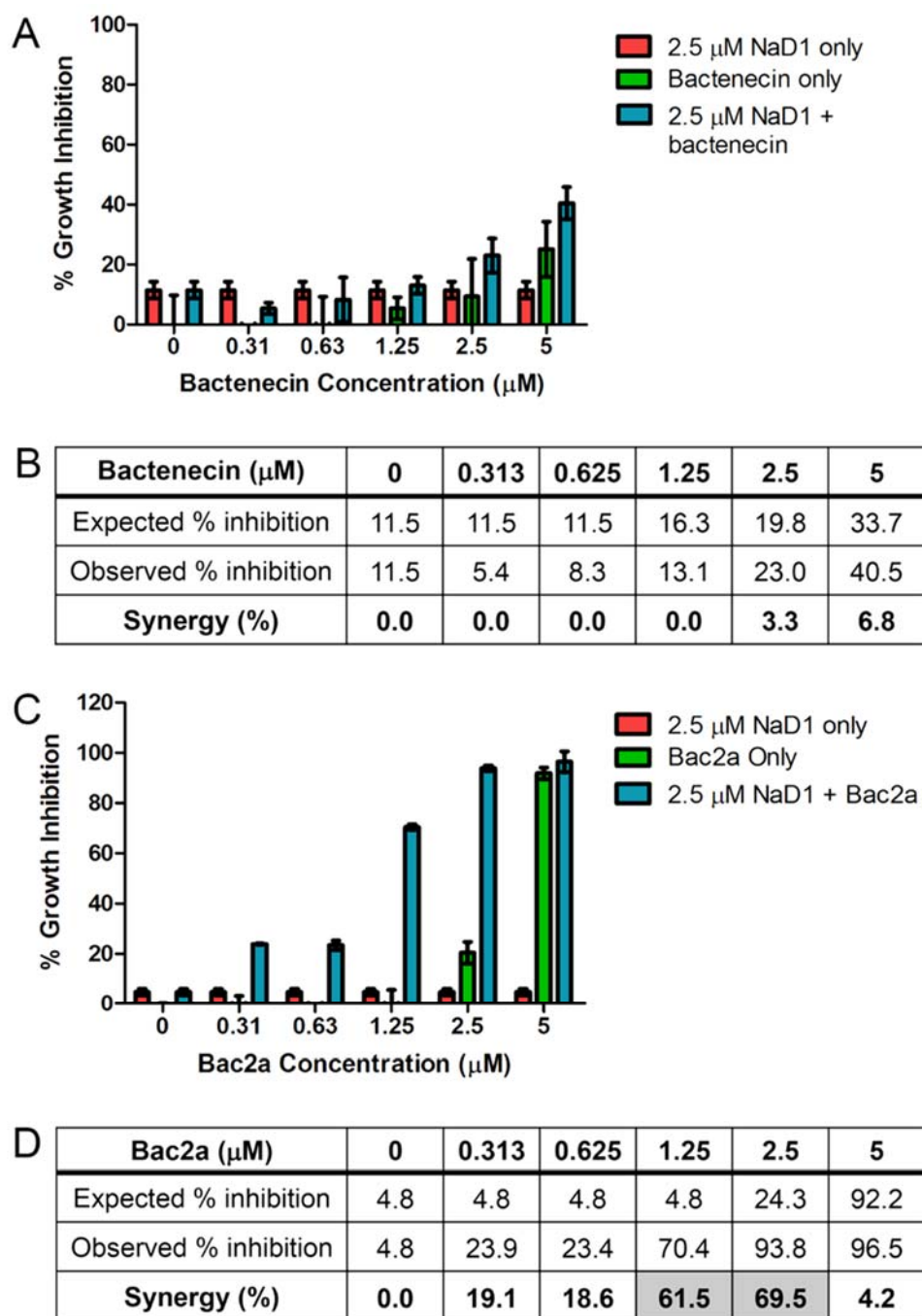


Figure 2.24 Synergy of NaD1 with two AMPs against *A. flavus* 5310

Growth inhibition of *A. flavus* 5310 in the presence of 2.5 μM NaD1 only, peptide only and NaD1 and peptide combined for (A) bactenecin and (C) Bac2a at multiple concentrations. Data are from one representative experiment. Error bars represent standard deviation from two replicates. Synergy between the peptides and NaD1 was calculated using Limpel's formula and is shown for various concentrations of (B) bactenecin and (D) Bac2a. Concentrations that displayed high or very high synergy with NaD1 are shaded in grey. The percentage inhibition expected to be purely additive and the observed percentage inhibition are also shown.

The serine protease inhibitor BPTI produced synergy when combined with NaD1 in the growth assays with *A. niger* 5181 and *A. flavus* 5310. At 2.5 μM , BPTI alone had no effect on the growth of *A. niger* 5181, but in the presence of 2.5 μM NaD1 the observed growth inhibition was 88.1% (compared to an expected inhibition of 15.8%). There was high or very high synergy values at all tested concentrations (0.313 μM to 5 μM BPTI) (Figure 2.25A and B). The combination of BPTI and NaD1 was also synergistic against *A. flavus* 5310. This peptide combination resulted in high synergy values at three BPTI concentrations (1.25 μM , 2.5 μM and 5 μM) (Figure 2.26A and B).

The cysteine protease inhibitor NaCys2 also displayed synergy with NaD1 against both *Aspergillus* pathogens. NaCys2 had no to very low inhibitory activity at any of the tested concentrations, but it enhanced the antifungal activity of NaD1. The combination of 5 μM NaCys2 and 2.5 μM NaD1 led to 91% growth inhibition of *A. niger* 5181, which was substantially higher than the expected inhibition of 9.9%. The combination of NaD1 and NaCys2 resulted a very high synergy value at 5 μM NaCys2 and a high level of synergy at 2.5 μM (Figure 2.25C and D). NaCys2 also displayed synergy with NaD1 in growth assays with *A. flavus* 5310. However, only medium (at 1.25 μM NaCys2) and low levels of synergy were obtained.

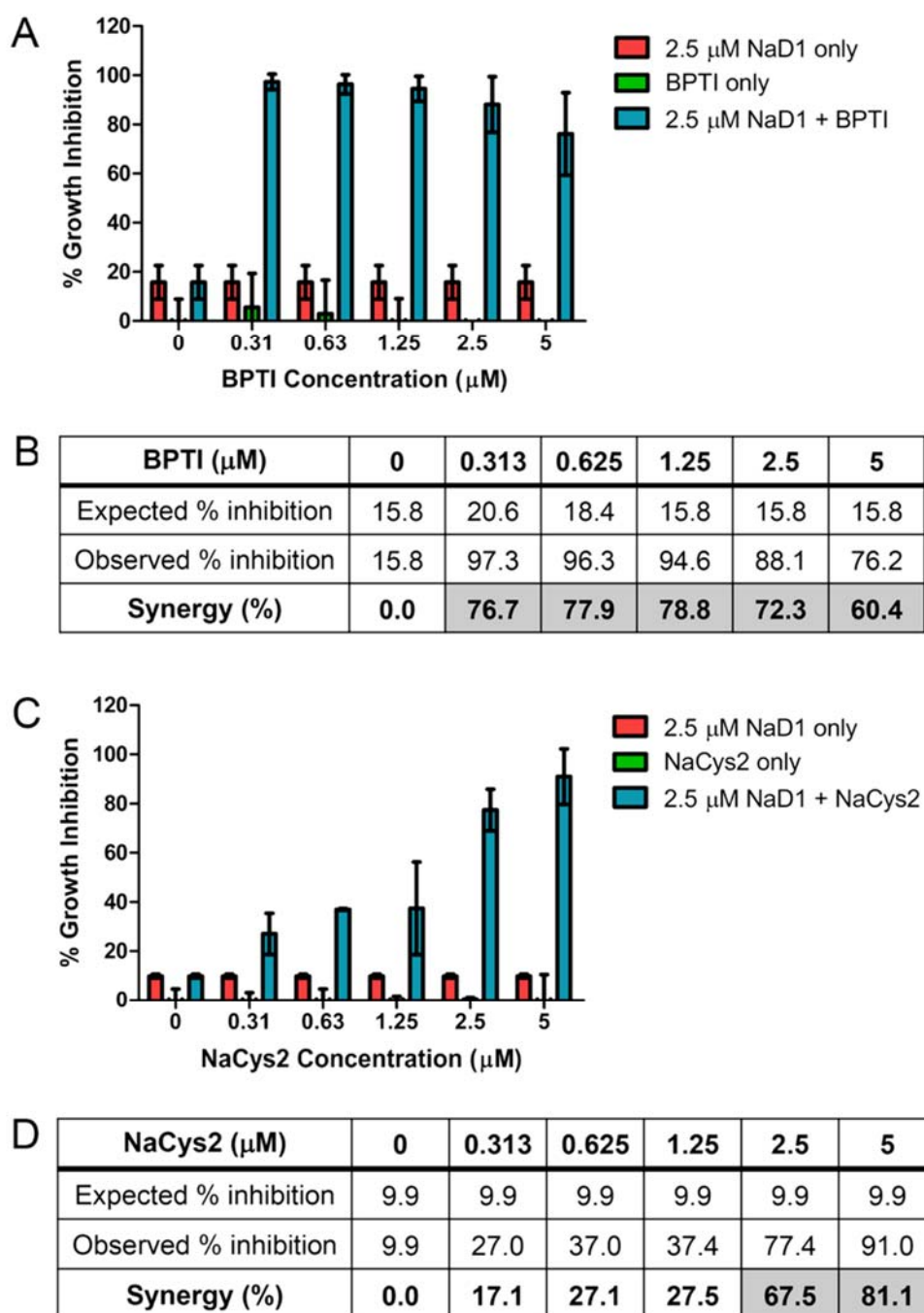


Figure 2.25 Synergy between NaD1 and two protease inhibitors against *A. niger* 5181

Growth inhibition of *A. niger* 5181 in the presence of 2.5 μM NaD1 only, peptide only and NaD1 and peptide combined for (A) BPTI and (C) NaCys2 at multiple concentrations. Data are relative to a no-protein control. Data are a representative example from three independent experiments. Error bars represent standard deviation from two replicates. Synergy between the peptides and NaD1 was calculated using Limpel's formula and is shown for various concentrations of (B) BPTI and (D) NaCys2. Concentrations of peptide that produced high or very high synergy with NaD1 are shaded in grey. The expected and observed inhibitions are also shown.

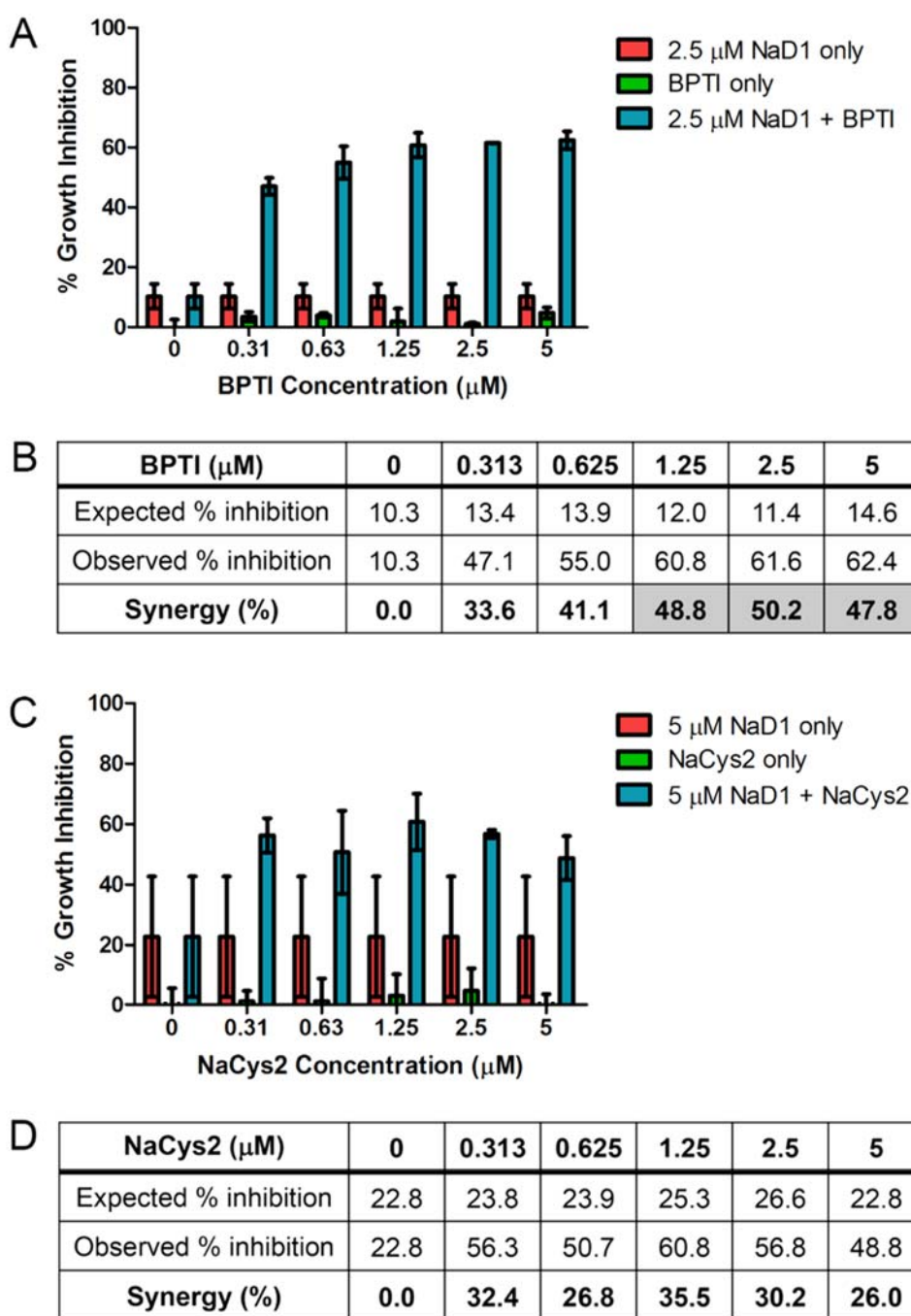


Figure 2.26 Synergy between NaD1 and two protease inhibitors against *A. flavus* 5310

Growth inhibition of *A. flavus* 5310 in the presence of 2.5 μM (BPTI) or 5 μM (NaCys2) NaD1 only, peptide only and NaD1 and peptide combined for (A) BPTI and (C) NaCys2 at multiple concentrations. Data are relative to a no-protein control. Data are a representative example from three independent experiments. Error bars represent standard deviation from two replicates. Synergy between the peptides and NaD1 was calculated using Limpel's formula and is shown for various concentrations of (B) BPTI and (D) NaCys2. Concentrations of peptide that produced high or very high synergy with NaD1 are shaded in grey. The expected and observed inhibitions are also shown.

2.3.8.1.3 Synergy assays with *C. albicans*

Both batenecin and Bac2a displayed synergy with 1 μ M NaD1 against the human pathogen *C. albicans*. The combination of batenecin and NaD1 resulted in high synergy values at 1 μ M and 2 μ M batenecin (Figure 2.27A and B). Similarly, the combination of Bac2a and NaD1 resulted in synergy. However, Bac2a displayed high levels of synergy with NaD1 at lower concentrations than batenecin (high synergy at 0.5 μ M and 1 μ M Bac2a) (Figure 2.27C and D).

Both protease inhibitors were also synergistic with NaD1 against *C. albicans*. The combination of BPTI and NaD1 resulted in high levels of synergy at 1.25 μ M, 2.5 μ M and 5 μ M BPTI (Figure 2.28A and B). The combination of NaCys2 and NaD1 gave high synergy values at three NaCys2 concentrations (1.25 μ M, 2.5 μ M and 5 μ M) (Figure 2.28C and D).

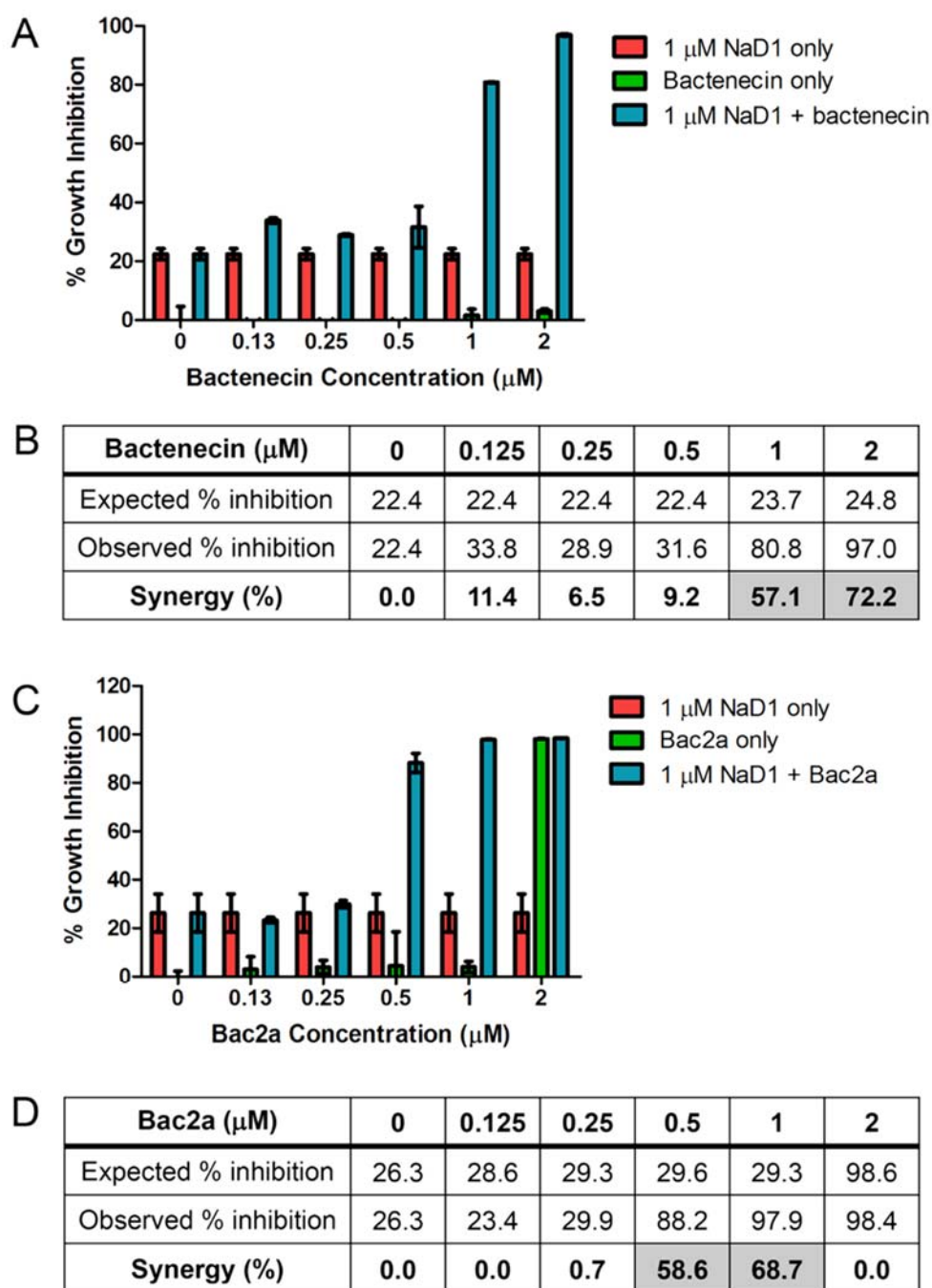


Figure 2.27 Synergy between NaD1 and two AMPs against *C. albicans* DAY185

Growth inhibition of *C. albicans* DAY185 in the presence of 1 μM NaD1 only, peptide only and NaD1 and peptide combined for (A) bactenecin and (C) Bac2a at multiple concentrations. Data are relative to a no-protein control. Data are a representative example from three independent experiments. Error bars represent standard deviation from two replicates. Synergy between the peptides and NaD1 was calculated using Limpel's formula and is shown for various concentrations of (B) bactenecin and (D) Bac2a. Concentrations of peptide that produced high or very high synergy with NaD1 are shaded in grey. The expected and observed inhibitions are also shown.

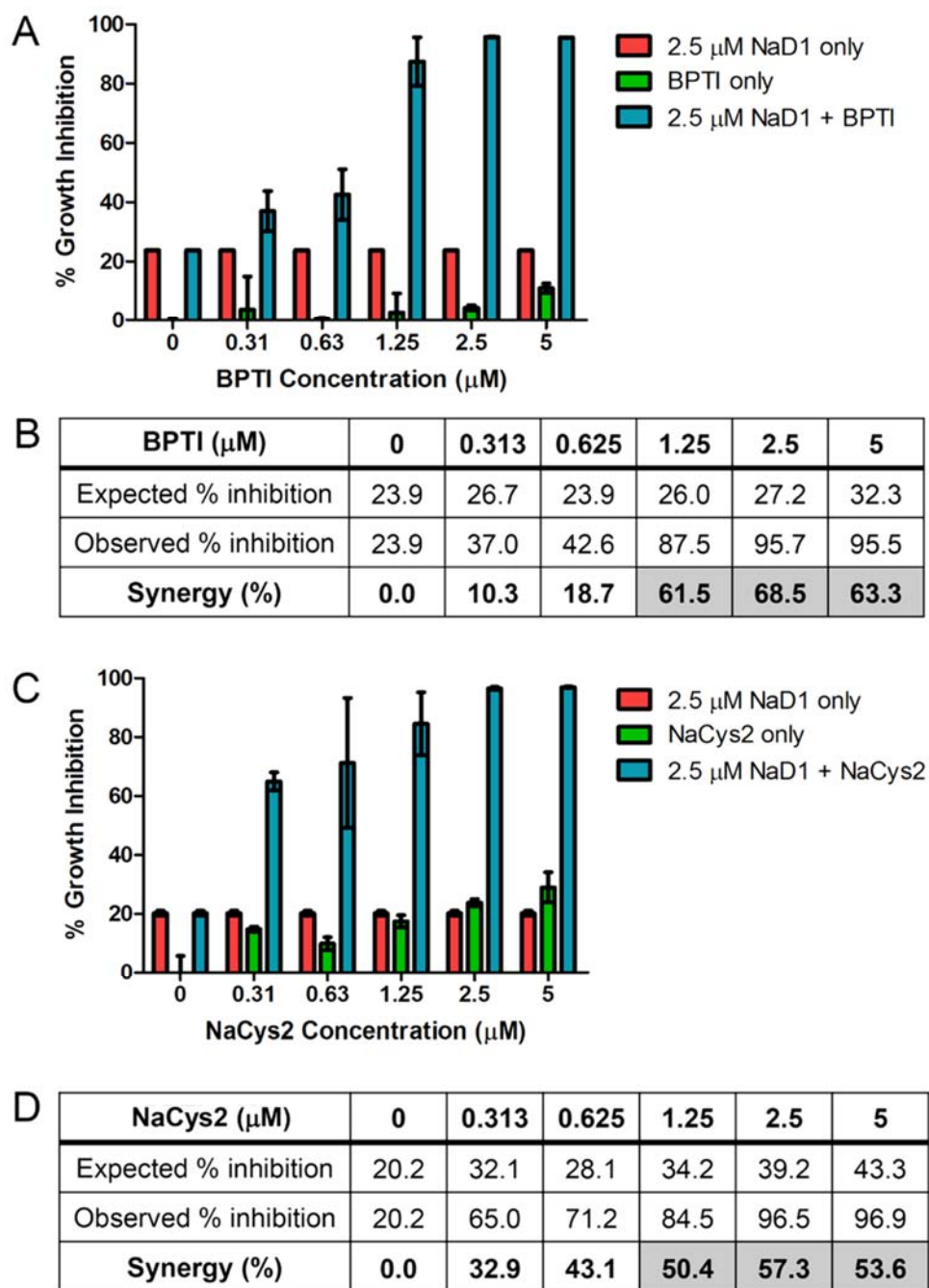


Figure 2.28 Synergy between NaD1 and two protease inhibitors against *C. albicans*

Growth inhibition of *C. albicans* DAY185 in the presence of 2.5 μM NaD1 only, peptide only and NaD1 and peptide combined for (A) BPTI and (C) NaCys2 at multiple concentrations. Data are relative to a no-protein control. Data are a representative example from three independent experiments. Error bars represent standard deviation from two replicates. Synergy between the peptides and NaD1 was calculated using Limpel's formula and is shown for various concentrations of (B) BPTI and (D) NaCys2. Concentrations of peptide that produced high or very high synergy with NaD1 are shaded in grey. The expected and observed inhibitions are also shown.

2.3.8.2 Synergy of NaD1 and two other plant defensins against *C. albicans*

The class II defensin NaD1 was tested for synergy with two class I plant defensins. The first defensin was DmAMP1 from *D. merckii*. The second peptide was NaD2, from the ornamental tobacco *N. alata*. These two class I defensins were chosen because they are likely to have different mechanisms of action (van der Weerden et al., 2013). Both defensins were tested in combination with 2.5 μ M NaD1 against the pathogen *C. albicans* DAY185.

According to Limpel's formula, the combination of 0.625 μ M DmAMP1 and 2.5 μ M NaD1 resulted in an inhibition difference value of 43.2 (Figure 2.29A and B). NaD2 was also highly synergistic in combination with NaD1 at two concentrations. High levels of synergy were observed at 1.25 μ M and 2.5 μ M NaD2 (Figure 2.29C and D).

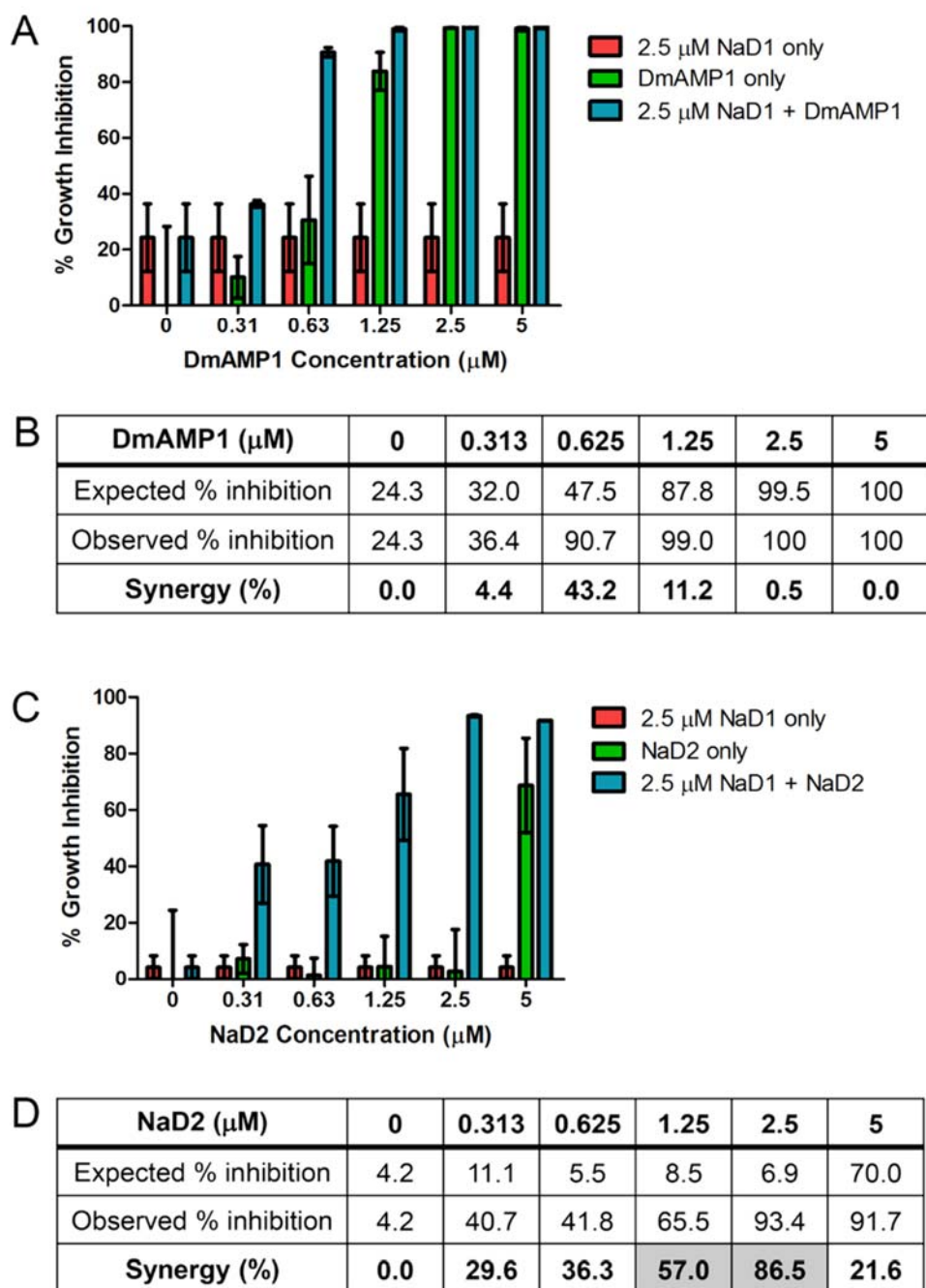


Figure 2.29 Synergy between NaD1 and two plant defensins against *C. albicans*

Growth inhibition of *C. albicans* DAY185 in the presence of 2.5 μM NaD1 only, peptide only and NaD1 and peptide combined for (A) DmAMP1 and (C) NaD2 at multiple concentrations. Data are relative to a no-protein control. Data are a representative example from three independent experiments. Error bars represent standard deviation from two replicates. Synergy between the peptides and NaD1 was calculated using Limpel's formula and is shown for various concentrations of (B) DmAMP1 and (D) NaD2. Concentrations of peptide that produced high or very high synergy with NaD1 are shaded in grey. The expected and observed inhibitions are also shown.

2.3.8.3 Synergy of NaD1 with two human antifungal peptides against *C. albicans*

NaD1 was tested for synergy with the human antifungal peptides h β D2 and histatin 5 against the human pathogen *C. albicans*. According to Limpel's formula, NaD1 at 2.5 μ M produced high synergy values with 2 μ M and 4 μ M histatin 5 (Figure 2.30A and B). NaD1 at 2.5 μ M was also highly synergistic with 0.625, 1.25 and 2.5 μ M of human defensin h β D2 (Figure 2.30C and D).

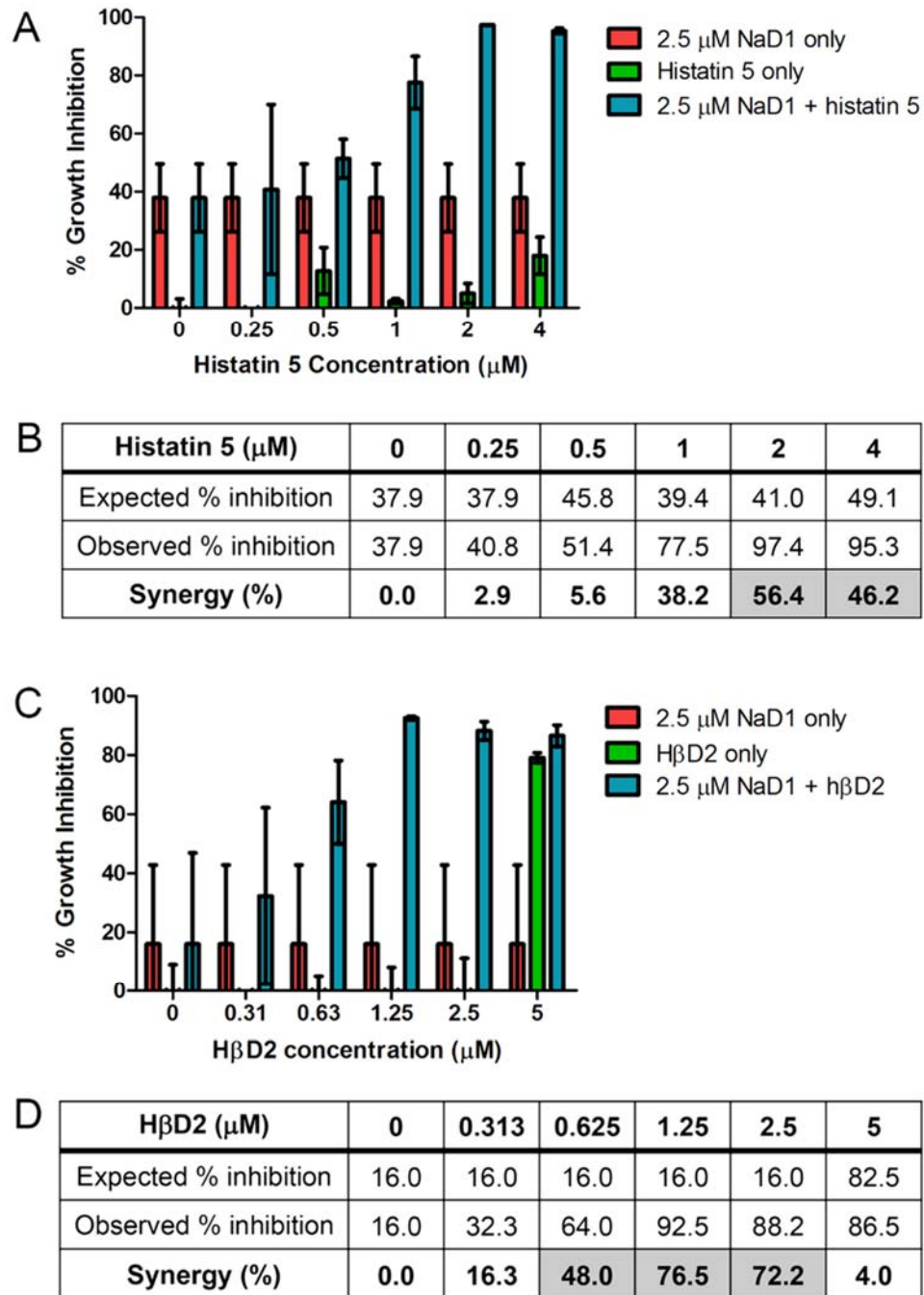


Figure 2.30 Synergy between NaD1 and two human AFPs against *C. albicans*

Growth inhibition of *C. albicans* DAY185 in the presence of 2.5 μM NaD1 only, peptide only and NaD1 and peptide combined for (A) histatin 5 and (C) h β D2 at multiple concentrations. Data are relative to a no-protein control. Data are a representative example from three independent experiments. Error bars represent standard deviation from two replicates. Synergy between the peptides and NaD1 was calculated using Limpel's formula and is shown for various concentrations of (B) histatin 5 and (D) h β D2. Concentrations of peptide that produced high or very high synergy with NaD1 are shaded in grey. The expected and observed inhibitions are also shown.

2.3.8.4 Synergy between NaD1 and the chemical fungicide amphotericin B against *C. albicans*

Lastly, NaD1 was tested for synergy with an antifungal chemical that is currently in use in the clinic. The chemical fungicide amphotericin B was tested at various concentrations in combination with 1.25 μM NaD1 against the pathogen *C. albicans*. Synergy was observed when *C. albicans* was treated with the combination of amphotericin B and NaD1. However, only low and medium synergy values were obtained (at 0.25 $\mu\text{g/mL}$ and 0.5 $\mu\text{g/mL}$, respectively) (Figure 2.31).

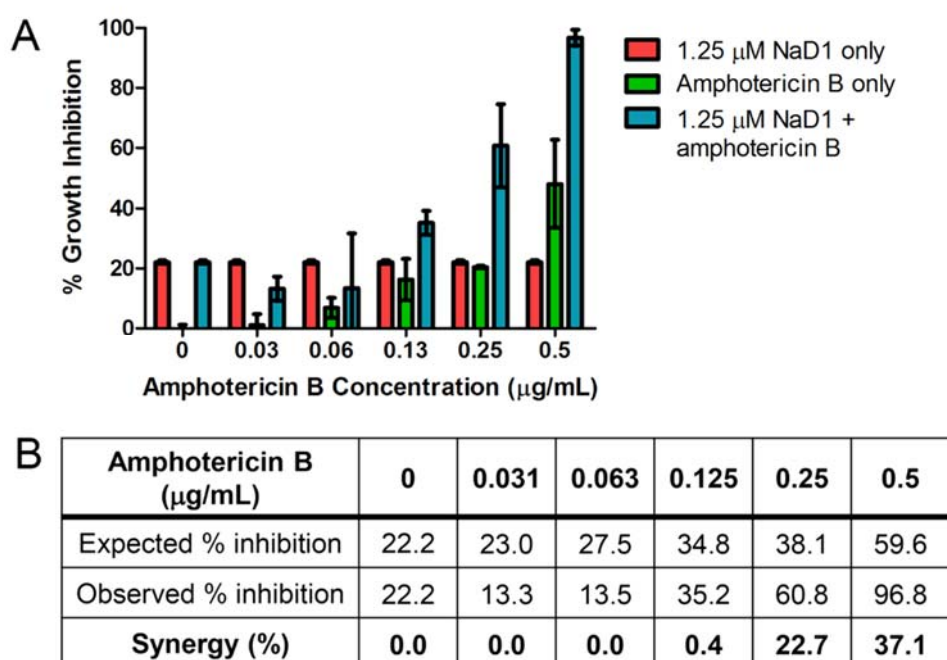


Figure 2.31 Synergy between NaD1 and amphotericin B against *C. albicans*

(A) Growth inhibition of *C. albicans* DAY185 in the presence of 1.25 μM NaD1 only, amphotericin B only and NaD1 and amphotericin B combined at multiple concentrations. Data are relative to a no-protein control. Data are a representative example from three independent experiments. Error bars represent standard deviation from two replicates. (B) Synergy between amphotericin B and NaD1 was calculated using Limpel's formula and is shown for various concentrations of amphotericin B. Concentrations of amphotericin B that produced high or very high synergy with NaD1 are shaded in grey. The expected and observed inhibitions are also shown.

2.4 Discussion

In this study I wanted to evaluate the potential of NaD1's use as a therapeutic treatment for human fungal disease. The first step in doing so was to investigate NaD1's antifungal activity against human fungal pathogens. NaD1 was initially reported to have activity against several filamentous plant pathogens. At this time it was also reported that NaD1 had little activity against the yeast *C. albicans* and *Saccharomyces cerevisiae*, although it was active against the filamentous species *Aspergillus nidulans* (van der Weerden et al., 2008). Considering that the yeast species were resistant, but filamentous pathogens were sensitive to NaD1, it was questioned whether NaD1 acts specifically on filamentous fungi. Some AFPs have been reported to have preferential activity for one fungal morphology over the other. For example, cathelicidin peptides (including BMAP-27 and BMAP-28, protegrin 1 and indolicidin) have activity against yeast but greatly reduced antifungal activity against filamentous fungi (Benincasa et al., 2006). For this reason, both filamentous and yeast pathogens of humans were tested for sensitivity to NaD1.

The growth media and starting cell density used in inhibition assays have a marked effect on antifungal activity. All subsequent fungal inhibition assays were performed with half-strength PDB, a medium that is regularly used for growth of plant fungal pathogens, so a better comparison could be made between the activity of NaD1 against filamentous plant and human pathogens. Starting cell densities were chosen that were consistent with those used in previously published studies for each pathogen. For example, the filamentous *Aspergillus* species were tested at 5×10^4 spores/mL, to be consistent with our already published method for filamentous plant pathogens.

C. albicans was retested with this new method and NaD1 had activity against this pathogen with an IC_{50} of 2.3 μ M (Figure 2.7). I have also recently reported that NaD1 is active against the yeast *S. cerevisiae* (Hayes et al., 2013). It is possible that the difference in NaD1's inhibitory activity in YPD and half-strength PDB is due to the increased growth rate in YPD. If cells multiply faster, the number of cells that replicate before succumbing to NaD1's effects may increase and continue to increase exponentially over following generations. Conversely, the slower growth in half-strength PDB could mean that are less likely to replicate before coming in contact with NaD1 and will not be able to continue contributing to the following generations. In half-strength PDB medium the doubling time of *C. albicans* cells was approximately 2 h (Figure 2.8). This was slightly slower than the

1.5 h doubling time observed when *C. albicans* cells were grown in YPD with uridine (Nobile & Mitchell, 2009). Considering that *C. albicans* cell death was observed within 15 min of NaD1 treatment in survival assays (Figure 2.9), this hypothesis is unlikely. Instead, a component of YPD media may reduce NaD1's ability to inhibit fungal growth.

As well as *C. albicans*, I also tested the ability of NaD1 to inhibit human pathogens in the *Cryptococcus* and *Aspergillus* genera. NaD1 inhibited the growth of all the *Cryptococcus* strains, as well as *A. niger* and *A. paraciticus* (Section 2.3.7). However, the *A. flavus* strains were not inhibited by NaD1 at the tested concentrations. In contrast, the peptides Bac2a and HXP4 inhibited the growth of these NaD1 resistant strains (Figure 2.19).

Bac2a and HXP4, as well as the pore forming peptides CP29 and BMAP-28, were also tested against the other human fungal pathogens (peptides reviewed in Section 2.1). The peptides, except BMAP-28, have not been well characterised for their activity against fungi. They were chosen to represent a range of antifungal mechanisms. The purpose of screening many peptides, particularly those with differing mechanisms, is for selection of peptides for combinatorial use. Peptides with differing mechanisms may prove to be effective in synergy and may help reduce the possibility of resistance occurring to a particular mechanism.

Bac2a consistently had the best antifungal activity against the tested pathogens, with the exception of *C. neoformans* H99, which was considerably more resistant to Bac2a than any of the other *C. neoformans* strains (Figure 2.16). Bac2a was also significantly more effective than its parent peptide, bactenecin, against all the tested pathogens (Section 2.3.7). That is, removal of the disulphide bond to create a linear peptide produces a better antifungal molecule. This is unusual, as removing the disulphide bond and structure usually abolishes antimicrobial activity of peptides, including NaD1 (Tamamura et al., 1993; van der Weerden et al., 2008).

NaD1 was generally the second most effective peptide against *Cryptococcus* yeast strains, with the exception of *C. neoformans* JEC21 and H99 to which HXP4 was the most effective (Section 2.3.7.1). These peptides had the same activity against the yeast *C. albicans* (Figure 2.10). These results were interesting, considering HXP4 is more active than NaD1 against filamentous plant pathogens in the *Fusarium* genus (personal communication, Dr Nicole van der Weerden, La Trobe University) and also against the filamentous strains

tested in this study (except *A. niger* 5181) (Section 2.3.7.2). HXP4 may be a better antifungal peptide than NaD1 against filamentous pathogens, but not yeast. If this is true, it may be due to differences in targets on the cell surface. Yeast and hyphal cell walls have different compositions (Bartnicki-Garcia, 1968; Bowman & Free, 2006). If HXP4's target on the cell wall is in lower abundance in yeast, this could result in decreased HXP4 binding and lower susceptibility. However, a much larger screen of yeast and filamentous pathogens would be required to confirm this. Alternatively, other differences in the mechanisms of action of NaD1 and HXP4 could also contribute to this.

The linear peptides, CP29 and BMAP-28, were active against the *C. neoformans* strains (although less than batenecin, Bac2a, NaD1 or HXP4) but had little or no activity against *C. gattii* and *Aspergillus* (with the exception of *A. paraciticus* 4469 which was significantly more sensitive to all peptides tested) (Section 2.3.7). CP29 also displayed activity against *C. albicans*, although less so than NaD1 and Bac2a (Figure 2.10). In contrast, BMAP-28 was the least active of the peptides against *C. albicans* (Figure 2.10). This is consistent with the report that BMAP-28 was generally less active against *C. albicans* strains than 17 *C. neoformans* strains tested (Benincasa et al., 2006). Also consistent with this thesis, Benincasa and co-workers found BMAP-28 had low activity against filamentous pathogens, including species of *Aspergillus* (Benincasa et al., 2006). However, there were two exceptions, *A. paraciticus* 4469 and also *A. niger* 5181, which were inhibited by this peptide (Section 2.3.7.2).

In general, the *Aspergillus* species were the most resistant to the antimicrobial peptides. However, NaD1 has previously been reported to have activity against *A. nidulans* with an IC₅₀ of 0.8 µM (van der Weerden et al., 2008). The *A. paraciticus* 4469 strain was also significantly more sensitive to NaD1 and the other antimicrobial peptides. This variance between activities against pathogens in the same genus may present an obstacle in treatment of disease, as the species and even strain may need to be identified to make an informed decision on the best course of treatment.

I was also interested in investigating the ability of NaD1 to act in synergy with other antimicrobial peptides. Synergy is when the combined activity of two peptides is greater than that expected from addition of their individual activities. Exploiting this synergistic activity may allow great reductions in the concentrations of peptides required to inhibit fungal pathogens. By choosing peptides with differing mechanisms of action, it may also be possible to reduce the emergence of resistant strains. NaD1 was tested in synergy with Bac2a and batenecin and two protease inhibitors NaCys2 and bovine pancreatic trypsin inhibitor (BPTI) against *Cryptococcus* species, *Aspergillus* species and *C. albicans*. NaD1 was used for synergy assays, rather than HXP4, as native NaD1 could be readily purified from flowers in the quantities required, whereas production of HXP4 was much more time consuming and yields were low. Protease inhibitors increase the activity of NaD1 against the plant pathogen *F. graminearum* (McKenna, 2012). One possible explanation for this effect is that NaD1 treatment makes the cell surface of fungi more permeable to other peptides which can then enter the cells and aid in inhibiting growth. This has been shown for the protease inhibitor NaCys1, where confocal microscopy was used to monitor uptake of fluorescently tagged NaCys1 with and without NaD1 treatment. NaCys1 entered the cytoplasm of *F. graminearum* hyphae only in the presence of NaD1 (McKenna, 2012). Protease inhibitors are expressed in plants as part of the defence mechanism against insects and fungi (Stevens et al., 2012; Walling, 2009). NaCys2 is a cysteine protease inhibitor (cystatin) from *N. alata* and is one of four similar cystatins from this plant species. NaCys2 had the best synergy with NaD1 against *F. graminearum* in comparison to NaCys1, 3 or 4 (McKenna, 2012). BPTI is a highly stable peptide with trypsin, chymotrypsin and serine protease inhibitory activity (Ascenzi et al., 2003). This mammalian peptide has synergistic activity with NaD1 against *F. graminearum* (McKenna, 2012) and can itself inhibit the growth of *C. albicans* (Bleackley et al., 2014a).

The molecular basis for the synergy between the cystatins and NaD1 has not been elucidated. Bleackley and co-workers (2014a) recently reported that BPTI inhibits Mg^{2+} uptake by interacting with the plasma membrane magnesium transporter, Alr1p. Treatment of *S. cerevisiae* with BPTI and a well characterised magnesium channel inhibitor, hexamine(III)cobalt chloride, results in growth arrest, with fewer cells in S-phase and an increased number of cells in G₀/G₁ and G₂ phases. One hypothesis for the mechanism of synergy between NaD1 and BPTI involves NaD1 interacting with a cell surface target that is more abundant during G₀/G₁ and G₂ phases of the cell cycle. However, NaD1's activity at different stages of the cell cycle still needs to be assessed.

All four of the tested peptides (Bac2a, bactenecin, BPTI and NaCys2) were synergistic with 1 μ M NaD1 at various concentrations against *C. gattii* R265 and *C. albicans* (Section 2.3.8). The peptides and protease inhibitors were tested against two *Aspergillus* pathogens, one which was more sensitive to NaD1 (*A. niger* 5181) and one which was more resistant to NaD1 (*A. flavus* 5310). The four peptides were synergistic with NaD1 at varying concentrations against *A. niger* 5181 (Figure 2.23, Figure 2.25). Bac2a, BPTI and NaCys2 were also synergistic with NaD1 against *A. flavus* 5310 (Figure 2.24, Figure 2.26).

NaD1 was also tested in synergy with the plant defensins DmAMP1 and NaD2. DmAMP1 was synergistic with 2.5 μ M NaD1 at 0.625 μ M and NaD2 was synergistic with 2.5 μ M NaD2 at various concentrations. Interestingly, NaD1 and NaD2 are both expressed in the flowers of *N. alata* (Dracatos et al., 2013). Perhaps *N. alata* expresses two different defensins in its flowers to produce a synergistic effect directly in this tissue. The expression of more than one defensin or antifungal molecule would also broaden the range of fungal pathogens affected. NaD1 was also synergistic with human peptides histatin 5 and h β D2. Histatin 5 is produced in saliva (Oppenheirn et al., 1988), whereas H β D2 is secreted from epithelial cells in the lung and thymus upon fungal infection (Alekseeva et al., 2009). If NaD1 was to be used therapeutically in a human system, there is the possibility that its antifungal activity could be greatly increased by the expression of the naturally occurring human antifungal peptides in the infected tissues.

The cause of synergy between NaD1 and the various antimicrobial peptides still needs to be elucidated. Perhaps synergy is observed when peptides with different mechanisms of action are combined. Many aspects of DmAMP1's and NaD1's mechanism of action are different (Table 0.1). For example, DmAMP1 binds mannosyldiinositolphosphorylceramide(M(IP)₂C) (Thevissen et al., 2004), while NaD1 binds phosphatidylinositol 4,5-bisphosphate (PI(4,5)P₂) (Poon et al., 2014). In contrast, histatin 5 binds to the heat shock proteins, Ssa1/2, on the cell wall and is internalised into the cytoplasm by the Dur3p and Dur31p polyamine transporters (Kumar et al., 2011; Li et al., 2003; Puri & Edgerton, 2014). Bac2a and NaD1 both permeabilise the membrane and enter into the cytoplasm of *Fov* hyphae (van der Weerden et al., 2010). Presumably their target on the cell wall and mechanism inside the cell are different. More research is required to clarify how synergy occurs.

After confirming that NaD1 inhibits the growth of a number of human fungal pathogens and can also act in synergy with protease inhibitors and AMPs (including the naturally occurring human AMPs histatin 5 and h β D2), I examined whether NaD1's activity against yeast pathogens is fungicidal or fungistatic (i.e. that NaD1 kills fungal cells rather than just inhibiting their growth). Fungicidal activity would be better suited for therapeutic use, as the pathogens are killed and cannot overcome the antifungal treatment. To determine this, yeast survival assays were performed. In these assays, rather than starting with a small number of cells and monitoring the ability of the cells to grow over a 24 h period, a large number of cells were treated with NaD1 for a short time and the numbers of viable cells after treatment were counted. This assay was used to demonstrate that NaD1 is a fungicidal peptide. At an OD₆₀₀ of 1.0, 50% of cells were killed by a concentration of 10 μ M NaD1 (Figure 2.9). The ability of NaD1 to kill *C. albicans* cells is consistent with earlier results of van der Weerden and co-workers (2010), who demonstrated that *Fov* is killed by NaD1 with 50% survival at approximately 2.5 μ M (shown using an MTT cell viability assay). The increased NaD1 concentration required to kill 50% of *C. albicans* cells in the survival assays, compared to the IC₅₀ of 2.3 μ M in inhibition assays, was due to an increase in starting cell density used at the start of the experiment (5000 cells/mL in inhibition assays versus an OD₆₀₀ of 1.0, or approximately 1.5×10^7 cells/mL, in survival assays). Interestingly, the amount of cell death did not alter significantly after the 15 min, 30 min or 60 min time points (Figure 2.9). This indicates that the majority of NaD1's activity had occurred within 15 min.

I was also interested in determining whether other aspects of NaD1's activity are consistent across yeast and filamentous fungi, including the kinetics of membrane permeabilisation by NaD1 and the reduction of activity in the presence of divalent cations. In the kinetic assays, membrane permeabilisation was monitored using the fluorescent molecule SYTOX green. This molecule is not membrane permeable so only enters cells after disruption of the plasma membrane. When it enters the cell, it binds to nucleic acids and fluoresces. In a permeabilisation kinetics assay with Fov, a lag phase of 15 min preceded NaD1 induced permeabilisation (van der Weerden et al., 2010). Against *C. albicans* the fluorescent intensity only began to increase significantly after 40 min (Figure 2.13). Considering that in survival assays cell death occurred in 15 min, this indicates that the permeabilisation observed may not contribute to cell death, but may instead be a secondary effect that occurs after NaD1 has interacted with its target in the cytoplasm. In contrast, CP29 and BMAP-28 rapidly permeabilise the membrane of both *C. albicans* and Fov (Figure 2.13 and van der Weerden et al., 2010). The ability of divalent cations to block NaD1 activity is also consistent between Fov and *C. albicans*. Both Mg^{2+} and Ca^{2+} were able to stop NaD1 induced killing of *C. albicans*, although Ca^{2+} was able to block killing at lower concentrations. Mg^{2+} completely rescued the *C. albicans* cells at 10 mM, while Ca^{2+} could do so at 1 mM (Figure 2.12). This has also been observed in Fov, where Ca^{2+} abolished NaD1 activity at a 20-fold lower concentration than Mg^{2+} (van der Weerden, 2007). This discrepancy indicates that it is not simply a charge effect. Instead it could be similar to the effect of $CaCl_2$ (or $MgCl_2$ at higher concentrations) on histatin 5 activity. Addition of $CaCl_2$ (or $MgCl_2$ to a lesser degree) reduced binding of fluorescently labelled histatin 5 to *C. albicans* cells and also reduced ATP release from cells (Dong et al., 2003). Perhaps addition of divalent cations blocks interaction of NaD1 with its target on the cell surface.

If NaD1 is to be used for the treatment of human pathogens it must retain activity under physiological conditions. There was no difference between NaD1 activity when fungal inhibition assays were conducted at 30°C or 37°C (Figure 2.11). In the presence of untreated serum, the IC_{50} of NaD1 doubled, although the activity still remained in the low micro-molar range (Figure 2.14). This reduction in activity may be due to charge. Half-strength PDB has a pH of about 5.0 and addition of serum increases this pH to about 7.0 (data not shown). At pH 7.0, NaD1 is less positively charged than at pH 5.0 (NaD1 has a theoretical isoelectric point of 9.08, calculated using ProtParam), which could contribute to the reduction in antifungal activity. In addition, *C. albicans* DAY185 appeared to grow better in the presence of serum (the optical density reached by *C. albicans* was greater in

the presence of serum, data not shown) which could mean that the cells are growing quickly, reducing the effectiveness of NaD1 as observed in the fungal inhibition assays conducted in YPD medium. The activity of Bac2a remained the same in serum, while CP29 activity increased. However, CP29 antifungal activity also increased in the presence of BSA (Figure 2.15), indicating that the increase in activity with serum may be due to the serum reducing the adhesion of CP29 to the plastic of the microtitre plate in which the experiments were conducted. Interestingly, the activity of NaD1 was reduced even further when the serum was heat inactivated (Figure 2.14). There is a possibility that this is due to the heat inactivation of other molecules in the serum, such as protease inhibitors, that could be acting synergistically with NaD1 to increase antifungal activity.

Overall, the hypothesis that NaD1 only acts on filamentous species has been disproved. As well as plant pathogens, NaD1 has activity against several human pathogens, including filamentous and yeast species. Indeed, NaD1 may be more active against *Cryptococcus* yeast species than the plant pathogen Fov, given that NaD1 has an IC_{50} of 1 μ M against Fov (when tested with a starting cell density of 5×10^4 spores/mL) (van der Weerden et al., 2008) and an IC_{50} of 0.91 μ M against *C. neoformans* JEC20 (despite a greater starting cell density of 1.5×10^6 cells/mL). Additionally, NaD1's activity is retained under physiological conditions and could be greatly enhanced by combination with other antifungal molecules. Furthermore, *C. albicans* is a good model for investigating the mechanism of NaD1, as many of the important features of activity (including permeabilisation and inhibition by Ca^{2+}) are conserved between Fov and *C. albicans*.

In this Chapter I revealed that NaD1 kills *C. albicans* cells. Many aspects of NaD1's mechanism was also found to be conserved in *C. albicans* and Fov. For example, NaD1's ability to permeabilise the membrane and the reduction of NaD1's activity in the presence of divalent cations. Another important aspect of NaD1's mechanism against Fov is its uptake into the cytoplasm. Thus, in Chapter 3, I examine how NaD1 gains access to the cytoplasm of fungal cells.

Chapter 3

Uptake of NaD1 into fungal cells

3.1 Introduction

NaD1's mechanism of action requires passage through the plasma membrane into the cytoplasm of *Fusarium* hyphae. This hypothesis was based on the observation that fluorescently labelled NaD1 enters *Fusarium oxysporum f. sp. vasinfectum* (Fov) hyphae, NaD1 was visualised in the cytoplasm in immuno-gold labelling experiments and NaD1 could be detected in cytoplasmic fractions after treatment of cells (van der Weerden et al., 2008).

However, the mechanism by which NaD1 gains access to the cytoplasm has not been elucidated. Potential methods of uptake are discussed below.

3.1.1 Endocytosis

Endocytosis is a process by which cells internalise extracellular material. This occurs through invagination of the plasma membrane and formation of intracellular vesicles. In mammalian cells two forms of endocytosis exist: phagocytosis and pinocytosis. Phagocytosis is performed by specialised cells, such as macrophages, which engulf large particles like bacteria. The second form of endocytosis, pinocytosis, can be further divided into categories such as macropinocytosis, clathrin-mediated endocytosis (CME), caveolin-dependent and clathrin/caveolin independent endocytosis (Conner & Schmid, 2003; Doherty & McMahon, 2009). Pinocytosis is also shared by other eukaryotic organisms including yeast. The most well understood form of pinocytosis is clathrin-mediated endocytosis. During this process, three heavy clathrin subunits and three light clathrin subunits assemble at the plasma membrane, forming clathrin coated pits. Other endocytic machinery is then recruited and membrane invaginations form and eventually pinch off to create clathrin coated vesicles (Reviewed in Conner & Schmid, 2003; Geli & Riezman, 1998). In *Saccharomyces cerevisiae*, clathrin is not required for invagination, but is needed for recruitment of the endocytic machinery (Kaksonen et al., 2005). This process is energy dependent. In the absence of ATP, molecules are sequestered into invaginated pits, but do not form vesicles, as the scission internalisation step is ATP dependent (Geli & Riezman, 1998; Schmid & Smythe, 1991). In mammalian cells, the GTPase dynamin is also important for this process. Dynamin localises to the neck of membrane invaginations and is involved in constriction and scission of the membrane (Conner & Schmid, 2003; Geli & Riezman, 1998; Sever et al., 2000). Dynamin is also involved in phagocytosis and clathrin-

independent endocytosis (Conner & Schmid, 2003). However, in *S. cerevisiae* dynamin does not have a direct role in internalisation (Kaksonen et al., 2006).

Researchers working with yeast have also highlighted the importance of actin in CME. Actin polymerisation begins when the clathrin coat and membrane begin to invaginate and ends when scission has occurred (Kaksonen et al., 2006). Disruption of actin polymerisation in *S. cerevisiae* using the inhibitor latrunculin A, which prevents actin assembly into filaments, blocks endocytosis (Figure 3.1) (Ayscough et al., 1997; Dutta & Donaldson, 2012). Similarly, actin mutants are unable to internalise the α -pheromone mating receptor Ste2 by endocytosis (Kubler & Riezman, 1993). However, actin does not seem to be essential for endocytosis in mammalian cells (Conner & Schmid, 2003; Kaksonen et al., 2006). Although in mammals actin polymerisation is required for the formation of membrane protrusions in macropinocytosis (Conner & Schmid, 2003; Dutta & Donaldson, 2012).

Once internalised, endocytic vesicles deliver molecules to endosomes. Cargo can be recycled back to the plasma membrane by early endosomes, as occurs with receptors, or directed to the *trans*-Golgi network (TGN) or sorted to late endosomes for transport to the lysosome (mammalian cells) or vacuole (fungi) for degradation (Bonifacino & Rojas, 2006; Geli & Riezman, 1998; Saksena et al., 2007). Sorting and trafficking of endosomes requires the ESCRT (endosomal sorting complexes required for transport) machinery. ESCRT complexes also control formation of late endosomes or multivesicular bodies (MVBs) (Henne et al., 2011; Saksena et al., 2007). Deletion of yeast genes encoding components of this pathway, termed vacuolar protein sorting (*VPS*) genes, results in mislocalisation of cargo (Saksena et al., 2007). The movement of endosomes and lysosomes in mammalian cells requires microtubules. Depolymerisation of microtubules using nocodazole, blocks movement of endosomes and lysosomes and also stops cargo transfer between early and late endosomes (Figure 3.1) (Apodaca, 2001; Matteoni & Kreis, 1987).

Various cellular inhibitors have been employed to study different aspects of endocytosis and protein transport. As mentioned previously, latrunculin A inhibits formation of actin filaments, which in turn blocks most forms of endocytosis (Ayscough et al., 1997; Dutta & Donaldson, 2012). The microtubule polymerisation inhibitor nocodazole, as mentioned above, blocks movement of endosomes and transfer of molecules to late endosomes (Apodaca, 2001; Matteoni & Kreis, 1987). Transfer from endosomes to and from the TGN (termed retrograde and anterograde transport, respectively) can be blocked by the inhibitor brefeldin A (Figure 3.1). Brefeldin A induces deformation of the protein transport network, by fusing the Golgi to the endoplasmic reticulum (ER) and to early endosomes (Lippincott-Schwartz et al., 1991; Wood et al., 1991). The target of brefeldin A in mammalian cells is a group of Sec7 GTP-exchange factors that are required for the activity of the ADP-ribosylation factor ARF1, which recruits coat proteins to membranes. ARF1 controls recruitment of the coatomer COPI and the clathrin adapter protein AP-1 to the *trans*-Golgi membrane (Jackson & Casanova, 2000; Nebenführ et al., 2002; Scales et al., 2000). Treatment with brefeldin A blocks the action of several toxins, including ricin, shiga toxin and pertussis toxin, which require retrograde transport to the Golgi to exert their effects (el Baya et al., 1997; Sandvig et al., 2002; Xu & Barbieri, 1995).

Inhibitors which effect endocytosis and protein transport were selected to further characterise NaD1's mechanism of uptake into cells (Figure 3.1).

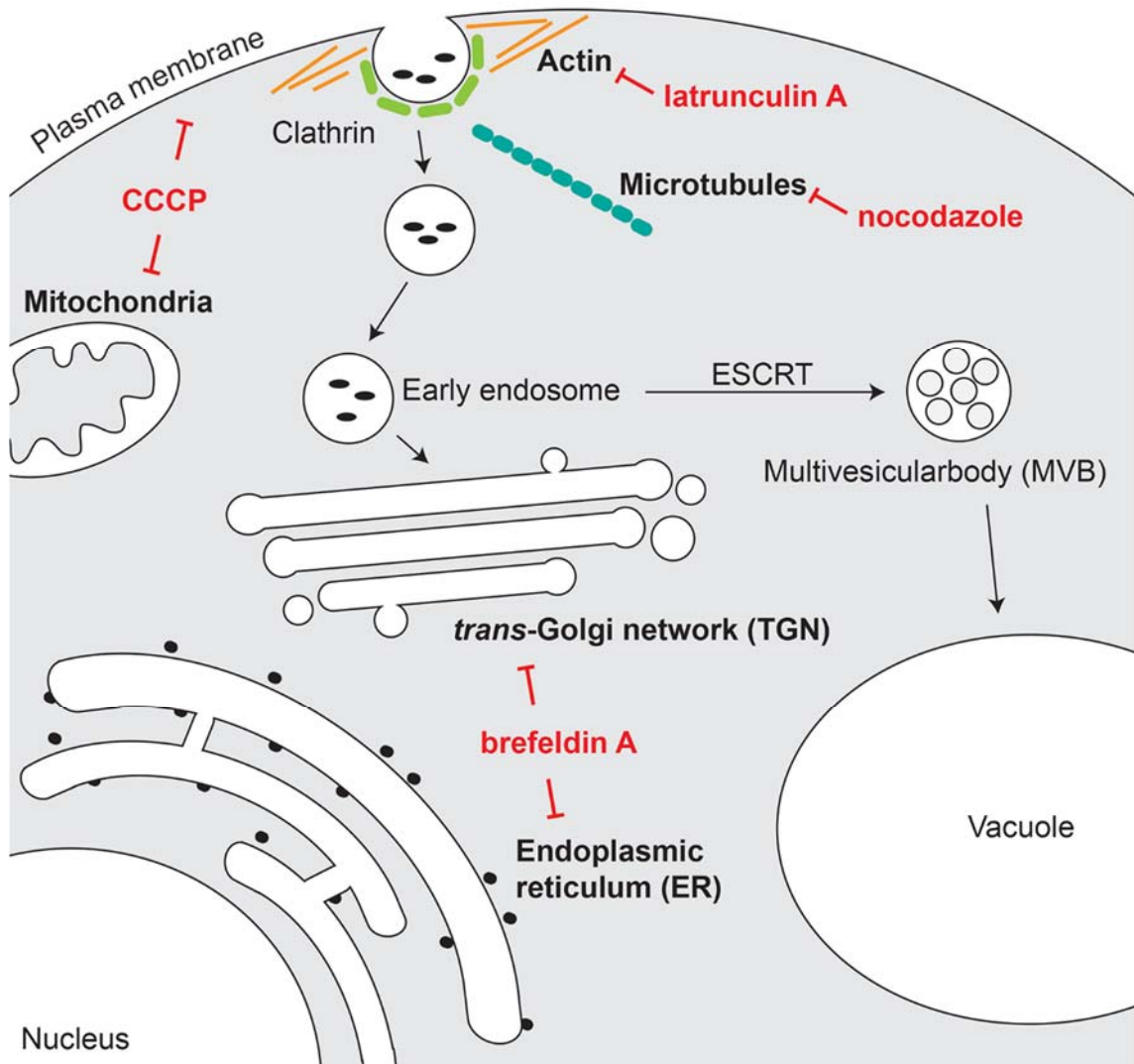


Figure 3.1 Inhibitors of endocytosis and protein trafficking

Latrunculin A affects endocytosis by preventing actin assembly. CCCP perturbs the mitochondrial and plasma membranes by inhibiting oxidative phosphorylation. Nocodazole and brefeldin A both affect internal protein transport. Nocodazole blocks microtubule polymerisation and brefeldin A deforms the *trans*-Golgi network and endoplasmic reticulum.

3.1.2 Polyamine transporters

Polyamine transporters are another route for entry of molecules into cells. These transporters internalise polyamines (putrescine, spermidine and spermine) which are involved in many cellular functions including protein synthesis and control of gene expression (Childs et al., 2003; Igarashi & Kashiwagi, 2010). They are members of the ABC (ATP binding cassette) transporter family which require energy for transport (Igarashi & Kashiwagi, 1999).

Polyamine transporters have been associated with uptake of cationic peptides. For example, the human antifungal peptide, histatin 5, enters *Candida albicans* cells via the polyamine transporters Dur3p and Dur31p. Deletion of these transporters reduced histatin 5 antifungal activity. In addition, when the polyamines spermidine or spermine were added along with histatin 5, cells were more resistant to the peptide. Furthermore, spermidine reduced uptake of FITC labelled histatin 5 into *C. albicans* (Kumar et al., 2011). More recently, Tati and co-workers reported that expression of Dur3p and Dur31p in resistant *Candida glabrata* strains render them sensitive to histatin 5 (Tati et al., 2013).

Histatin 5 uptake into *C. albicans* is also reduced after treatment with the inhibitor carbonyl cyanide m-chlorophenyl hydrazone (CCCP) (Jang et al., 2010). CCCP is an uncoupler of oxidative phosphorylation. It depolarises mitochondrial and plasma membranes and blocks mitochondrial ATP synthesis (Figure 3.1) (Heytler & Prichard, 1962; Mohr & Fewtrell, 1987). Thus, CCCP may inactivate the polyamine transporter which requires ATP to function. In confirmation of this, CCCP also blocks the uptake of spermidine into *C. albicans* cells (Kumar et al., 2011).

3.1.3 Passive transport

Passive transport is another mode of entry for molecules into cells. This is the mechanism by which some cell-penetrating peptides (CPPs) access the cytoplasm. These peptides are small (less than 30 amino acids long) and positively charged (Deshayes et al., 2005). The process these peptides employ to enter cells is debated. For example, some CPPs which were originally hypothesised to enter through receptor and energy independent mechanisms, are now thought to enter via endocytosis (Heitz et al., 2009; Lindgren & Langel, 2011). In contrast, other peptides are thought to enter through transient pores or by direct penetration driven by the membrane potential (Deshayes et al., 2005; Lindgren & Langel, 2011). Molecules which enter by direct penetration have a positive charge that allows interaction with negatively charged phospholipid headgroups (Deshayes et al., 2005). For the transient pore model, it is hypothesised that charged side chains insert into the membrane and initiate the formation of a pore, which allows translocation into the cell. Using molecular dynamics simulations with the HIV cell-penetrating peptide Tat, Herce and Garcia (2007) proposed that at high peptide concentrations the arginine residues of the peptide insert into the bilayer due to attraction to the phosphate groups on the inner leaflet. The cell membrane repair mechanisms can then mend and mask the damage, and stop leakage of intracellular molecules (Herce & Garcia, 2007; Lindgren & Langel, 2011; Palm-Apergi et al., 2009).

An example of a CPP that has been proposed to act in an energy independent mechanism is the synthetic peptide transportan. This peptide is a 27 residue variant of the peptide galparan which was derived by fusing the neuropeptide galanin with a wasp venom peptide called mastoparan (Lindgren et al., 2004). Passage of this peptide across the plasma membrane and entry into the cytoplasm is not inhibited by low temperatures (4°C) nor is it blocked by phenylarsine oxide, an inhibitor of clathrin-mediated endocytosis, phagocytosis and macropinocytosis (Dutta & Donaldson, 2012; Lindgren et al., 2004). This peptide is thus presumed to enter through direct penetration, rather than endocytosis (Deshayes et al., 2005).

Although NaD1 is larger than known CPPs, it does have the characteristic positive charge of this peptide family. Also, CPPs can facilitate the entry of much larger proteins. For example, transportan (2.8 kDa) linked to GFP or avidin (27 kDa and 66 kDa, respectively) is still internalised (along with its linked cargo) into cells (Pooga et al., 2001), indicating that this pathway is not size limited.

The proposal that some antimicrobial peptides transit the plasma membrane and act within the cytoplasm is not novel. Several antifungal peptides travel to specific areas of the cell. For example, histatin 5 was co-located with MitoTracker orange in mitochondria of *C. albicans* (Helmerhorst et al., 1999). In another example, the plant defensin Psd1 from *Pisum sativum* co-localises with the nuclear stain DAPI in *F. solani* hyphae. A yeast two-hybrid experiment also identified cyclin F as a possible binding partner of Psd1 in the nucleus. Furthermore, analysis of the DNA content of *N. crassa* conidia after Psd1 treatment indicated that cell cycles had been impaired (Lobo et al., 2007).

This Chapter will focus on the mechanism of uptake of NaD1 into fungal cells using *C. albicans* as a model organism. Uptake of fluorescently labelled NaD1 into yeast cells was monitored by confocal microscopy, to confirm that the three step mechanism of uptake observed in filamentous fungi (cell surface binding, membrane disruption and uptake) was conserved in *C. albicans*. The method of uptake of NaD1 into the cytoplasm of *C. albicans* cells was also investigated using the inhibitors, CCCP and latrunculin A as well as *S. cerevisiae* endocytosis mutants. The involvement of internal protein transport machinery was tested using the inhibitors brefeldin A and nocodazole and *C. albicans* strains with deletions of various components of the ESCRT pathway.

3.2 Materials and Methods

3.2.1 BODIPY-labelling of NaD1

Proteins were labelled on the C-terminus with a BODIPY fluorescent tag as described in van der Weerden et al. (2010). Protein (approximately 2.5 mg in 360 μ L milliQ water) was mixed with 40 μ L of 1 M MES buffer, pH 4.5 prior to addition of 1.5 mg of 4,4-difluoro-5,7-dimethyl-4-bora-3a,4a-diaza-s-indacene-3-propionyl ethylenediamine (BODIPY-FL-EDA, Life Technologies) dissolved in 100 μ L of 0.1 M MES buffer (pH 4.5) and EDC (1-ethyl-3-(3-dimethylaminopropyl)carbodiimide, 40 μ L of a 20 mg/mL stock in 0.1 M MES buffer pH 4.5, Sigma). The mixture was incubated at room temperature in the dark for 2 - 3 h before precipitated protein was removed by centrifugation at 13,000 rpm for 10 min. Excess BODIPY-FL-EDA and EDC was removed from the supernatant using a 3000 MWCO Vivaspin 500 column (Sartorius) spun at 13,000 rpm for 5 min. The centrifugation step was repeated until flow through was clear (with addition of extra milliQ water after each spin). The flow through from the last wash and the labelled peptide were placed in storage at 4°C.

A small amount of BODIPY-NaD1 was purified further using RP-HPLC (1200 series HPLC, ZORBAX 300SB-C8 column, flow rate 3 ml/min, Agilent Technologies) with a 40 min linear gradient of 0–100% Buffer B (60% acetonitrile, 0.089% trifluoroacetic acid). Eluted protein was lyophilised and dissolved in milliQ water. The protein concentration was then determined by BCA protein assay (Pierce) and the protein was stored at 4°C. The BODIPY labelled NaD1 was tested for its ability to inhibit the growth of *F. graminearum* (see Section 3.2.2).

3.2.2 Fungal growth inhibition assays

Growth inhibition assays were performed essentially as described in Broekaert et al. (1990). For *F. graminearum* assays, fungus was grown on half-strength potato dextrose agar (PDA, Becton Dickson) for 14 days before spores were collected by flooding plates with 10 mL of half-strength potato dextrose broth (PDB, Becton Dickinson). Spores were filtered through Miracloth (Merck Millipore), counted using a haemocytometer and diluted to 5×10^4 spores/mL in half-strength PDB. A $5 \times$ stock of the test protein was serially diluted (two-fold), to a final volume of 20 μ L and in triplicate, into the wells of a 96 well microtitre plate (Greiner) by a TECAN Evo100 liquid handling robot. Diluted spores (80 μ L) were

added to the wells of the microtitre plate. Hyphal growth from spores was monitored by measuring absorbance at 595 nm, in a SpectraMAX M5 plate reader (Molecular Devices), using the 9 well-scan. Measurements were taken before and after 24 h incubation at 25°C.

For antifungal assays in the presence of cellular inhibitors, *C. albicans* DAY185 cells were grown overnight in yeast peptone dextrose medium (YPD, 3 mL, 30°C, 250 rpm). The cells from overnight cultures were then counted with a haemocytometer and diluted to 5000 cells/mL with half-strength PDB. Each inhibitor was serially diluted (two-fold) down a 96 well microtitre plate (Greiner) to leave a final volume of 10 µL in each well. The top (final) concentration of each inhibitor was: 40 µM Brefeldin A (Sigma), 20 µM Nocodazole (Sigma) or 20 µM latrunculin A (AdipoGen). A no-inhibitor control was also included. NaD1 (in MilliQ H₂O, 10 µL, 25 µM) was then added to each well to a final concentration of 2.5 µM followed by the cells (80 µL) and an overnight incubation at 30°C. Growth was monitored by measuring absorbance at 595 nm in a SpectraMAX M5 plate reader (Molecular Devices).

For growth inhibition assays with *S. cerevisiae* mutants, strains were obtained from the Yeast MATa collection (Thermo Scientific). Each strain was grown overnight in YPD (30°C, 250 rpm) and then diluted to an OD₆₀₀ of 0.01 with half-strength PDB. NaD1 (20 µL) was serially diluted down a microtitre plate (Greiner) from a top final concentration of 10 µM. Diluted cells (80 µL) were then added and plates were incubated overnight at 30°C prior to measuring absorbance at 595 nm.

For testing the antifungal activity of NaD1 against the *C. albicans* ESCRT mutants (kind gift from Professor Aaron Mitchell, Carnegie Mellon University), the cells were counted using a haemocytometer and diluted to 5000 cells/mL in half-strength PDB. Cells (80 µL) were added to a microtitre plate containing 20 µL of protein (serially diluted from a top concentration of 10 µM). OD₅₉₅ measurements were taken before and after 24 h incubation at 30°C.

3.2.3 Confocal microscopy of *C. albicans* and Fov hyphae

Fusarium oxysporum f. sp. vasinfectum (Fov) spores from a glycerol stock were grown in half-strength PDB for 48 h on a circular mixer at RT. Spores were then filtered through sterile Miracloth (Merck Millipore), counted with a haemocytometer and diluted to 5×10^4 spores/mL in 10 mL of half-strength PDB in a 50 mL tube, before incubation overnight at RT on a circular mixer. Hyphae (200 μ L) from the overnight culture were added to the well of an 8 well μ -slide (Ibidi) and propidium iodide (PI, 5 μ M) was then added to the hyphae and left for 10 min, before addition of BODIPY-NaD1 (5 μ M final concentration). Cells were monitored on a Leica TCS SP2 confocal microscope with excitation of BODIPY at 488 nm (Argon laser, emission detected with a long pass 515 nm filter) and PI at 543 nm (HeNe laser, emission detected with a long pass 590 nm filter). Images were analysed using the image processing software, FIJI (Schindelin et al., 2012).

C. albicans cells were grown overnight in 5 mL of YPD (30°C, 250 rpm). Cells were then diluted in half-strength PDB to an OD₆₀₀ of 0.1. Propidium iodide was added (5 μ M final concentration) to 200 μ L of cells and left for 10 min. BODIPY-NaD1 (10 μ M) was then added and cells were monitored using a Zeiss LSM510/ConfoCor confocal. BODIPY was excited at 488 nm (Argon laser), and emission was detected at 505 to 530 nm. PI was excited at 561 nm (DPSS laser), and fluorescence was monitored at 575 to 615 nm. For time course experiments images were taken every 5 sec. Images were captured using Zen2009 (Zeiss) software and analysed using FIJI (Schindelin et al., 2012).

To ensure that fluorescence in cells was due to uptake of BODIPY labelled protein and not free label, equal volumes of the final BODIPY wash and native unlabelled peptide (10 μ M NaD1) were also added to the *C. albicans* cells and visualised.

For the CCCP experiment, *C. albicans* cells were diluted to an OD₆₀₀ of 0.1 with half-strength PDB and 600 μ L was incubated with 50 μ M CCCP for 2h (30°C, 250 rpm). Cells were pelleted by centrifugation at 3,000 rpm for 5 min and then resuspended in 600 μ L of fresh half-strength PDB. PI (5 μ M) and BODIPY-NaD1 (10 μ M) were then added to 200 μ L of cells and which were visualised on the Zeiss LSM510/ConfoCor confocal microscope (with lasers as described above).

3.2.4 Monitoring of BODIPY-NaD1 uptake into *C. albicans* by flow cytometry

C. albicans DAY185 was grown overnight in 3 mL of YPD (30°C, 250 rpm). Cells were diluted to an OD₆₀₀ of 0.2 in half-strength PDB and grown for several hours until they reached an OD₆₀₀ of 1.0 (30°C, 250 rpm). Cells were then diluted to an OD₆₀₀ of 0.1 in half-strength PDB before 200 µL samples were withdrawn and treated with 0, 5, 10 or 20 µM of BODIPY labelled NaD1. Cells were incubated in the dark for 30 min (250 rpm) before they were washed twice with PBS (by centrifugation, 2 min, 13,000 rpm) and were resuspended in 200 µL of PBS. Cells were analysed using a BD FACSCanto II with excitation at 488 nm and emission detection with a 530/30 filter. Data was analysed using Weasel v3.0 (Walter and Eliza Hall Institute).

For monitoring the effect of CCCP on BODIPY-NaD1 uptake, cells (at an OD₆₀₀ of 0.1 in half-strength PDB) were pre-treated for 2h (30°C, 250 rpm) with 50 µM CCCP (Sigma). Cells were then treated with 10 µM BODIPY-NaD1 for 15 min (30°C, 250 rpm). After incubation, cells were washed twice with PBS (by centrifugation at 13,000 rpm for 2 min) and resuspended in 200 µL of PBS. Cells were then analysed using the BD FACSCanto II as described above.

3.2.5 Confirmation of correct gene deletions in *S. cerevisiae* mutants

PCR analysis was used to confirm that the correct gene had been disrupted in each of the *S. cerevisiae* deletion strains. A small amount of each mutant was scraped from a YPD plate and added to 200 µL of TE. Cells were then incubated at 90°C for 30 min prior to PCR.

Sequences for forward primers for each mutant were obtained from the *Saccharomyces* Gene Deletion Project (http://www-sequence.stanford.edu/group/yeast_deletion_project/downloads.html#strainsavail). The forward (Fw) primer was designed to start amplification 200 – 400 bp upstream of the start codon in the 5' untranslated region (UTR). The kanB primer (CTGCAGCGAGGAGCCGTAAT) amplified from the KanMX4 module which was inserted into the genes of interest (Figure 3.2).

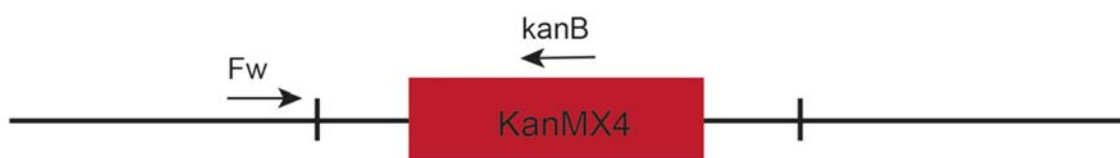


Figure 3.2 PCR with kanB primer

KanB, as well as a forward (Fw) primer for the gene of interest, were used in a PCR with genomic DNA from the deletion mutants to check for insertion of the KanMX4 module into the correct gene.

Treated cells (3 μ L) were added to 12.5 μ L of 2 \times GoTaq master mix (Promega), primers (1 μ L of 10 μ M Fw and kanB) and water, to a total volume of 30 μ L. The PCR conditions were 94°C for 3 min, 30 cycles of 94°C for 1 min, 51°C for 1 min and 72°C for 1 min, followed by 72°C for 7 min. PCR products were separated on a 1% agarose gel.

3.3 Results

3.3.1 Antifungal activity of BODIPY-labelled NaD1

Fluorescently labelled NaD1 was produced to determine whether the uptake of NaD1 that had been reported for *Fov* (van der Weerden et al., 2010; van der Weerden et al., 2008) also occurs in the human pathogen *C. albicans*. The antifungal activity of BODIPY-NaD1 was tested to ensure that the fluorescent tag on the C-terminus had not impaired the activity of NaD1. The IC₅₀ of the labelled NaD1 was the same as the native protein when tested against *F. graminearum* (Figure 3.3).

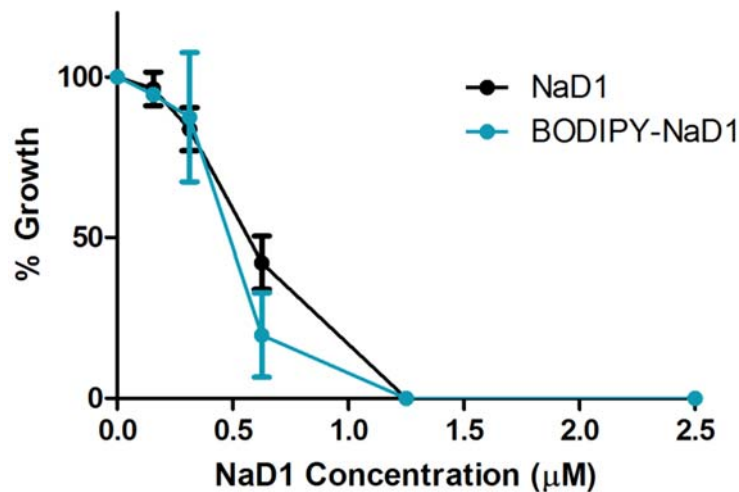


Figure 3.3 The effect of BODIPY-labelled NaD1 on fungal growth

Various concentrations of NaD1 and BODIPY-labelled NaD1 were tested against the plant fungal pathogen *F. graminearum*. Hyphal growth is relative to a no-protein control. Data are from one experiment. Error bars represent SD (n=3).

3.3.2 Uptake of NaD1 into *Fusarium oxysporum f. sp. vasinfectum* hyphae

To confirm that the newly labelled BODIPY-NaD1 was internalised into the cytoplasm in the same manner as previously reported, the BODIPY-NaD1 was tested against Fov hyphae and monitored on the confocal microscope. After 10 min exposure to the BODIPY-NaD1 some, but not all, of the cells in the hyphae had NaD1 in the cytoplasm (Figure 3.4). These cells had also taken up propidium iodide (PI) and had a granular appearance. PI is impermeable and only fluoresces when bound to DNA, making it a marker of cell disruption and viability. Neighbouring cells had NaD1 on the cell surface and appeared viable. That is, the cytoplasm had not become granulated and PI had not entered.

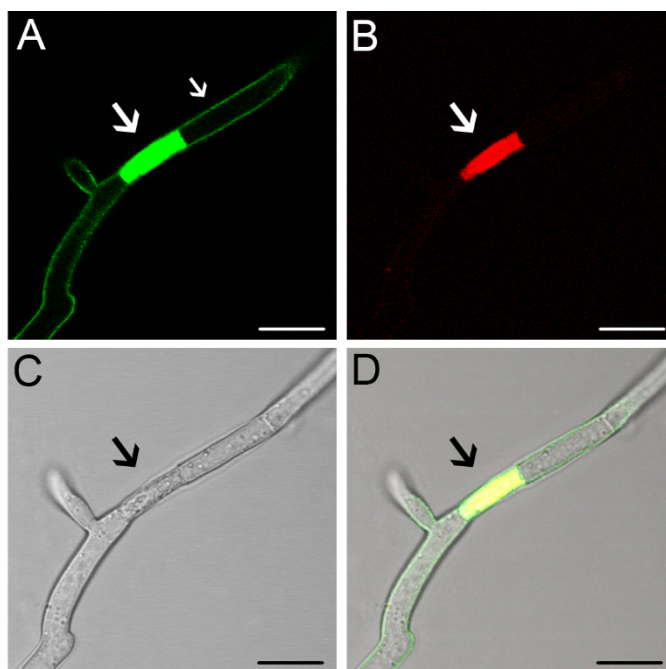


Figure 3.4 NaD1 binds to the cell surface and is internalised into Fov hyphae

Fov hypha treated with BODIPY labelled NaD1 (5 μ M, 10 min) and Propidium iodide. (A) and (B) show BODIPY-NaD1 and PI fluorescence, respectively. A white light image and overlay are shown in (C) and (D), respectively. Arrows mark the area of the hypha which had internalised NaD1 and PI into the cytoplasm. The smaller arrow in (A) point to NaD1 on the cell surface. Scale bars = 20 μ m. Images are a representative example of three independent experiments, which gave equivalent results.

3.3.3 Uptake of NaD1 into *C. albicans*

C. albicans (DAY185) cells were immersed in 10 μ M BODIPY-NaD1 and PI and were observed by confocal microscopy. No fluorescence from BODIPY-NaD1 was observed at time zero (data not shown). The appearance of the cells after 10 min exposure to BODIPY-NaD1 is presented in Figure 3.5. The labelled NaD1 had accumulated on the cell surface, but had not entered the cytoplasm. The cells were still viable (as ascertained by the lack of PI staining).

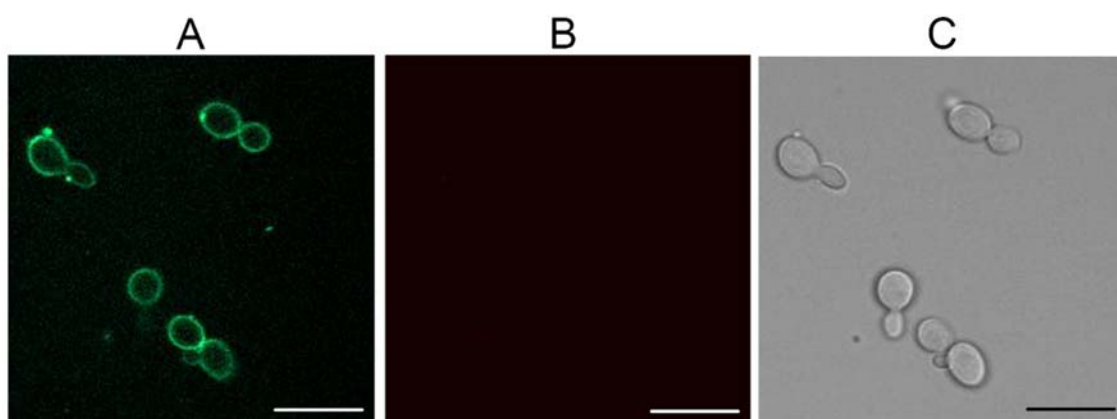


Figure 3.5 BODIPY-NaD1 accumulated on the cell surface of *C. albicans* cells

C. albicans cells 10 min after treatment with 10 μ M BODIPY-NaD1 and 5 μ M PI. (A) BODIPY-NaD1 fluorescence, (B) PI fluorescence and a (C) white light image are shown. Scale bars = 20 μ m. Images are a representative example of three independent experiments, which gave equivalent results.

After a 15 min incubation with the 10 μ M BODIPY-NaD1 and PI mixture, both the BODIPY-NaD1 and PI had entered into the cytoplasm of the yeast cells. Cells which had not taken up the BODIPY-NaD1 had not taken up PI and thus were still viable. Furthermore, these living cells did not have a granulated cytoplasm like the cells which had taken up PI (Figure 3.6).

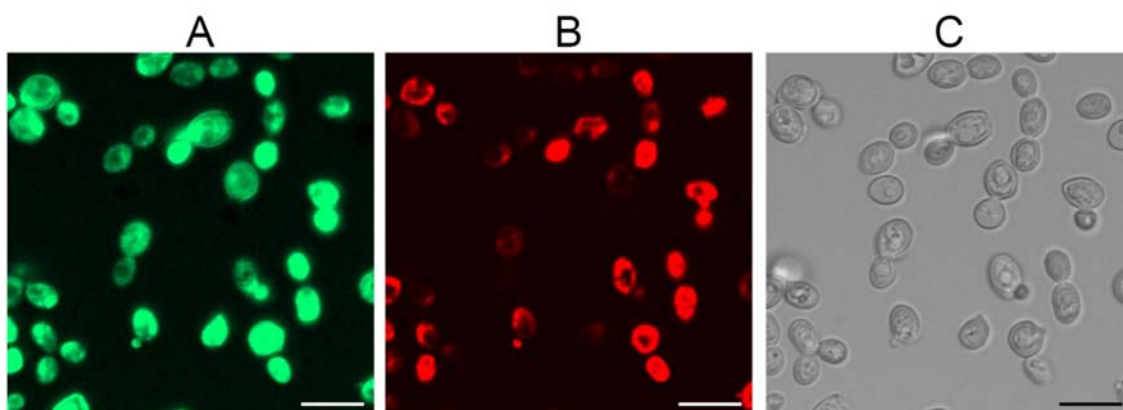


Figure 3.6 NaD1 uptake into *C. albicans* cells

C. albicans cells 15 min after treatment with 10 μ M BODIPY-NaD1 and 5 μ M PI. (A) BODIPY-NaD1 fluorescence, (B) PI fluorescence and a (C) white light image are shown. Scale bars = 10 μ m. Images are a representative example of three independent experiments, which gave equivalent results.

Interestingly, BODIPY-NaD1 uptake into *C. albicans* cells appeared to have occurred prior to PI uptake. The appearance of the cells over a 7 min time course after treatment with BODIPY-NaD1 and PI is shown in Figure 3.7. The cell marked by an arrow in Figure 3.7, had accumulated BODIPY-NaD1 on the cell surface at 3 min. By 5 min, the BODIPY-NaD1 had entered the cytoplasm but no PI uptake was observed. By 7 min, PI had begun to accumulate in the cytoplasm. PI uptake also followed BODIPY-NaD1 uptake in the surrounding cells.

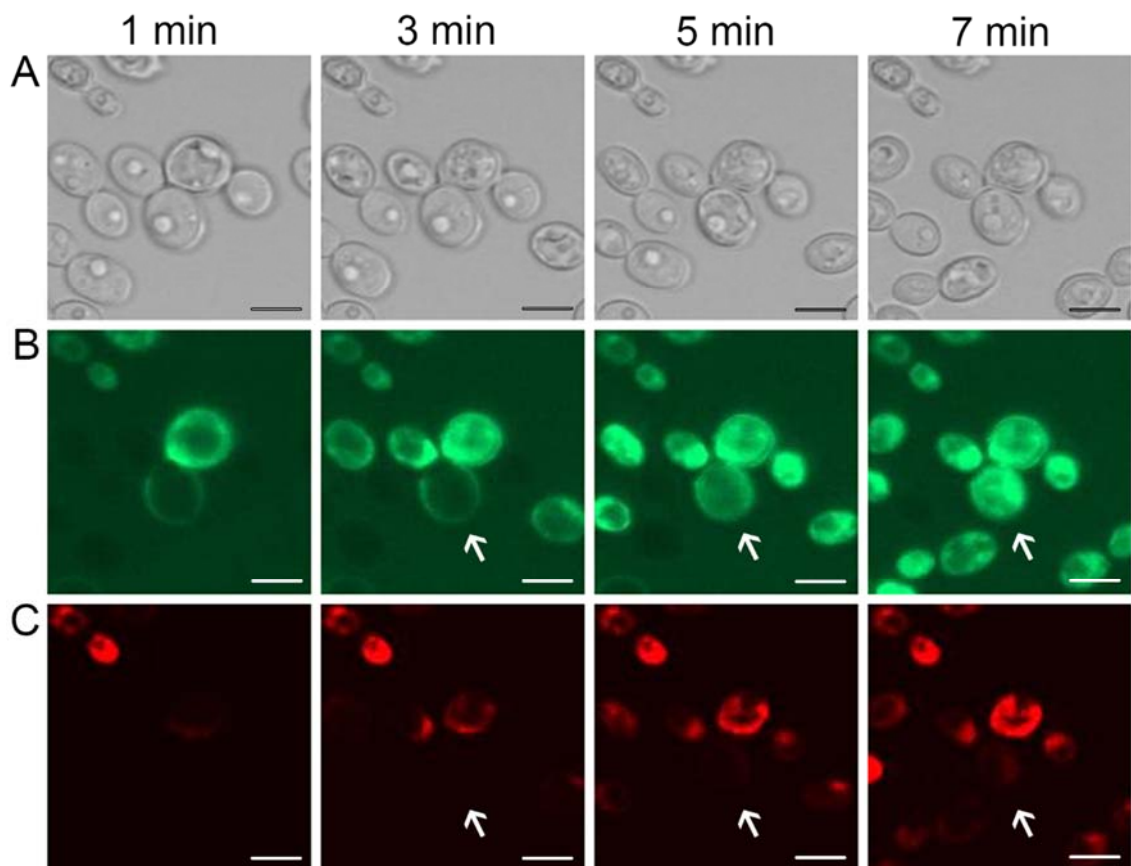


Figure 3.7 BODIPY-NaD1 uptake occurs prior to PI fluorescence

C. albicans DAY185 was treated with 10 μ M BODIPY-NaD1 and 5 μ M PI with images at 2 min intervals. (A) White light, (B) BODIPY-NaD1 and (C) PI images are shown for each time point. The cell marked by a white arrow shows BODIPY-NaD1 uptake prior to PI uptake. The cells which were stained with PI in the first minute of the time course were not viable. Scale bars = 5 μ m. Images are a representative example of three independent experiments, which gave equivalent results.

To confirm that the BODIPY fluorescence in the cytoplasm was due to entrance of NaD1 and not due to any free BODIPY that had remained in the sample after labelling, some of the BODIPY-NaD1 was purified by RP-HPLC. A single peak was collected from the HPLC and microscopy was performed with the purified sample. As with the original *C. albicans* microscopy, all cells which had taken up PI had also accumulated BODIPY-NaD1 in the cytoplasm (Figure 3.8).

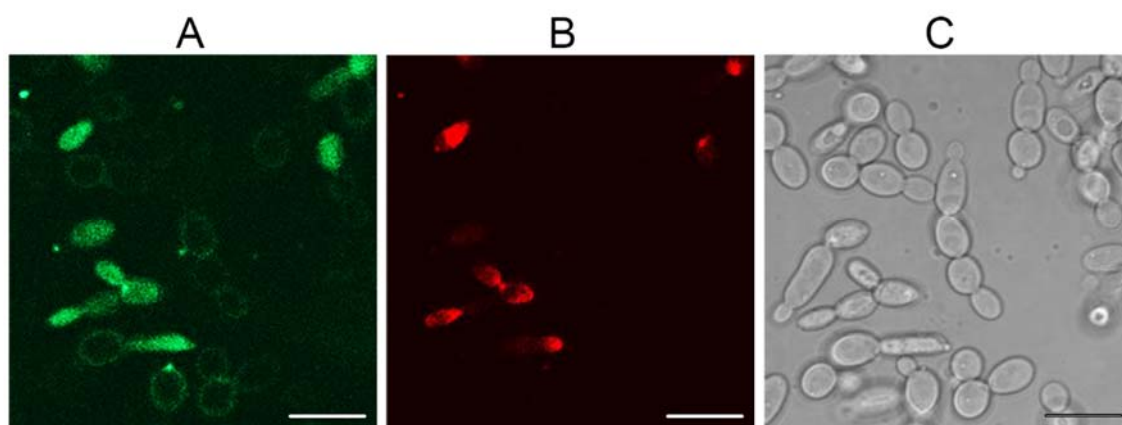


Figure 3.8 Uptake of HPLC purified BODIPY-NaD1 into *C. albicans*

C. albicans cells 14 min after treatment with 10 μ M of HPLC purified BODIPY-NaD1 and 5 μ M PI. (A) BODIPY-NaD1 fluorescence, (B) PI fluorescence and a (C) white light image are shown. Scale bars = 10 μ m. Images are a representative example of three independent experiments, which gave equivalent results.

Uptake of BODIPY-NaD1 into *C. albicans* was also monitored using flow cytometry (Figure 3.9). *C. albicans* DAY185 cells at an OD₆₀₀ of 0.1 were treated with various concentrations of BODIPY-NaD1. After incubation, cells were washed twice to ensure that any BODIPY-NaD1 which had not bound to the cell surface or entered cells had been removed. A concentration dependent increase in fluorescence was observed (Figure 3.9). As the concentration of BODIPY-NaD1 was increased there was a corresponding shift to the right on the flow cytometer, indicating that more cells had a higher level of fluorescence signal and therefore more BODIPY-NaD1 had been retained.

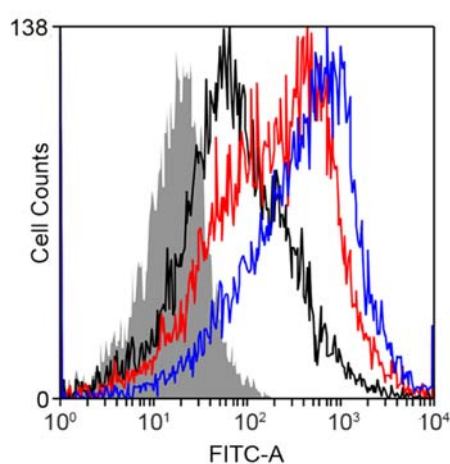


Figure 3.9 BODIPY-NaD1 uptake monitored by flow cytometry

Flow cytometry was used to observe the uptake of fluorescently labelled NaD1 (BODIPY-NaD1) into *C. albicans*. BODIPY-NaD1 was added at 5 μ M (black lines), 10 μ M (red lines) and 20 μ M NaD1 (blue lines) and incubated for 30 min. A no-treatment control is shown shaded in grey. Cells were then washed to leave only BODIPY-NaD1 that had bound to the cell surface or had entered the cells. The vertical and horizontal axes represent cell counts and fluorescent intensity, respectively. Data are a representative example of three independent experiments, which gave equivalent results.

3.3.4 Determination of the mechanism of NaD1 uptake into yeast cells

Inhibitors of endocytosis (latrunculin A) and oxidative phosphorylation (CCCP) were tested with NaD1, to determine whether NaD1 uptake occurs through endocytosis and if uptake is an energy dependent process. *S. cerevisiae* mutants with deletions in several genes important for endocytosis were also tested against NaD1. These mutants had deletion of genes involved in actin regulation and formation of the clathrin coat (Figure 3.10).

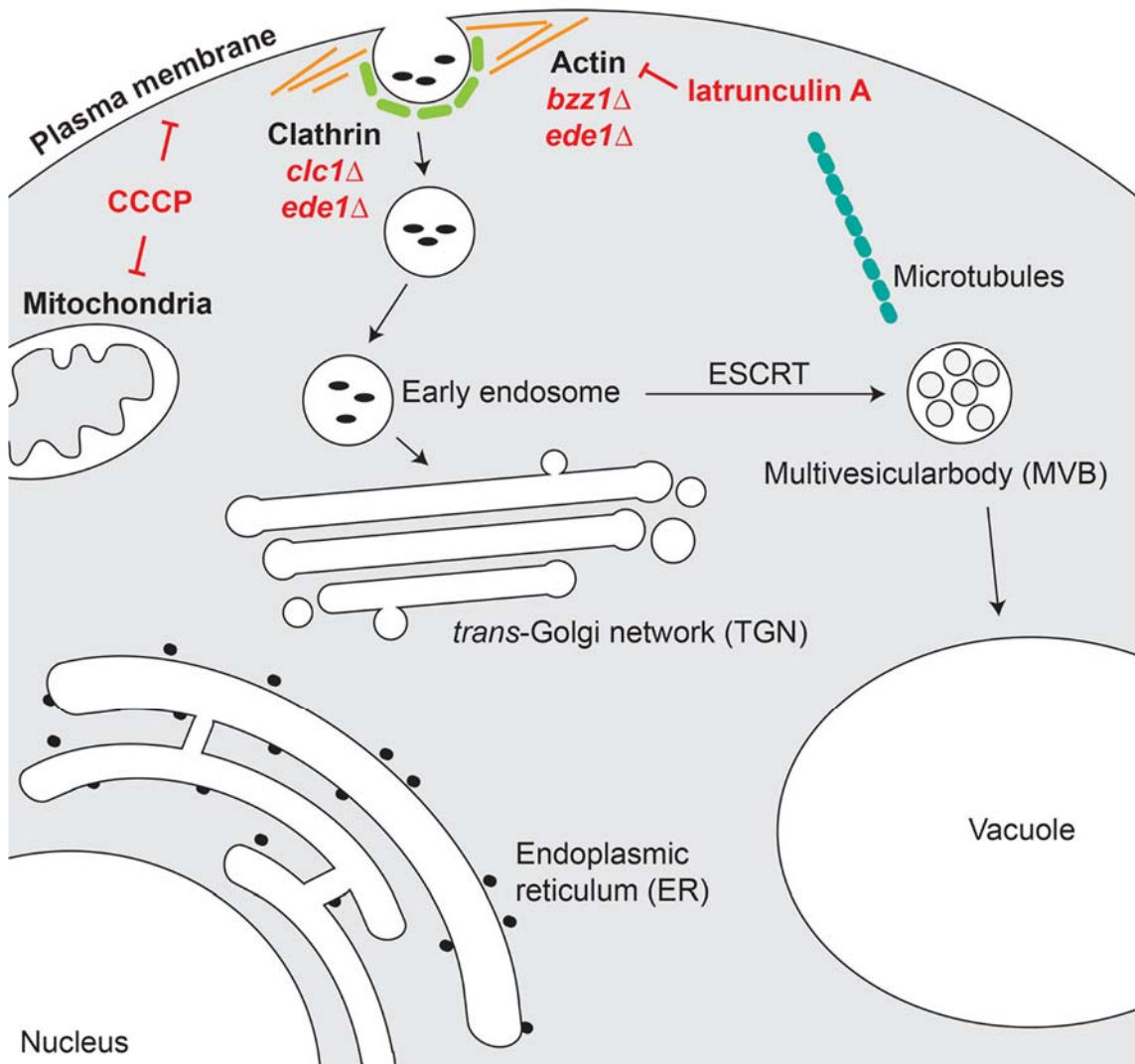


Figure 3.10 Uptake inhibitors and endocytosis deletion mutants

Inhibitors of endocytosis (latrunculin A) and oxidative phosphorylation (CCCP) were tested for their ability to block NaD1 activity. *S. cerevisiae* mutants with deletion of genes involved in the clathrin coat and actin polymerisation were also tested for resistance to NaD1.

3.3.4.1 Latrunculin A

Addition of latrunculin A reduced the ability of NaD1 to inhibit growth of *C. albicans* (Figure 3.11). Latrunculin A rescued *C. albicans* from NaD1 inhibition and reverted cell growth to the level obtained in the latrunculin A only control.

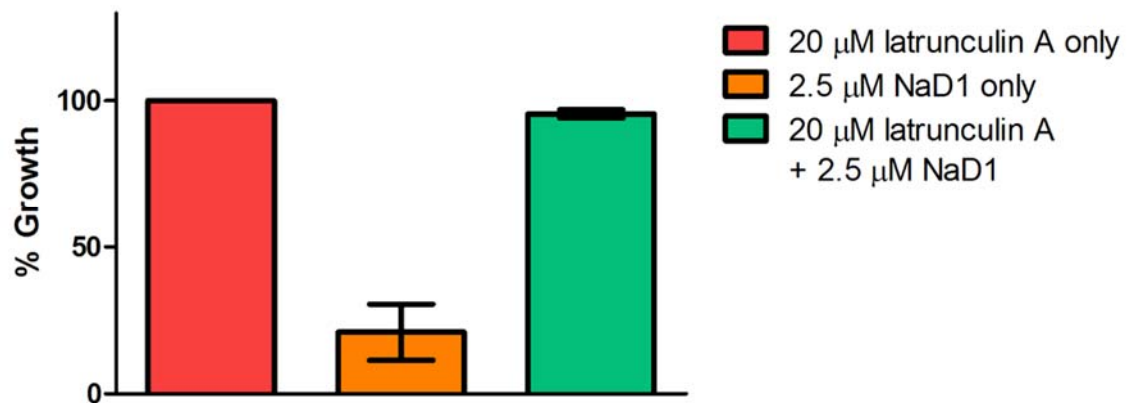


Figure 3.11 Latrunculin A reduces the effect of NaD1 against *C. albicans*

C. albicans DAY185 was treated with 20 μM latrunculin A only, 2.5 μM NaD1 only or 20 μM latrunculin A and 2.5 μM NaD1 in combination. Data are relative to the 20 μM latrunculin A only control. Errors bars represent SEM (n=3).

3.3.4.2 CCCP

In initial growth inhibition assays, the uncoupler of oxidative phosphorylation, CCCP, killed all cells at the concentrations tested (data not shown). However, at the higher cellular density used in flow cytometry assays, 50 μM CCCP affected uptake of BODIPY-NaD1 into *C. albicans* cells (Figure 3.12). This result was confirmed using confocal microscopy (Figure 3.13). Both BODIPY-NaD1 uptake and disruption of the cell membrane (ascertained by lack of PI fluorescence) were reduced after CCCP treatment (Figure 3.13).

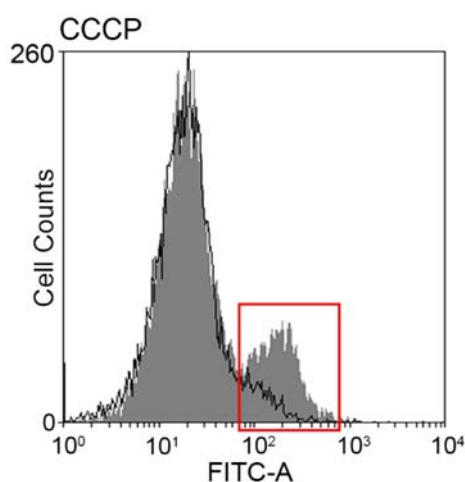


Figure 3.12 Flow cytometry monitoring BODIPY-NaD1 uptake after treatment with CCCP

Flow cytometry was used to observe the uptake of fluorescently labelled NaD1 (BODIPY-NaD1) into *C. albicans* after treatment with CCCP. Cells were pre-treated with 50 μM CCCP for two hours and then incubated with 10 μM BODIPY-NaD1 for 15 min. Black lines are BODIPY-NaD1 (10 μM) plus inhibitor and shaded in grey are NaD1 only controls (10 μM NaD1, no inhibitor). A red box surrounds the peaks which correspond to cells which BODIPY-NaD1 had bound to the cell wall or entered. The vertical and horizontal axes represent cell counts and fluorescent intensity, respectively. Data are representative examples of three independent experiments, which gave equivalent results.

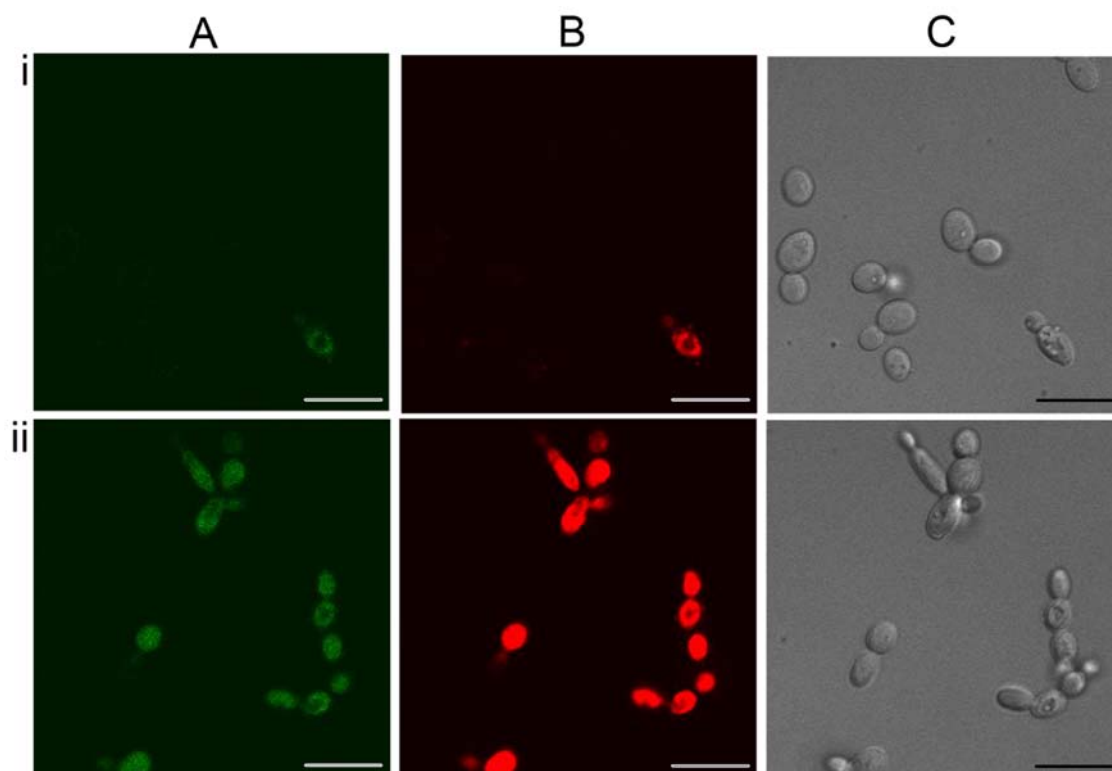


Figure 3.13 Confocal microscopy monitoring BODIPY-NaD1 and PI uptake after CCCP treatment

Confocal microscopy was used to monitor uptake of BODIPY-NaD1 into *C. albicans* DAY185 after pre-treatment with CCCP. (i) CCCP pre-treated cells and (ii) no-inhibitor control cells were treated with 10 μ M BODIPY-NaD1 for 15 min. (A) BODIPY-NaD1 and (B) PI and (C) white light images are shown. Scale bars = 40 μ m. Images are a representative example of three independent experiments, which gave equivalent results.

3.3.4.3 Endocytosis mutants

Several *S. cerevisiae* endocytosis mutants were also screened for resistance to NaD1. These mutants have knockouts in genes that affect the early immobile phase (*ede1Δ* and *clc1Δ*) and the last mobile phase (*bzz1Δ*) of endocytosis (Boettner et al., 2012). Deletion of the genes *EDE1* and *BZZ1* increased the tolerance of the *S. cerevisiae* cells to NaD1 (Figure 3.14A). The phenotypes of both these mutants were NaD1 specific, as they were not resistant to the antimicrobial peptide LL-37 (Figure 3.14B). A *clc1Δ* mutant, which lacks the clathrin light chain, only differed from wildtype at the low concentration of 1.5 μM NaD1. All the mutants were completely inhibited by NaD1 at concentrations above 3.5 μM (Figure 3.14).

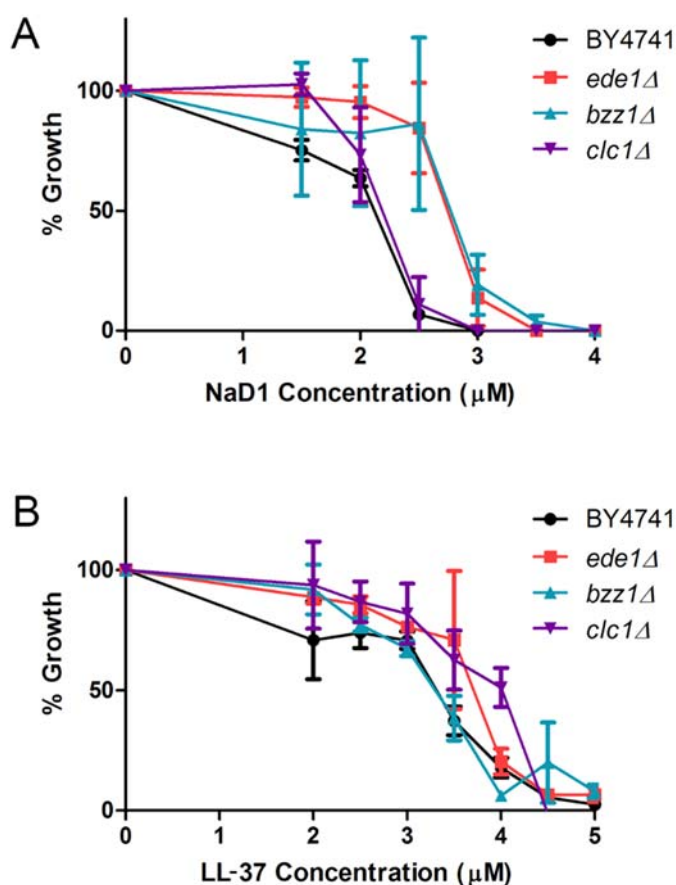


Figure 3.14 The effect of NaD1 on growth of *S. cerevisiae* endocytosis mutants

S. cerevisiae BY4741 (WT), *ede1Δ*, *bzz1Δ*, and *clc1Δ* were treated with various concentrations of (A) NaD1 or (B) LL-37. Data is relative to a no-protein control. Results shown are a representative example of three independent experiments. Error bars represent SD (n=3).

The *S. cerevisiae* endocytic mutants were confirmed by PCR using the KanB primer. The PCR products from *clc1* Δ , *ede1* Δ and *bzz1* Δ matched the expected sizes of 572, 684 and 696 bp, respectively (Figure 3.15). As expected, no amplification was observed in the wildtype.

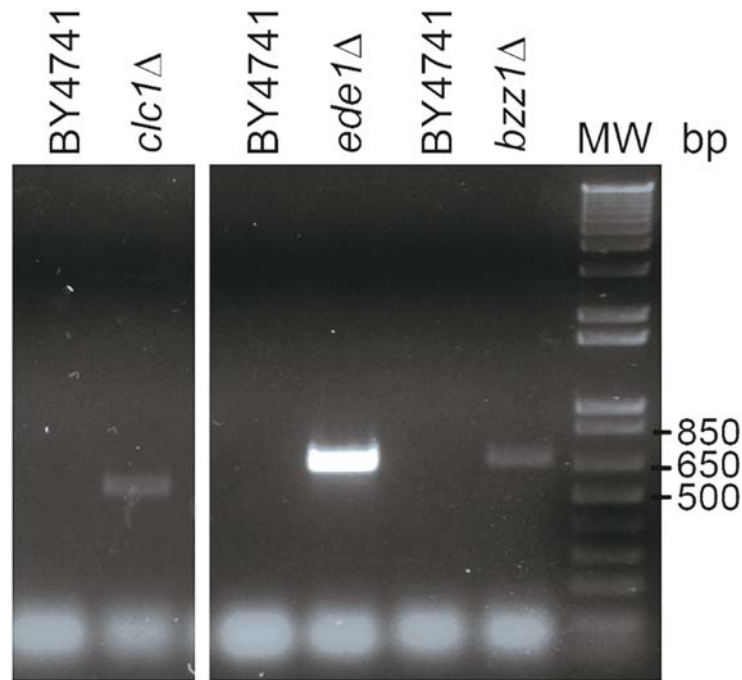


Figure 3.15 PCR check of *S. cerevisiae* *clc1* Δ , *ede1* Δ and *bzz1* Δ mutants

Amplification of genomic DNA from BY4741, *clc1* Δ , *ede1* Δ and *bzz1* Δ strains with KanB primer and *clc1* Fw, *ede1* Fw and *bzz1* Fw primers. Bands of the expected size appeared for all the mutants. As expected, no amplification was observed in the wildtype (BY4741).

3.3.5 Investigation of the involvement of protein transport in NaD1's activity

Since inhibitors of endocytosis and oxidative phosphorylation reduced NaD1 activity, the next experiments were designed to determine whether internal protein transport is required for antifungal activity. Two protein transport inhibitors were tested to determine whether they blocked NaD1 activity in *C. albicans*. The two inhibitors block internal protein transport by inhibiting polymerisation of microtubules (nocodazole) and Golgi/ER function (brefeldin A). *C. albicans* mutants with deletions of genes encoding several ESCRT components were also tested (Figure 3.16).

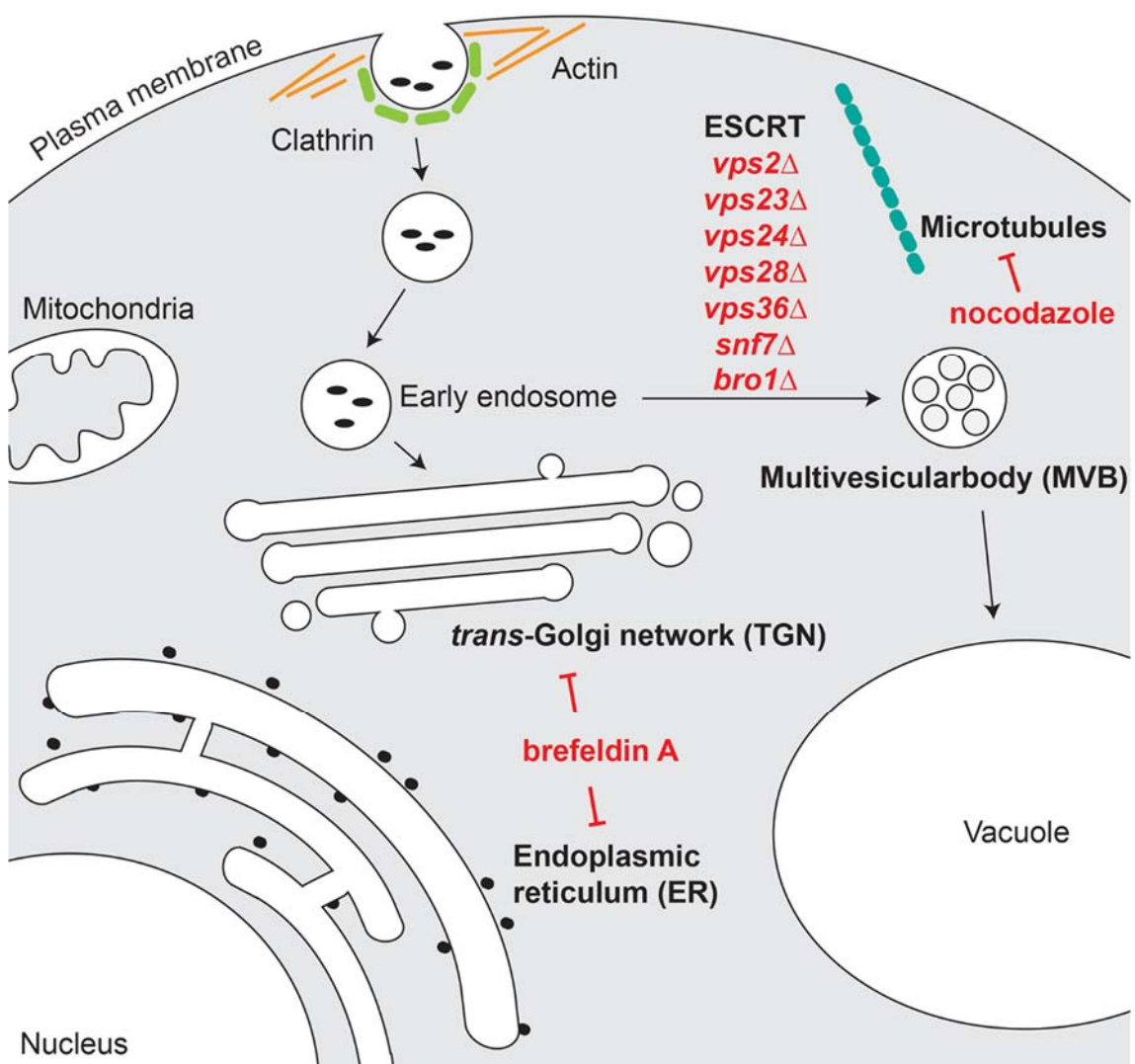


Figure 3.16 Protein transport inhibitors and ESCRT machinery deletion mutants

Two inhibitors of protein transport were tested for their ability to reduce NaD1's antifungal activity. Nocodazole blocks microtubule polymerisation and brefeldin A blocks normal Golgi and ER function. *C. albicans* mutants with deletion of ESCRT machinery genes were also tested for resistance to NaD1.

3.3.5.1 Brefeldin A and nocodazole

NaD1 treatment concurrently with brefeldin A or nocodazole treatment did not reduce the antifungal activity of NaD1 against *C. albicans* (Figure 3.17). The level of growth did not differ in the presence of nocodazole. In the presence of brefeldin A, growth inhibition increased.

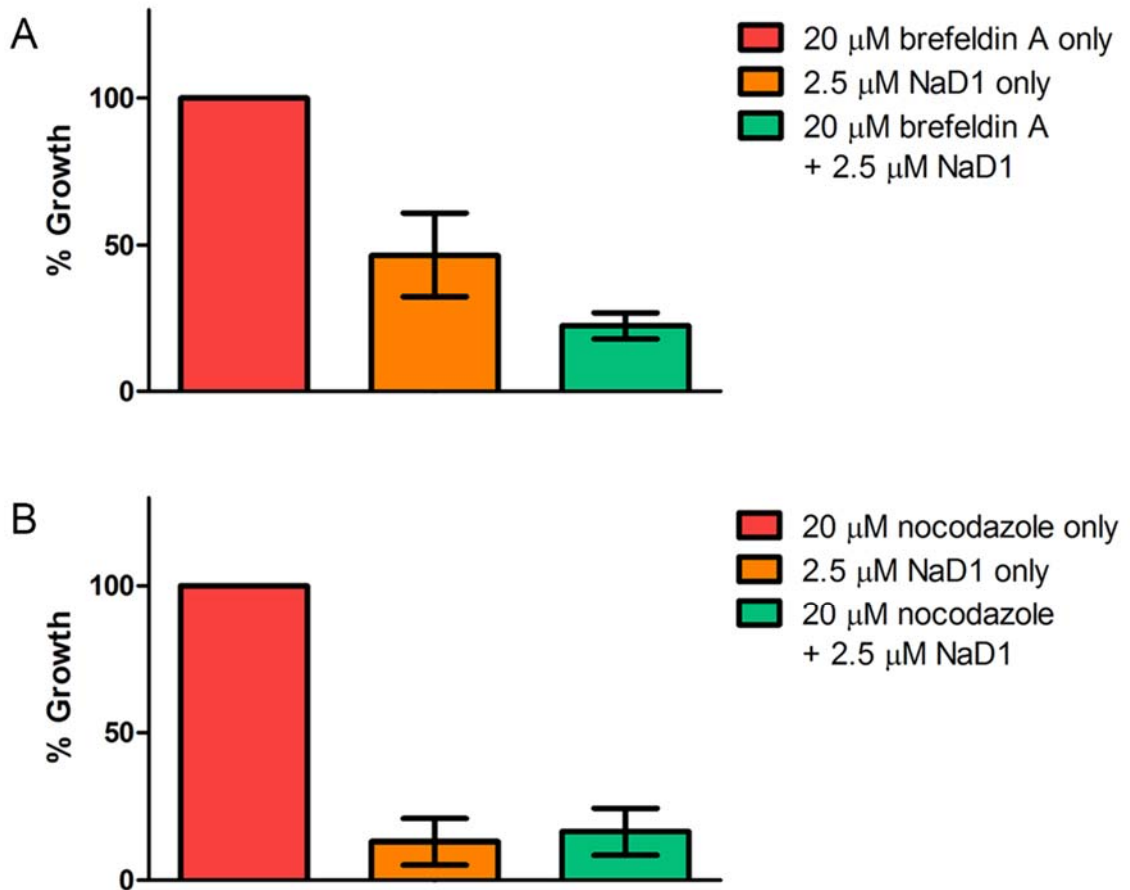


Figure 3.17 Brefeldin A and nocodazole do not affect the activity of NaD1 against *C. albicans*

C. albicans DAY185 was treated with 2.5 μM NaD1 only, inhibitors only or 2.5 μM NaD1 and (A) 20 μM brefeldin A or (B) 20 μM nocodazole in combination. Data are relative to the inhibitor only controls. Errors bars represent SEM (n=3).

3.3.5.2 ESCRT deletion mutants

C. albicans ESCRT mutants were also tested for sensitivity/resistance to NaD1. The growth of the tested mutants did not differ from wildtype when tested with NaD1 (Figure 3.18). Disruption of the correct genes in these mutants had been verified previously by Dr Mark Bleackley (La Trobe University) using PCR.

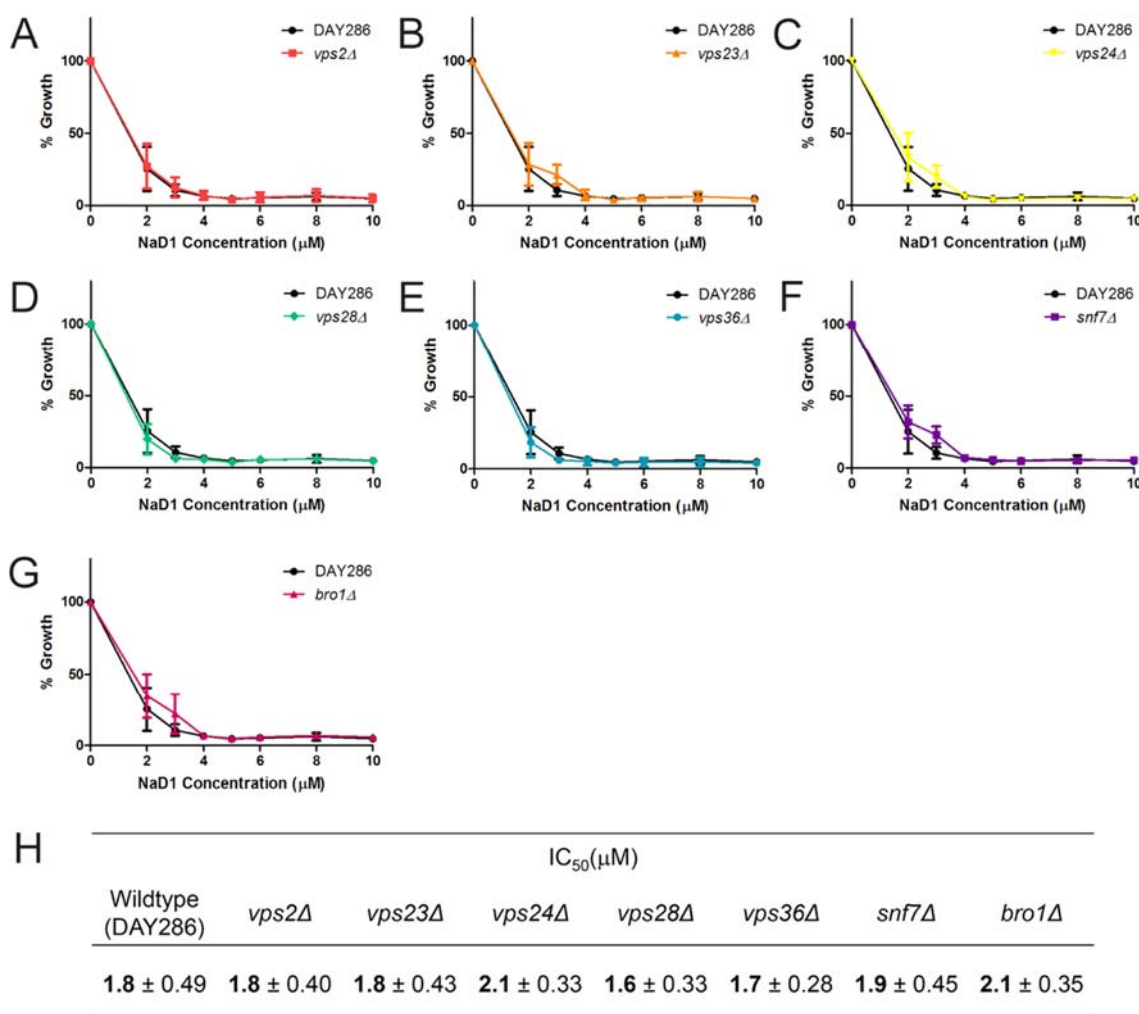


Figure 3.18 The effect of NaD1 on the growth of *C. albicans* ESCRT mutants

C. albicans DAY286 (WT), (A) *vps2Δ*, (B) *vps23Δ*, (C) *vps24Δ*, (D) *vps28Δ*, (E) *vps36Δ*, (F) *snf7Δ* and (G) *bro1Δ* were treated with various concentrations of NaD1. Data is relative to a no-protein control and are from three independent experiments. Error bars represent SEM (n=4). (H) $IC_{50} \pm$ standard deviation of *C. albicans* ESCRT mutants treated with NaD1 (n=4). No values were significantly different from wildtype ($p > 0.05$).

3.4 Discussion

The overall aim of this Chapter was to determine how NaD1 crosses the plasma membrane and enters the cytoplasm of fungal cells. This follows on from observations by van der Weerden et al., who used various procedures, such as monitoring uptake of fluorescently tagged NaD1, immunogold electron microscopy and fractionation of cells, to demonstrate that NaD1 enters the cytoplasm of Fov hyphae (van der Weerden et al., 2008). In this study, uptake of BODIPY-NaD1 into Fov hyphae was confirmed. The uptake of NaD1 was accompanied by PI uptake and cell death within 10 min for some hyphae. The observation that NaD1 entered the cytoplasm and killed cells led to the question of whether NaD1 had only entered the cell after disruption of the plasma membrane and cell death had occurred or whether cell death occurred after NaD1 had entered the cell and interacted with an intracellular target. To address this, experiments were conducted in the yeast *C. albicans*, which was more amenable to time lapse microscopy experiments on the confocal microscope.

A time course experiment with *C. albicans* revealed that BODIPY-NaD1 uptake occurred prior to PI fluorescence. First, BODIPY-NaD1 accumulated on the cell surface of yeast cells. After further incubation, BODIPY-NaD1 began to enter into the cytoplasm of the cells. At this time, no PI fluorescence was observable in the cell. As BODIPY-NaD1 continued to accumulate in the cytoplasm, PI fluorescence was finally apparent. Thus, it is likely that disruption of the cell surface and cell death occurs after NaD1 internalisation. However, there is also the possibility that BODIPY-NaD1 uptake occurs faster than PI uptake, as PI has to reach and bind to DNA before fluorescing.

Having demonstrated that NaD1 enters the cytoplasm, and most likely does so prior to disruption of the plasma membrane, this led to the question of how NaD1 passes through the plasma membrane. Treatment with the endocytosis inhibitor latrunculin A, which blocks formation of actin filaments, reduced NaD1 activity in growth inhibition assays (Figure 3.11). In agreement with this, deletion of *ede1* or *bzz1* in *S. cerevisiae* rendered the yeast less sensitive to NaD1 treatment. The *EDE1* gene is involved in early immobile phase of clathrin mediated endocytosis (CME), and deletion of this gene results in defects in endocytosis and minor alteration to the actin cytoskeleton (Boettner et al., 2012; Gagny et al., 2000). *Bzz1* is involved in the mobile phase of endocytosis and is required for actin polymerisation (Boettner et al., 2012; Galletta et al., 2010). Deletion of the *S. cerevisiae*

clathrin light chain (*clc1Δ*) did not affect NaD1 activity to the same degree as *ede1* and *bzz1* deletion (Figure 3.14). However, deletion of *clc1Δ* resulted in a decreased growth phenotype (Silveira et al., 1990), which made comparisons difficult. Further study is required, including testing a clathrin heavy chain deletion mutant, to determine whether NaD1 uptake is clathrin dependent. In contrast, these mutants were not resistant to LL-37. In support of this data, Ordonez and co-workers (2014) reported that azide has no effect on LL-37 antifungal activity. Together with the *Scede1* and *Scbzz1* data, this indicates that LL-37's mechanism of action does not involve internalisation by endocytosis. A small amount of LL-37 is internalised into *C. albicans* cells after treatment, but this is likely to occur through an energy independent process, and is not believed to be part of LL-37's primary mechanism. Instead, it is hypothesised that cell death occurs through direct membrane permeabilisation (Den Hertog et al., 2005; Ordonez et al., 2014).

Interestingly, binding of LL-37 to actin was recently reported to protect LL-37 from degradation by bacterial proteases. In antibacterial assays with exogenous proteases, LL-37 activity was reduced. However, antibacterial activity was restored if actin filaments were also added (Sol et al., 2014). As *ede1Δ* and *bzz1Δ* mutants were not resistant to LL-37, this indicates that resistance of these mutants to NaD1 was due to disruptions to endocytosis rather than mere blockage of actin polymerisation.

In further support of endocytosis as the mechanism of NaD1's uptake, NaD1 internalisation appeared energy dependent. NaD1 uptake was reduced after addition of CCCP, an uncoupler of oxidative phosphorylation (Figure 3.12, Figure 3.13). In addition, NaD1's antifungal activity was reduced on *S. cerevisiae rho⁰* (petite) mutants, which have reduced mitochondrial function (Hayes et al., 2013).

However, CCCP has multiple cellular effects and as such could decrease the activity of NaD1 through mechanisms aside from decreasing energy available for endocytosis. For example, CCCP reduces the activity and blocks uptake of the human antifungal peptide histatin 5. Mitochondrial petite mutants are also resistant to histatin 5 (Gyurko et al., 2000; Jang et al., 2010). Two distinct mechanisms of uptake have been observed for this peptide. The first involves histatin 5 translocation to the cytoplasm by the Dur3p and Dur31p polyamine transporters (Jang et al., 2010; Kumar et al., 2011). The second involves endocytic uptake and sequestration into the vacuole (Jang et al., 2010). Cells eventually undergo vacuolar expansion and cell death. However, as deletion of genes important for

endocytosis or treatment with latrunculin A does not make cells more sensitive to histatin 5, vacuolar expansion is a secondary effect that does not contribute to toxicity (Jang et al., 2010). In this case, CCCP induced resistance is due to the blockage of energy dependent uptake through polyamine transporters. CCCP treated cells have reduced cytosolic histatin 5 and spermidine uptake was also blocked by the inhibitor (Jang et al., 2010).

Polyamine transporters were also examined as a possible method of uptake for NaD1. Deletion of the polyamine transport regulator Agp2, reduces the antifungal activity of several cationic peptides, including NaD1, h β D2, CP29, BMAP-28 and Bac2a (Bleackley et al., 2014b). Agp2 regulates the expression of many genes, including the polyamine transporters Dur3 and Sam3 (Aouida et al., 2013). Both the antifungal activity and uptake of NaD1 is reduced in *agp2* Δ mutants and addition of spermidine protects against NaD1 induced membrane permeabilisation (Bleackley et al., 2014b). However, deletion of the polyamine transporters themselves (*sam3* Δ , *dur3* Δ and *sam3* Δ *dur3* Δ) does not affect NaD1 activity. This indicates that NaD1 and the other cationic peptides are not internalised by a polyamine transporter, but that a reduction in spermidine uptake results in accumulation of positively charged polyamines at the membrane, which in turn blocks access of positively charged antimicrobial peptides (Bleackley et al., 2014b).

NaD1 could also potentially cross the membrane through a non-endocytic process that is dependent on membrane permeabilisation or direct penetration of the membrane. However, when combined with the data demonstrating that mutants defective in endocytosis have increased tolerance to NaD1, it is most likely that the decreased uptake of, and subsequent resistance to, NaD1 observed in CCCP treated cells was due to less energy being available to drive the endocytic process.

Similar to NaD1, the *Penicillium* antimicrobial peptide PAF also appears to be internalised by endocytosis. An inhibitor of actin polymerisation similar to latrunculin A, called latrunculin B, blocked PAF internalisation into *Aspergillus nidulans* hyphae (Oberparleiter et al., 2003). Also, PAF did not enter cells in the presence of CCCP and uptake of PAF was blocked at 4°C. Collectively, this data indicates that endocytosis is the mechanism of uptake (Oberparleiter et al., 2003).

However, NaD1 itself may not be internalised by endocytosis, but rather a target of NaD1 on the plasma membrane requires turnover or regulation by endocytosis. This occurs with the ether-phospholipid edelfosine in *S. cerevisiae*. Edelfosine is internalised into *S. cerevisiae* cells, but not through endocytosis, and its uptake is not required for toxicity. Instead, edelfosine works by inducing endocytic uptake of the plasma membrane H⁺ pump Pma1p, which is transported to the vacuole for degradation. Treatment of endocytosis mutants with edelfosine resulted in a reduction in antifungal activity, despite the fact that edelfosine uptake was not reduced in these mutants. Instead, blocking endocytosis reduced antifungal activity by stopping internalisation of Pma1p (Cuesta-Marbán et al., 2013). In addition, mutants with deletion of genes encoding proteins required for protein recycling and transport, including ESCRT complexes, resulted in resistance to edelfosine. However, uptake and transport of edelfosine to the ER in these mutants was not altered. Resistance was attributed to higher levels of Pma1p in the membrane as a result of decreased protein turnover in the membranes of these mutants (Cuesta-Marbán et al., 2013). As mutants in the ESCRT pathway are not resistant to NaD1 we can eliminate increased presence of a target protein in the membrane as a mechanism for resistance in endocytosis mutants.

Having established that NaD1 is likely to gain access to the cytoplasm by endocytosis, I wanted to address the question of whether NaD1 is trafficked throughout the cell by endosomal vesicles, like pertussis, ricin and shiga toxins which require retrograde transport to the Golgi for activity (el Baya et al., 1997; Sandvig et al., 2002). Brefeldin A, which inhibits retrograde transport by deforming the protein transport network (Lippincott-Schwartz et al., 1991; Wood et al., 1991), and nocodazole, an inhibitor of microtubule polymerisation, did not affect NaD1 activity against *C. albicans* cells (Figure 3.17). Similarly, mutants with deletion of ESCRT complex components, which are responsible for endosome sorting and production of multivesicular bodies (MVBs) (Henne et al., 2011; Saksena et al., 2007), were not hypersensitive or resistant to NaD1 (Figure 3.18), indicating that retrograde transport is not essential for NaD1's activity and cell wall repair mechanisms are not likely to be required to tolerate NaD1's activity.

Endocytosis may not be the only mechanism by which NaD1 enters into cells. At high NaD1 concentrations a second mechanism of entry may be involved in uptake. The *S. cerevisiae* endocytosis mutants were less sensitive to NaD1 at concentrations below 2.5 μM (Figure 3.14). However, above 3.5 μM NaD1, the *bzz1* and *ede1* deletion mutants were completely inhibited, suggesting that endocytosis may no longer be required for NaD1 activity at these higher concentrations. Perhaps high NaD1 concentrations directly damage the plasma membrane leading to cell death. A similar mechanism may occur with histatin 5 at high concentrations. In energy depleted cells with increased cell wall accumulation of histatin 5, cell death occurs through direct interaction with the membrane. Thus, it has been proposed that histatin 5 causes membrane permeabilisation and lysis at higher concentrations (Jang et al., 2010). However, endocytosis is not completely absent in these mutants, only decreased. At high NaD1 concentrations, the limited amount of endocytosis occurring may still be sufficient to internalise a lethal concentration of NaD1.

In this Chapter I showed that NaD1 is internalised into *C. albicans* cells and this uptake is likely to occur prior to disruption of the cell surface and cell death. I also showed that NaD1 uptake is an energy dependent process, most likely endocytosis. A summary of cellular components essential for NaD1 activity is shown in Figure 3.19.

Since NaD1 is internalised, we have hypothesised that NaD1 has an intracellular target. If an intracellular target could be identified, this would support the hypothesis that NaD1 needs to be internalised for its antifungal activity to occur. In the following Chapter, I describe a screen of a *C. albicans* deletion mutants, performed to gain further insight into NaD1's mechanism of action and to potentially identify an intracellular target.

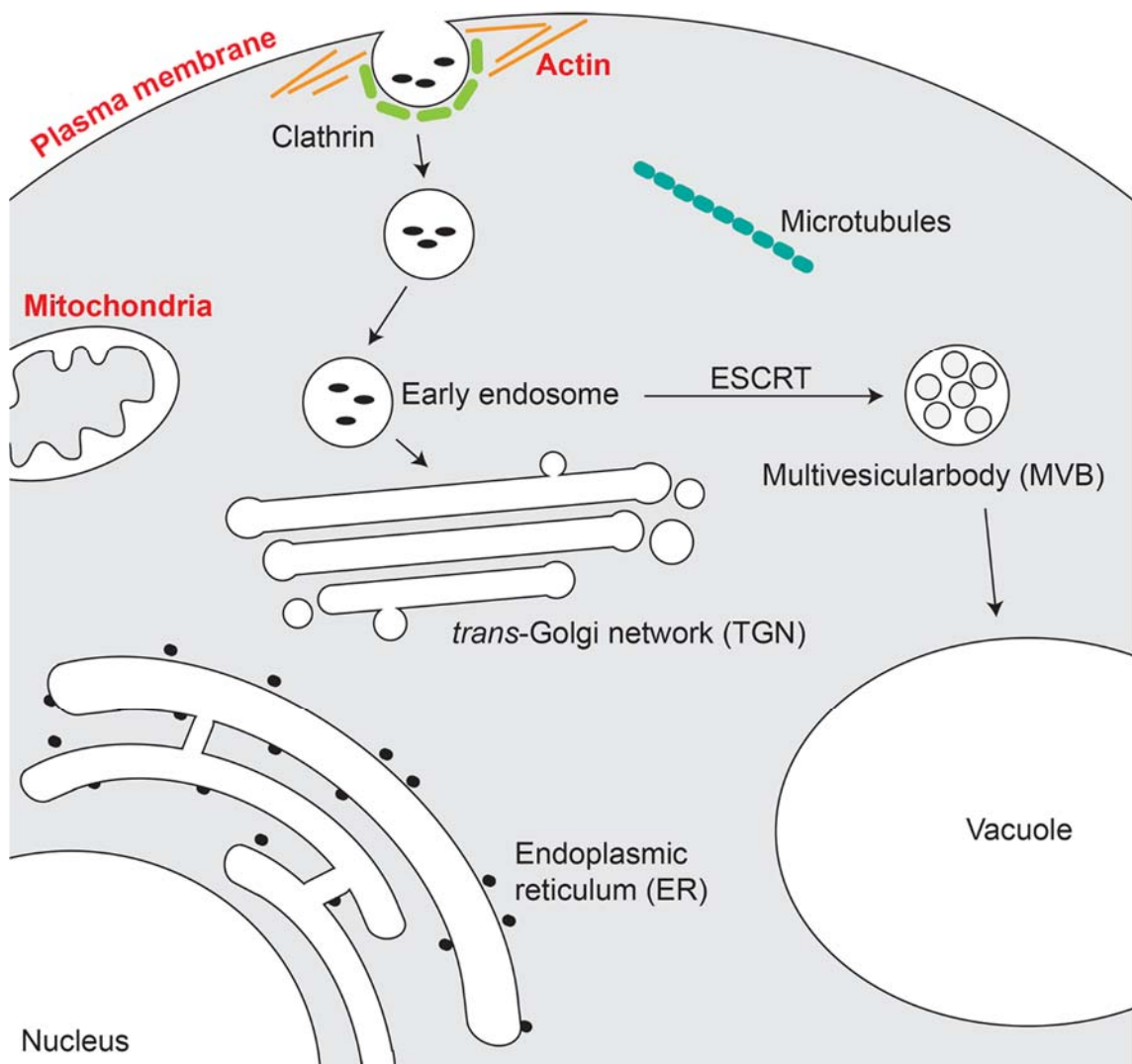


Figure 3.19 Yeast components essential for NaD1 internalisation

Mutants or inhibitors that disrupt ATP production in the mitochondria (or plasma membrane potential) and actin polymerisation reduce NaD1's antifungal activity (in red). Inhibitors that disrupt endosomal sorting trafficking do not affect NaD1 activity.

Chapter 4

Mechanism of action of NaD1 against *Candida albicans*

4.1 Introduction

As discussed in the Introduction to this thesis, the mechanism of action of NaD1 against filamentous fungi involves a three step process which includes interaction with a component of the cell wall, passage through the plasma membrane and entrance into the cytoplasm (van der Weerden et al., 2008). However, many details of this process are unknown. Chapter 2 has a description of the cytotoxic effect of NaD1 on *Candida albicans* and in Chapter 3 I showed that NaD1's antifungal activity is likely to require internalisation and interaction with an intracellular target. In order to gain further insight into the mechanism of NaD1, I employed the advanced genetics and tools that are available for yeast species, but not filamentous fungi. Deletion libraries, for example, are a powerful tool for gaining knowledge of biological mechanisms as they allow experimentation of altered phenotype after disruption of single genes. Yeast are particularly suited for construction of deletion libraries as directed disruptions are possible.

The deletion libraries used in these studies were constructed in *C. albicans* by the Mitchell laboratory (Blankenship et al., 2010; Nobile & Mitchell, 2005; Norice et al., 2007) and were obtained from the Fungal Genetic Stock Center. The three libraries included deletions in genes required for cell wall biosynthesis and cell wall structure, as well as genes encoding kinases and transcription factors. The protein kinase deletion library was constructed for examination of signal transduction pathways, particularly those related to cell wall regulation. The genes that were deleted represent a spectrum of signalling pathways (Blankenship et al., 2010). The transcription factor library was originally constructed for an investigation of biofilm formation and contains deletions in putative transcription factor genes (Nobile & Mitchell, 2005). The cell wall deletion library was also constructed for the study of biofilm formation and consists of deletions in genes predicted to encode cell wall proteins or proteins required for cell wall synthesis (Norice et al., 2007). These libraries did not contain deletions in all genes required for these processes and deletions in essential genes were not included. Nevertheless, screening of these libraries was expected to give some insight into the target or mechanism of NaD1.

Most of the gene deletions were constructed by transposon insertion. As *C. albicans* is diploid, production of homozygous deletions required two rounds of disruption to knockout both alleles of the gene (Enloe et al., 2000; Hernday et al., 2010). The transposon insertion mutants were created using the UAU1 cassette method in the BWP17 strain (which is an *arg4*, *ura3* and *his1* auxotroph). This method is unique in that only a single transformation is required to yield homozygous deletions. The procedure utilises a transposon (Tn7) that is linked to a UAU1 (*ura3-ARG4-ura3*) cassette. The full gene of interest is cloned from *C. albicans* and the Tn7-UAU1 cassette is inserted into the open reading frame (ORF). The ORF containing the Tn7-UAU1 cassette is then transformed into the BWP17 strain where it is inserted into the gene of interest to produce a heterozygous mutant (Blankenship et al., 2010; Enloe et al., 2000; Nobile & Mitchell, 2009; Norice et al., 2007). This UAU1 cassette contains functional *ARG4* and two halves of non-functional *URA3* which share some homologous sequence allowing for excision of *ARG4* and recombination of an intact *URA3* gene. During the first allele disruption, the transposon and UAU1 cassette are inserted into the gene of interest. As the UAU1 cassette contains a functional *ARG4*, transformed strains can be selected on arginine deficient medium. The yeast can then become homozygous for the UAU1 cassette through gene conversion or spontaneous mitotic recombination events. Some of the homozygous transformants will recombine the *URA3* marker, excising *ARG4*, resulting in an *ARG4+*, *URA3+* phenotype. Homozygous mutants are then selectable on arginine and uracil deficient medium (Figure 4.1) (Enloe et al., 2000; Nobile & Mitchell, 2009).

Some mutants were also constructed using two rounds of transformation. In this method the *URA3* and *ARG4* selectable markers are flanked by 100 bp of DNA that is homologous to the 3' untranslated region (UTR) and 5' UTR of the gene of interest. After the first transformation the *URA3* marker is inserted by homologous recombination leading to removal of the first allele of the gene of interest. A second transformation with the *ARG4* marker then replaces the second allele (Figure 4.2) (Hernday et al., 2010).

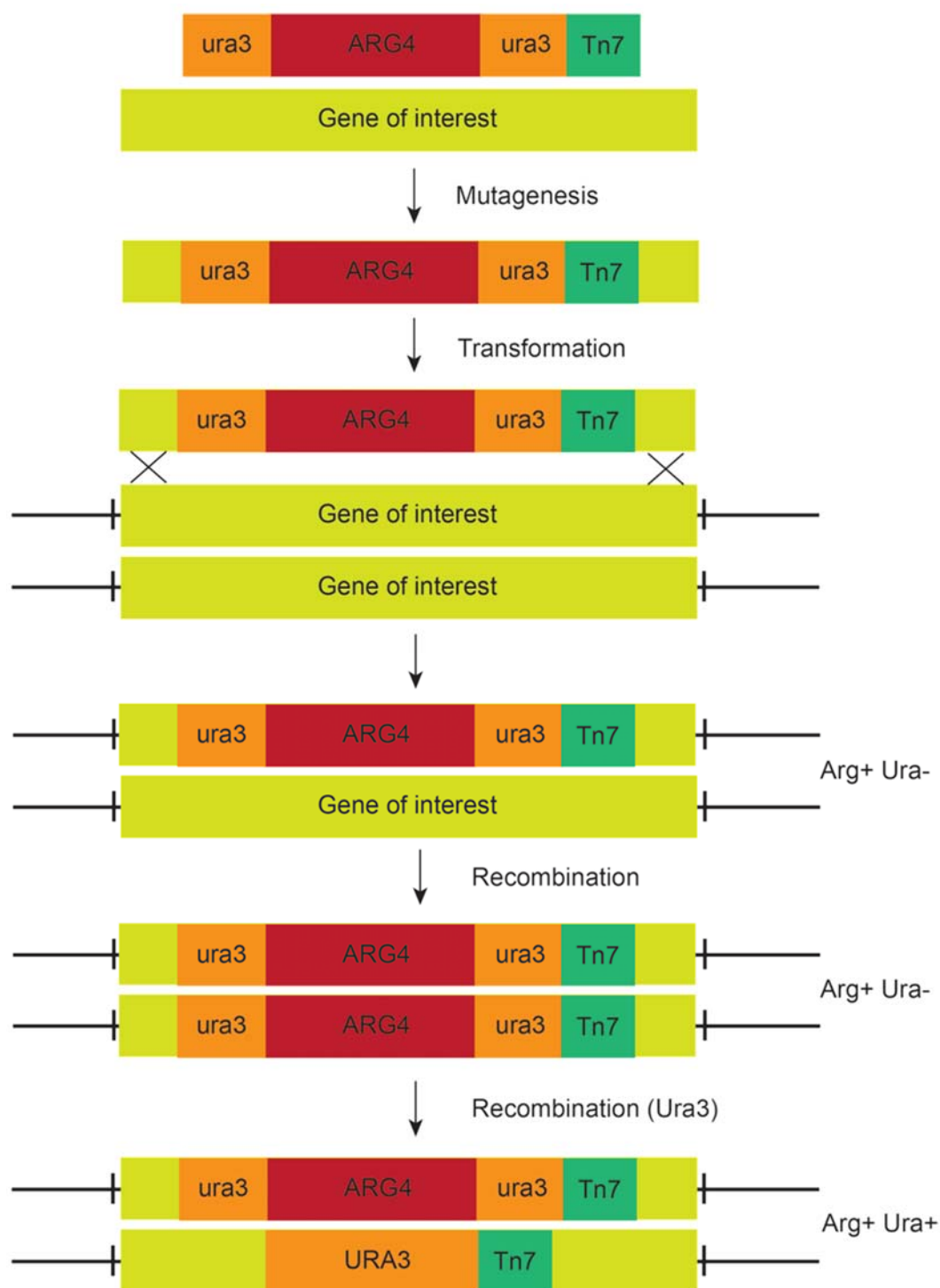


Figure 4.1 Transposon insertion method of gene deletion used to construct *C. albicans* homozygous deletion mutants

The *Tn7* transposon and *UAU1* cassette are inserted into the ORF of interest using transposon mutagenesis. The ORF-*UAU1*-*Tn7* is then transformed into *C. albicans*. The 1st allele is replaced by the insert containing the intact *ARG4* gene and two inactive halves of *URA3*. Resulting colonies are *ARG4+*, *ura3-*. Homozygotes are produced by spontaneous recombination events which result in an intact *URA3* gene. Homozygous deletion colonies are *ARG4+*, *URA3+*.

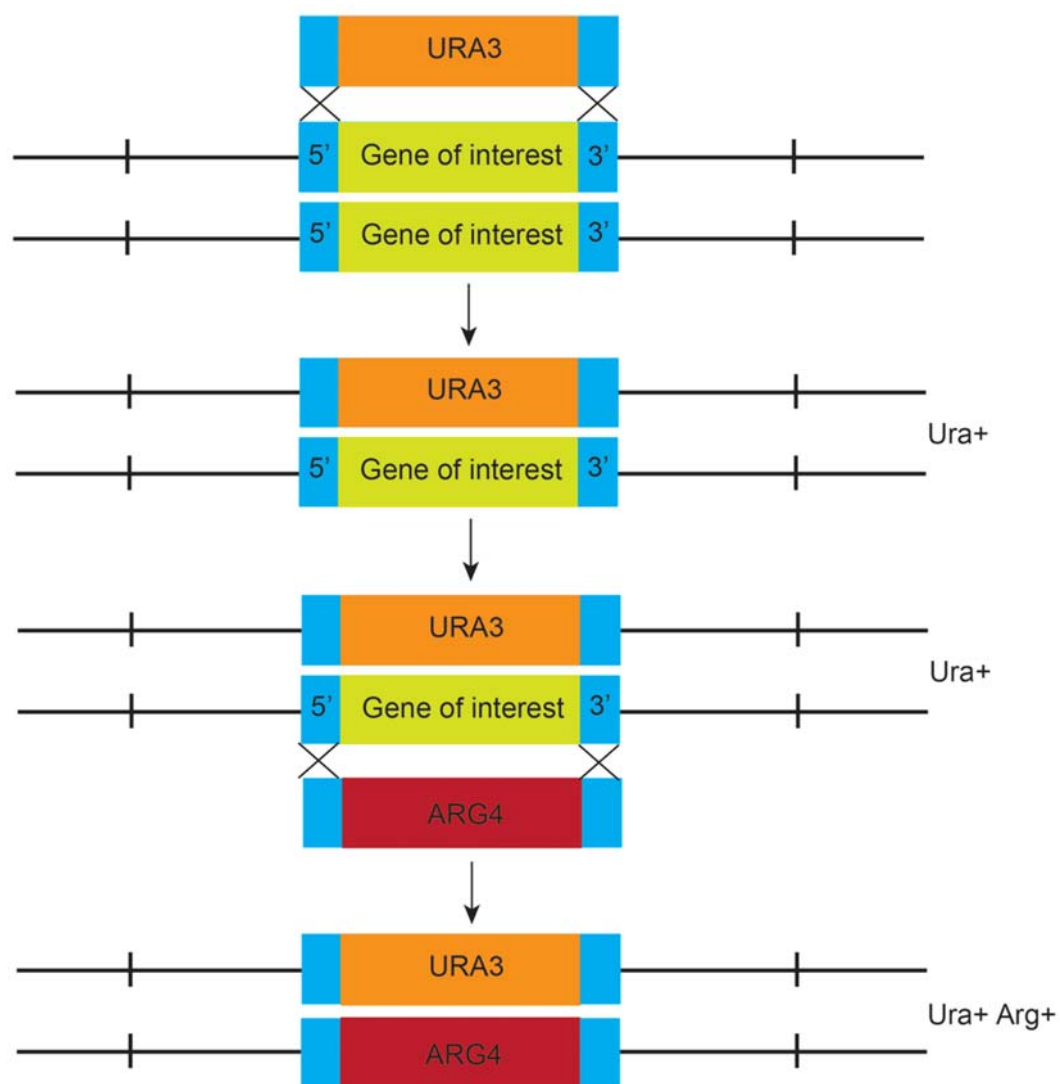


Figure 4.2 Homologous recombination method of gene deletion used to construct *C. albicans* homozygous deletion mutants

Selectable markers are flanked by regions homologous to the 5' and 3' UTR of the gene of interest. The *URA3* gene is first inserted into the gene of interest by homologous recombination. A second round of homologous recombination is used to insert the *ARG4* marker into the second allele.

The cell wall and kinase libraries contain two independent deletion mutants for each gene of interest. This gives increased confidence in positive hits if both independent copies share the same phenotype. The libraries were screened for both sensitivity and resistance to NaD1. Resistant mutants would most likely have disruptions of genes which are targets for NaD1 and required for its antifungal activity. Sensitive mutants are likely to be disrupted in genes that serve as tolerance mechanisms for survival of the yeast after NaD1 exposure.

Although the libraries contain only a small subset of non-essential genes, these libraries were still able to give interesting information about the interaction between NaD1 and the fungal cell. Most of the work described in this Chapter has been published in Hayes et al, (2013) (Appendix AI).

4.2 Materials and Methods

4.2.1 *C. albicans* deletion library screen

C. albicans homozygous transposon deletion libraries were prepared by the Mitchell laboratory (Blankenship et al., 2010; Nobile & Mitchell, 2005; Norice et al., 2007) and were obtained from the Fungal Genetic Stock Center. These libraries were constructed by transposon insertion into the BWP17 strain background (*ura3::imm434/ura3::imm434 iro1/iro1::imm434 his1::hisG/his1::hisG arg4/arg4*), resulting in homozygous mutations. The libraries were obtained in 96 well microtitre plates and were stored in 20% glycerol. Plates were duplicated using an Agilent Bravo robot. *C. albicans* mutants (5 μ L) were inoculated into 100 μ L of fresh yeast peptone dextrose (YPD, in microtitre plates) and grown overnight, at 30°C with shaking. Overnight cultures were then diluted 1/20,000 in 100 μ L half-strength potato dextrose broth (PDB, approximately 5000 cells/mL) containing NaD1. NaD1 was added to the wells at a final concentration of 2 μ M or 5 μ M (Figure 4.3). These concentrations were selected because they were slightly lower and greater than the IC₅₀ of NaD1 (2.3 μ M, Chapter 2). Plates were incubated for 24 h at 30°C and growth was monitored by measuring OD at 595 nm using a SpectraMAX M5e plate reader (Molecular Devices). For mutant screening, the wildtype strain was DAY286 (*ARG4+*, *URA3+*, *his1-*) (Davis et al., 2002). Growth of mutants in the presence of NaD1 was compared to no-protein controls. The screen was repeated three times. An OD₅₉₅ of 0.1 was used as a cut-off value when selecting sensitive and resistant mutants. To confirm hits, IC₅₀ values were obtained using fungal inhibition assays as described in Section 2.2.5.

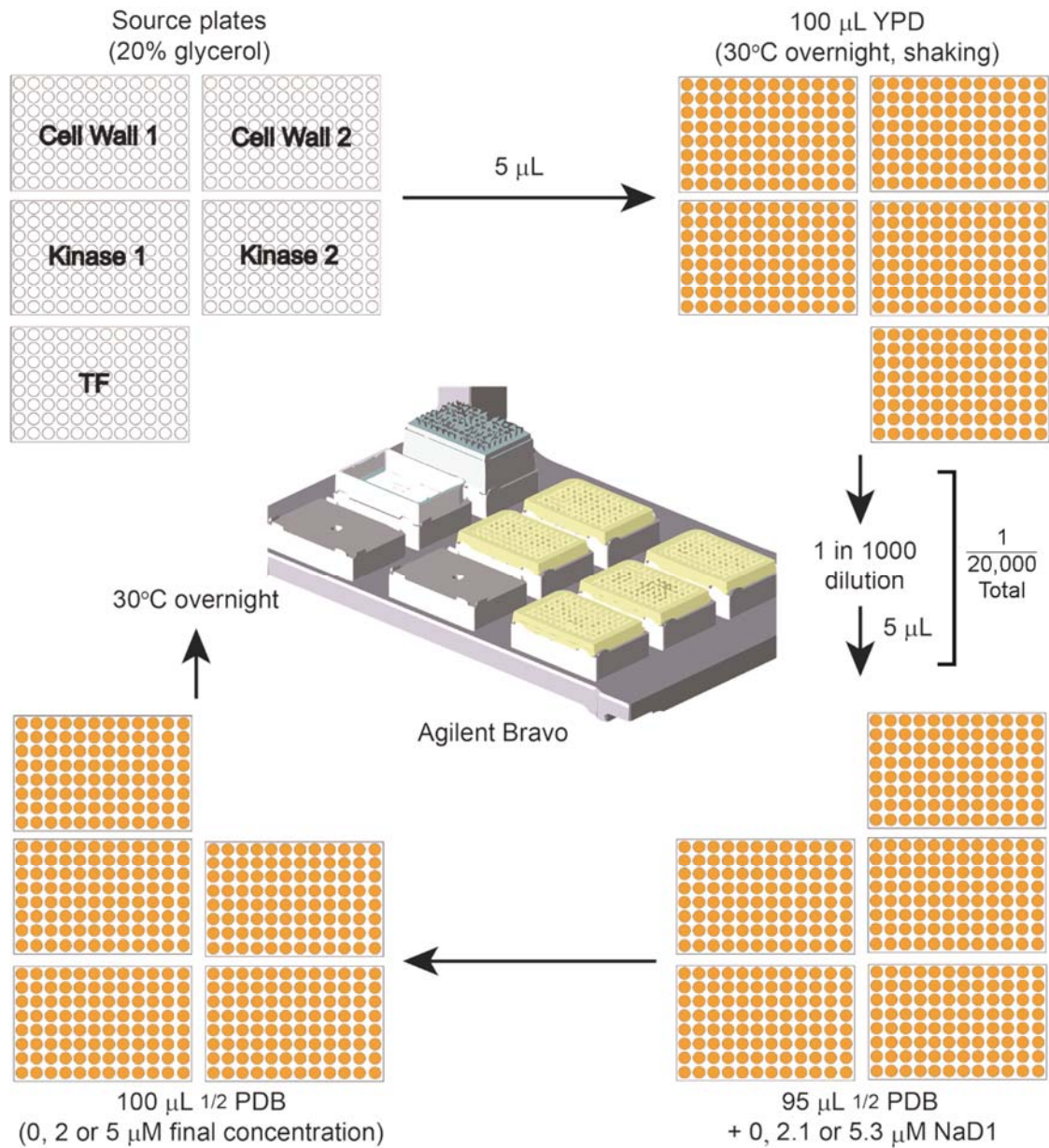


Figure 4.3 Sample preparation for *C. albicans* library screens

Microtitre plates containing *C. albicans* mutants were duplicated using an Agilent Bravo robot, diluted 1/20,000 into 1/2 PDB and containing NaD1.

4.2.2 Complementation of *C. albicans* *HOG1* and *PBS2* genes

4.2.2.1 Genomic DNA extraction from *C. albicans*

C. albicans genomic DNA was extracted using a method modified from Biss et al. (2014). *C. albicans* (BWP17) cells from overnight cultures (5 mL, 50 mL tubes) were pelleted by centrifugation (4000 rpm, 5 min). The cells were disrupted by addition of 200 μ L of buffer A (2% Triton X-100, 1% SDS, 100 mM NaCl, 10 mM Tris-HCl pH 8, 1 mM EDTA pH 8), 200 μ L phenol: chloroform: isoamyl alcohol (25:24:1) and 200 μ L of glass beads (180 μ m, Sigma) followed three 1 min cycles in a bead-beater (placed on ice for 1 min between each run). TE buffer (200 μ L, 10 mM Tris-HCl pH 8.0, 0.1 mM EDTA) was then added and the samples were centrifuged for 5 min at $10,000 \times g$. The supernatant was removed, added to 1 mL of 100% ethanol (RT) and mixed by inversion. Samples were spun for 2 min at $4,000 \times g$ and the DNA pellet was resuspended in of 400 μ L TE. Ammonium acetate (10 μ L, 4 M) and 1 mL of 100% ethanol were then added and mixed by inversion. The samples were centrifuged again at $4,000 \times g$ (2 min), the supernatant was removed and the pellet was air dried and resuspended in 50 μ L TE.

4.2.2.2 Cloning of *PBS2* and *HOG1* genes from *C. albicans*

PBS2 and *HOG1* genes were amplified from genomic DNA (from Section 4.2.2.1). For amplification of each gene, the forward primer (Fw) was designed to begin amplification 1000 bp upstream of the starting ATG (within the 5' untranslated region [UTR]). The reverse primer (Rv) was designed 500 bp downstream of the STOP codon (in the 3' UTR). Each primer also contained 40 bp from the multiple cloning site (MCS) of the pDDB78 vector (underlined sequence).

For amplification of the *PBS2* gene, the following primers were used:

Fw: TTCACACAGGAAACAGCTATGACCATGATTACGCCAAGCTTAAAACA
 GTTTCTAAATAGTCTG and Rv: TCGACCATATGGGAGAGCTCCCAACGCGTT
GGATGCATAGGTCGAATTAATTAGACGTGATT.

The following primers were used for the amplification of the *HOG1* gene:

Fw: TTCACACAGGAAACAGCTATGACCATGATTACGCCAAGCTCTTAAAGA
TTCATCCAATGATGG and Rv: TCGACCATATGGGAGAGCTCCCAACGCGTTG
GATGCATAGCAGAAGACAATCTTTTGAACTAT.

PCR was performed using Expand High Fidelity Polymerase (Roche). Expand Polymerase (1 μ L) was added to 1 μ L of genomic DNA, along with 0.5 μ L 25 mM dNTPs, 3 μ L 25 mM MgCl₂, 5 μ L Expand buffer (10 \times) and primers (1 μ L of Fw and Rv), to a total volume of 50 μ L.

The PCR conditions were 94 $^{\circ}$ C for 3 min, 35 cycles of 94 $^{\circ}$ C for 45 sec, 50-55 $^{\circ}$ C for 30 sec (50 $^{\circ}$ C *HOG1*, 55 $^{\circ}$ C *PBS2*) and 68 $^{\circ}$ C for 4 min, followed by 68 $^{\circ}$ C for 7 min. The PCR product (5 μ L) was then examined by electrophoresis on a 1% agarose gel to check for successful amplification of the genes.

4.2.2.3 Preparation of linearised pDDB78 vector for insertion of HOG1 and PBS2 PCR products

The pDDB78 vector (2-3 μ g) was digested with *NotI* (Promega) and *EcoRI* (Promega). The digestion was performed in a final volume of 50 μ L, which included 1 μ L of both *NotI* and *EcoRI*, 5 μ L of 10 \times buffer H (Promega), 5 μ L of 10 \times BSA and pDDB78. After overnight incubation at 37 $^{\circ}$ C, 5 μ L was run on a 1% agarose gel to check for successful digestion.

4.2.2.4 Transformation of PCR product and digested pDDB78 into *S. cerevisiae* BY4741 Δ trp

Linearised pDDB78 (Section 4.2.2.3) and the *HOG1* and *PBS2* PCR products (Section 4.2.2.2) were transformed into *Saccharomyces cerevisiae* for circularisation and homologous recombination. A 5 mL culture of BY4741 Δ trp was grown overnight in YPD at 30°C. From this culture, 500 μ L was transferred to a microfuge tube (per transformation) and spun at 3000 rpm for 5 min. The supernatant was discarded and then 45 μ L of the amplified *HOG1* and *PBS2* DNA, 12 μ L of linearised pDDB78 and 10 μ L of calf thymus DNA (pre-heated to 95°C for 10 min) was added. The tube was vortexed briefly and then 500 μ L PLATE (40 % PEG, 0.1 M LiOAc, 1x TE) was added. Cells were left stationary at 30°C overnight. The following day cells were spun at 3000 rpm for 5 min and the pellet was washed with 1 mL of milliQ water. The cells were then resuspended in 100 μ L of milliQ water and spread onto tryptophan dropout plates (see Appendix AII). Plates were incubated at 30°C for 3 days.

4.2.2.5 Miniprep to isolate pDDB78-PBS2 and pDDB79-HOG1 plasmids from BY4741 Δ trp

Colonies were selected from tryptophan dropout plates (Section 4.2.2.4) and grown in 10 mL of minus tryptophan medium at 30°C overnight. Plasmid DNA was isolated using the Qiagen ‘QiaPrep’ kit. The manufacturer’s method was altered to include a bead-beater step. In brief, after addition of buffer P2 (Qiagen), 250 μ L of glass beads (180 μ m, Sigma) were added. The tube was placed in a bead-beater for 2 min, incubated on ice for 1 min, and then placed back into the bead-beater for a further 2 min. The samples were then incubated on ice for 5 min before plasmid DNA isolation was continued according to the manufacturer’s protocol.

4.2.2.6 Transformation of *E. coli* with pDDB78-PBS2 and pDDB78-HOG1

Plasmid DNA, isolated as described in Section 4.2.2.5, was transformed into NEB 10-beta Competent *E. coli* cells (New England Biolabs) according to the manufacturer’s protocol.

4.2.2.7 Plasmid purification from *E. coli*

Colonies were picked, placed into 5 mL of LB ampicillin medium and grown overnight at 37°C. Plasmid DNA was isolated from the *E. coli* (Section 4.2.2.6) using the Wizard Plus SV miniprep DNA Purification kit (Promega).

4.2.2.8 Screening of pDDB78-PBS2 and pDDB78-HOG1

Plasmids were screened for correct insertion of genes by PCR. Plasmid (1 µL from Section 4.2.2.7) was added to 1 µL of Expand polymerase (Roche), 5 µL of 10 × Expand buffer (Roche), 3 µL 25 mM MgCl₂, 0.5 µL 25 mM dNTPs, primers (1 µL of Fw and Rv, from Section 4.2.2.2) and water, to a total volume of 50 µL. The PCR conditions were 94°C for 3 min, 30 cycles of 94°C for 45 sec, 50°C for 30 sec and 68°C for 3.5 min, followed by 68°C for 7 min. The PCR products were separated on a 1% agarose gel.

Clones identified as positive by PCR were sequenced by AGRF (Melbourne, Australia). Primers were designed to sequence the entire length of the *PBS2* and *HOG1* genes (1638 and 1134 bp, respectively). The first forward primer (Fw1) was designed to begin 100 bp upstream of the starting ATG. The following forward primers were spaced every 500 bp throughout the genes. The reverse primer (Rv) was designed to begin amplification 200 bp downstream of the STOP codon.

For sequencing of pDDB78-*PBS2* the following primers were used:

Fw1: GAGGGACAGCGAGAATGAAAAC, Fw2: CCCAAACCAAACCTTGAAATT AAGTG, Fw3: GAGGTTTCGTTGGATAGAATATTTGG, Fw4: TTAAGACCATCTT ACGCGGCATTAT and Rv: ATTAGTGTGATTTCTGGTGTGGGG.

HOG1 sequencing was conducted with the following primers:

Fw1: CTGATTCAATCAAGATTCAAGTCGT, Fw2: ACATTCATTCTGCCGGTGT TATTC, Fw3: ACCCATCCTTATATGGAGGCAT and Rv: CATTTTACATATTCAC TGTTTCCCC.

4.2.2.9 Linearising plasmids for transformation into *C. albicans*

Restriction digests were performed with *Nru*I (New England Biolabs). Approximately 5 µg of plasmid was digested with 2 µL of *Nru*I, in the presence of 5 µL of 10× buffer (New England Biolabs) and 5 µL of 10× BSA in a total volume of 50 µL. Restriction digests were conducted at 37°C for 2 h.

4.2.2.10 Transformation of *C. albicans* deletion mutants

C. albicans transformations were performed essentially as described in Hernday et al. (2010). Cultures (5 mL) of *C. albicans hog1Δ/hog1Δ* and *pbs2-/pbs2-* were grown in YPD with 80 µg/mL uridine, overnight at 30°C, with shaking (250 rpm). The following day, a 50 mL culture was prepared with an OD₆₀₀ of 0.2 and grown for 5 h at 30°C before the cells were pelleted by centrifugation at 2800 rpm for 5 min. The cells were resuspended and washed in 50 mL of milliQ water and pelleted again at 2800 rpm for 5 min. The cell pellet was resuspended in 500 µL of TE/LiOAc (100 µL per transformation) and approximately 5 µg linearised plasmid (from Section 4.2.2.9) and 10 µL of calf thymus DNA (pre-heated to 95°C for 10 min and cooled on ice) was added. The cells were mixed by pipetting and left to sit at room temperature for 30 min. After incubation 700 µL of PLATE (40% PEG, 0.1 M LiOAc, 1x TE) was added and the cells were left to sit at room temperature overnight. The following day, cells were heat shocked at 44°C for 15 min and then spun down at 5000 rpm for 1 min. The cells were washed in 1 mL of YPD, re-pelleted and the supernatant was discarded. The pelleted cells were resuspended in 100 µL of YPD and spread onto selective plates (agar deficient in uracil, arginine and histidine). The plates were then incubated for 3 days at 30°C.

4.2.3 Fungal growth inhibition assays

Growth inhibition assays were performed essentially as described in Broekaert et al. (1990). *C. albicans* DAY185, DAY286, *pbs2-/pbs2-*, *hog1Δ/Δ*, *pbs2-/pbs2- + PBS2*, *hog1Δ/Δ + HOG1*, and other *C. albicans* strains were grown overnight at 30°C in YPD with uridine. NaD1 was serially diluted, to a final volume of 20 µL and each dilution was added in triplicate, into the wells of a 96 well microtitre plate (Greiner) by a TECAN Evo100 liquid handling robot. Diluted cells (80 µL, 5000 cells/mL in ½ PDB) were added to the wells of the microtitre plate. Growth was monitored by measuring absorbance at 595 nm, in a SpectraMAX M5e

plate reader (Molecular Devices), using the 9 well-scan. Measurements were taken before and after 24 h incubation at 30°C.

For ascorbate and sorbitol inhibition assays, 10 µL of protein was added to each well along with 10 µL of either ascorbate (50 mM) or sorbitol (500 mM). Cells (80 µL) were then added as described above.

4.2.4 Detection of Hog1 activation by Western blot

Western blots to detect Hog1 phosphorylation were based on a method modified from Alonso-Monge et al. (2003). Overnight cultures (5 mL) of *C. albicans* DAY185 and *hog1Δ/Δ* cells were diluted to an OD₆₀₀ of 0.2 in half-strength PDB (100 mL) and grown for a further 5 h at 30 °C (250rpm). Cells were then diluted to an OD₆₀₀ of 1.0 and 10 mL aliquots were treated with 10 µM NaD1, 20 µM NaD1 or 1 M NaCl for 5, 10 or 15 min. Cells were pelleted by centrifugation (3000 rpm, 5 min) and washed in 500 µL of cold MilliQ water. The cell pellets were then frozen with liquid nitrogen. Trichloroacetic acid (TCA, 20% w/v, 100 µL) was added to the frozen pellet, the cells were disrupted by vortexing in the presence of glass beads (180 µm, Sigma) and then the supernatant was collected. The glass beads were washed with 500 µL of 10% TCA and the supernatant was collected and pooled with the supernatant from the previous step. Precipitated proteins were pelleted by centrifugation at 14,000 rpm for 5 min and the pellet was washed with 1 mL of ice cold acetone. Proteins were separated on Bio-Rad AnyKD mini Tris-glycine gels and transferred to polyvinyl difluoride (PVDF) membranes. The membranes were probed overnight at 4°C with Phospho-p38 MAPK (Thr180/Tyr182) (Cell Signalling) or HOG1(y-215) (Santa Cruz Biotechnology) antibodies that had been diluted 1/200 in 5% (w/v) skim milk (Diploma) in TBST (Tris-buffered saline and 0.05% Tween 20). After washing with TBST, the membranes were incubated overnight at 4°C with the secondary antibody (ECL anti-Rabbit IgG linked to horseradish peroxidase, GE Healthcare, 1/20,000 dilution in TBST). Proteins that bound the antibody were detected using ECL detection reagent (GE Healthcare) with a Bio-Rad ChemiDoc MP imaging system. Hog1 levels were quantified using Bio-Rad Image Lab 3.0 and levels of phosphorylated Hog1 were calculated relative to total Hog1 levels.

4.2.5 Microscopy with ROS probe DHR 123

Reactive oxygen species were detected using dihydrorhodamine 123 (DHR 123) and a method modified from van der Weerden et al. (2008). Overnight cultures of *C. albicans* DAY185 (5 mL) were diluted to an OD₆₀₀ of 0.1 with half-strength PDB. DHR 123 (25 µM, Molecular Probes) was added to 200 µL of cells and incubated for 2 h (RT, 250 rpm, in the dark). Propidium iodide (PI, Sigma, 5 µM) was added 10 min prior to visualisation. After the 10 min incubation at RT, NaD1 (10 µM) was then added and cells were visualised immediately using a Zeiss LSM510/ConfoCor confocal microscope with Argon and DPSS lasers. DHR 123 was excited at 488 nm and emitted light detected at 505-530 nm. PI was excited at 561 nm and emitted light was detected at 575-615 nm. Images were captured using Zen2009 (Zeiss) software and analysed using FIJI (Schindelin et al., 2012).

4.2.6 Flow cytometry with DHR 123 and DAF-FM

An overnight culture of *C. albicans* DAY185 (5 mL) was diluted to an OD₆₀₀ of 0.2 in half-strength PDB and grown for several hours until it reached an OD₆₀₀ of 1.0 (30°C, 250 rpm). Cells were then diluted to an OD₆₀₀ of 0.1 in half-strength PDB before 200 µL was treated with DHR 123 or DAF-FM (25 µM, in DMSO, Molecular Probes) and incubated for an hour at 30°C (250 rpm). NaD1 (in water) was added (at 5, 10 or 20 µM final concentration) 15 min prior to flow cytometry. Cells were analysed using a BD FACSCanto II with excitation at 488 nm and emission detection with a 530/30 filter. Data was analysed using Weasel v3.0 (Walter and Eliza Hall Institute).

4.2.7 Survival assays

Survival assays were performed essentially as described in Section 2.2.7. For survival assays with sorbitol, overnight cultures of *C. albicans* DAY185 were diluted to an OD₆₀₀ of 0.2 in half-strength PDB and grown to an OD₆₀₀ of 1.0. Cells were then pre-treated for an hour with 1 M sorbitol (30°C, 250 rpm) before exposure to NaD1 (at 5, 10 or 20 µM) for 15 min (30°C, 250 rpm). Cells were then diluted to 1/1000 or 1/10,000 in water and 20 µL was plated onto YPD agar plates. Colonies were counted after overnight incubation at 30°C. Survival assays were also performed against DAY185 at OD₆₀₀ of 0.1, to match the OD₆₀₀ used in flow cytometry.

4.3 Results

4.3.1 NaD1 sensitive and resistant mutants identified in the screen of the *C. albicans* deletion libraries

The three *C. albicans* deletion libraries were screened for both resistance and hypersensitivity to NaD1. Each gene deletion in the libraries was represented by two independent clones. The libraries were screened three times with both 2 μ M NaD1 (to select for sensitive mutants) and 5 μ M NaD1 (to select for resistant mutants). The distribution of mutants from these screens was constructed by plotting percentage growth inhibition for each mutant tested, from lowest to highest inhibition. As was expected for the 2 μ M NaD1 screen there was a normal distribution of growth inhibition (Figure 4.4). At 5 μ M NaD1 more mutants exhibited growth inhibition approaching 100% (Figure 4.5). This was expected, given that 5 μ M NaD1 is above the IC₅₀ of NaD1 (2.3 μ M) against this pathogen.

Only thirteen deletion mutants, out of a total of 436 mutants, had consistent phenotypes across the multiple screens of the three deletion libraries (Table 4.1). Each of these mutants was tested further to obtain growth curves and IC₅₀ values (Figure 4.6 - Figure 4.8) for comparison against the wildtype (DAY286).

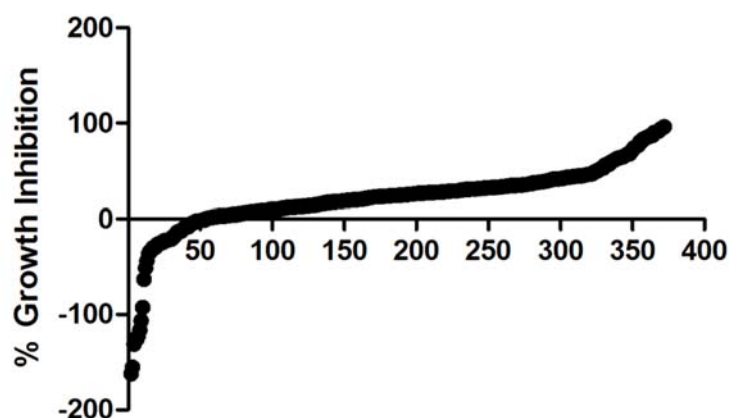


Figure 4.4 The distribution of deletion mutants from the 2 μ M NaD1 sensitivity screen

Distribution of percentage growth inhibition for all mutants (from all three deletion libraries) screened with 2 μ M NaD1.

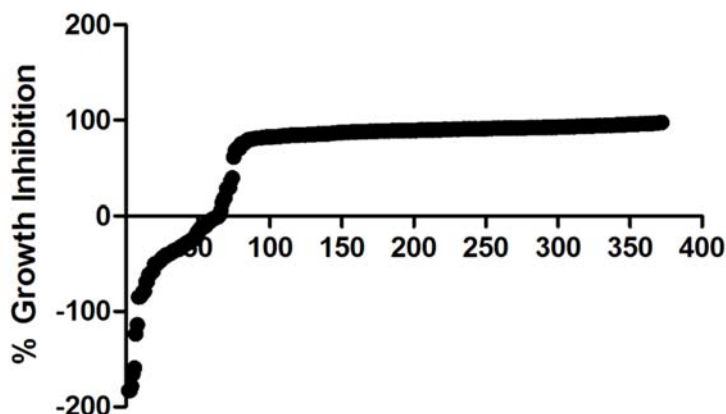


Figure 4.5 The distribution of deletion mutants from the 5 μM NaD1 resistance screen
Distribution of percentage growth inhibition for all mutants (from all three deletion libraries) screened with 5 μM NaD1.

Table 4.1 The mutant hits identified in the NaD1 screen of *C. albicans* deletion libraries

Genes deleted from mutants that were hits in two or more screens of the *C. albicans* deletion library. Hits from the resistance screen are shown in red and hits from the sensitivity screen are shown in blue.

Gene	Function	Mutant Library
<i>IRS4</i>	Cell wall integrity	Cell wall
<i>SAP8</i>	Secreted aspartyl protease	Cell wall
<i>ECM5</i>	Unknown	Cell wall
<i>ECM33.3F</i>	GPI-anchored cell wall protein	Cell wall
<i>PLB2</i>	Putative phospholipase B	Cell wall
<i>CHS5</i>	Putative chitin biosynthesis protein	Cell wall
<i>PBS2</i>	MAPKK, osmotic and oxidative stress response	Kinase
<i>KIS1</i>	Snf1p complex scaffold protein	Kinase
<i>SSN3</i>	Putative cyclin-dependent protein kinase	Kinase
<i>orf19.223</i>	Putative serine/threonine protein kinase	Kinase
<i>HOG1</i>	MAPK, osmotic and oxidative stress response	Kinase
<i>BCR1</i>	Zinc finger transcription factor	Transcription factor
<i>orf19.6845</i>	Putative transcription factor with bZIP DNA-binding motif	Transcription factor

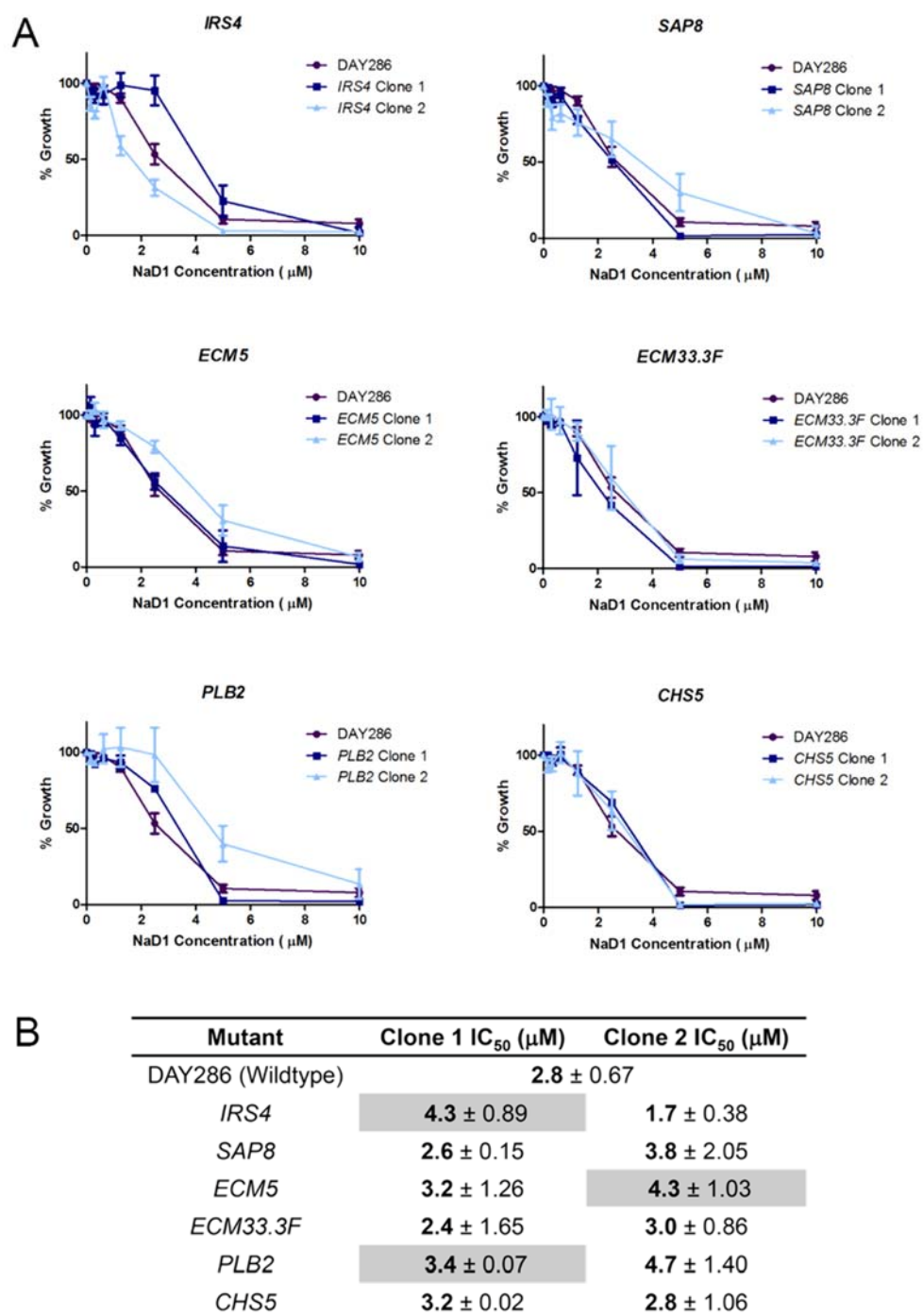


Figure 4.6 The effect of NaD1 on the growth of *C. albicans* cell wall deletion mutants

(A) Growth inhibition assays on cell wall deletion mutants which were hits in the *C. albicans* library screens (from Table 4.1). Two independent clones of each deletion mutant were tested and are shown compared to wildtype (DAY286). All data is shown relative to a no-protein control. Error bars = SEM (n=3). (B) Mean IC₅₀ (μM) values ± SD for each *C. albicans* mutant in (A). All IC₅₀ values highlighted in grey were significantly different from wildtype (p-values < 0.05) when compared to wildtype using an independent samples t-test (using IBM SPSS Statistics, version 19).

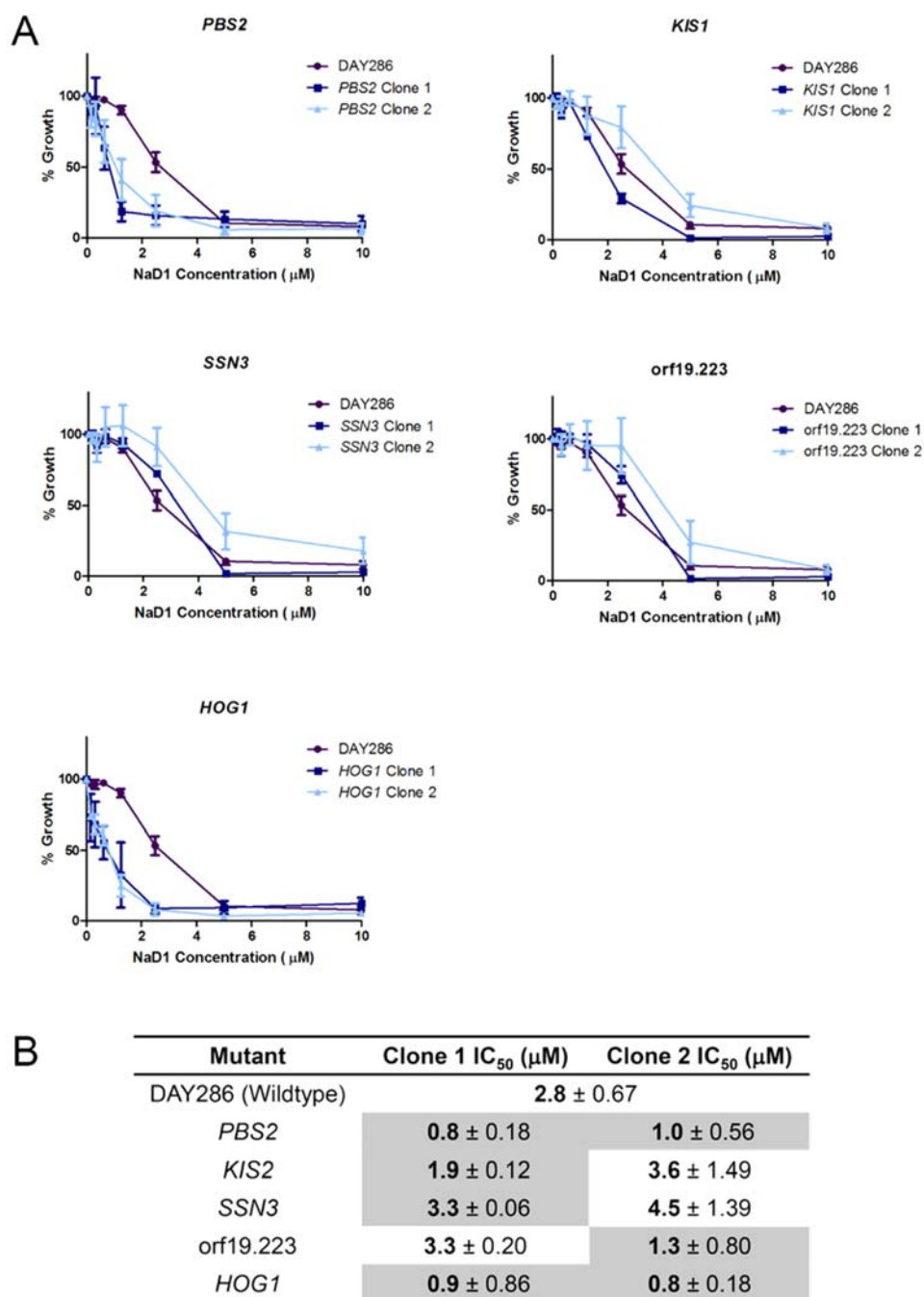


Figure 4.7 The effect of NaD1 on the growth of *C. albicans* kinase deletion mutants

(A) Growth inhibition assays on kinase deletion mutants which were hits in the *C. albicans* library screens (from Table 4.1). Two independent clones of each deletion mutant were tested and are shown compared to wildtype (DAY286). All data is shown relative to a no-protein control. Error bars = SEM (n=3). (B) Mean IC₅₀ (μM) values ± SD for each *C. albicans* mutant in (A). All IC₅₀ values shaded in grey were significantly different from wildtype (p-values < 0.05) when compared to wildtype using an independent samples t-test (using IBM SPSS Statistics, version 19).

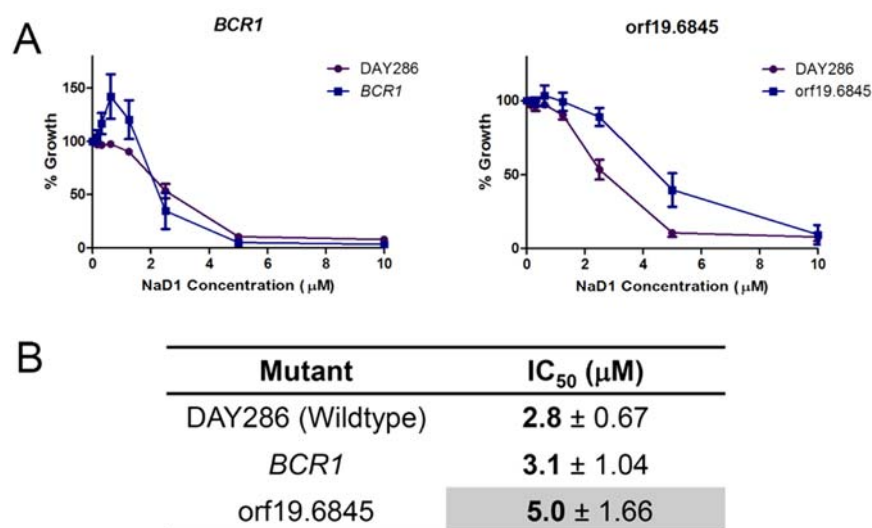


Figure 4.8 The effect of NaD1 on the growth of *C. albicans* transcription factor deletion mutants

(A) Growth inhibition assays on transcription factor deletion mutants which were hits in the *C. albicans* library screens (from Table 4.1). Deletion mutants are shown compared to wildtype (DAY286). These gene deletions were only represented by a single clone in the transcription factor deletion library. All data is shown relative to a no-protein control. Error bars = SEM (n=3). (B) Mean IC₅₀ (µM) values ± SD for each *C. albicans* mutant in (A). All IC₅₀ values shaded in grey were significantly different from wildtype (p-values<0.05) when compared to wildtype using an independent samples t-test (using IBM SPSS Statistics, version 19).

Mutants that had consistent phenotypes across both clones are listed in Table 4.2. Of these mutants, only one was resistant to NaD1. This unidentified ORF (orf19.6845) is a putative transcription factor with a bZIP DNA-binding motif. The IC₅₀ of this mutant was 4.2 µM compared to 2.3 µM against the wildtype.

There were also two sensitive mutants. These mutants lacked the MAPK Hog1 and its upstream MAPKK Pbs2. These mutants displayed IC₅₀'s of about 1 µM compared to the wildtype IC₅₀ of 2.3 µM (Table 4.2).

Table 4.2 Growth inhibition of mutants from the *C. albicans* library screens by NaD1

IC₅₀'s are mean ± SD from at least three independent experiments. P-values were calculated using an independent samples t-test (IBM SPSS Statistics v19) as compared to wildtype and are shown in brackets. Significant changes in IC₅₀ values from wildtype are highlighted in grey (p<0.05).

<i>C. albicans</i> strain	Function	NaD1 IC ₅₀ (μM)
Wildtype (DAY286)		2.3 ± 0.55
<i>pbs2</i> ^{-/-}	MAPK Kinase, regulation of Hog1	1.0 ± 0.56 (p=0.001)
<i>hog1Δ/Δ</i>	MAP Kinase, osmotic and oxidative stress response	0.8 ± 0.32 (p=0.000)
<i>orf19.6845</i> ^{-/-}	bZIP transcription factor	4.2 ± 0.56 (p=0.000)

4.3.2 Complementation of *HOG1* and *PBS2* genes

To confirm the hypersensitivity phenotype of the *hog1* and *pbs2* deletion mutants, the *HOG1* and *PBS2* genes were complemented into their respective mutants. The two genes were amplified from wildtype *C. albicans* by PCR. The expected size of the amplified *HOG1* and *PBS2* DNA was 2,730 bp and 3,230 bp, respectively. Amplicons of approximately these sizes were observed on agarose gels after amplification with PCR (Figure 4.9).

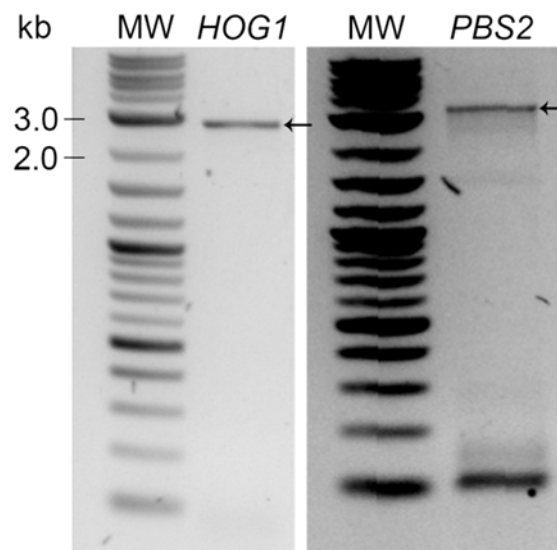


Figure 4.9 The amplification of *PBS2* and *HOG1* genes

The *PBS2* and *HOG1* genes were amplified from *C. albicans* wildtype genomic DNA by PCR. The amplified DNA (arrowed) matched the expected size of *HOG1* and *PBS2*, at 2,730 bp and 3,230 bp, respectively.

Amplified genes and digested pDDB78 (*EcoRI/NotI*) were transformed into *S. cerevisiae* BY4741 Δ trp for homologous recombination. DNA from colonies (on tryptophan dropout medium) was then isolated and transformed into *E. coli* for amplification. The resulting DNA was subjected to PCR with the original *HOG1* and *PBS2* amplification primers to screen for positive insertion of the genes into the pDDB78 vector. Two *PBS2* transformants (PBS2-3 and PBS2-4) had amplicons of approximately 3000 bp, consistent with the size of the *PBS2* gene (3,230 bp) and indicative of successful insertion of the *PBS2* gene into the pDDB78 vector (Figure 4.10). One *HOG1* transformant had an amplicon of between 2000 and 3000 bp, which was consistent with the expected size of the *HOG1* gene (2,730 bp) and successful insertion into the pDDB78 vector (Figure 4.10). These plasmids were then sent for sequencing which verified that the plasmids contained the *HOG1* and *PBS2* genes, with no mutations (see Appendix AIII). PBS2-4, did have the *PBS2* gene, but with mutations (not shown).

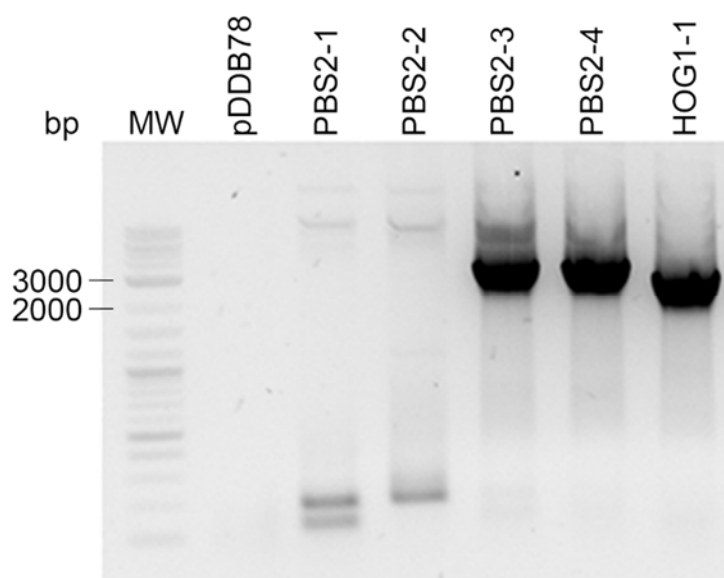


Figure 4.10 Amplified DNA from the *PBS2* and *HOG1* transformants

DNA from colonies which grew on tryptophan deficient selective medium were subjected to PCR using the original *HOG1* and *PBS2* primers to check for successful recombination of pDDB78 and the *HOG1* and *PBS2* genes. PBS2-3, PBS2-4 and HOG1-1, but not PBS2-1 or PBS2-2, had the fragments of interest. Also included was the pDDB78 empty plasmid control.

DNA from positive clones was linearised with *Nru*I and transformed into *hog1Δ/Δ* or *pbs2-/-* *C. albicans* cells. These *C. albicans* complements were then tested for susceptibility to NaD1 treatment. The two mutants had growth of only 20% in the presence of 1.25 μM NaD1 compared to the wildtype, which retained 80% growth. The complemented strains were not hypersensitive to NaD1 and had returned to the wildtype phenotype (Figure 4.11).

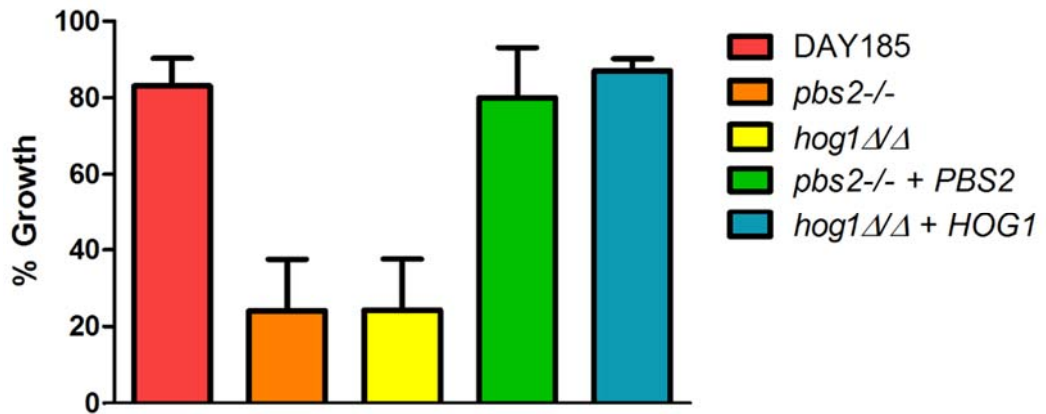


Figure 4.11 The effect of NaD1 to growth of *hog1Δ* and *pbs2Δ* mutants and complements

Fungal inhibition assay showing growth of *C. albicans* DAY185, deletion mutants and complements 24 hours after challenge with 1.25 μM NaD1. The mutants displayed hypersensitivity to NaD1. The complemented strains displayed the same growth as the DAY185 wildtype. Percentage growth was calculated based on growth of no-protein controls. Error bars represent SEM (n=3).

4.3.3 Detection of Hog1 phosphorylation in response to NaD1

To test whether NaD1 treatment causes Hog1 activation in *C. albicans*, antibodies to Hog1 (for total Hog1 levels) and phosphorylated Hog1 (activated Hog1) were used. Hog1 phosphorylation was observed at all NaD1 concentrations and all time points tested, although to a lesser extent than the Hog1 phosphorylation that occurred in the 1 M NaCl positive control. There was no Hog1 phosphorylation in the no-treatment, negative control or when *hog1Δ/Δ* was treated with NaD1 (Figure 4.12).

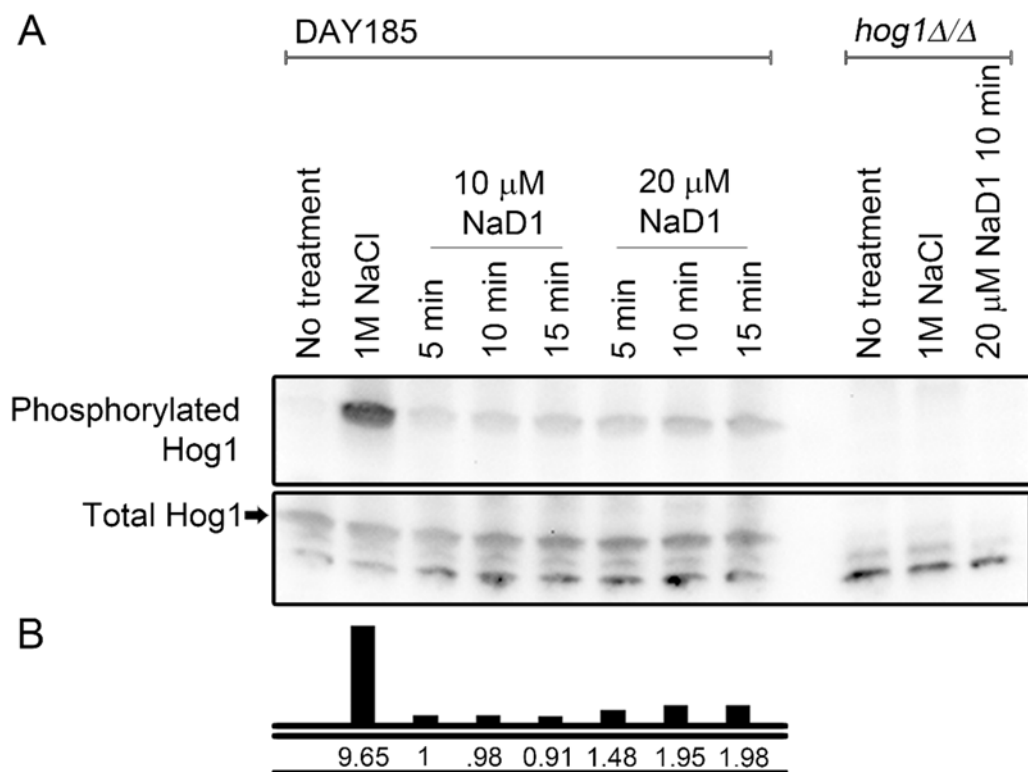


Figure 4.12 Hog1 is activated by NaD1 treatment

(A) Western blots showing levels of phosphorylated Hog1 (after probing with antibodies against phospho-p38 MAPK), against total Hog1 levels (detected with Hog1 antibody). DAY185 and *hog1Δ/Δ* were treated with 1 M NaCl and NaD1. Total Hog1 levels are shown with a black arrow. Hog1 phosphorylation was detected after treatment with the NaCl positive control and with 10 μM or 20 μM NaD1. No p-Hog1 was detected in the *hog1Δ/Δ* strain or in the no-treatment control. (B) Density of p-Hog1 bands from Western blots. Densities were normalised to total hog1 levels, and are shown relative to the 5 min, 10 μM NaD1 treatment.

4.3.4 Production of reactive oxygen species

Hog1 has a dual role in responding to oxidative and osmotic stress. To determine which of these stresses results in Hog1 activation after NaD1 treatment, *C. albicans* cells were first subjected to confocal microscopy and flow cytometry to examine if reactive oxygen species (ROS) are produced after treatment with the defensin. *C. albicans* cells were pre-incubated with propidium iodide (PI) which was used to monitor cell permeability and the fluorescent probe DHR 123 which was used to detect ROS production. After NaD1 treatment, ROS production was only detected with DHR 123 in cells that PI had also entered (Figure 4.13). Flow cytometry revealed that the number of ROS positive cells increased with increasing NaD1 concentration (Figure 4.14). In the absence of NaD1, only 1% of cells displayed DHR 123 fluorescence. As the NaD1 concentration was increased to 5, 10 and 20 μM , the number of ROS positive cells increased to 22%, 81.2% and 88.6%, respectively. Nitric oxide (NO) was also produced upon NaD1 treatment, with the number of NO positive cells increasing from 7.2% with 5 μM NaD1, to 62.9% and 88.2% with 10 μM and 20 μM NaD1 treatment, respectively (Figure 4.14). Survival assays under the same test conditions (OD_{600} of 0.1 and a 15 min NaD1 treatment) revealed that the level of cell death was consistent with the levels of ROS positive cells observed during flow cytometry (Figure 4.15).

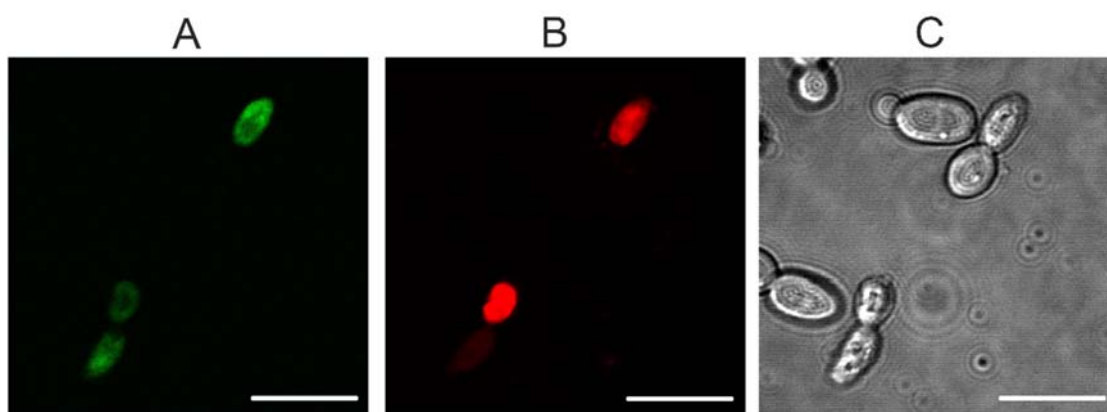


Figure 4.13 ROS production in *C. albicans* cells after NaD1 treatment

ROS production in *C. albicans* cells 30 min after treatment with 10 μM NaD1. (A) DHR 123 fluorescence, (B) PI fluorescence and a (C) white light image are shown. Scale bars = 10 μm . Images are a representative example of three independent experiments, which gave equivalent results.

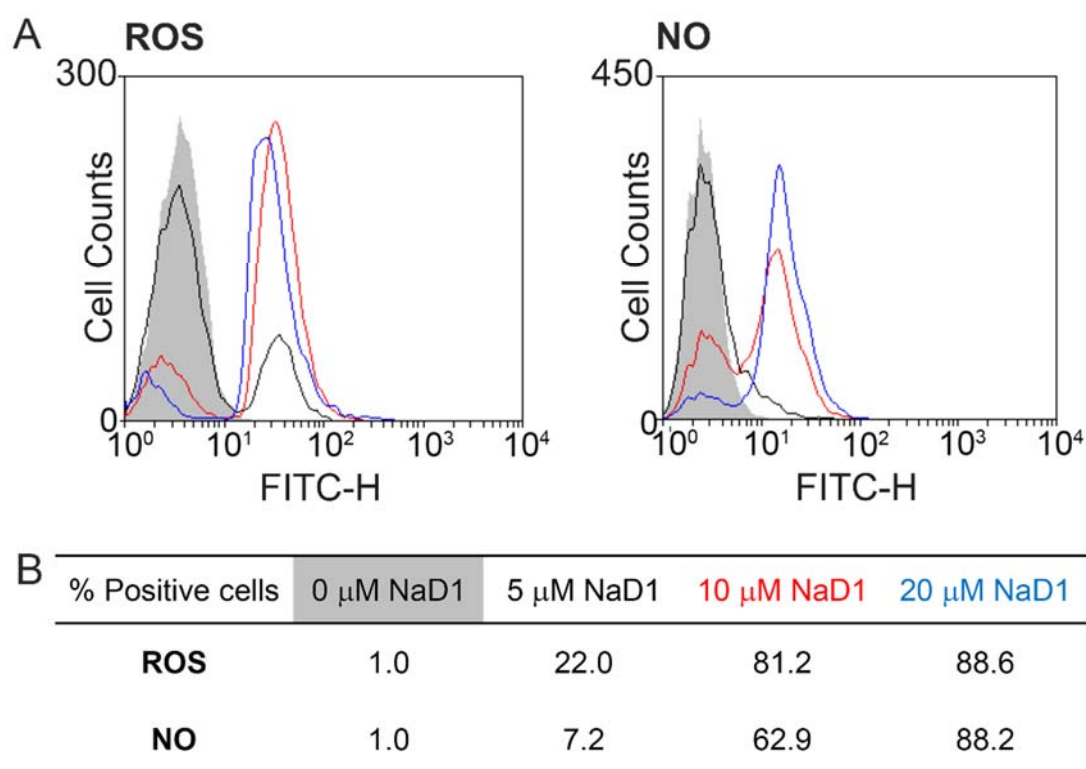


Figure 4.14 Flow cytometry monitoring DHR 123 and DAF-FM fluorescence after treatment with NaD1

(A) Flow cytometry was used to observe the number of ROS (DHR 123) and NO (DAF-FM) positive cells obtained with increasing concentrations of NaD1. NaD1 was added at 5 μM (black lines), 10 μM (red lines) and 20 μM NaD1 (blue lines). A no-protein control is represented by grey shading. The vertical and horizontal axes represent cell counts and fluorescent intensity, respectively. Data are representative examples of three independent experiments, which gave equivalent results. (B) The percentage ROS and NO positive cells from the flow cytometry in (A).

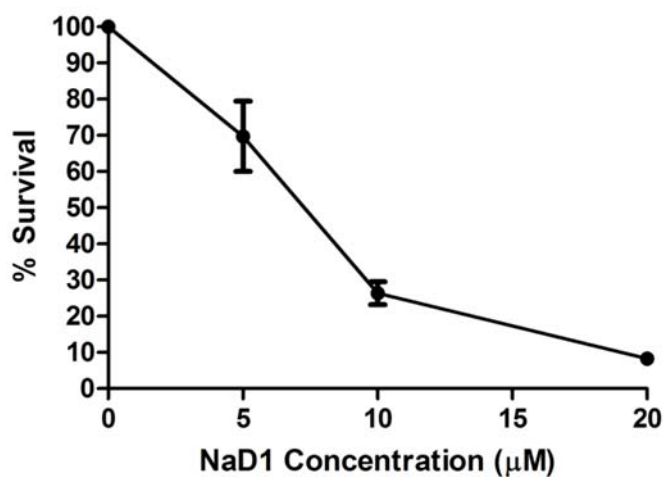


Figure 4.15 The survival of *C. albicans* in the presence of various concentrations of NaD1

Cell survival of *C. albicans* DAY185 treated with varying concentrations of NaD1 for 15 min, relative to a no-protein control. Cells were treated at an OD600 of 0.1 to match the OD600 of cells used in flow cytometry analysis. Error bars represent SEM (n=3).

4.3.5 Fungal inhibition of *C. albicans* by NaD1 in the presence of ascorbate

Since ROS were produced when *C. albicans* was treated with NaD1, I next examined whether reducing the amount of ROS, by addition of the antioxidant ascorbate, could protect against NaD1. Inhibition of *C. albicans* by NaD1 was reduced when cells were co-treated with ascorbate. The IC₅₀ of NaD1 doubled from 2.5 μ M to approximately 5 μ M in the presence of 50 mM ascorbate (Figure 4.16).

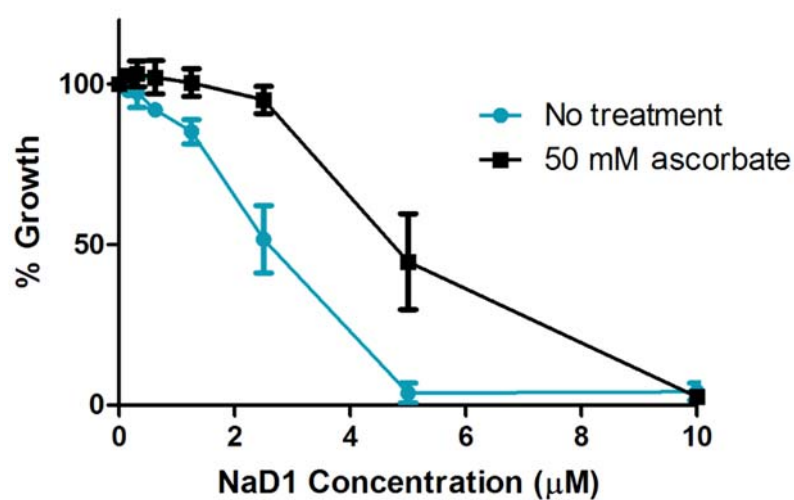


Figure 4.16 The effect of ascorbate on NaD1 activity against *C. albicans*

C. albicans was treated with various concentrations of NaD1 in the presence or absence of 50 mM ascorbate. Data is shown relative to a no-NaD1, no-ascorbate control. Error bars represent SEM (n=3).

4.3.6 Survival of *C. albicans* by NaD1 in the presence of sorbitol

To determine if NaD1 induces osmotic stress, the effect of sorbitol on NaD1 activity was examined. Sorbitol is an osmotic stressor. However, pre-treatment with sorbitol can also aid in stabilising osmotic pressure, by priming the cells for further osmotic stress. When *C. albicans* cells were treated with NaD1 concurrently with sorbitol (to induce osmotic stress) in growth inhibition assays, there was no effect on NaD1 activity. Also, sorbitol did not affect the activity of NaD1 in cell survival assays after pre-treatment with sorbitol (with sorbitol acting as an osmotic stabiliser) (Figure 4.17).

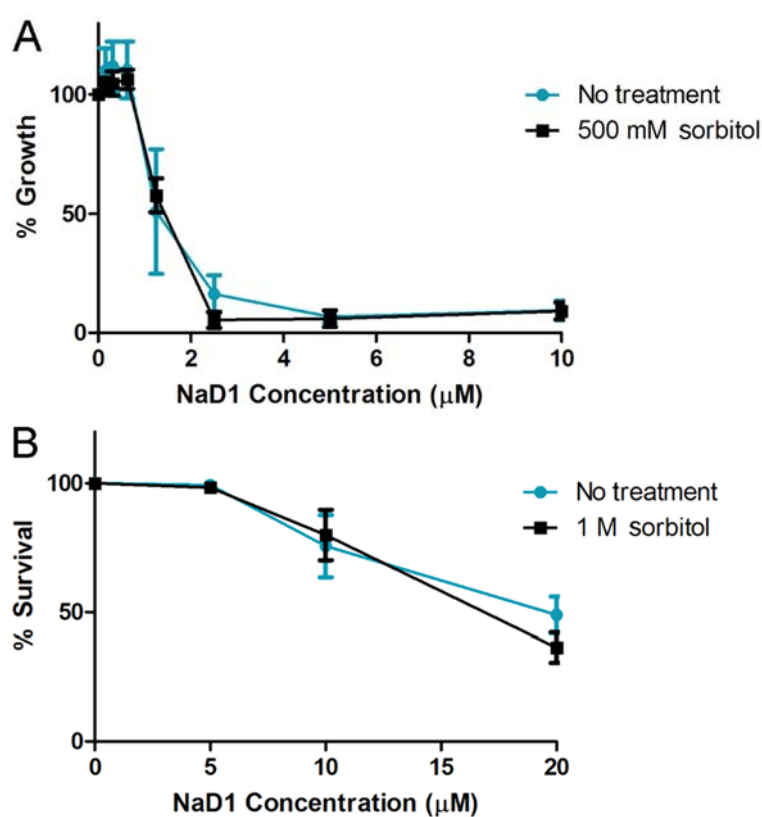


Figure 4.17 The effect of sorbitol on NaD1 activity against *C. albicans*

(A) *C. albicans* DAY185 growth inhibition assay with varying concentrations of NaD1 in the presence of 500 mM sorbitol. Data is shown relative to a no-protein control. Error bars represent SEM (n=4).
(B) *C. albicans* DAY185 survival assay after pre-treatment with 1 M sorbitol. Data is shown relative to a no-protein control. Error bars represent SEM (n=3).

4.4 Discussion

Three *C. albicans* deletion libraries were screened for altered susceptibility to NaD1, with the aim of uncovering information about NaD1's target(s) and mechanism of action. Although many hits were revealed in the screen, only three of the deletions had consistent phenotypes in following experiments. Two independent clones of each mutant were present in the libraries. No subsequent experiments were performed when the two clones behaved differently in response to NaD1, although it is possible that some of these were genuine hits. Without further study, we are unable to ascertain if the differences in sensitivity of the two clones were due to incorrect assignment of gene deletions. This could account for the low number of genes identified in the deletion library screen. We were particularly surprised to find no hits in the cell wall deletion library, as the cell wall has been reported to be important for NaD1's activity (van der Weerden et al., 2010). NaD1's three step mode of action involves binding to the cell surface, movement through the plasma membrane and entrance into the cytoplasm. Previous experimentation revealed that pre-treatment of Fov hyphae with β -glucanase and proteinase K treatment protected Fov hyphae from NaD1. This led to the hypothesis that a cell wall protein was acting as a receptor for NaD1 in filamentous fungi (van der Weerden et al., 2010). The failure to find a hit in the cell wall library of *C. albicans* may have occurred because the library did not contain genes encoding all cell wall proteins. That is NaD1's cell wall target was not present in the library. Another explanation is that multiple proteins are required for NaD1 interaction with the cell surface, and that single disruptions are not sufficient to observe a phenotypic change.

Screening of the *C. albicans* kinase deletion libraries revealed that in the absence of the Hog1 MAPK, cells were more susceptible to NaD1. Both *hog1 Δ/Δ* and *pbs2^{-/-}* - deletion mutants were hypersensitive to NaD1 indicating that activation of the HOG pathway provides some protection against the toxic effects of NaD1. Confirmation of activation of the Hog1 pathway by NaD1 was obtained with the observation that Hog1 was phosphorylated in response to NaD1 treatment (Figure 4.12). The Hog1 pathway has been reported to function in the protection of *C. albicans* from two other antifungal peptides, histatin 5 and human beta-defensin 2 (h β D2), and is the sole stress signalling pathway that functions in response to these peptides (Argimon et al., 2011; Vylkova et al., 2007). Interestingly, *C. albicans* mutants with overactive Hog1 (*ptc1 Δ* mutants) have been reported to be more sensitive to growth inhibition than wildtype by the plant defensin HsAFP1 (Aerts et al., 2011). The Ptc1 phosphatase is responsible for inactivation of the

Hog1 pathway through dephosphorylation of Hog1p (Aerts et al., 2011). Thus, increased activation of Hog1 is actually detrimental to the fungus during HsAFP1 exposure. This is in contrast to observations with h β D2, histatin 5 and NaD1, where Hog1 activation has a protective role.

As the Hog1 pathway has a dual role in both osmotic and oxidative stress response, I examined whether NaD1 induced production of reactive oxygen species and/or osmotic stress in *C. albicans*. Histatin 5, which also causes activation of the Hog1 pathway, has been reported to produce a primary osmotic stress, followed by a secondary oxidative stress (Vylkova et al., 2007). That is, oxidative stress induced by H₂O₂ did not affect histatin 5 activity, whereas pre-treatment of *C. albicans* with sorbitol reduced the toxicity of histatin 5 by preconditioning cells to osmotic stress (Vylkova et al., 2007). In contrast, sorbitol pre-treatment did not reduce the activity of NaD1. This indicates that, unlike histatin 5, Hog1 activation in response to NaD1 is not based on osmotic stress. Next, I questioned whether NaD1 was creating oxidative stress in cells. Cells naturally produce ROS at low levels to allow cells to adapt to stress by causing an increase in beneficial mutations. However, when ROS levels increase, it is no longer beneficial, and leads to cell death by damaging protein, lipids and DNA (Belenky et al., 2013; Belenky & Collins, 2011). Several antifungal peptides increase ROS production in yeast, including the radish defensin RsAFP2 (Aerts et al., 2007). Our laboratory has previously reported that NaD1 causes ROS production in the filamentous plant pathogen *F. oxysporum f. sp. vasinfectum* (Fov) (van der Weerden et al., 2008). In the current study, microscopy and flow cytometry with the ROS sensitive dye DHR 123 were used to confirm that NaD1 also induces ROS production in *C. albicans*. To further prove the involvement of ROS in NaD1's activity, I tested whether the antioxidant ascorbate could rescue cells from the toxic effects of NaD1. Ascorbate has been reported to protect *C. albicans* from RsAFP2 treatment (Aerts et al., 2007). Treatment with ascorbate provided partial protection from NaD1. Treatment with 50 mM ascorbate did not give complete resistance to NaD1, but did reduce NaD1's antifungal activity two-fold. This signifies that ROS production is part of the mechanism of NaD1, but may not be the only process by which NaD1 brings about cell death. However, it is also possible that full protection was not observed because some ROS still remained after treatment with 50 mM ascorbate. The role of NaD1 in inducing oxidative stress was tested further by examining the effect of NaD1 on *S. cerevisiae* rho⁰ mutants, which are deficient in mitochondrial respiration. These mutants were less susceptible to

NaD1 treatment (Hayes et al., 2013). Overall, this means that oxidative, not osmotic stress, is an important feature of NaD1's activity.

Interestingly, some of the mutants which were hits in the initial library screens, but were disregarded because both mutant clones did not show consistent phenotypes, have been reported to be involved in the cell wall integrity, oxidative stress or osmotic stress responses. One of these mutants, the cell wall associated protein *Irs4*, has been reported to be involved in virulence and cell wall integrity in *C. albicans* (Badrane et al., 2005). *C. albicans Irs4Δ* mutants are hypersensitive to caspofungin treatment (Badrane et al., 2005). In *S. cerevisiae*, *Irs4* has been reported to negatively regulate the cell wall integrity pathway and to lower phosphatidylinositol 4,5-bisphosphate (PI(4,5)P₂) levels by activation of the PI(4,5)P₂ phosphatase *Inp51* (Morales-Johansson et al., 2004). Interestingly, NaD1 binds PI(4,5)P₂ and other phosphatidylinositols (Poon et al., 2014). The *irs4* deletion mutant would have increased PI(4,5)P₂ levels. It is possible that increased PI(4,5)P₂ in the *irs4* mutant could lead to increased NaD1 binding to the cells and increased antifungal activity (i.e. hypersensitivity in the mutant). However, when treated with NaD1 in fungal inhibition assays, one *irs4Δ* clone was resistant and the other sensitive to NaD1. Further study and verification of the correct gene disruptions is required. Also of interest are the *Kis1* and *Ssn3* kinases. *Kis1Δ* mutants are reported to be hypersensitive to oxidative stress, osmotic stress and caspofungin, indicating roles in the oxidative and osmotic stress responses and maintenance of cell wall integrity (Blankenship et al., 2010). However, in fungal inhibition assays only one of the *kis1Δ* clones had increased sensitivity to NaD1. The sensitivity of the second clone was the same as wildtype. The *ssn3Δ* mutant has also been reported to have increased sensitivity to oxidative stress (Blankenship et al., 2010). In this study, one *ssn3Δ* clone was resistant to NaD1 treatment and the second clone behaved like wildtype. Thus, the clones of the *kis1* and *ssn3* mutants should be tested to ensure they have the correct gene deletions. Nevertheless, their appearance as putative hits in the three replicates of the kinase library screen, supports the involvement of oxidative stress in the mechanism of NaD1.

A summary of Hog1 involvement in *C. albicans* tolerance to NaD1 is presented in Figure 4.18.

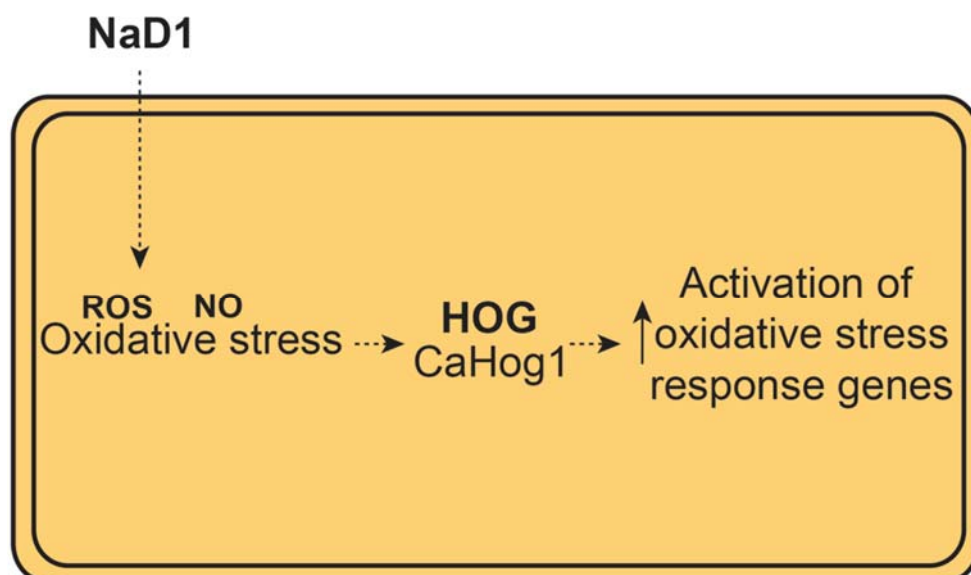


Figure 4.18 Overview of NaD1's mechanism against *C. albicans*

NaD1 enters into *C. albicans* cells and induces production of reactive oxygen species. The cell activates the Hog1 pathway in response to this stress.

It is becoming increasingly apparent that stress signalling pathways in fungi are important to the activity of many antifungal peptides. These pathways give fungi a protective response to many antifungal peptides. Given that, histatin 5, h β D2 and NaD1 all activate the HOG pathway in *C. albicans* it has been proposed that alteration or blocking of this stress response pathway may increase the toxicity of certain antifungal peptides (Argimon et al., 2011; Vylkova et al., 2007). However, for broad plant protection it is important to determine whether NaD1 activates Hog1 in other fungal pathogens. If so, the HOG pathway would be an interesting target for future antifungal treatments and a viable option for NaD1 combinatorial treatment on a broad-spectrum of fungal pathogens.

Chapter 5

The impact of stress signalling pathways on the potency of plant defensins on fungal pathogens

5.1 Introduction

In Chapter 4 of this thesis, I described the role of the HOG pathway in enhancing tolerance of *Candida albicans* to NaD1. Although CaHog1 responds to both osmotic and oxidative stress, only oxidative stress was identified as part of NaD1's mechanism. As well as the HOG pathway, several other pathways are activated in response to oxidative stress in *C. albicans*. These include the CaCap1 transcription factor and the cell wall integrity (CWI) pathway (Figure 5.1) (Alarco & Raymond, 1999; Enjalbert et al., 2006; Navarro-García et al., 2005). For a review of HOG, CWI and Cap1 signalling see Chapter 1.

The aim of this Chapter was to investigate whether pathways apart from the HOG pathway enhance tolerance to NaD1 in *C. albicans*. I investigated whether deletion of *Camkc1* (the terminal MAPK of the *C. albicans* CWI pathway) or *Cacap1* enhances NaD1 sensitivity. In addition, I also tested mutants of the calcineurin stress response and mating pathways. The calcineurin pathway responds to many of the same stresses as the CWI pathway (Bader et al., 2003; Cruz et al., 2002; Levin, 2011) and has been implicated in tolerance to many chemical fungicides (reviewed in Chapter 1). The mating pathway is involved in protection of *F. graminearum* against the toxic effects of the plant defensins RsAFP2, MsDef1 and MtDef4 (Ramamoorthy et al., 2007b). The mating pathway, and the GPCR that activates it, is described in the following paragraph.

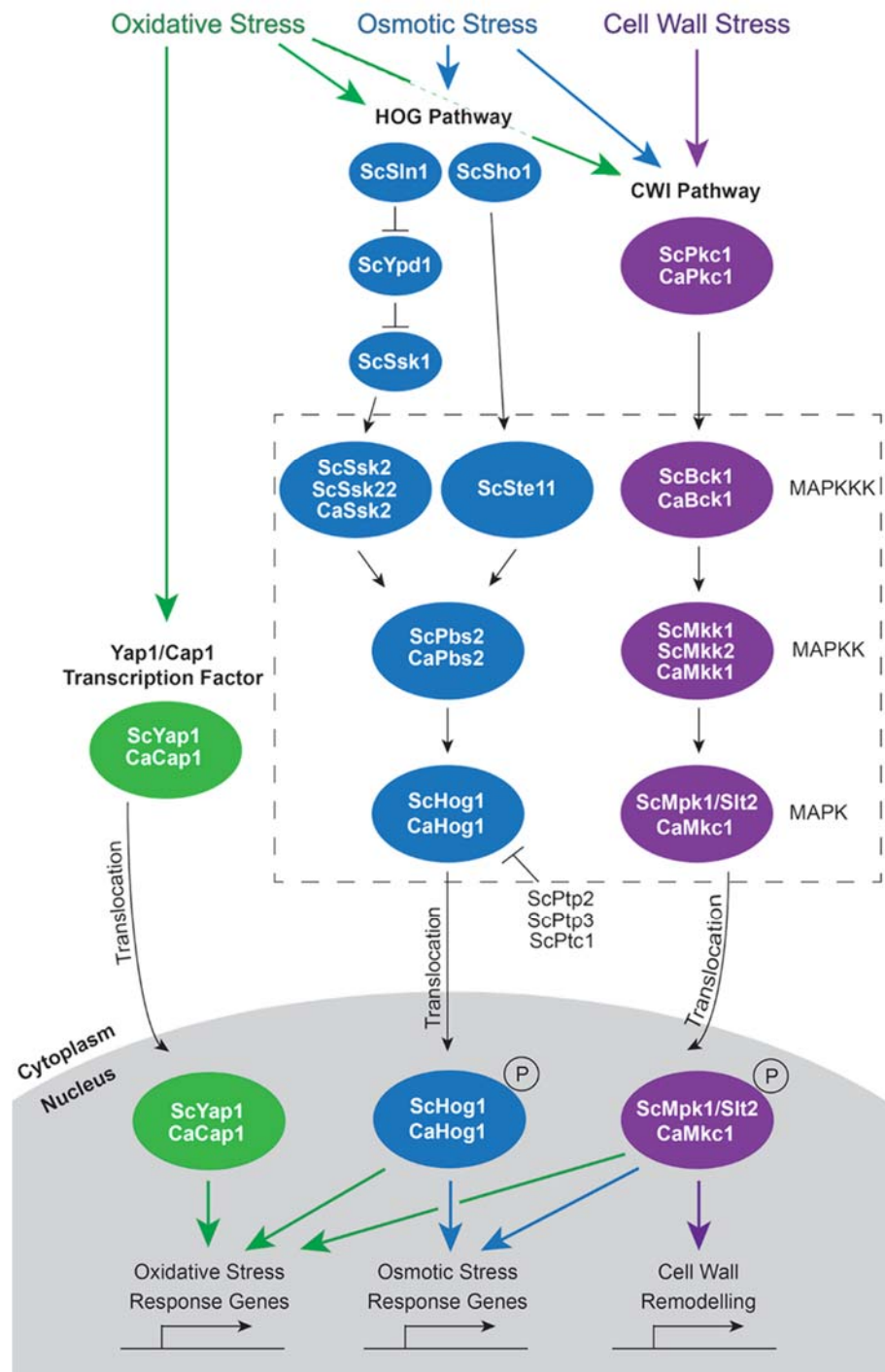


Figure 5.1 Oxidative, osmotic and cell wall stress response pathways in *C. albicans* and *S. cerevisiae*

The HOG and CWI MAPK pathways and the ScYap1/CaCap1 transcription factor can all be activated upon oxidative stress in *S. cerevisiae* and *C. albicans*. Phosphorylation cascades result in activation of a terminal MAPK which translocates to the nucleus and affects expression of stress response genes. The ScYap1/CaCap1 transcription factor resides in the cytoplasm until activated by oxidative stress, whereupon it moves to the nucleus and regulates gene expression. Purple arrows represent cell wall stress, blue arrows represent osmotic stress and green arrows are oxidative stress. Sc, *Saccharomyces cerevisiae*; Ca, *Candida albicans*.

Like the HOG and CWI pathways, the mating pathway requires successive phosphorylation events that end with phosphorylation of a terminal MAPK (Fus3 in *S. cerevisiae* and Cek2 in *C. albicans*) (Figure 5.2) Activation of this pathway begins with stimulation of the Ste2 (α -factor) and Ste3 (a-factor) G-protein coupled receptors by pheromone (Correia & Pla, 2010; Miyajima et al., 1987; Versele et al., 2001). G-protein coupled receptors detect extracellular signals and activate trimeric G-proteins which induce a cellular response. Trimeric G-proteins consist of α , β and γ subunits, with the α subunit responsible for GDP binding. When GDP is bound, $G\alpha$ is associated with a $G\beta\gamma$ dimer and the G-protein is inactive. Upon receptor stimulation the $G\alpha$ loses affinity for GDP which is replaced by GTP. The $G\alpha$ subunit then dissociates from the $G\beta\gamma$ dimer and the receptor (Hamm & Gilchrist, 1996). There are two known GPCRs in *S. cerevisiae* (Figure 5.3). The first is involved in mating. Pheromone binding to Ste2 or Ste3 causes dissociation of the $G\alpha$ subunit (ScGpa1/CaCag1) from the $G\beta\gamma$ subunit (Ste4 and Ste18). This results in signalling through the MAPKKK, ScSte11/CaSte11, and the MAPKK, ScSte7/CaHst7, and ends with phosphorylation of ScFus3/CaCek2. ScFus3 can then continue on to alter transcription of pheromone induced genes and to halt the cell cycle at G1 phase, which is required for mating (Correia & Pla, 2010; Miyajima et al., 1987; Monge et al., 2006; Versele et al., 2001). Another GPCR exists in *S. cerevisiae*, which responds to glucose in the surroundings. Binding of glucose to this receptor, Gpr1, activates the $G\alpha$ protein Gpa2 which activates the adenylate cyclase Cyr1 and results in increased cyclic AMP (cAMP) synthesis and activation of cAMP-dependent protein kinase (also known as PKA). Activation of PKA results in a number of transcriptional changes, among them the switch to fermentative growth and repression of stress activated genes (Griffioen & Thevelein, 2002; Nakafuku et al., 1988; Tamaki, 2007; Versele et al., 2001).

The mating pathway shares the ScSte7/CaHst7 MAPKK and the Ste11 MAPKKK with the ScKss1/CaCek1 pathway responsible for pseudohyphal and invasive growth upon nutrient starvation (Figure 5.2). ScSte7 has a higher affinity for ScKss1, except in the presence of the scaffold protein ScSte5, which is specifically recruited after pheromone binding and directs signalling through the ScFus3 pathway (Correia & Pla, 2010; Monge et al., 2006; Saito, 2010).

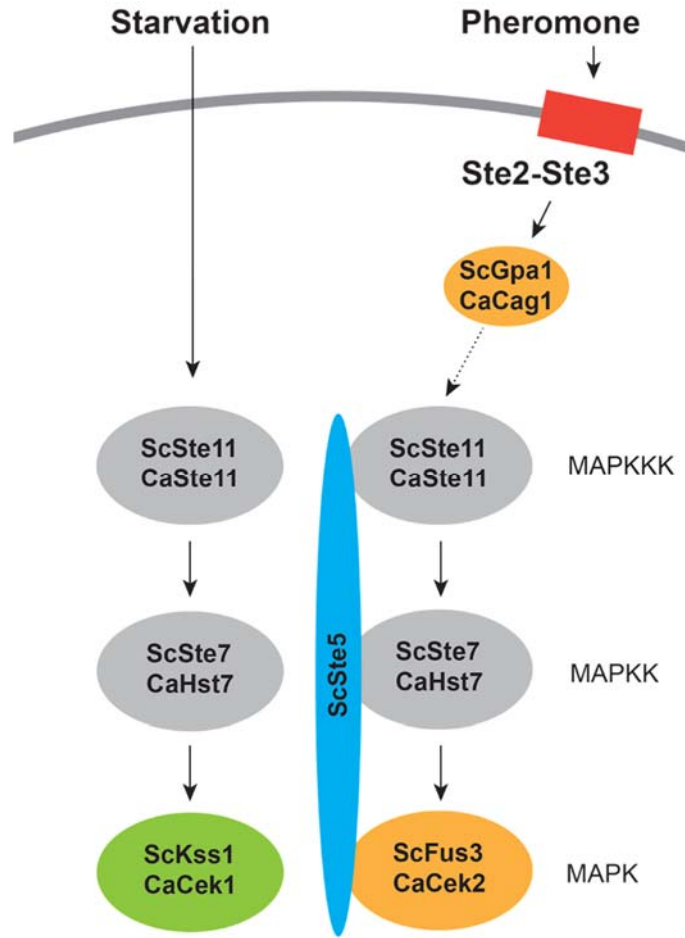


Figure 5.2 The *S. cerevisiae* Fus3 and Kss1 signalling pathways

Pseudohyphal and invasive growth (ScKss1/CaCek1) and mating (ScFus3/CaCek2) pathways share the MAPKKK Ste11 and the MAPKK ScSte7/CaHst7. Shared components are coloured grey. The scaffold protein ScSte5 is required for signalling through the ScFus3 pathway, and is only recruited upon pheromone binding to the Ste2-Ste3 G-protein coupled receptors.

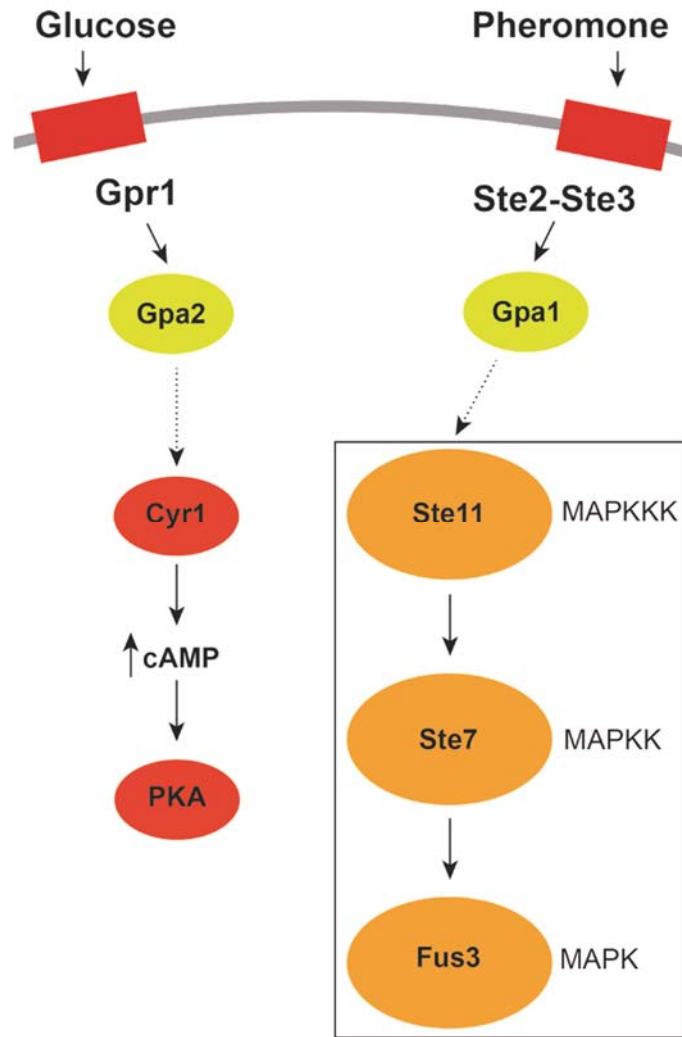


Figure 5.3 Two GPCRs exist in *S. cerevisiae*

Two GPCRs exist in *S. cerevisiae* that are responsible for glucose sensing (Gpr1) and pheromone sensing (Ste2 or Ste3). Glucose binding to Gpr1 activates the adenylate cyclase Cyr1 which results in increased cAMP synthesis and activation of PKA. Pheromone binding to the receptors results in signalling through the Fus3 MAPK cascade.

It is not uncommon for antifungal molecules to induce signalling through multiple MAPK pathways. For example, the echinocandin drug caspofungin activates both the HOG and CWI pathways. The activation of the CWI pathway relates to caspofungin's primary mechanism of decreasing β -1,3-glucan levels in the *C. albicans* cell wall. A compensatory increase in chitin cell wall levels after caspofungin treatment requires signalling through CWI, HOG and calcineurin (Walker et al., 2008). Caspofungin also causes oxidative stress in *C. albicans* triggering activation of CaHog1 and the CaCap1 transcription factor (Kelly et al., 2009). Thus it is likely that response to NaD1 requires multiple stress response pathways.

In addition to NaD1, I also investigated whether HOG and CWI signalling are important for tolerance of *C. albicans* to two other plant defensins. They are the class I defensins (Figure 0.1) NaD2 (from *N. alata*) and DmAMP1 (from *D. merckii*). NaD2 has antifungal activity, although less so than NaD1 against all plant fungal pathogens tested (Dracatos et al., 2013). However, its mechanism of action is unknown. DmAMP1 is better characterised, and its mechanism differs greatly from NaD1. RsAFP2, with which DmAMP1 has high sequence identity and shares many similarities in mechanism, activates CWI signalling in *C. albicans* (Thevissen et al., 2012; van der Weerden et al., 2013). The current literature regarding the mechanism of DmAMP1 is reviewed briefly below.

The antifungal mechanism of DmAMP1 involves membrane binding, alteration of the membrane potential, production of reactive oxygen species (ROS), programmed cell death and finally permeabilisation of the plasma membrane. The membrane binding site for DmAMP1 has been identified. Radio-labelling and mutational analysis revealed that DmAMP1 binds to mannosyldiinositolphosphoryl-ceramide (M(IP)₂C) (Thevissen et al., 2004), a sphingolipid that is present in the plasma membrane and cell wall of *Saccharomyces cerevisiae* (Patton & Lester, 1991). DmAMP1 also causes changes to membrane potential. The defensin induces a release of K⁺ and uptake of Ca²⁺ into fungal hyphae (Thevissen et al., 1996). Alterations to Ca²⁺ concentrations may have a significant impact on hyphal elongation, because a Ca²⁺ gradient at the hyphal tip is required for growth (Robson et al., 1991; Theis & Stahl, 2004). Membrane permeabilisation also occurs after DmAMP1 treatment. However, there is a delay between the time of initial DmAMP1 treatment and permeabilisation, indicating that the membrane disruption is a secondary effect to the antifungal activity of the defensin (Aerts et al., 2008).

In addition to investigating these pathways in *C. albicans*, the research in this Chapter was directed towards investigating the response of *S. cerevisiae* signalling mutants to NaD1, to determine whether these stress responses are conserved across different fungal species. *S. cerevisiae* mutants with deletions in the mating, CWI, HOG and calcineurin pathways, as well as the *Scyap1* transcription factor, were tested with NaD1.

Lastly, to investigate if stress signalling pathway inhibitors have potential in increasing the efficacy of antifungal peptides I investigated whether NaD1 and NaD2 have synergistic activity with chemical inhibitors of the CWI and calcineurin pathways.

5.2 Materials & Methods

5.2.1 Fungal growth inhibition assays

Growth inhibition assays were performed essentially as described in Broekaert et al. (1990). *C. albicans* DAY286 and mutants were grown overnight at 30°C in yeast peptone dextrose (YPD) with 80 µg/mL uridine (250 rpm). NaD1, NaD2 or DmAMP1 were serially diluted, to a final volume of 20 µL and each dilution was added in triplicate, into the wells of a 96 well microtitre plate (Greiner) by a TECAN Evo100 liquid handling robot. Diluted cells (80 µL, 5000 cells/mL in half-strength PDB) were added to the wells of the microtitre plate. Growth was monitored by measuring absorbance at 595 nm, in a SpectraMAX M5e plate reader (Molecular Devices), using the 9 well-scan. Measurements were taken before and after 24 h incubation at 30°C.

For *S. cerevisiae* mutants, NaD1 (20 µL) was added to microtitre plates (Greiner) at final concentrations of 0, 1, 1.2, 1.4, 1.6, 1.8 and 2 µM in triplicate. After overnight growth in YPD (30°C, 250 rpm) cells were diluted to an OD₆₀₀ of 0.01 with half-strength PDB and 80 µL was added to each well of the plate. The plates were incubated at 30°C, with measurement of optical density (OD₅₉₅) before and after 24 h incubation.

For testing susceptibility of *C. albicans* DAY185 and *S. cerevisiae* BY4741 to hydrogen peroxide, overnight cultures (in 3 mL YPD, 30°C, 250 rpm) of both species were diluted to 5000 cells/mL with half-strength PDB. Hydrogen peroxide (20 µL, 30% w/v) was added to a microtitre plate (Greiner) at a top concentration of 1.5 % (final) and serially diluted down the plate. Cells (80 µL) were added and grown at 30°C. Absorbance (OD₅₉₅) was measured after 24 h.

For antifungal assays in the presence of pertussis toxin, *C. albicans* DAY185 cells were grown overnight in YPD (3 mL, 30°C, 250 rpm). The cells were then counted with a haemocytometer and diluted to 5000 cells/mL with half-strength PDB. Pertussis toxin (with a top final concentration of 10 ng/µL, List Biological Laboratories) was serially diluted down a microtitre plate (Greiner) to leave a final volume of 10 µL in each well. NaD1 (10 µL) was then added to each well to a final concentration of 2.5 µM followed by cells (80 µL) and an overnight incubation at 30°C. Growth was monitored by measuring absorbance at 595 nm in a SpectraMAX M5 plate reader (Molecular Devices).

For *S. cerevisiae* growth assays in the presence of pertussis toxin, overnight cultures of *S. cerevisiae* BY4741 (3 mL, 30°C, 250 rpm) were diluted to an OD₆₀₀ of 0.01 with half-strength PDB. Pertussis toxin (List Biological Laboratories, 10 µL) was then serially diluted down a microtitre plate (Greiner) with a top final concentration of 10 ng/µL. NaD1 (10 µL, 2.5 µM final concentration) and 80 µL of cells were then added. Plates were incubated overnight at 30°C and growth was monitored by measuring absorbance at 595 nm.

When pertussis toxin and brefeldin A were tested in combination, *C. albicans* cells were prepared as above. Firstly, pertussis toxin (10 µL, 100 ng/µL) was added to wells of a microtitre plate (Greiner) for a final concentration of 10 ng/µL followed by brefeldin A (5 µL) to give final concentrations of 0, 5, 10 and 20 µM. NaD1 was then added to each well (5 µL, 80 µM for a final concentration of 4 µM) and cells (80 µL) were added prior to overnight incubation at 30°C. OD₅₉₅ measurements were taken before and after 24 h incubation.

For testing the activity of NaD1 against *C. albicans* in the presence of dextrose, DAY185 overnight cultures were diluted to 5000 cells/mL in half-strength PDB. NaD1 (10 µL) was serially diluted down a microtitre plate (Greiner) to a top final concentration of 10 µM. Twenty per cent dextrose or water (10 µL) was added to the wells before addition of diluted cells (80 µL) and overnight incubation at 30°C. Growth was monitored by measuring absorbance at 595 nm.

5.2.2 Confirmation of correct gene deletions in *C. albicans* mutants

5.2.2.1 Extraction of genomic DNA from *C. albicans* cells

Genomic DNA extracts from *C. albicans* were prepared using DNAzole reagent (Life Technologies) essentially as described by the manufacturer. Scrapings of *C. albicans* DAY286 and the mutants were taken directly from YPD agar plates and were added to 1 mL of milliQ water. DNAzole reagent (1 mL, Life Technologies) was added along with 200 μ L of acid-washed glass beads (180 μ m, Sigma) in microfuge tubes. The samples were vortexed for 2 min and then centrifuged for 10 min at 12,000 rpm. The supernatant was moved to a fresh tube and 500 μ L of 100% ethanol was added. The ethanol-supernatant mix was incubated at room temperature for 15 min and then spun for 2 min at 4,000 \times g. The supernatant was discarded and the DNA pellet was resuspended in 1 mL of 70% ethanol. The contents of the tube were mixed by inversion and pelleted again (1 min at 4,000 \times g). The ethanol wash was repeated once more before the ethanol was removed from the tube and the pellet was dried by heating for 1 min at 60°C. The dried pellet was then resuspended in 20 μ L of milliQ water. Successful genomic DNA extraction was confirmed by examining samples after electrophoresis on a 1% agarose gel.

5.2.2.2 PCR screen using *ARG4* detect primers

PCR was used to check for insertion of *ARG4* into the genes of interest in selected deletion mutants. The protocol was adapted from Nobile and Mitchell (2009). The *ARG4* detect primer (GGAATTGATCAATTATCTTTTGAAC), which is homologous to the *ARG4* insert, was added along with primers that were complementary to regions 100 bp upstream and downstream of the ORF of the gene of interest (Figure 5.4). Strains were also replated on uracil dropout medium (see Appendix AII).



Figure 5.4 PCR with *ARG4* detect primers

ARG4 detect, as well as forward (Fw) and reverse (Rv) primers for the gene of interest, were used in PCRs with genomic DNA from the deletion mutants to check for insertion of the *ARG4* marker into the correct gene.

The following primers were used:

bck1^{-/-}

Fw: ATAAAGTCAAATTGCTGCATCC and

Rv: GAAACAAAGATGCAGAACAAC.

cap1^{-/-}

Fw: TTGAATTCGCCTCCTCCC and

Rv: AAATAATTACAAAATAAAAACGTATAACG.

cna1^{-/-}

Fw: CAAATCAATCATTAGCTATATTTGATC and

Rv: CAAATAGATGATTCAACTCTGAC.

crz1^{-/-}

Fw: TTTAATCTGGTCATTTCAATTTCCC and

Rv: CAAAATAAAAACAAATCATTCGTAAAAC.

cek2^{-/-}

Fw: CAAAAGTGAGGGAAGTTATCAACC and

Rv: CTATCAGGAGGGGACAGGG.

hst7^{-/-}

Fw: CACACACACATATACCACTCG and

Rv: GCTGTTGTTTAAGTTTATCGACTTG.

Genomic DNA (5 μ L) was added to 10 μ L of 2 \times Phusion master mix (Thermo Fisher), primers (1 μ L of 10 μ M Fw, Rv and *ARG4* detect) and water, to a total volume of 20 μ L. The PCR conditions were 98°C for 30 sec, 30 cycles of 98°C for 10 sec, 51°C for 30 sec and 72°C for 2 min, and then 72°C for 10 min. PCR products were separated on a 1% agarose gel.

The *bck1*^{-/-} and DAY286 genomic DNA was also subjected to restriction digest with *Sac*II (New England Biolabs) for 1 h at 37°C before amplification with *ARG4* detect and *bck1*^{-/-} Fw and Rv primers as described above. The *Sac*II enzyme cuts within the *BCK1* gene but does not cut within the *ARG4* marker.

5.2.3 Confirmation of correct deletions in *S. cerevisiae* mutants

S. cerevisiae mutants were verified according to the method presented in Section 3.2.5. In brief, cells were scraped from a YPD agar plate, placed in 200 μ L of TE and incubated at 90°C for 30 min. Forward primers were ordered based on sequences from the *Saccharomyces* Gene Deletion Project (http://www.sequence.stanford.edu/group/yeast_deletion_project/downloads.html#strainsavail). PCR was performed with a forward primer and the *kanB* primer (CTGCAGCGAGGAGCCGTAAT). Treated cells (3 μ L) were added to 12.5 μ L of 2 \times GoTaq master mix (Promega), primers (1 μ L of 10 μ M Fw and *kanB*) and water, to a total volume of 30 μ L. The PCR conditions were 94°C for 3 min, 30 cycles of 94°C for 1 min, 51°C for 1 min and 72°C for 1 min, followed by 72°C for 7 min. The PCR products were separated on a 1% agarose gel.

5.2.4 BODIPY-NaD1 uptake into *C. albicans* monitored by flow cytometry

Flow cytometry was performed essentially as described in Section 3.2.4. *C. albicans* DAY185 (3 mL) was grown overnight at 30°C (250 rpm). Cells were diluted to an OD₆₀₀ of 0.2 in half-strength PDB and grown for several hours until they reached an OD₆₀₀ of 1.0 (30°C, 250 rpm). Cells were then diluted to an OD₆₀₀ of 0.1 in half-strength PDB. Cells (200 μ L) were then pre-treated for 2h (30°C, 250 rpm) with 10 ng/ μ L pertussis toxin (List Biological Laboratories) or 40 μ M Brefeldin A (Sigma), followed by 10 μ M BODIPY-NaD1 for 15 min (in the dark, 30°C, 250 rpm). After incubation, cells were washed twice with PBS (by centrifugation at 13,000 rpm for 2 min) and resuspended in 200 μ L of PBS. Cells were analysed using a BD FACSCanto II with excitation at 488 nm

and emission detection with a 530/30 filter. Data was analysed using Weasel v3.0 (Walter and Eliza Hall Institute).

5.2.5 Detection of Hog1 phosphorylation in response to NaD2

Western blots were performed essentially as described in Section 4.2.4. This method was adapted from Alonso-Monge et al. (2003). Overnight cultures (5 mL) of DAY185, *hog1Δ/Δ* and *mkc1-/-* cells were diluted to an OD₆₀₀ of 0.2 in 50 mL half-strength PDB and grown to an OD₆₀₀ of 1.0 (30°C, 250 rpm). Aliquots (10 mL) were treated with NaD₂ for 20 min. For detection of Hog1 activation, 1 M NaCl (10 min treatment) was used as a positive control. Proteins were extracted and concentrated using the TCA precipitation method described in Section 4.2.4 before they were separated on Bio-Rad AnyKD mini Tris-glycine gels and transferred to polyvinyl difluoride (PVDF) membranes. For detection of Hog1 activation, Phospho-p38 MAPK (Thr180/Tyr182) (Cell Signalling) or HOG1(y-215) (Santa Cruz Biotechnology) antibodies were used that had been diluted 1/200 in 5% (w/v) skim milk (Diploma) in TBST (Tris-buffered saline and 0.05% Tween 20). All membranes were probed overnight at 4°C with the primary antibodies, they were washed three times with TBST (10 min washes) and probed overnight at 4°C with secondary antibody (ECL anti-Rabbit IgG linked to horseradish peroxidase, GE Healthcare, 1/20,000 dilution in TBST). Immunoreactive proteins were detected using ECL detection reagent (GE Healthcare) with a Bio-Rad ChemiDoc MP imaging system.

5.2.6 Synergy with FK506 and cercosporamide

Synergy assays were performed essentially as described in Section 2.2.9. This method was adapted from Anderson et al. (2009). In brief, NaD1 or NaD2 (10 μ L of a 10 \times stock) were serially diluted four times down a microtitre plate (Greiner) using a TECAN Evo100 liquid handling robot. Cercosporamide (Tocris Biosciences, 10 μ L of a 100 μ g/mL stock) or FK506 (Abcam Biochemicals, 10 μ L of a 300 μ g/mL stock) were serially diluted six times across the same microtitre plate. *C. albicans* cells (80 μ L, 5000 cells/mL in half-strength PDB) were added and the plates were incubated for 24 h at 30°C. Fungal growth was determined by measuring absorbance at 595 nm (SpectraMAX M5e plate reader, Molecular Devices). Synergy was calculated using Limpel's formula (Richer, 1987).

Limpel's Formula:

$$Ee = x + y - \left(\frac{xy}{100}\right)$$

Ee = expected inhibition

x = inhibition by protein 1

y = inhibition by protein 2

$$\text{Inhibition difference (ID)} = I_o - Ee$$

Synergy is occurring when the observed fungal inhibition is greater than the level of inhibition expected if the antifungal activities of individual molecules were working additively.

5.3 Results

5.3.1 NaD1's effect on calcineurin signalling, the Cap1 oxidative stress response and the cell wall integrity and mating pathways in *C. albicans*

To determine whether the Cap1 transcription factor, the CWI pathway, the mating pathway or calcineurin signalling are involved in survival of cells in the presence of NaD1, *C. albicans* mutants with homozygous deletion of critical genes of these pathways were tested for their relative sensitivity to NaD1. The CWI stress response pathway mutants had deletions of the *BCK1* and *MKC1* genes (see Figure 5.1). The genes deleted in the mating pathway mutants were *STE11*, *HST7* and *CEK2* (see Figure 5.2) and calcineurin mutants lacked either a calcineurin subunit (*cna1Δ*) or a downstream transcription factor (*crz1Δ*). The last mutant lacked Cap1, a transcription factor which is involved in oxidative stress response independent of Hog1 (Figure 5.1).

The *mkc1Δ* and *bck1Δ* mutant phenotypes did not differ from wildtype in their response to NaD1. The *cap1Δ*, *cna1Δ*, *crz1Δ*, *cek2Δ*, *hst7Δ* and *ste11Δ* mutants also responded like wildtype to NaD1 treatment (Figure 5.5, Table 5.1).

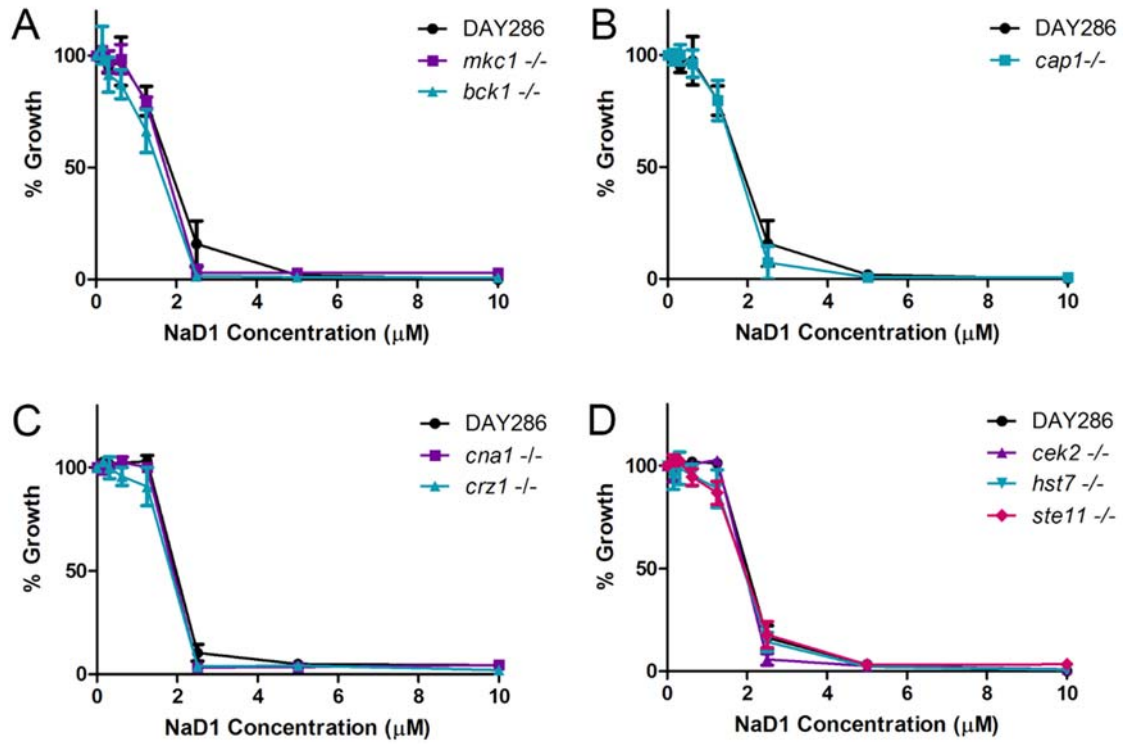


Figure 5.5 The effect of NaD1 on the growth of CWI, Cap1 oxidative stress response, calcineurin and mating pathway deletion mutants

C. albicans DAY286, (A) *mkc1*^{-/-}, *bck1*^{-/-}, (B) *cap1*^{-/-}, (C) *cna1*^{-/-}, *crz1*^{-/-}, (D) *cek2*^{-/-}, *hst7*^{-/-} and *ste11*^{-/-} were grown in the presence of various concentrations of NaD1. Data is shown relative to no-protein controls. Error bars represent SEM (n=3).

Table 5.1 The effect of NaD1 on the growth of *C. albicans* wildtype and mutants in various stress signalling pathways

IC₅₀'s are mean ± SD from at least three independent experiments. P-values were calculated using an independent samples t-test (IBM SPSS Statistics v19) as compared to wildtype and are shown in brackets. Significant changes in IC₅₀ from wildtype are highlighted in grey.

Gene Knockout	Function	NaD1 IC ₅₀ (μM)
Wildtype (DAY286)		2.3 ± 0.60
<i>pbs2</i>	MAPK Kinase, regulation of Hog1	1.0 ± 0.60 (p=0.001)
<i>hog1</i>	MAP Kinase, osmotic and oxidative stress response	0.8 ± 0.30 (p=0.000)
<i>bck1</i>	MAPK Kinase, regulation of Mkc1	1.7 ± 0.33 (p=0.058)
<i>mkc1</i>	MAP Kinase, cell wall integrity and stress	1.7 ± 0.05 (p=0.125)
<i>cap1</i>	Transcription factor, oxidative stress response	1.9 ± 0.25 (p=0.148)
<i>cna1</i>	Calcineurin subunit	2.0 ± 0.06 (p=0.143)
<i>crz1</i>	Transcription factor, downstream of calcineurin	1.8 ± 0.24 (p=0.098)
<i>ste11</i>	MAPKK Kinase, regulation of Hst7	1.9 ± 0.33 (p=0.180)
<i>hst7</i>	MAPK Kinase, regulation of Cek2	2.2 ± 0.85 (p=0.926)
<i>cek2</i>	MAP Kinase, mating pathway	2.3 ± 0.77 (p=0.989)

To verify that *C. albicans* mutants contained the *ARG4* insert in the appropriate genes, genomic DNA was extracted and subjected to PCR with the *ARG4* detect primer, and upstream and downstream primers homologous to the ORF of interest. Mutants were also grown on uracil deficient medium to ensure they contained the *URA3* selection marker.

The *mkc1*^{-/-} mutant had previously been verified for correct deletion of the *MKC1* gene by Western blotting in the Traven lab (Monash University). The remainder of the mutants were verified using the PCR method. An agarose gel showing examples of the PCR products is shown in Figure 5.6. Amplification from the wildtype genomic DNA with Cap1, Cek2 and Crz1 primers yielded DNA fragments of the expected sizes of approximately 1700 bp, 1319 bp and 2396 bp, respectively. No amplification of the wildtype amplicons was observed in the genomic DNA from mutant strains. In the remainder of the mutants, DNA fragments of the expected size were amplified from the wildtype but not the mutants (data not shown).

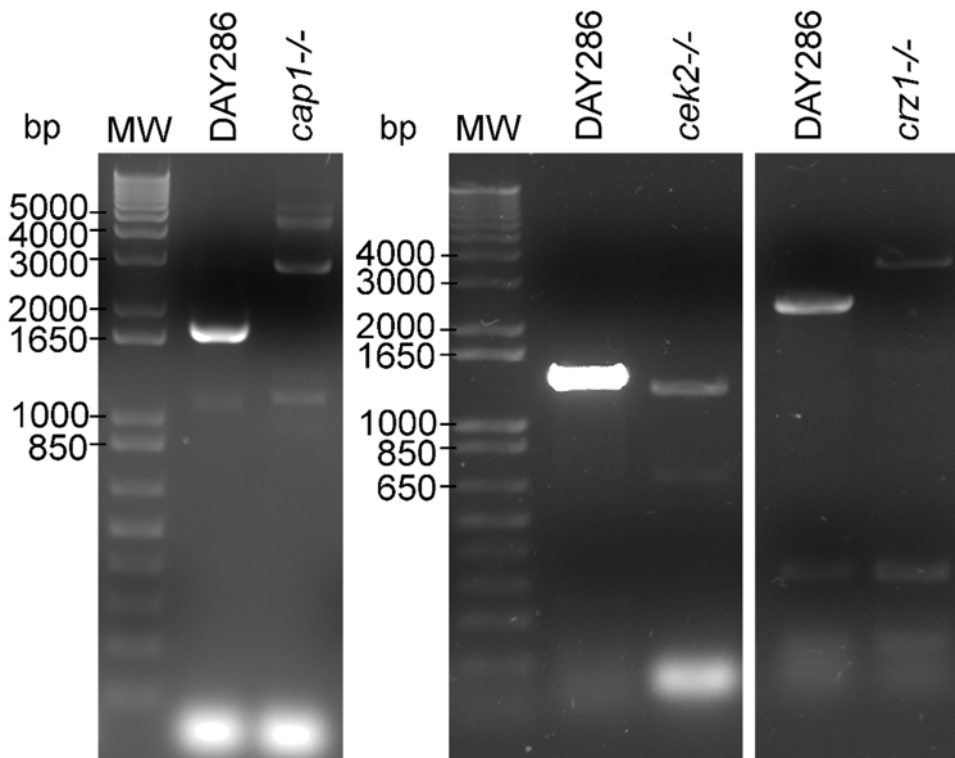


Figure 5.6 PCR screen of *cap1*^{-/-}, *cek2*^{-/-} and *crz1*^{-/-} mutants

Amplification of genomic DNA from DAY286, *cap*^{-/-}, *cek2*^{-/-} and *crz1*^{-/-} with *ARG4* detect, Fw and Rv primers for the gene of interest.

5.3.2 The effect of NaD1 on the growth of *S. cerevisiae* *hog1*, *mpk1*, *cna1*, *yap1* and *fus3* deletion mutants

To see if these signalling pathways contribute to tolerance to NaD1 in other yeast species, *S. cerevisiae* *hog1* Δ , *mpk1* Δ (homologous to *C. albicans* *mkc1* Δ), *cna1* Δ , *yap1* Δ (homologous to *Cacap1* Δ) and *fus3* Δ (homologous to *Cacek2* Δ) were tested for hypersensitivity to NaD1.

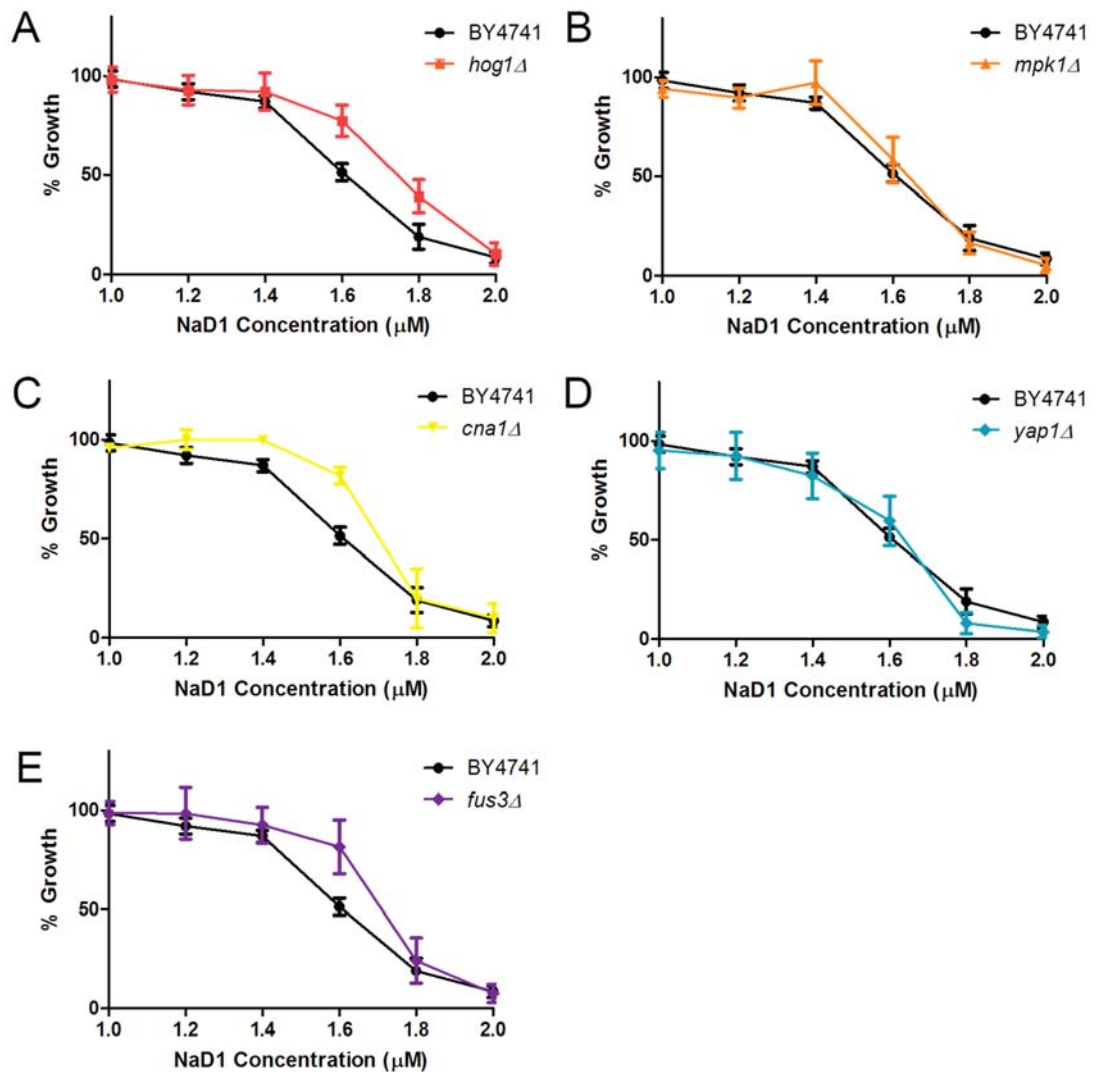


Figure 5.7 The effect of NaD1 on the growth of *S. cerevisiae* with mutations in the HOG, CWI, calcineurin and Yap1 transcription factor pathways

Growth of *S. cerevisiae* BY4741, (A) *hog1* Δ , (B) *mpk1* Δ , (C) *cna1* Δ , (D) *yap1* Δ and (E) *fus3* Δ mutants were monitored in the presence of various concentrations of NaD1. Data is shown relative to a 0 μ M NaD1 control. Data is from three independent experiments. Error bars represent SEM (n=3).

As observed with *C. albicans*, the *Scmpk1Δ* and *Scyap1Δ* mutants were not more sensitive to NaD1 than wildtype cells. In contrast, the *S. cerevisiae hog1Δ* mutant was slightly resistant to NaD1, rather than sensitive like *C. albicans*. The *Scna1Δ* and *Sefus3Δ* mutants were also slightly more resistant to NaD1 than wildtype (Figure 5.7, Table 5.2).

Table 5.2 The effect of NaD1 on growth of *S. cerevisiae* wildtype and mutants in various stress signalling pathways

IC₅₀'s are mean ± SD from at least three independent experiments. P-values were calculated using an independent samples t-test (IBM SPSS Statistics v19) as compared to wildtype and are shown in brackets. Significant changes in IC₅₀ from wildtype are highlighted in grey.

Gene Knockout	Function	NaD1 IC ₅₀ (μM)
Wildtype (BY4741)		1.6 ± 0.04
<i>hog1</i>	MAP Kinase, osmotic and oxidative stress response	1.8 ± 0.05 (p=0.003)
<i>mpk1</i>	MAP Kinase, cell wall integrity and stress	1.6 ± 0.06 (p=0.604)
<i>yap1</i>	Transcription factor, oxidative stress response	1.6 ± 0.08 (p=0.911)
<i>cna1</i>	Calcineurin subunit	1.7 ± 0.07 (p=0.022)
<i>fus3</i>	MAP Kinase, mating pathway	1.7 ± 0.04 (p=0.009)

The *S. cerevisiae* mutants were checked for the correct gene deletions by PCR with kanB primer (Rv) and a primer in the upstream UTR (Fw) for the gene of interest. As expected, there was no amplification in any of the BY4741 genomic DNA with kanB and Fw primers (Figure 5.8). The *hog1Δ*, *mpk1Δ*, *cna1Δ*, *yap1Δ* and *fus3Δ* mutants had bands which matched the expected sizes of 679 bp, 609 bp, 675 bp, 523 bp and 557 bp, respectively. These sizes were consistent with sizes expected from correct deletion of the genes.

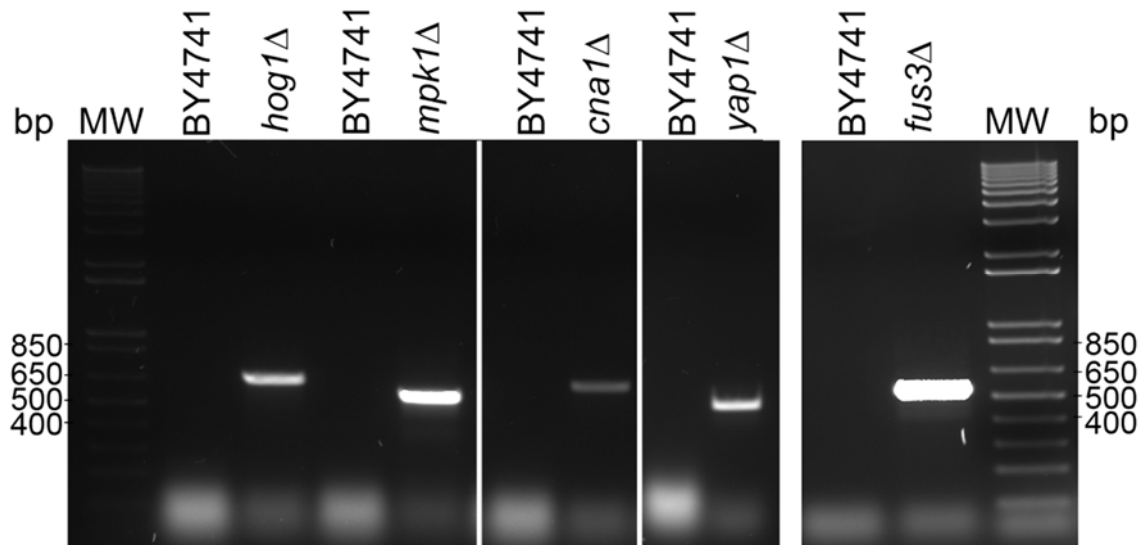


Figure 5.8 PCR screen to confirm gene deletions in *S. cerevisiae* *hog1Δ*, *mpk1Δ*, *cna1Δ*, *yap1Δ* and *fus3Δ*

Amplification of genomic DNA from BY4741, *hog1Δ*, *mpk1Δ*, *cna1Δ*, *yap1Δ* and *fus3Δ* strains with KanB primer and *hog1* Fw, *mpk1* Fw, *cna1* Fw, *yap1* Fw or *fus3* Fw primers. Amplicons of the expected size were obtained for all the mutants. As expected, no amplified DNA was obtained from the wildtype (BY4741).

The *hog1Δ* deletion phenotype was much more pronounced in *C. albicans* than in *S. cerevisiae*. In addition, the *S. cerevisiae hog1Δ* mutant was more resistant to NaD1, rather than more sensitive as observed in *C. albicans* (Table 5.1, Table 5.2). To determine whether there were differences in oxidative stress tolerance between *C. albicans* and *S. cerevisiae* that could account for the difference in phenotype in the *hog1Δ* mutant, *C. albicans* DAY185 and *S. cerevisiae* BY4741 were tested for susceptibility to hydrogen peroxide at various concentrations. *S. cerevisiae* did not reach the same cell density as *C. albicans* in the no-protein control after 24 h incubation (data not shown) However, when data was expressed as percentage growth (relative to the no-protein control) the *C. albicans* and *S. cerevisiae* growth curves overlapped (Figure 5.9).

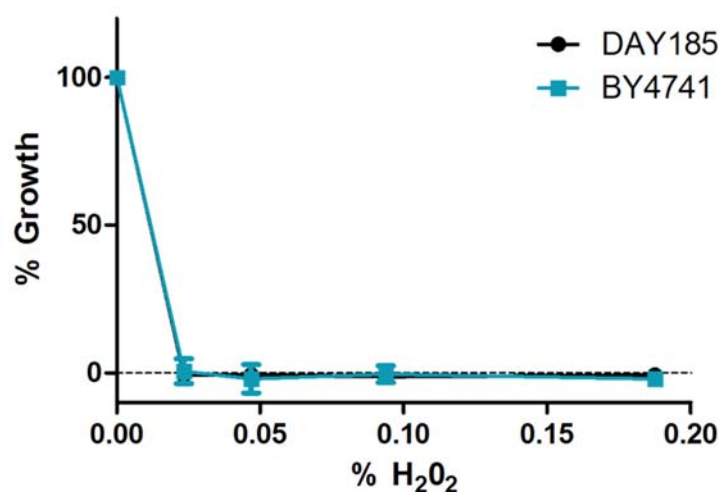


Figure 5.9 The effect of hydrogen peroxide on the growth of *C. albicans* and *S. cerevisiae*

C. albicans DAY185 and *S. cerevisiae* BY4741 growth was monitored after incubation with various concentrations of H₂O₂. Data is shown relative to a no treatment control. Data is a representative example of three independent experiments. Error bars represent SD (n=2).

5.3.3 *S. cerevisiae* deletions in genes which function upstream of Hog1

Hog1 activation can occur through signals emanated by either of two cell surface osmosensors, Sho1 and Sln1, in *S. cerevisiae* (Figure 5.1) (Maeda et al., 1995). Another transmembrane protein, ScMsb2, is involved in activation of the ScSho1 branch of ScHog1 activation, and can also cause ScHog1 activation independently of ScSho1 (Tatebayashi et al., 2007). In *C. albicans*, activation of CaHog1 only occurs through the CaSln1 osmosensor (Cheetham et al., 2007; Smith et al., 2010). To determine if the upstream signal that activates Hog1 after NaD1 treatment differs between *C. albicans* and *S. cerevisiae*, *Scsho1Δ*, *Scmsb2Δ* and *Scsln1Δ* mutants were tested for differences in NaD1 sensitivity relative to wildtype. Like the *Schog1Δ* mutant (Figure 5.7A), both the *Scsho1Δ* and *Scmsb2Δ* mutants were more resistant to NaD1 than wildtype (Figure 5.10). The *ScSLN1* gene is essential for growth, so a heterozygous mutant was tested. This mutant behaved like wildtype after treatment with NaD1 (Figure 5.10).

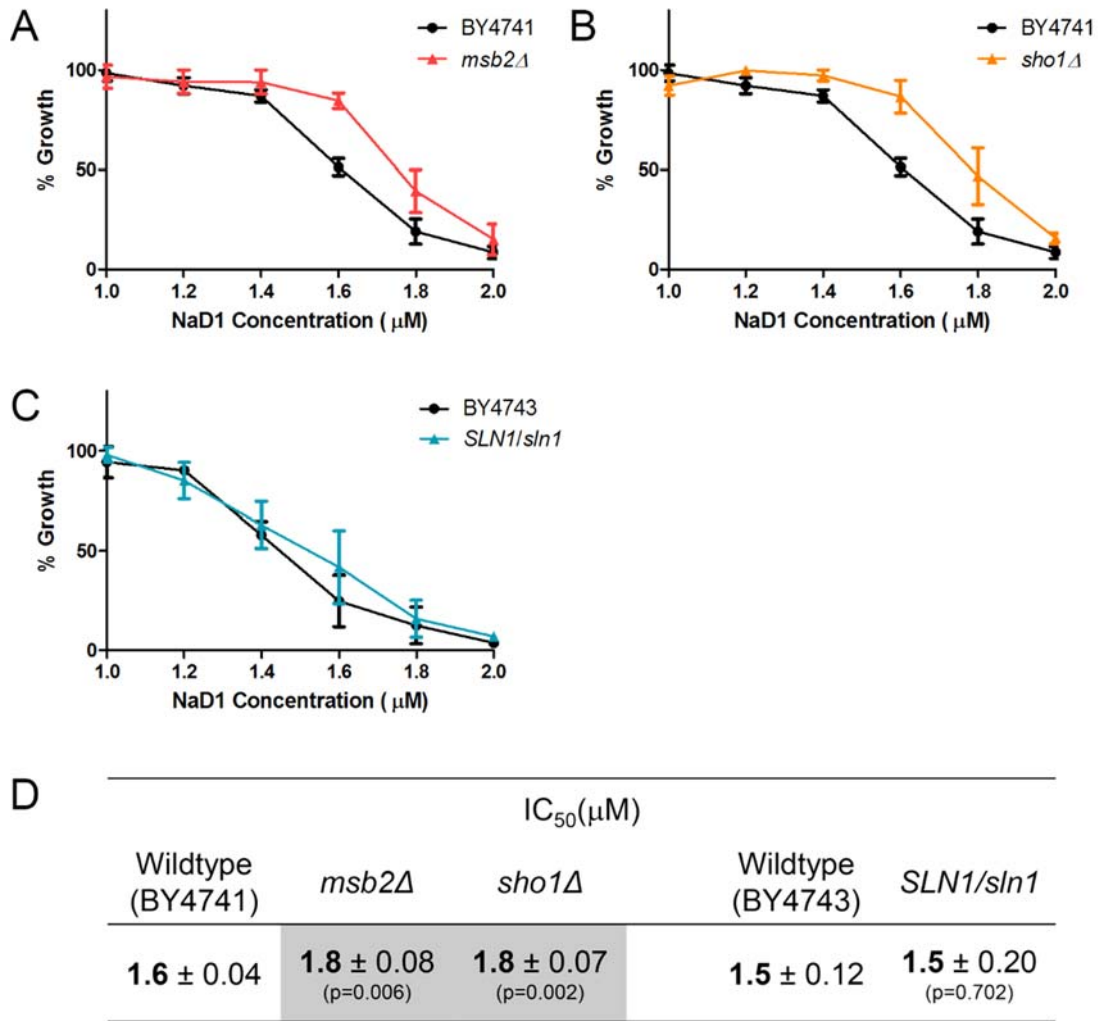


Figure 5.10 The effect of NaD1 on the growth of *S. cerevisiae* mutants from the two alternative osmosensing pathways of Hog1 activation

S. cerevisiae homozygous mutants (A) *msb2Δ*, (B) *sho1Δ* and a heterozygous *sln1* deletion mutant were treated with various concentration of NaD1. For *sho1Δ* and *msb2Δ*, growth was compared to the wildtype strain BY4741. For the *SLN1/sln1* heterozygous mutant the wildtype strain was BY4743. Data is shown relative to a 0 μM NaD1 control. Data is from three independent experiments. Error bars represent SEM (n=3). (D) IC₅₀'s are means ± SD from at least three independent experiments. P-values were calculated using an independent samples t-test (IBM SPSS Statistics v19) as compared to wildtype and are shown in brackets. Significant changes in IC₅₀ values from wildtype are highlighted in grey.

The *S. cerevisiae* mutants were verified for correct gene deletions by PCR with the kanB primer (Rv) and forward primers (Fw) for the gene of interest. As expected, there was no amplification from the BY4741 genomic DNA (Figure 5.11). The *hog1Δ*, *msb2Δ*, *sho1Δ* and *SLN1/sln1Δ* mutants had amplified DNA which matched the expected sizes of 679, 623, 699 and 645 bp, respectively. These sizes were consistent with sizes expected from correct deletion of the genes.

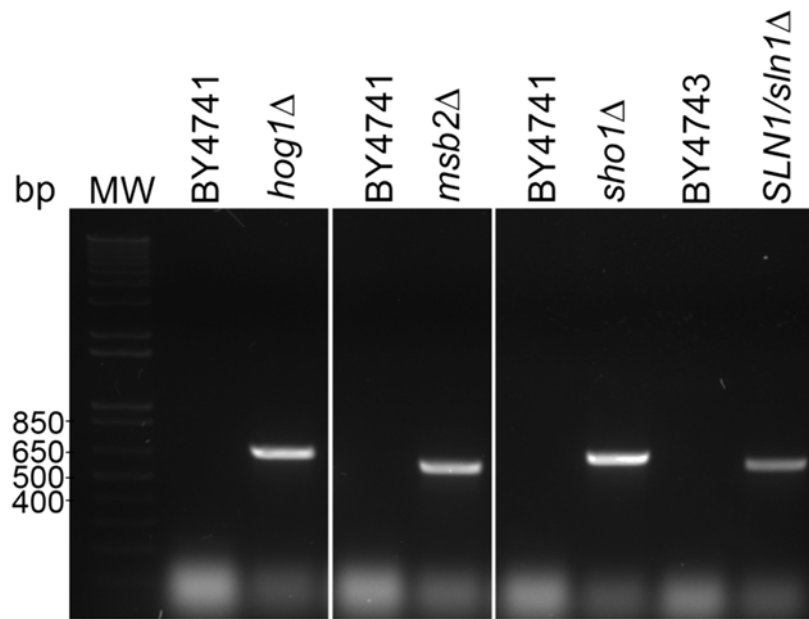


Figure 5.11 PCR screen to confirm gene deletions in the *S. cerevisiae* *hog1Δ*, *msb2Δ*, *sho1Δ* and *SLN1/sln1Δ* mutants

Amplification of genomic DNA from BY4741 (or BY4743 for heterozygous mutants), *hog1Δ*, *msb2Δ*, *sho1Δ* and *SLN1/sln1Δ* strains with KanB primer and *hog1* Fw, *msb2* Fw, *sho1* Fw or *sln1* Fw primers. Amplicons of the expected size appeared for all the mutants. As expected, the primers did not produce amplicons from the wildtype (BY4741 or BY4743).

5.3.4 G-protein coupled receptors

The mating pathway is activated when the ScSte2 or ScSte3 G-protein coupled receptors are stimulated by pheromone (Figure 5.3) (Versele et al., 2001). As the phenotype of the mating pathway mutants *Scfus3Δ* and *Cacek2Δ* differed, I was interested in whether an inhibitor of G-protein coupled receptors, pertussis toxin, would affect the activity of NaD1 against *C. albicans* and *S. cerevisiae*.

Pertussis toxin at 10 ng/μL blocked the growth inhibitory activity of NaD1 against *C. albicans* (Figure 5.12A). This phenomenon also occurred in *S. cerevisiae*, although NaD1's activity was reduced by 50% rather than blocked in the presence of pertussis toxin (Figure 5.12B).

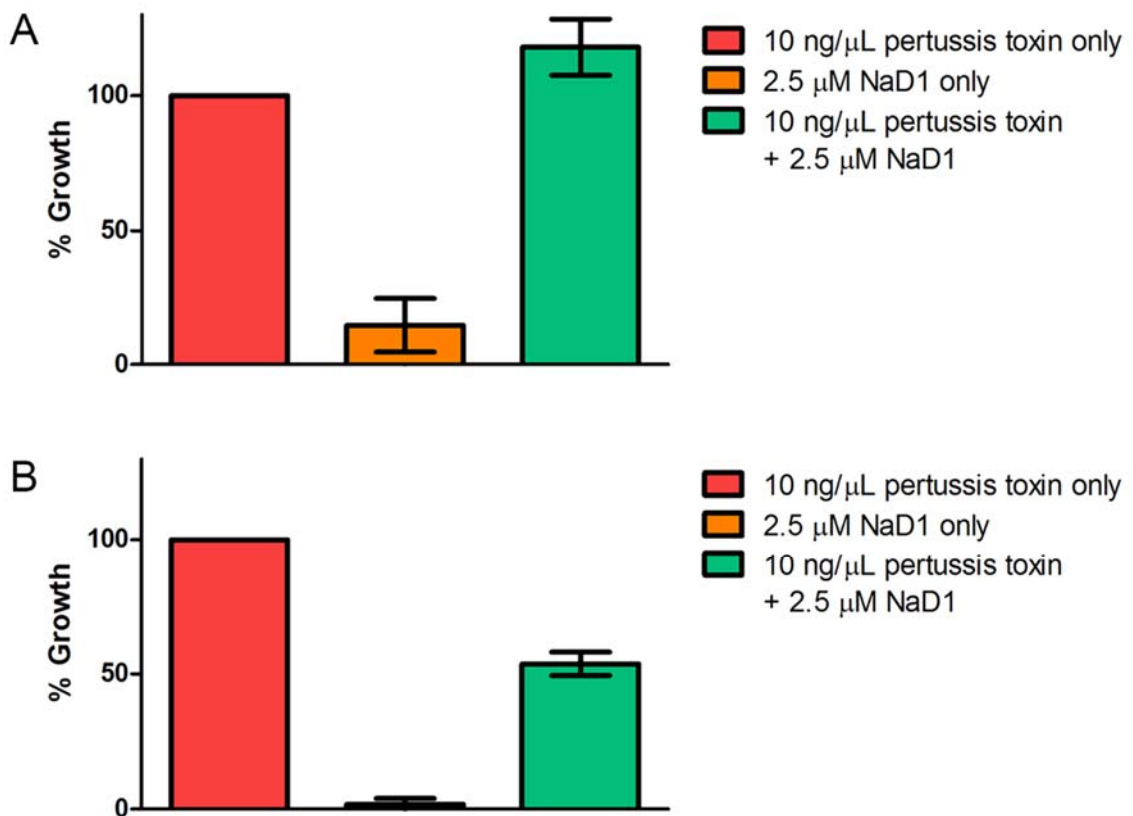


Figure 5.12 Pertussis toxin reduces the effect of NaD1 against *C. albicans* and *S. cerevisiae*

(A) *C. albicans* DAY185 or (B) *S. cerevisiae* were treated with 2.5 μM NaD1 only, 10 ng/μL pertussis toxin only or 2.5 μM NaD1 and 10 ng/μL pertussis toxin in combination. Data are relative to the pertussis toxin only controls. Errors bars represent SEM (n=3).

The effect of pertussis toxin on NaD1 activity was also investigated using flow cytometry. *C. albicans* cells were treated with pertussis toxin (and brefeldin A as a control), incubated with BODIPY-NaD1, washed to remove any NaD1 which had not been internalised or tightly bound to the cell wall and then the fluorescing cells were counted using flow cytometry (Figure 5.13).

C. albicans cells which had been treated with BODIPY-NaD1 and pertussis toxin had lower levels of fluorescence than cells which had been treated with BODIPY-NaD1 alone (Figure 5.13A). In contrast, brefeldin A treatment did not reduce fluorescence in cells.

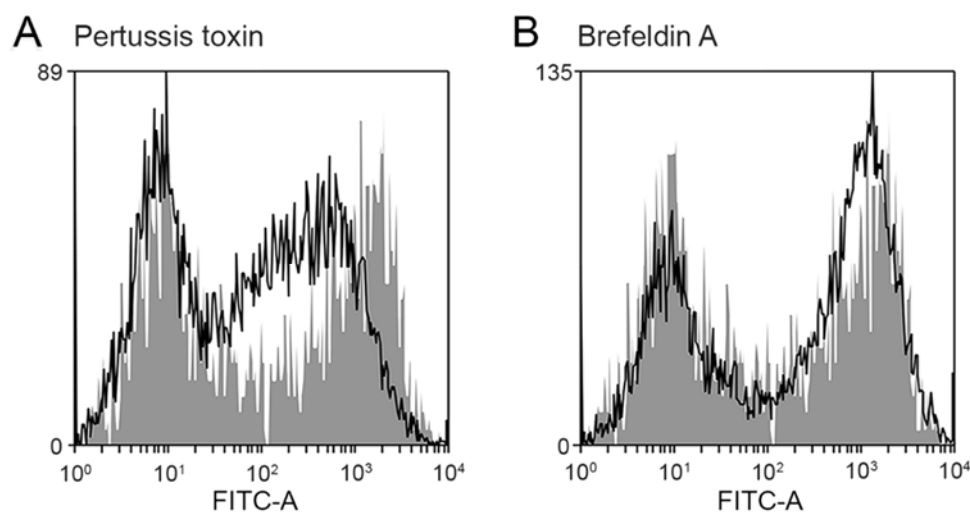


Figure 5.13 Flow cytometry monitoring BODIPY-NaD1 uptake after treatment with cellular inhibitors

Flow cytometry was used to monitor the uptake of fluorescently labelled NaD1 (BODIPY-NaD1) into *C. albicans* after treatment with (A) pertussis toxin or (B) brefeldin A. Black lines are BODIPY-NaD1 (10 μM) plus inhibitor and shaded in grey are NaD1 only controls (10 μM, no inhibitor). Cells were then washed to leave only BODIPY-NaD1 that had entered cells or was bound to the cell wall. The vertical and horizontal axes represent cell counts and fluorescent intensity, respectively. Data are representative examples of three independent experiments, which gave equivalent results.

Pertussis toxin reduced the activity of NaD1 in fungal growth inhibition assays and reduced the amount of BODIPY-NaD1 fluorescence in flow cytometry experiments (Figure 5.12, Figure 5.13). The effect of pertussis toxin examined further by performing growth inhibition assays in the presence of both pertussis toxin and brefeldin A. Brefeldin A renders pertussis toxin inactive by blocking uptake and transport of the toxin (el Baya et al., 1997; Xu & Barbieri, 1995). When brefeldin A was added to growth assays with pertussis toxin and NaD1, the protective effect of pertussis toxin against the growth inhibitory activity of NaD1 was partially reversed (Figure 5.14). That is, addition of brefeldin A led to less cell growth compared to the combination of pertussis toxin and NaD1 alone. This effect was concentration dependent, with cell growth decreasing with increasing brefeldin A concentrations.

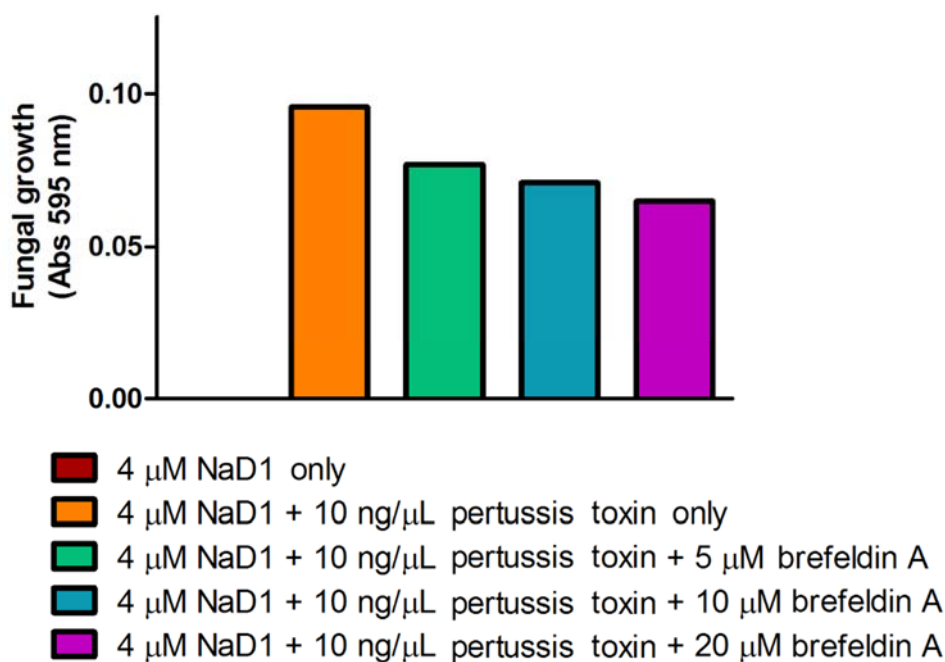


Figure 5.14 Addition of brefeldin A reduces rescue of NaD1 growth inhibition of *C. albicans* by pertussis toxin

C. albicans DAY185 was treated with 4 μ M NaD1 only, NaD1 with 10 ng/ μ L pertussis toxin and NaD1, pertussis toxin and 5, 10 or 20 μ M brefeldin A. Growth was quantified by measuring absorbance at 595 nm after 24 h incubation. Data is a representative example of three independent experiments which gave equivalent results.

As the resistance phenotype of the mating pathway MAPK deletion mutants was specific to *S. cerevisiae*, but pertussis toxin reduced NaD1 inhibition in both *S. cerevisiae* and *C. albicans*, I examined whether deletion of the second *S. cerevisiae* GPCR, Gpr1, affected NaD1 activity. I also tested mutants with deletions of the pheromone sensing GPCRs, *Scste2* and *Scste3*, and the MAPKKK *Scste11* and MAPKK *Scste7*, which are shared by the mating and invasive growth pathways.

The growth inhibitory activity of NaD1 on the *S. cerevisiae* *gpr1Δ*, *ste2Δ*, *ste3Δ*, *ste7Δ* and *ste11Δ* mutants was and compared to wildtype (BY4741) (Figure 5.15). In the presence of NaD1, the growth of the *gpr1Δ* mutant did not differ significantly from wildtype (Figure 5.15A). However, the *fus3Δ*, *ste2Δ*, *ste3Δ*, *ste7Δ* and *ste11Δ* mutants were slightly more resistant to NaD1 growth inhibition than wildtype (Figure 5.15B-D).

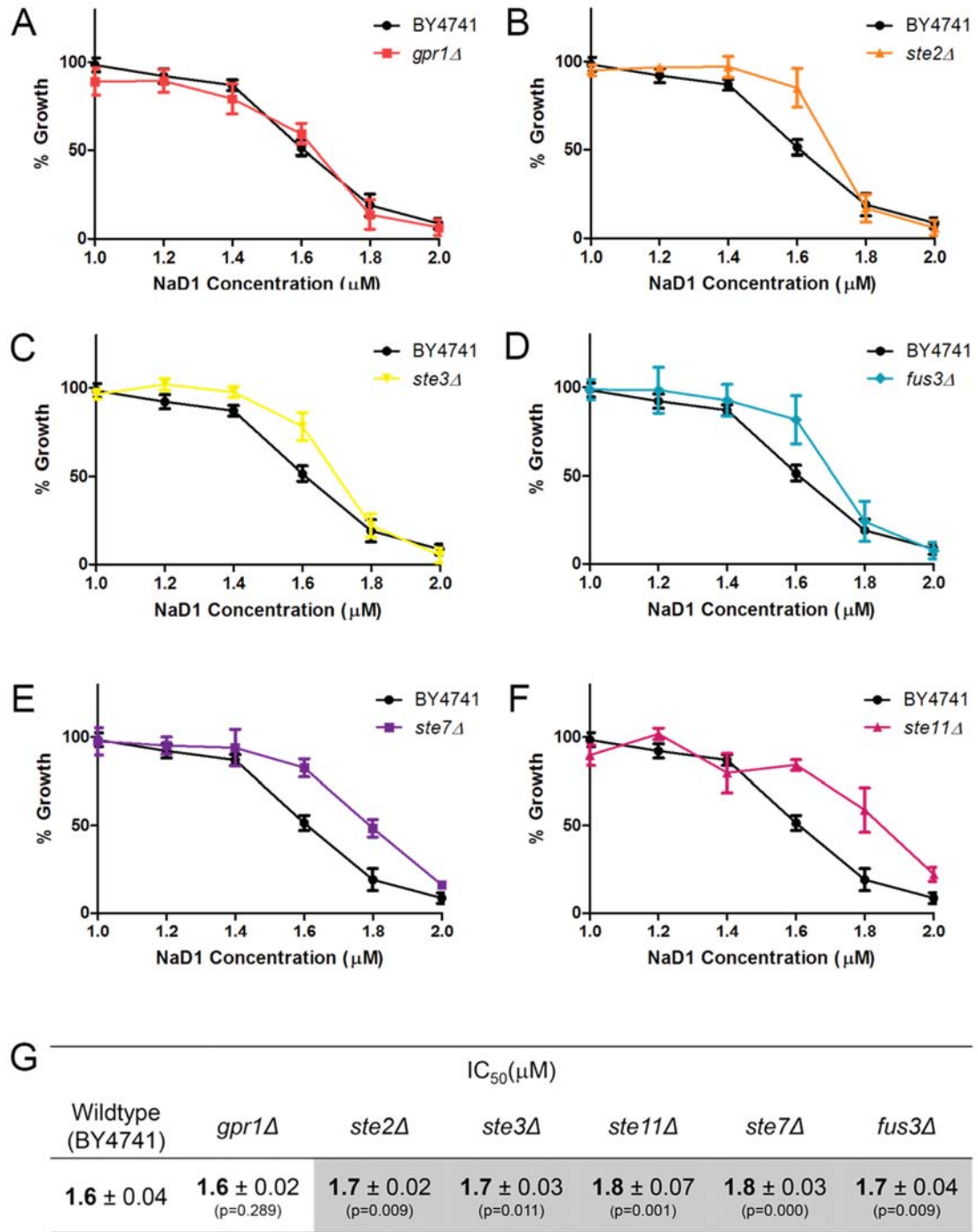


Figure 5.15 The growth inhibitory activity of NaD1 against *S. cerevisiae* GPCR and Fus3 mating pathway mutants

S. cerevisiae BY4741 (WT), (A) *gpr1Δ*, (B) *ste2Δ*, (C) *ste3Δ*, (D) *fus3Δ*, (E) *ste7Δ* and (F) *ste11Δ* were treated with various concentrations of NaD1 and growth monitored for 24 h. Data is relative to a 0 μM NaD1 control. Results shown are from three independent experiments. Error bars represent SEM (n=3). (G) IC₅₀'s are means ± SD from at least three independent experiments. P-values were calculated using an independent samples t-test (IBM SPSS Statistics v19) as compared to wildtype and are shown in brackets. Significant changes in IC₅₀ values from wildtype are highlighted in grey.

To determine if the *S. cerevisiae* mutants had the correct deletions, the strains were subjected to PCR with the kanB primer (Rv) and a primer in the upstream UTR (Fw) for the gene of interest. As the deletions were constructed by insertion of a KanMX4 module into the gene, amplification using these primers was only expected in strains that had successful deletions. As expected, there was no amplification from wildtype genomic DNA when using the above primers (Figure 5.16). The *gpr1Δ*, *ste2Δ*, *ste3Δ*, *ste7Δ* and *ste11Δ* mutants had amplicons which matched the expected sizes of 700, 677, 621, 634 and 558 bp, respectively. The deletion in the *fus3Δ* mutant was verified previously (Figure 5.8).

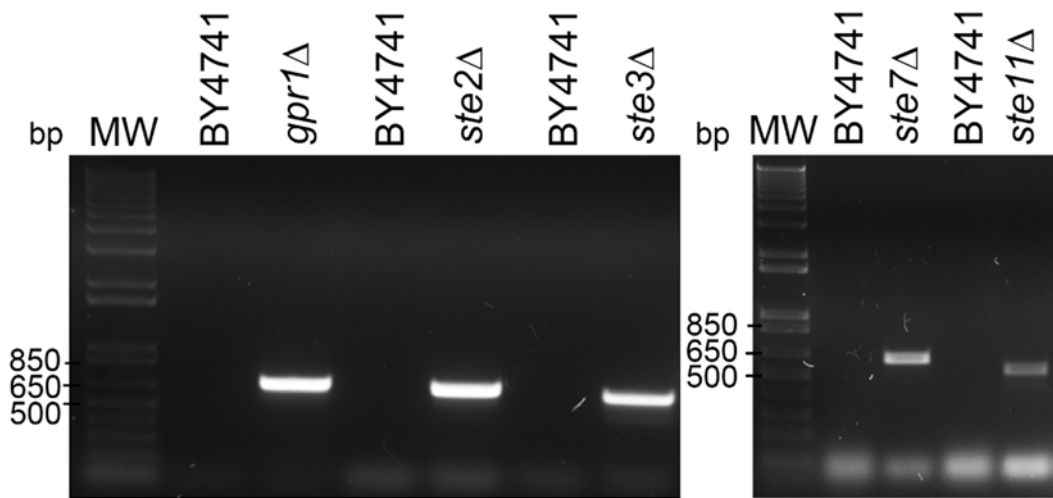


Figure 5.16 PCR screen to confirm gene deletions in the *S. cerevisiae fus3Δ*, *ste3Δ*, *ste2Δ* and *gpr1Δ* mutants

Amplification of genomic DNA from BY4741, *gpr1Δ*, *ste2Δ*, *ste3Δ*, *ste7Δ* and *ste11Δ* strains with KanB primer and *gpr1* Fw, *ste2* Fw, *ste3* Fw, *ste7* Fw or *ste11* Fw primers. Amplicons of the expected size appeared for all the mutants. As expected, the primers did not produce amplicons from the wildtype (BY4741).

The GPCR encoded by *GPR1* functions in glucose sensing. Thus, I examined whether increasing the amount of glucose affected the activity of NaD1 against *C. albicans* DAY185 and *S. cerevisiae* BY4741. An additional two per cent dextrose was added to the half-strength PDB medium (PDB already contains 2% dextrose). The activity of NaD1 was not altered by addition of extra dextrose to half-strength PDB (Figure 5.17).

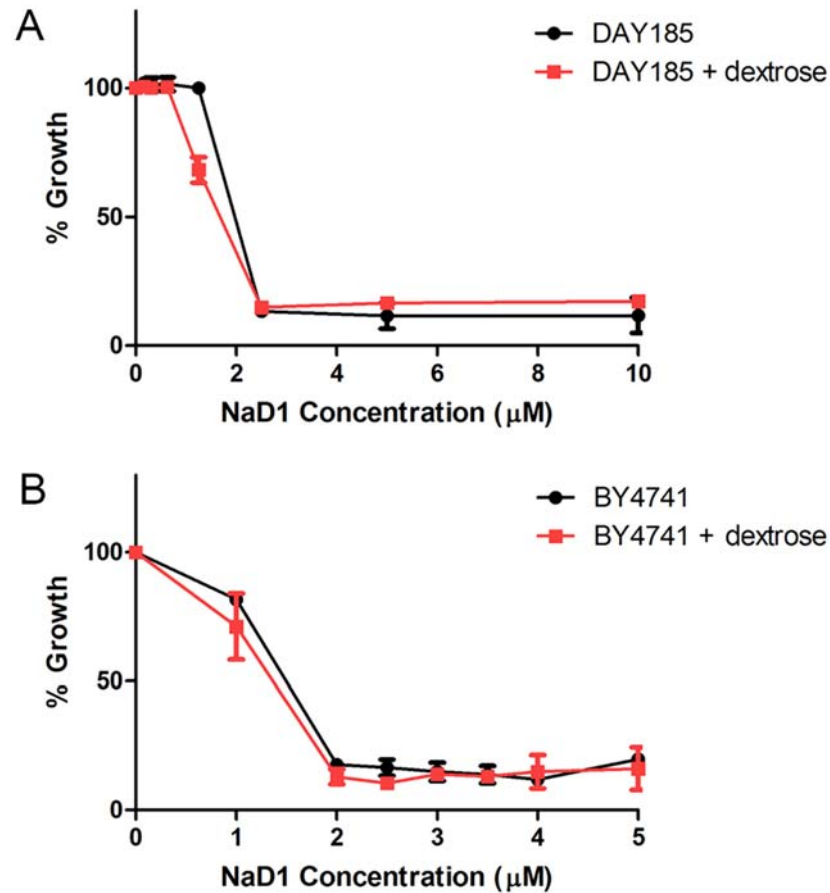


Figure 5.17 The effect of additional dextrose on the activity of NaD1 against *C. albicans* and *S. cerevisiae* in half-strength PDB

(A) *C. albicans* DAY185 and (B) *S. cerevisiae* BY4741 were treated with various NaD1 concentrations in the presence and absence of an additional 2% dextrose. Data is shown relative to a no-protein control. Data a representative example. Error bars represent SD (n=3).

5.3.5 The effect of other plant defensins on the growth of *C. albicans* signalling mutants

To determine whether other plant defensins trigger the same stress response pathways, *C. albicans* signalling mutants were tested for susceptibility to two plant defensins from different phylogenic groups (van der Weerden & Anderson, 2012b). They were the class I defensins NaD2 (from *N. alata*) and DmAMP1 (from *D. merckii*). Interestingly, both the *hog1* and *mkc1* deletion mutants were sensitive to NaD2 and DmAMP1 (Figure 5.18), whereas only the *hog1* deletion mutant was sensitive to NaD1 (Table 5.1).

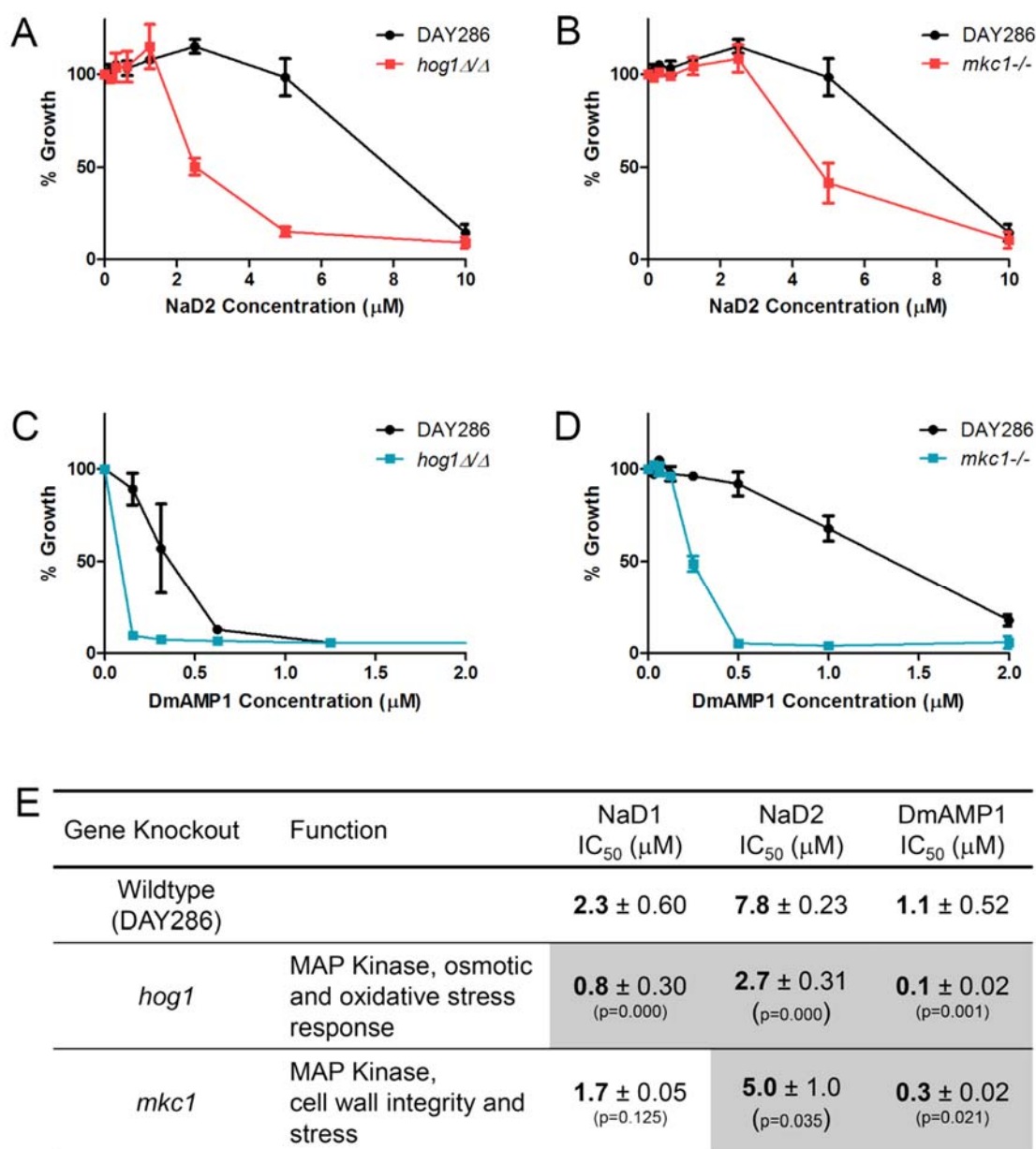


Figure 5.18 The effect of the plant defensins NaD1, NaD2 and DmAMP1 on the growth of *C. albicans* wildtype and *hog1Δ* and *mkc1Δ* mutants

Growth inhibition assays with various concentrations of NaD2 against *C. albicans* (A) *hog1Δ/Δ* and (B) *mkc1-/-* or DmAMP1 against (C) *hog1Δ/Δ* and (D) *mkc1-/-*. Data is shown relative to a no-protein control. Data is from three independent experiments. Error bars represent SEM (n=3). (E) IC₅₀'s are mean ± SD from at least three independent experiments. P-values were calculated using an independent samples t-test (IBM SPSS Statistics v19) as compared to wildtype and are shown in brackets. Significant changes in IC₅₀ values from wildtype are highlighted in grey. The data corresponding to NaD1 is presented in Table 5.1.

5.3.6 Detection of *C. albicans* Hog1 phosphorylation in response to NaD2

The enhanced sensitivity of the *C. albicans* Hog1 deletion mutant to NaD2 suggests that the Hog1 pathway is activated by NaD2 in the wildtype. Phosphorylation of Hog1 in wildtype *C. albicans* after NaD2 treatment was thus monitored by Western blotting. In the absence of NaD2, no phosphorylated Hog1 was detected. However, phosphorylated Hog1 appeared after treatment with 1 M NaCl or 20 μ M NaD2 (Figure 5.19A). No Hog1, in either the phosphorylated or non-phosphorylated form, was detected in the *hog1* deletion mutant (Figure 5.19A). Using densitometry, the level of phosphorylation after NaD2 treatment was calculated relative to the 1 M NaCl treated sample after taking differences in total Hog1 levels into account. The level of phosphorylated Hog1 in the NaD2 was 0.82 of the 1 M NaCl control (Figure 5.19B).

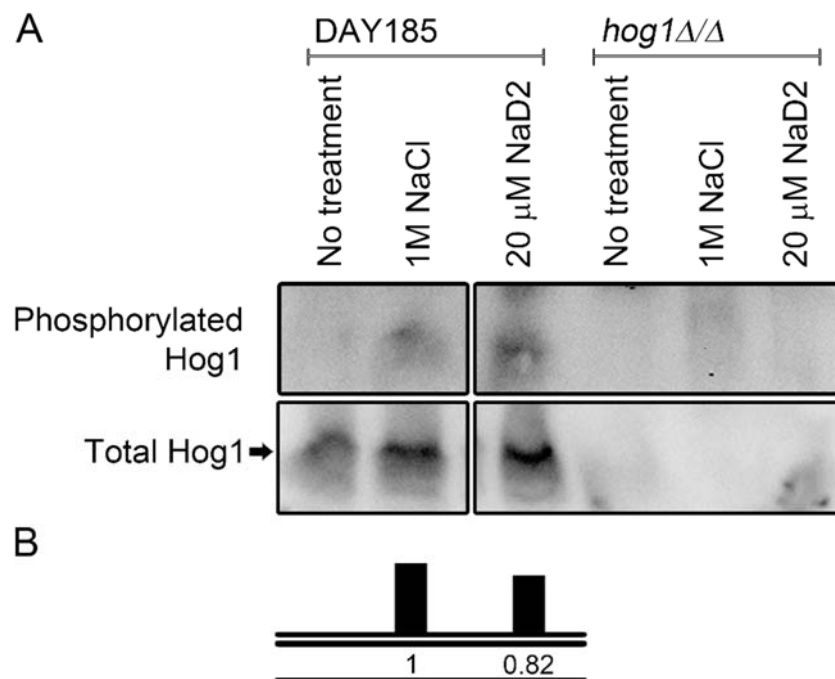


Figure 5.19 The Hog1 pathway is activated in *C. albicans* by NaD2 treatment

(A) Western blots showing levels of phosphorylated Hog1 (after probing with antibodies against phospho-p38 MAPK), against total Hog1 levels (detected with Hog1 antibody). DAY185 and *hog1* Δ/Δ cells were treated with 1 M NaCl (10 min) or 20 μ M NaD1 (20 min). Total Hog1 levels are shown with a black arrow. Hog1 phosphorylation was detected after treatment with the NaCl positive control and with 20 μ M NaD2. No p-Hog1 was detected in the *hog1* Δ/Δ strain after treatment with 1 M NaCl, 20 μ M NaD2 or in the no-treatment control. (B) Density of p-Hog1 bands from Western blots. Densities were normalised to total Hog1 levels, and are shown relative to the 1M NaCl control.

5.3.7 The effect of inhibitors of the calcineurin and cell wall integrity pathways on the antifungal activity of NaD1 and NaD2

In previous sections of this Chapter I described the effects of mutations in various stress pathways and the mating pathway on the activity of NaD1 and NaD2. Deletion of genes in the HOG pathway enhanced sensitivity to both defensins whereas impairment of the CWI pathway enhanced NaD2 sensitivity but had no effect on sensitivity to NaD1. This work was continued using chemical inhibitors of calcineurin and the CWI pathway to establish their effect on the activity of NaD1 and NaD2 against *C. albicans*.

The calcineurin inhibitor FK506 and the CWI pathway inhibitor cercosporamide enhanced the activity of NaD1 against *C. albicans* in a synergistic manner. Synergy levels were classified as low, medium, high or very high as defined in Table 2.2. According to Limpel's formula, the combination of cercosporamide and NaD1 resulted in only medium (at 5 µg/mL cercosporamide) or low levels of synergy (Figure 5.20A and B). In contrast, the combination of NaD1 and 30µg/mL FK506 resulted in very high synergy and 7.5 µg/mL or 15 µg/mL FK506 produced high synergy (Figure 5.20C and D).

NaD2 also displayed synergy with cercosporamide and FK506 against *C. albicans*. The combination of NaD2 and cercosporamide resulted in high synergy values at two concentrations of cercosporamide (2.5 µg/mL and 5 µg/mL) (Figure 5.21). While, the combination of NaD2 and FK506 resulted in a high synergy when 30 µg/mL FK506 was used (Figure 5.21C and D).

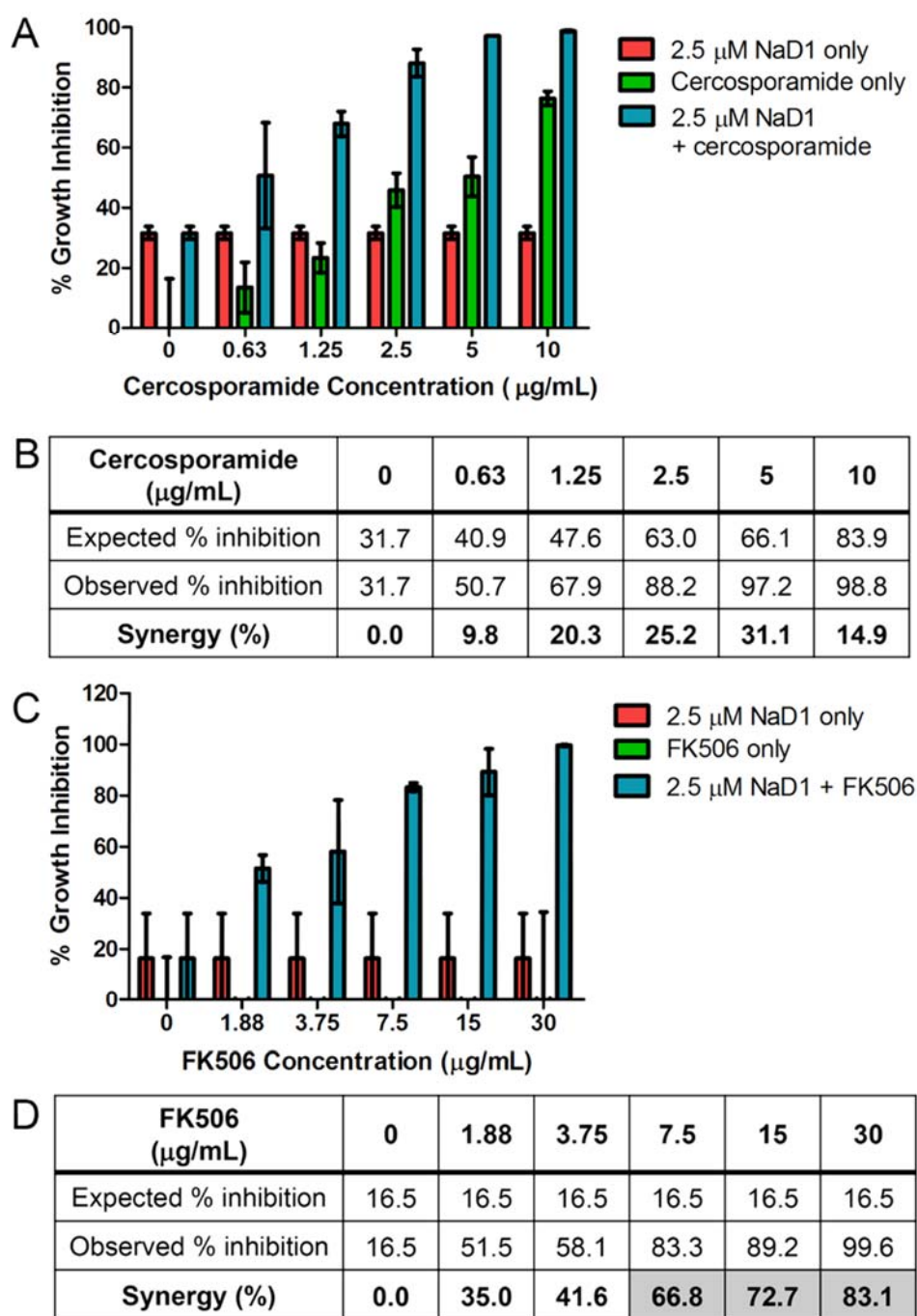


Figure 5.20 Synergy of NaD1 with FK506 and cercosporamide against *C. albicans*

Growth inhibition of *C. albicans* DAY185 in the presence of 2.5 μM NaD1 only, inhibitor only and NaD1 and inhibitor combined for (A) cercosporamide and (C) FK506 at various concentrations. Data is relative to a no-protein control. Data are representative examples from three independent experiments. Error bars represent standard deviation from two replicates. Synergy between the inhibitors and NaD1 was calculated using Limpel's formula and is shown for various concentrations of (B) cercosporamide and (D) FK506. Concentrations of inhibitor that produced high or very high synergy with NaD1 are shaded in grey. The expected and observed inhibitions are also shown.

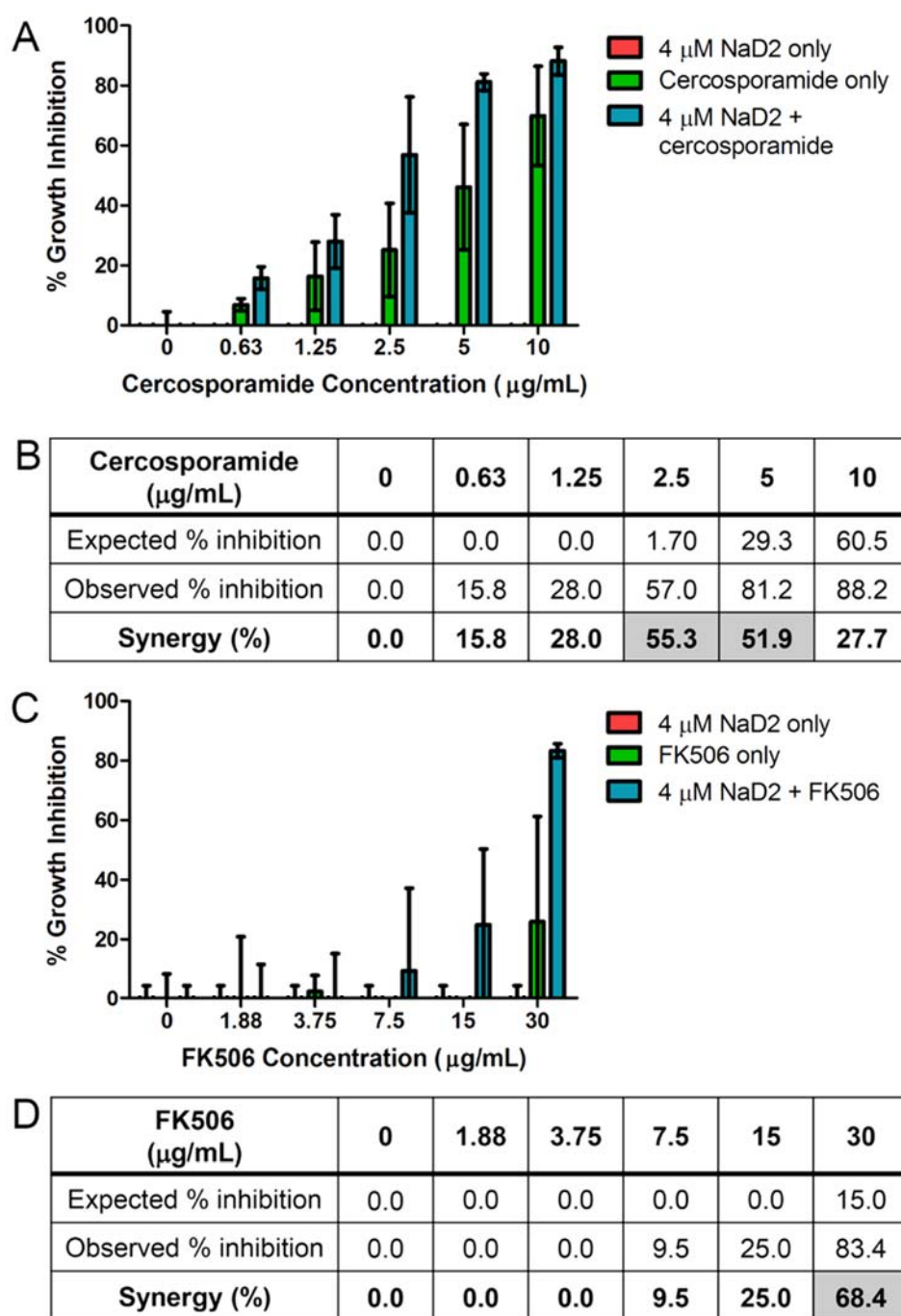


Figure 5.21 Synergy of NaD2 with FK506 and cercosporamide against *C. albicans*

Growth inhibition of *C. albicans* DAY185 in the presence of 4 µM NaD2 only, inhibitor only and NaD2 and inhibitor combined for (A) cercosporamide and (C) FK506 at various concentrations. Data is relative to a no-protein control. Data is a representative example from three independent experiments. Error bars represent standard deviation from two replicates. Synergy between the inhibitors and NaD2 was calculated using Limpel's formula and is shown for various concentrations of (B) cercosporamide and (D) FK506. Concentrations of inhibitor that produced high or very high synergy with NaD2 are shaded in grey. The expected and observed inhibitions are also shown.

5.4 Discussion

In Chapter 4, I reported that NaD1 causes oxidative stress (through production of ROS) in *C. albicans* cells and the CaHog1 pathway is activated by the fungus in an attempt to overcome the stress. This observation led to the question of whether *Cacap1Δ* and CWI mutants would also be more susceptible to NaD1. CaCap1 is a transcription factor that responds to oxidative stress independently from CaHog1 (Enjalbert et al., 2006). The CWI pathway is primarily activated in response to cell wall stress, but can also be activated by oxidative stress (Navarro-García et al., 2005). However, neither *Cacap1Δ* nor CWI deletion mutants (*Camkc1Δ* and *Cabck1Δ*) were more susceptible to NaD1 than wildtype. Thus, *C. albicans* tolerance to NaD1 induced oxidative stress does not require the CaCap1 transcription factor or the CWI pathway.

C. albicans calcineurin signalling responds to many of the same stresses as the CWI pathway (Bader et al., 2003; Cruz et al., 2002), so the requirement of this pathway in the NaD1 response was also tested. Like the CWI deletion mutants, mutants deficient in Ca-calcineurin signalling, with deletion of either the Ca-calcineurin subunit *Cacna1* or the transcription factor *Cacrz1*, were not sensitive to NaD1 treatment. Likewise, mutants with deletions in the *C. albicans* mating pathway (*Cacek2Δ* and *Cahst7Δ*) did not differ from wildtype in their NaD1 response.

In summary, *C. albicans* appears to respond to NaD1 induced ROS solely through the CaHog1 pathway. A summary of *C. albicans* stress signalling in response to NaD1 is presented in Figure 5.22.

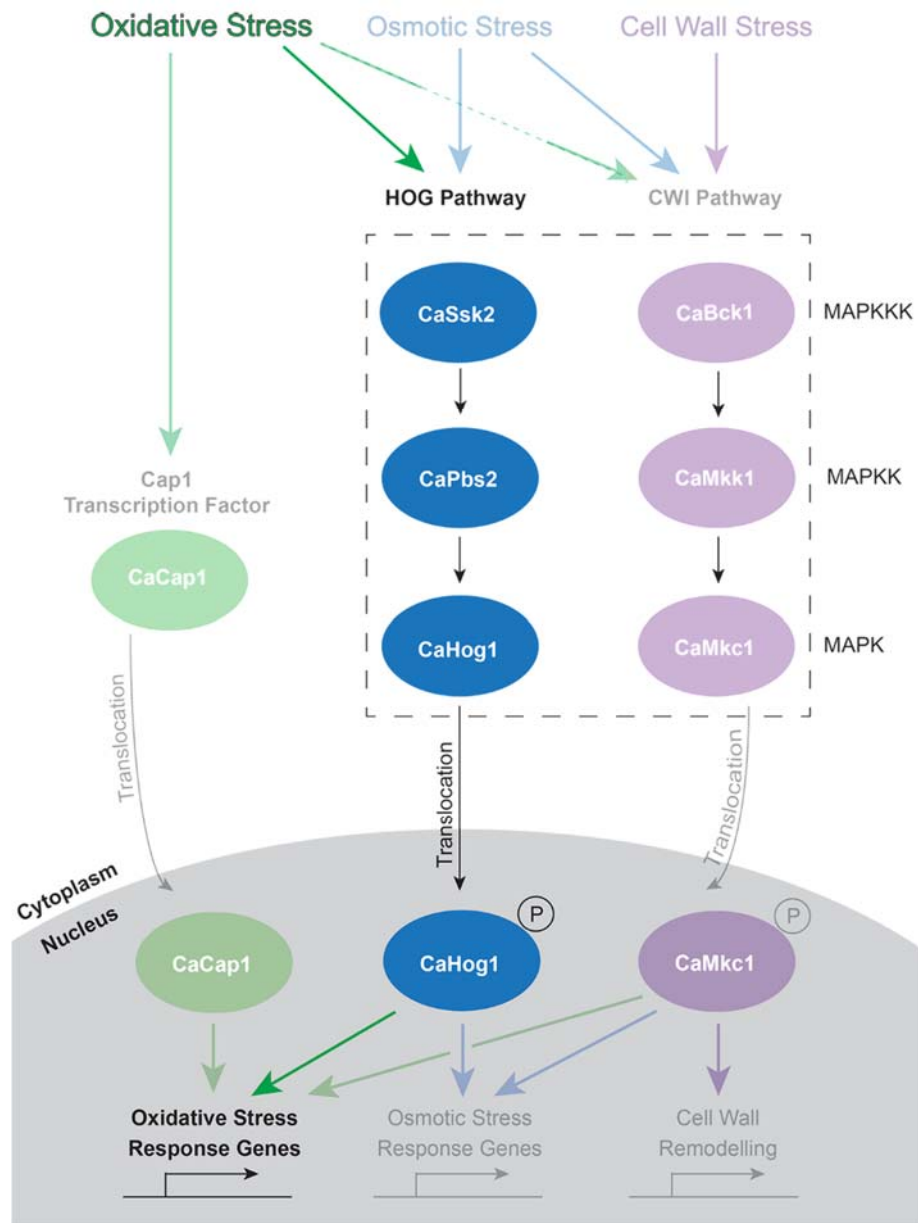


Figure 5.22 *C. albicans* stress signalling in response to NaD1

When treated with NaD1, *C. albicans* activates the Hog1 MAPK pathway. Oxidative stress, not osmotic stress, is responsible for activation of this pathway. The CWI pathway and Cap1 do not respond to NaD1 treatment.

The mating pathway of *F. graminearum* has also been associated with tolerance to the plant defensins RsAFP2, MsDef1 and MtDef4 (Ramamoorthy et al., 2007b). However, deletion of the MAPK, MAPKK and MAPKKK (CaCek2, CaHst7 and CaSte11, respectively) of the *C. albicans* mating pathway did not alter NaD1's ability to inhibit fungal growth.

Next, *S. cerevisiae* stress signalling mutants were also analysed. The *S. cerevisiae hog1Δ* mutant did have an altered phenotype compared to wildtype, but it was slightly more resistant to NaD1 rather than sensitive like the *C. albicans hog1* deletion. That is, in *S. cerevisiae* it appears that ScHog1 activation contributes to NaD1's antifungal activity, rather than enhancing tolerance. Sc-calcineurin also appears to be involved in NaD1's mechanism against *S. cerevisiae*, as the *Scna1Δ* mutant was also more resistant to NaD1. Again, this observation contrasts to the behaviour of *C. albicans*, where the phenotype of both the *Cacna1Δ* and *Cacrz1Δ* mutants was the same as the wildtype. Lastly, the *S. cerevisiae* mating pathway may be involved in NaD1's antifungal activity as *Scfus3Δ* was slightly resistant to NaD1 treatment, whereas deletion of the MAPK of this pathway in *C. albicans* (CaCek2) did not alter NaD1's antifungal activity. In summary, ScHog1, the mating pathway (ScFus3) and Sc-calcineurin may modulate NaD1's antifungal activity against *S. cerevisiae*.

Deletion of Hog1 rendered *C. albicans* more sensitive to NaD1, whereas *S. cerevisiae* with the Hog1 deletion was more tolerant. To determine whether the differences in the NaD1 response in the *hog1Δ* mutants in *C. albicans* and *S. cerevisiae* arise from differences in sensitivity to oxidative stress, wildtype *C. albicans* (DAY185) and *S. cerevisiae* (BY4741) were grown in the presence of various concentrations of hydrogen peroxide. Although *S. cerevisiae* did not grow to the same optical density as *C. albicans* during the incubation period, the degree of growth inhibition relative to a no-treatment control was the same for both species. Thus, is unlikely to be due to differences in sensitivity to oxidative stress.

I also investigated pathway components upstream of Hog1 that are essential for NaD1 activity, to determine whether they contribute to differences in the *C. albicans* and *S. cerevisiae hog1* Δ phenotype. The upstream signalling cascades that activate Hog1 are complex, and react to stress differently in *S. cerevisiae* and *C. albicans*. These differences may explain why the phenotype of the *hog1* Δ mutants are different in the two yeast species.

In *S. cerevisiae*, osmotic stress induced ScHog1 activation occurs through two independent signalling cascades. The first begins with the histidine kinases ScSln1, ScYpd1 and ScSsk1, which signal to the MAPKKKs ScSsk2 and ScSsk22. In the second pathway ScSho1 signals to the MAPKKK ScSte11. These two pathways converge at the MAPKK ScPbs2, which activates ScHog1 (Figure 5.1) (Maeda et al., 1995; Posas et al., 1996). The two branches are not redundant, with ScSln1 activated at moderate concentrations of the osmo-stressor KCl and both ScSln1 and ScSho1 causing changes to gene expression at high KCl concentrations (O'Rourke & Herskowitz, 2004). In *S. cerevisiae*, it is also known that the ScSho1 and ScSln1 branches react to stimuli at different speeds, with the ScSln1 branch producing faster Hog1 activation than the ScSho1 branch (Hersen et al., 2008; Maeda et al., 1995). Two transmembrane osmosensors ScMsb2 and ScHrk1 also exist upstream of ScSho1 (Tatebayashi et al., 2007). ScMsb2 can also activate the ScHog1 pathway independently of the ScSho1 branch (O'Rourke & Herskowitz, 2002; Tatebayashi et al., 2007). In addition, ScMsb2 and ScSho1 are also involved in activation of the ScKss1 invasive growth pathway (Cullen et al., 2004). Less is known about the *S. cerevisiae* upstream signalling in response to oxidative stress. However, *Scsho1* Δ and a *Scsln1-ssk1* double deletion are sensitive to hydrogen peroxide (although not to other oxidants), signifying that both branches of signalling may be involved in oxidative stress response (Singh, 2000). Signalling is further complicated by sharing of components between pathways. For example, ScSte11 is shared between the ScFus3, ScKss1 and ScHog1 pathways and both ScSte7 and ScSte11 are shared by ScFus3 and ScKss1 (Qi & Elion, 2005). Prevention of cross-talk between the pathways is complicated and involves several regulatory steps, including the binding of scaffold proteins which, when bound, favour signalling through one pathway (Saito, 2010). For example, the ScSte5 scaffold protein is only recruited after pheromone exposure and directs signalling through the ScFus3 pathway (Correia & Pla, 2010; Saito, 2010). ScPbs2 and ScSho1 act as co-scaffolds to direct signalling to ScHog1 (Saito, 2010). Other upstream components exist in these pathways but will not be discussed here. A simplified illustration of MAP kinase signalling in *S. cerevisiae* is shown in Figure 5.23. Collectively, this data means that in *S. cerevisiae*, the

oxidative stress produced by NaD1 could activate the Hog1 pathway through either the ScSln1 or ScSho1 branches. Therefore, *Scsln1*, *Scsho1* and *Scmsb2* deletion mutants were tested with NaD1.

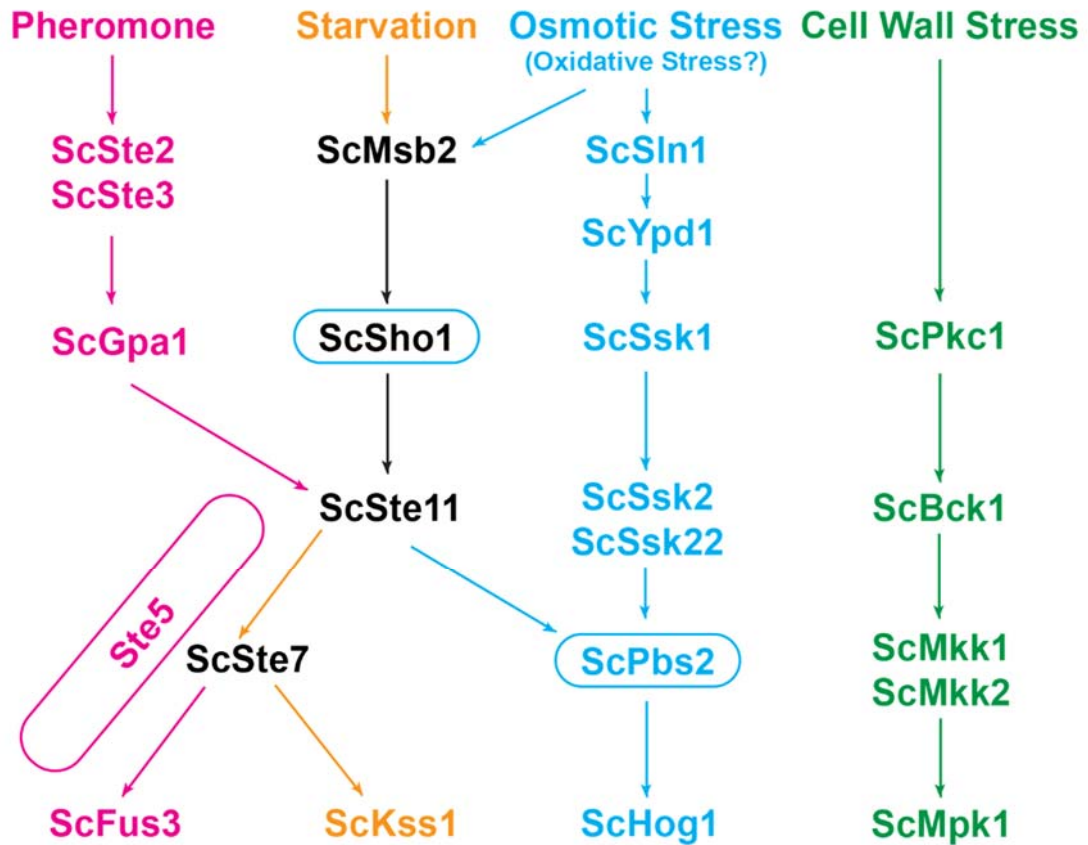


Figure 5.23 MAP kinase signalling in *S. cerevisiae*

Mating (pheromone induced, pink), invasive growth (starvation induced, orange), osmotic (and oxidative?) stress response (blue) and cell wall stress response (green) are regulated by the MAPK ScFus3, ScKss1, ScHog1 and ScMpk1, respectively. ScMsb2, ScSho1, ScSte11 and ScSte7 are involved in multiple pathways and are shown in black. Scaffold proteins that aid in preventing cross-talk between the pathways have a rounded rectangle around the protein name. The colour of the rectangle identifies the pathway towards which that scaffold protein directs signalling.

In *C. albicans*, signalling in response to both osmotic and oxidative stress occurs through a single MAPKKK CaSsk2 to the MAPKK CaPbs2, as *Cassk2* deletion impairs Hog1 phosphorylation to both of these stresses. In contrast, deletion of *Castell1* does not affect CaHog1 phosphorylation in response to osmotic or oxidative stress (Cheetham et al., 2007). Upstream of CaSsk2, deletion of *Cassk1* also blocks CaHog1 activation in response to oxidative stress (Chauhan et al., 2003; Román et al., 2005). CaYpd1 and CaSln1 do appear to be involved in CaHog1 regulation in *C. albicans*, but their roles have not been fully elucidated. Sln1 and Ypd1 negatively regulate the Hog1 pathway, so deletion of the *SLN1* and *YPD1* genes results in constitutive activation of Hog1 in both *S. cerevisiae* and *C. albicans* (Maeda et al., 1994; Mavrianos et al., 2014; Posas et al., 1996; Román et al., 2005). However, *Caypd1Δ* and *Casln1Δ* are still able to increase CaHog1 phosphorylation (above the constitutive level) upon hydrogen peroxide treatment (Mavrianos et al., 2014; Román et al., 2005). Upstream of CaSte11, CaSho1 does appear to play a role in resistance to oxidative stress, but is hypothesised to be mostly independent of CaHog1, as deletion of *Casho1* does not affect CaHog1 phosphorylation (Román et al., 2005). Interestingly, the deletion mutants *Casho1Δ*, *Cassk1Δ* and double deletion of *Casho1* and *Cassk1* still phosphorylate CaHog1 in response to osmotic stress, indicating that another upstream pathway may signal to CaSsk2 in response to osmotic stress in *C. albicans* (Chauhan et al., 2003; Román et al., 2005). Furthermore, CaMsb2 does not appear to have a major role in CaHog1 activation, as *Camsb2* deletion does not block osmotic stress induced CaHog1 activation. CaMsb2 does contribute to osmotic stress tolerance in the absence of CaSsk1 and CaSho1, although this tolerance is CaHog1 independent (Román et al., 2009). However, the involvement of CaMsb2 in CaHog1 activation during oxidative stress has not been investigated. Instead it appears that the primary roles of CaSho1 and CaMsb2 are in activation of CaCek1 (ScKss1 homolog) signalling (Román et al., 2009; Román et al., 2005). A simplified illustration of MAP kinase signalling in *C. albicans* is shown in Figure 5.23. In contrast to *S. cerevisiae*, oxidative stress, and therefore NaD1, must activate *C. albicans* Hog1 through only the CaSln1 branch.

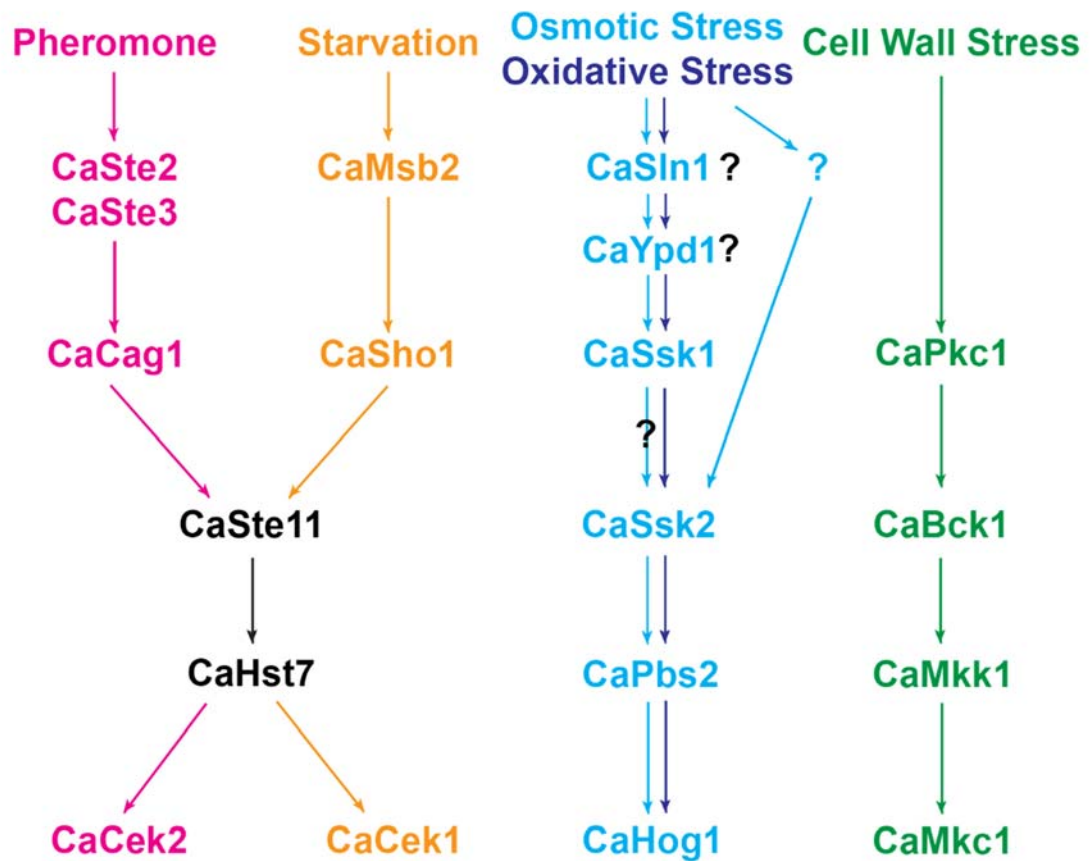


Figure 5.24 MAP kinase signalling in *C. albicans*

Mating (pheromone induced, pink), invasive growth (starvation induced, orange), osmotic (light blue) and oxidative (dark blue) stress response and cell wall stress response (green) are regulated by the MAPK CaCek2, CaCek1, CaHog1 and CaMkc1, respectively. CaSte11 and CaHst7 are involved in multiple pathways and are shown in black. Black question marks represent aspects of the CaHog1 pathway which require further analysis. The blue question mark represents unknown alternative signalling in the CaHog1 pathway.

In response to NaD1, *S. cerevisiae* *Scmsb2* and *Scsho1* deletion mutants both had the same phenotype as *Schog1Δ*. That is, with slightly higher tolerance to NaD1 than wildtype. In contrast, the *ScSLN1/sln1* heterozygous mutant (*ScSln1* is essential for survival) had the same sensitivity to NaD1 as wildtype. As the *Sho1* branch does not signal to *CaHog1* in *C. albicans* (Figure 5.24), this indicates that NaD1 induced *Hog1* activation occurs through different upstream signalling cascades in *S. cerevisiae* and *C. albicans*. Perhaps the cross-over between the *ScHog1* pathway and *ScFus3* pathways in *S. cerevisiae* (via the shared MAPKKK *ScSte11*) could also account for the *ScFus3* phenotype (i.e. resistance of *ScFus3*, *ScSte7* and *ScSte11* deletion mutants to NaD1, Figure 5.15). Although considering the *ScSte2* and *ScSte3* (components of the pheromone sensing GPCR) deletion mutants are also slightly resistant, this indicates that the signalling most likely originates from the GPCR of the *ScFus3* pathway.

The differences in *hog1Δ* phenotypes in *C. albicans* and *S. cerevisiae* could also result from differences in gene expression after *Hog1* activation. Unlike *S. cerevisiae*, *C. albicans* lacks a general stress response. That is, *C. albicans* does not appear to have a set of genes that are up-regulated commonly by all stresses. In contrast, osmotic, oxidative and heat stress in *S. cerevisiae* can activate many of the same genes and exposure to one stress can give cross protection with other stresses. For example, a mild heat shock can protect against a subsequent osmotic stress (Enjalbert et al., 2003). In fact, the gene *GPD1*, which encodes a glycerol-3-phosphate dehydrogenase, is only induced by osmotic stress in *C. albicans* but is also induced by heat and oxidative stress in *S. cerevisiae* (Enjalbert et al., 2003). Perhaps NaD1's mechanism against *S. cerevisiae* is similar to the action of the chemical fungicide fludioxonil against various filamentous fungi. It is hypothesised that treatment of *Neurospora crassa* with fludioxonil results in *os-2* (*Hog1* homolog) activation and over accumulation of glycerol that contributes to cell death. In this case, deletion of *os-2* reduces sensitivity of *N. crassa* to fludioxonil (Zhang et al., 2002). Similarly, hyperactivation of *CaHog1* (by deletion of the negative regulator *CaPtc1*) renders *C. albicans* hypersensitive to the plant defensin HsAFP1 (Aerts et al., 2011). Furthermore, *S. cerevisiae* deletion of the negative regulators *Scsln1* and *Scydp1* or mutations to *ScHog1* also lead to hyperactive *ScHog1* and increased cell death (Posas et al., 1996; Yaakov et al., 2003). Activation of *S. cerevisiae* *Hog1* by oxidative stress after NaD1 treatment could result in overaccumulation of glycerol and cell death.

Interestingly, the actin cytoskeleton is required for ScMsb2 to activate ScHog1 after osmotic stress (Tanaka et al., 2014). In Chapter 3, I showed that latrunculin A and deletion of several genes which affect actin (*Scede1Δ* and *Scbzz1Δ*) resulted in resistance to NaD1. In this Chapter I also showed that deletion of *Scmsb2* (and *Scsho1* and *Schog1*) results in a slight resistance to NaD1. It could be that disruption of the actin cytoskeleton by latrunculin A and these deletions results in reduced signalling to ScHog1 through ScMsb2. Considering the *Schog1Δ* mutant was also more resistant to NaD1, this could mean that the phenotypes observed in latrunculin A treated and *Scede1Δ* and *Scbzz1Δ* cells did not arise from defects in endocytosis, but to defects in ScHog1 signalling, which in *S. cerevisiae*, appear to contribute to cell death. However, the level of resistance observed in the endocytosis mutants was much greater than the phenotype of the *Schog1*, *Scsho1* and *Scmsb2* deletion mutants, pointing toward inhibition of endocytosis as the determining factor for this phenotype.

Considering there were differences in phenotype between *C. albicans* and *S. cerevisiae* cells with deletion of the MAPK of the mating pathways, I tested the effect of pertussis toxin on the two yeast species. Pertussis toxin blocks signalling through GPCRs by inducing ADP-ribosylation of the G α subunit and blocking activation of the G-protein (Kaslow & Burns, 1992; Lochter et al., 2011). The first known target of pertussis toxin was the mammalian G α_i protein (Katada, 2012), with which *S. cerevisiae* G α subunits (Gpa1 and Gpa2) are homologous (Miyajima et al., 1987; Nakafuku et al., 1988; Versele et al., 2001).

Treatment of *C. albicans* with pertussis toxin reduced the antifungal activity of NaD1 (Figure 5.12). In flow cytometry experiments, pertussis toxin treated cells had a lower level of fluorescence than with NaD1 treatment alone, indicating that BODIPY-NaD1 had bound to the cell surface but had not entered the cytoplasm (Figure 5.13). The ability of pertussis toxin treatment to reduce NaD1's antifungal activity was also observed in *S. cerevisiae* (Figure 5.12). This reduction in NaD1's activity against *C. albicans* was partially reversible by co-treating with both pertussis toxin and brefeldin A (Figure 5.14). This is consistent with previous observations, where the effect of pertussis toxin was abolished by brefeldin A (el Baya et al., 1997; Xu & Barbieri, 1995). It was not expected that pertussis toxin would affect NaD1's activity on both *C. albicans* and *S. cerevisiae*, given that *Cacek2Δ* was not resistant to NaD1. To determine if the glucose sensing GPCR ScGpr1 is involved in NaD1's activity, I tested a *Scgpr1* deletion mutant. Deletion of *Scgpr1* did not affect sensitivity of *S. cerevisiae* to NaD1 (Figure 5.15). The addition of an extra 2% glucose to *S. cerevisiae*

or *C. albicans* fungal inhibition assays had no effect on NaD1 activity (Figure 5.17). Next, mutants with deletion of the pheromone sensing GPCRs *Scste2* and *Scste3*, as well as the MAPKKK *Scste11* and the MAPKK *Scste7* were tested. All of these mutants had the same phenotype as the *Scfus3* Δ mutant, with a slight resistance to NaD1 treatment (Figure 5.15). Since all the ScFus3 pathway mutants were resistant to NaD1, there is likely to be a relationship between NaD1's activity and the ScFus3 pathway (Figure 5.23). The ScFus3 pathway could be required for NaD1 induced death in *S. cerevisiae*. If this is true, removal of key components of the pathway or the use of pertussis toxin to stop ScFus3 activation would result in NaD1 resistance. However, the level of resistance observed with pertussis toxin treatment was much greater than that obtained with the *Scste2*, *Scste3* and ScFus3 pathway deletion mutants. The reason for pertussis toxin induced NaD1 resistance in both *C. albicans* and *S. cerevisiae* is still unknown.

Deletion of components of the mating pathway (Figure 5.23) has been reported to enhance resistance of *S. cerevisiae* to the plant antifungal protein osmotin. As observed with NaD1, the *S. cerevisiae ste11* and *ste7* deletion mutants are resistant to osmotin. Yeast with deletion of *Scfus3* alone were not resistant, but cells with the *fus3/kss1* double deletion were (Yun et al., 1998). Cells with a deletion in the scaffold protein *Scste5*, which directs signalling to ScFus3, were also resistant to osmotin, indicating that ScKss1 and ScFus3 are both important for osmotin activity (Figure 5.23). Seemingly at odds with this, deletion of the receptor genes *Scste2* or *Scgpa1* did not cause resistance to osmotin. However, concurrent pheromone and osmotin treatment did increase osmotin susceptibility. Yun and colleagues (1998) thus hypothesised that osmotin's mechanism requires components of the pheromone signalling pathway, as well as another undefined upstream sensor.

G-protein inhibitors also block the movement of ions that occurs in filamentous fungi after exposure to the plant defensins RsAFP2 and DmAMP1. As mentioned previously (Table 0.1), RsAFP2 and DmAMP1 cause a release of K⁺ and uptake of Ca²⁺ into *Neurospora crassa* hyphae. Treatment with G-protein inhibitors reduced the alkalization of medium after exposure to RsAFP2 and DmAMP1 (although to a lesser extent than with RsAFP2) (Thevissen et al., 1996). This means that the movement of ions after treatment with RsAFP2, and DmAMP1 to a lesser extent, is mediated by a G-protein. Deletion of the GPCR *Gpr3* in *Botrytis cinerea* also enhances sensitivity to the defensin-like peptide VvAMP2 from *Vitis vinifera* (Nanni et al., 2013).

Another explanation for the phenotype of the ScFus3 pathway deletion mutants relates to endocytic uptake of the ScSte2 receptor from the pheromone induced mating pathway in *S. cerevisiae* (Figure 5.23) (Kubler & Riezman, 1993; Wolfe & Trejo, 2007). ScEde1 is involved in regulation of ScSte2 internalisation and *Scede1* Δ has a partial defect in internalising α -factor (Gagny et al., 2000; Shih et al., 2002). Activated ScSte2 is phosphorylated, internalised and sent to the vacuole for degradation (Riezman, 1993). Thus, the enhanced resistance to NaD1 observed in the *Scede1* Δ and *Scbzz1* Δ mutants and the latrunculin A treated cells could be due to reduced ScFus3 activation. That is, ScSte2 turnover would be reduced in these cells, resulting in reduced ScFus3 signalling. This is consistent with the finding that *S. cerevisiae fus3* Δ is resistant to NaD1. However, this hypothesis is complicated by the observation that *Scclc1* Δ was not resistant to NaD1 even though clathrin heavy and light chain (*Scchc1* Δ and *Scclc1* Δ) mutants also have reduced α -factor uptake (Boettner et al., 2012; Riezman, 1993). Also in conflict with this, the level of resistance in endocytosis mutants and latrunculin A treated cells was much greater than that observed in the ScFus3 pathway deletion mutants. Thus, it is more likely that blocking endocytosis reduces NaD1 activity by reducing NaD1 uptake, rather than by reducing ScFus3 signalling.

I also tested *C. albicans* HOG and CWI mutants with the antifungal peptides NaD2 and DmAMP1, to determine if the mechanism of action of these defensins was the same as NaD1. NaD2 is a class I defensin which produced by the same plant as NaD1; the ornamental tobacco *N. alata*. This peptide has lower antifungal activity than NaD1 against a number of plant pathogens (Dracatos et al., 2013). Both *Cahog1* Δ and *Camkc1* Δ mutants were more sensitive to NaD2 than wildtype cells, and NaD2 treatment led to CaHog1 phosphorylation. Very little is known about the mechanism of action of NaD2, but the hypersensitivity of the *Camkc1* deletion mutant indicates that NaD2 affects the cell wall of *C. albicans*. DmAMP1, a class I defensin from *D. merckii*, was also tested with these mutants. DmAMP1 has 49% identity and a similar antifungal mechanism to the defensin RsAFP2, which has recently been reported to activate the cell wall integrity pathway (Thevissen et al., 2012). As observed with NaD2, both *Cahog1* and *Camkc1* deletion mutants were hypersensitive to DmAMP1.

Considering that deletion of *Camkc1* enhances sensitivity to NaD2, an inhibitor of the CWI pathway was predicted to increase the activity of NaD2 against wildtype *C. albicans*. The CWI pathway inhibitor, cercosporamide, and the calcineurin inhibitor FK506 were

thus tested for synergy with NaD1 and NaD2. Cercosporamide is reported to increase the antifungal activity of the chemical fungicides micafungin, fluconazole and fenpropimorph (all of which target the cell wall or the plasma membrane) against *C. albicans* (LaFayette et al., 2010). The calcineurin inhibitor FK506 acts in synergy with fluconazole, caspofungin and fludioxonil against *C. neoformans* and with fluconazole, terbinafine, fenpropimorph and micafungin against *C. albicans* (Cruz et al., 2002; Del Poeta et al., 2000; Kojima et al., 2006; Onyewu et al., 2003; Singh et al., 2009). NaD2 displayed synergy with cercosporamide at all tested concentrations. It also displayed synergy with FK506, but required higher concentrations than cercosporamide. Interestingly, both cercosporamide and FK506 displayed synergy with NaD1, despite both Ca-calcineurin and *Camkc1A* mutants having no sensitivity to NaD1. Perhaps the synergy of NaD1 with these inhibitors arises because these inhibitors have toxic effects on their own (Odom et al., 1997; Sussman et al., 2004) (although FK506 was used at a sub-inhibitory concentration in these assays), resulting in greater stress to the cells.

The relationship between stress signalling pathways in fungi and their activation after exposure to plant defensins are complex. The response of these pathways to antifungal molecules can differ between fungal species. Furthermore, the stress pathways that are activated by antifungal peptides vary with their mechanisms of toxicity. Nevertheless, there is a clear role for stress response mechanisms in tolerance of fungi to antifungal molecules.

Chapter 6

Concluding remarks

6.1 Introduction

Fungal disease is a persistent problem in human health and agriculture (Brown et al., 2012; Fisher et al., 2012). Despite the use of chemical fungicides, the incidence and mortality of human disease from fungal pathogens is high and is increasing with the use of immunosuppressive therapies and incidence of HIV (Brown et al., 2012; Latge & Calderone, 2002). Antimicrobial peptides have been suggested as novel treatments for these infections (Brandenburg et al., 2012; Peters et al., 2010; Theis & Stahl, 2004). However, most antimicrobial peptides have only been characterised for antibacterial activity (van der Weerden et al., 2013). One class of antimicrobial peptides that display significant antifungal activity are the plant defensins (Thomma et al., 2002; van der Weerden & Anderson, 2012b). One of these defensins, NaD1, has been examined for its activity and mechanism against plant fungal pathogens. However, its ability to inhibit fungal pathogens of humans and its suitability for therapeutic use had not been assessed. In addition, aspects of NaD1's antifungal mechanism, such as how the peptide gains access to the fungal cytoplasm, had not been elucidated. In this thesis I aimed to answer some of these outstanding questions.

6.2 Findings of this study

6.2.1 NaD1 inhibits the growth of human fungal pathogens

NaD1 inhibits the growth of several species of fungi which frequently infect humans. Species of the *Aspergillus*, *Cryptococcus* and *Candida* genera most commonly cause invasive disease (Brown et al., 2012). NaD1 inhibits the growth of species within all three of these genera. NaD1 was most active against strains of *Cryptococcus neoformans* and *Cryptococcus gattii*. It also had inhibitory activity against *Aspergillus niger* and *Aspergillus paraciticus* strains. However, the three strains of *Aspergillus flavus* tested were resistant to NaD1. Investigating the differences between *A. flavus* and the other *Aspergillus* strains may provide insight into the cause of *A. flavus* resistance, and in turn may provide information about NaD1's mechanism of action. In contrast, the NaD1 derivative HXP4 inhibited the growth of these NaD1 resistant strains. Lastly, the growth of *Candida albicans* was inhibited by NaD1 at a low micromolar concentration.

Several other antimicrobial peptides were also tested against these pathogens. In particular, the peptide Bac2a had significant antifungal activity against all pathogens tested. NaD1 and HXP4 generally compared favourably to Bac2a, except for *A. flavus*, on which NaD1 had little activity.

In addition, NaD1 is fungicidal against *C. albicans*. That is, it kills *C. albicans* cells rather than merely inhibiting their growth. In survival assays against *C. albicans*, cell death did not increase with treatments longer than 15 min, indicating that NaD1's action had occurred within a 15 min time period. Most of the molecules currently used for the treatment of fungal disease are fungistatic rather than fungicidal. For example, ergosterol biosynthesis inhibitors, a major class of antifungals that are currently used in the clinic, do not usually kill fungal cells. Similarly, echinocandin drugs, which are the preferred treatment for invasive *C. albicans* infections, are fungistatic against filamentous fungi (LaFayette et al., 2010; Onyewu et al., 2003; Perlin, 2011). Fungicidal activity is preferred in disease treatment as it reduces the likelihood of resistant strains emerging.

NaD1 was originally hypothesised to only affect filamentous hyphae (van der Weerden et al., 2008). However, the data presented in this thesis disproves this hypothesis, as *Cryptococcus* and *C. albicans* are both yeast (although *C. albicans* also has a hyphal form). The change of the assay medium, from YPD to half-strength PDB, revealed that NaD1 does kill yeast.

Some antimicrobial peptides are inactive in serum (Maisetta et al., 2008). NaD1 was thus tested for antifungal activity under physiological conditions. NaD1 inhibited the growth of *C. albicans* in the presence of 5% fetal calf serum, although growth was slightly reduced. When *C. albicans* was grown at 37°C, the level growth inhibition by NaD1 was the same as when inhibition assays were performed at 30°C.

6.2.2 NaD1 acts in synergy with protease inhibitors and other antimicrobial peptides

NaD1 acts in synergy with proteinase inhibitors against plant fungal pathogens (Anderson et al., 2009; McKenna, 2012). In this thesis, I showed that NaD1 also acts in synergy with proteinase inhibitors against fungal pathogens of humans. Synergy and combined treatments with multiple AMPs (or chemical fungicides) have the potential of negating many of the problems associated with antifungal disease treatment. For example, the emergence of resistance to an antifungal therapy is less likely to occur if combinations of molecules with at least two different mechanisms of killing are used. The use of AMPs with different mechanisms of action may also broaden the spectrum of fungal pathogens that can be treated. In addition, synergistic activity may allow for decreased concentrations of antifungal molecules used in treatment, reducing the likelihood of negative side effects occurring in the host.

The molecules that had the best synergy with NaD1 were the antimicrobial peptide Bac2a and the protease inhibitor BPTI. Interestingly, NaD1 had better synergy with the plant defensin NaD2, than with a defensin from a different plant source, DmAMP1. Perhaps NaD1 and NaD2 act in synergy in the flowers of *Nicotiana glauca*. NaD1 also had high levels of synergy with the human antimicrobial peptides histatin 5 and h β D2. Therefore, if NaD1 was used therapeutically it could potentially act in synergy with these endogenous peptides. Lastly, NaD1 had medium synergy levels with the chemical fungicide amphotericin B, indicating that existing chemical fungicides and plant defensins could have synergistic activity, if combined for the treatment of human fungal disease.

6.2.3 The three step mechanism of NaD1 is conserved in *C. albicans*

As mentioned previously in this thesis, NaD1 has a three step mechanism of action against the filamentous plant pathogen *Fusarium oxysporum f. sp. vasinfectum*, that involves binding to the cell surface, disruption of the plasma membrane and uptake into the cytoplasm (van der Weerden et al., 2008). These steps are conserved in *C. albicans*. Using confocal microscopy with fluorescently labelled NaD1, the movement of the protein was tracked in live cells for 15 min after treatment. Shortly after addition of the protein, NaD1 bound to the cell surface. The protein then moved into the cytoplasm of the *C. albicans* cells. There was a delay between the uptake of BODIPY-NaD1 and propidium iodide fluorescence, indicating that NaD1 enters into the cell prior to cell death.

The uptake of the BODIPY-NaD1 was also confirmed using flow cytometry, which showed concentration dependent uptake of the peptide. Permeabilisation of the plasma membrane was also confirmed using a SYTOX green uptake assay, which monitored the fluorescence of the nucleic acid binding molecule SYTOX green over a three hour period. SYTOX green uptake occurred with NaD1 treatment, but much slower than peptides known to rapidly permeabilise the membrane (BMAP-28 and CP29) (van der Weerden et al., 2010).

6.2.4 NaD1 may be internalised by endocytosis, but does not appear to require internal protein transport

The method of uptake of NaD1 into cells was studied using inhibitors and mutants with defects in endocytosis and protein transport. The inhibitor latrunculin A, which blocks most forms of endocytosis (Dutta & Donaldson, 2012), reduced NaD1's activity against *C. albicans*. In addition, deletion of *Saccharomyces cerevisiae* genes involved in endocytosis resulted in resistance to NaD1. As endocytosis requires energy, an inhibitor of oxidative phosphorylation, CCCP (Heytler & Prichard, 1962), was also tested. Pre-treatment with CCCP reduced NaD1's activity and blocked uptake of the peptide into *C. albicans*. These results are also consistent with previous observations that *S. cerevisiae rho⁰* mutants, with a deficiency in mitochondrial respiration, are resistant to NaD1 (Hayes et al., 2013) and NaD1 induced permeabilisation of *Fusarium oxysporum f. sp. vasinfectum* (Fov) is blocked at 4°C (van der Weerden, 2007). Together, these results indicate that NaD1 is internalised by endocytosis, at least at concentrations below 2.5 µM. The *S. cerevisiae* endocytosis mutants were not less sensitive to NaD1 at concentrations above 2.5 µM, indicating that perhaps another mechanism of uptake, or direct cell lysis, occurs at higher NaD1 concentrations.

NaD1's activity does not require internal protein transport through the endosomal network after passage through the plasma membrane. NaD1 activity against *C. albicans* was not affected by brefeldin A, which blocks retrograde transport from endosomes to the *trans*-Golgi network (Lippincott-Schwartz et al., 1991; Wood et al., 1991), or nocodazole, which depolarises microtubules and affects endosome movement (Apodaca, 2001; Matteoni & Kreis, 1987). Likewise, deletion of components of the *C. albicans* ESCRT pathway, which is responsible for endosome trafficking and formation of late endosomes (or MVBs) (Henne et al., 2011; Saksena et al., 2007), did not reduce NaD1's antifungal activity. This indicates

that NaD1 is not likely to be trafficked to the vacuole for degradation, nor is there likely to be a target for NaD1 on the plasma membrane that requires recycling mechanisms.

6.2.5 *C. albicans* tolerates low NaD1 concentrations by activating Hog1

Upon NaD1 treatment, *C. albicans* activates the HOG pathway. The HOG pathway was initially identified as being involved in NaD1 tolerance in the *C. albicans* deletion library screen. *C. albicans hog1* (the terminal MAPK) and *pbs2* (the MAPKK that regulates Hog1) deletion mutants were more sensitive to NaD1, and this sensitivity was reversed after complementation of the genes in the mutants. Western blots revealed that Hog1 is phosphorylated, and therefore activated, after exposure to NaD1.

In addition, Hog1 is the sole *C. albicans* stress response pathway that is involved in tolerance to NaD1. Deletion of the MAPK and MAPKK of the mating and CWI pathways did not affect NaD1 tolerance, nor did deletion of the Cap1 transcription factor or a subunit of calcineurin.

6.2.6 NaD1 induces ROS, but not osmotic stress

After discovering the involvement of the *C. albicans* HOG pathway in tolerance to NaD1, I examined whether NaD1 induces osmotic or oxidative stress in *C. albicans*, since Hog1 can be activated in response to either of these stresses (Figure 5.24). Confocal microscopy and flow cytometry of *C. albicans* were used to demonstrate that NaD1 induces the production of reactive oxygen species (determined using the ROS probe DHR 123) and nitric oxide. Further evidence for the induction of oxidative stress by NaD1 was the reduction in NaD1 growth inhibition in the presence of the antioxidant ascorbate. In contrast, pre-treatment with sorbitol to prime the cells for osmotic stress did not reduce NaD1's antifungal activity. Furthermore, co-treatment with sorbitol (to induce osmotic stress) and NaD1 did not increase antifungal activity. Thus NaD1 induces oxidative, but not osmotic stress, in *C. albicans*.

6.2.7 NaD1 activates Hog1 through different upstream signalling cascades in *C. albicans* and *S. cerevisiae*

Although Hog1 is involved in NaD1 tolerance in *C. albicans*, it appears to be required for NaD1's toxicity in *S. cerevisiae*. That is, deletion of *Schog1* enhanced resistance to NaD1, rather than enhancing sensitivity. Given this, I questioned whether the signalling upstream of Hog1 differed between the two species in response to NaD1. In *C. albicans*, activation of Hog1 occurs through a single cascade which begins with the histidine kinase CaSln1 (Cheetham et al., 2007). In *S. cerevisiae*, activation can occur through signalling from ScSln1 or ScSho1 (Maeda et al., 1995; Posas et al., 1996). *S. cerevisiae hog1Δ and deletion mutants in the ScSho1 branch were slightly resistant to NaD1 treatment. In contrast, a *SLN1/sln1* heterozygous mutant (Sln1 is essential in *S. cerevisiae*) did not differ from wildtype. Since *C. albicans* can only signal through CaSln1, NaD1 must activate Hog1 through different upstream pathways in *S. cerevisiae* and *C. albicans*.*

6.2.8 *C. albicans* tolerates plant defensins with different stress response pathways

Different antimicrobial peptides and chemical fungicides activate different stress signalling pathways, and thus are likely to have different mechanisms of action (Chapter 1). The mechanism of action of antifungal peptides are known to differ (van der Weerden et al., 2013; Vriens et al., 2014). To determine if the examination of stress signalling pathways could give some indication of the mechanism of the plant defensins NaD2 and DmAMP1, I tested these peptides against *Cahog1* and *Camkc1* deletion mutants. While NaD1 only activates the HOG pathway, *C. albicans* tolerance to the plant defensins NaD2 and DmAMP1 involves both the HOG and the CWI pathways. Deletion of the MAPK of the CWI pathway (*Camkc1*Δ) resulted in sensitivity to both NaD2 and DmAMP1. Thus, these defensins are likely to damage the cell wall of fungi as part of their mechanism of action.

6.2.9 A GPCR may contribute to NaD1 activity

An inhibitor of G-protein coupled receptors, pertussis toxin (Kaslow & Burns, 1992; Locht et al., 2011), reduced the antifungal activity of NaD1 against both *C. albicans* and *S. cerevisiae*. This reduction in NaD1's antifungal activity was partially reversed by brefeldin A, which is known to block the action of pertussis toxin (el Baya et al., 1997). Of the two GPCRs in *S. cerevisiae*, inhibition of signalling from the Ste2-Ste3 pheromone receptors may contribute to NaD1 resistance, as deletion of *Scste2Δ*, *Scste3Δ* or components of the ScFus3 mating pathway (which this GPCR activates) resulted in slight resistance to NaD1. However, the level of resistance observed in these mutants was much less than that obtained with pertussis toxin treatment. In addition, the resistance phenotype of the mating pathway mutants in *S. cerevisiae* was not conserved in *C. albicans*. Therefore, the true cause for the resistance to NaD1 that is produced by pertussis toxin treatment needs to be elucidated.

6.2.10 NaD1 and NaD2 act in synergy in *C. albicans* growth assays with stress signalling inhibitors

NaD1 and NaD2 operated in synergy with the CWI inhibitor cercosporamide and the calcineurin inhibitor FK506 in cell growth assays. This was expected for NaD2, because the cell wall integrity pathway is involved in tolerance of NaD2. However, NaD1 also had synergy with these inhibitors. It is currently not known why NaD1 has synergistic activity with these inhibitors. As these inhibitors are also toxic to yeast (Odom et al., 1997; Sussman et al., 2004), the combination of the inhibitors and NaD1 could result in greater stress to the cells.

6.3 Future directions

6.3.1 What is NaD1's primary target?

Screening of the *C. albicans* deletion library for NaD1 resistance was used in an attempt to find a target for the antifungal activity of NaD1. The library screen revealed one gene deletion that enhanced NaD1 resistance in both clones. This gene, orf19.6845, encodes a putative bZIP transcription factor. The only information available for this gene is that it is induced in a *C. albicans* biofilm model (Nett et al., 2009). To discover more about this potential target for NaD1, it may be beneficial to add a fluorescent tag to monitor when this putative transcription factor is translocated to the nucleus. The gene targets of this putative transcription factor could be studied using transcriptome profiling of the deletion mutant or using chromatin immunoprecipitation (ChIP) techniques (Horak & Snyder, 2002; Johnson et al., 2007).

Several other resistant mutants were also identified in the initial screen and antifungal assays (*irs4* Δ , *sap8* Δ , *plb2* Δ , *kis2* Δ and *ssn3* Δ) but the resistance phenotype was not conserved in both clones. However, some of the mutants may not have the correct deletions. Consequently, they require PCR verification that the gene deletion had occurred and also further investigation into any involvement in NaD1's activity. The *irs4* Δ mutant, with deletion of gene that encodes a PI(4,5)P₂ phosphatase (Morales-Johansson et al., 2004), is of particular interest, as NaD1 binds PI(4,5)P₂ on lipid strips (Poon et al., 2014).

It would also be beneficial to screen the heterozygous *C. albicans* deletion collection as described in Xu et al. (2007). This library has 2868 heterozygous deletion mutants (45% of the *C. albicans* genome) and has barcodes incorporated for screening by microarray.

6.3.2 How does synergy occur?

To investigate a possible involvement of signalling in synergy, I initiated an RNAseq (Wang et al., 2009b) experiment to investigate changes in *C. albicans* gene regulation in response to singular plant defensins, and defensins in combination. However, due to time constraints these experiments were not completed for inclusion in this thesis. NaD1 and DmAMP1 were chosen for this experiment as they both have significant antifungal activity on their own, they have synergy in combination (Chapter 2) and they activate different stress signalling pathways (Chapter 5). Survival assays were performed with DmAMP1 and

NaD1 and DmAMP1 in combination to select the most appropriate concentrations for the RNAseq experiment. Preliminary cell treatments and RNA extractions were performed. The RNA from these extractions was of sufficient quality to sequence the mRNA transcriptome. Libraries will be prepared using Illumina sample prep kits and sequenced on an Illumina HiSeq. This experiment will not only give information about synergy, including whether stress signalling contributes to synergy, but could also give further information about NaD1's mechanism of action.

It would also be interesting to examine the mechanism of synergy between BPTI and NaD1. BPTI causes growth arrest in yeast, increasing the number of cells in the G₀/G₁ and G₂ phases of the cell cycle (Bleackley et al., 2014a). NaD1's activity should be investigated at the different phases of the cell cycle, to determine if NaD1 is more active at G₀/G₁ and G₂ stages. If NaD1 is more active during these phases, this could explain why BPTI and NaD1 synergy occurs.

6.3.3 NaD1 uptake by endocytosis

The data presented in this thesis led to the hypothesis that NaD1 is internalised by endocytosis. However, it is unknown whether this uptake is a clathrin dependent process. This could be resolved by testing a mutant with deletion of the clathrin heavy chain (*chc1Δ*). Preliminary experiments were performed with a *Scchc1Δ* mutant, but were not included in this thesis as the mutant could not be verified by PCR for correct deletion of the *CHC1* gene. Several other inhibitors could also be tested to identify the type of endocytosis involved in NaD1 uptake (Dutta & Donaldson, 2012). For example, the inhibitor chlorpromazine inhibits clathrin mediated endocytosis by moving clathrin from the cell surface and into endosomes (Dutta & Donaldson, 2012). In some mammalian cell types this inhibitor can also inhibit clathrin independent endocytosis. However, the fluorescent probes lactosylceramide (LacCer), which is internalised by clathrin independent endocytosis, and transferrin, which requires clathrin for endocytosis, could be used to ensure that only clathrin dependent endocytosis is affected (Vercauteren et al., 2010). The inhibitor amiloride can be used to block macropinocytosis, which is another process that requires actin (Conner & Schmid, 2003; Dutta & Donaldson, 2012). However, as the mechanisms of these inhibitors and probes have been determined in mammals, their use could potentially be complicated by mechanistic differences between mammals and yeast. It would also be beneficial to test other *S. cerevisiae* endocytosis mutants such as *end3Δ*

and *end4Δ*, which are defective in the internalisation step of endocytosis (Bénédicti et al., 1994; Raths et al., 1993; Wesp et al., 1997).

It is also necessary to confirm that NaD1 uptake was blocked in the *S. cerevisiae* endocytosis mutants and in *C. albicans* after latrunculin A treatment. These experiments could be performed using confocal microscopy or flow cytometry with the BODIPY tagged NaD1 and would confirm that the resistance phenotype of the endocytosis mutants was not due to reduced ScFus3 signalling or reduced activation of ScHog1 through the ScMsb2 osmosensor. Confocal microscopy and flow cytometry experiments would also assist in resolving whether a second mechanism of NaD1 uptake occurs at higher NaD1 concentrations. These assays could monitor uptake of high concentrations of BODIPY-NaD1 after treatment with latrunculin A. Considering the different phenotypes of Hog1 and mating pathway mutants in *S. cerevisiae* and *C. albicans* it may also be beneficial to create deletions of the endocytosis related genes in *C. albicans* to confirm that antifungal activity and uptake of NaD1 is affected in this species.

6.3.4 GPCRs and NaD1

The effect of pertussis toxin on NaD1 activity against *S. cerevisiae* and *C. albicans* requires further investigation. Although the ScFus3 mating pathway (which is activated by the Ste2-Ste3 pheromone sensing GPCR) appeared to be involved in pertussis toxin induced resistance in *S. cerevisiae*, deletion of components of the *C. albicans* mating pathway did not affect NaD1 sensitivity. Since, the pertussis toxin resistance phenotype was conserved in both *S. cerevisiae* and *C. albicans*, the resistance to NaD1 is not likely to be due to reduced activation of the mating pathway. A potential method to confirm this is to test diploid *S. cerevisiae* cells with pertussis toxin, as ScSte4 and ScSte18 are expressed only in haploid cells (Versele et al., 2001). This means that the GPCR cannot activate ScFus3 signalling in these cells. If pertussis toxin does not reduce NaD1 inhibition in diploid *S. cerevisiae* then the effect of pertussis toxin on NaD1 activity is independent of ScFus3 signalling.

In flow cytometry experiments NaD1 uptake was reduced in pertussis toxin treated samples. Confocal microscopy of NaD1 uptake into *C. albicans* and *S. cerevisiae* would be beneficial to determine if pertussis toxin results in accumulation of NaD1 on the cell surface, without uptake into the cytoplasm. If NaD1 is activating a G-protein directly it would be helpful to test mutants with deletions of the G α proteins Gpa2 (downstream of Gpr1) and Gpa1 (downstream of Ste2 and Ste3), as well as components of the G $\beta\gamma$ dimer that are associated with Gpa1, Ste18 and Ste4. Unfortunately, the full extent of the effects brought about by pertussis toxin in yeast are not known. Perhaps a screen of the *S. cerevisiae* full deletion collection with pertussis toxin would aid in narrowing down the list of possible NaD1 targets.

6.3.5 Fus3 and Hog1 activation in *S. cerevisiae*

The mating and HOG pathways both appear to contribute to NaD1 toxicity against *S. cerevisiae*. It would be beneficial to determine if ScHog1 and ScFus3 are phosphorylated after NaD1 treatment. It would also be interesting to observe how addition of glycerol affects NaD1 activity. The chemical fungicide fludioxonil causes hyperactivation of *Neurospora crassa* Hog1, leading to overaccumulation of glycerol and swelling and rupture of the cells (reviewed in Chapter 1). If NaD1 causes Hog1 hyperactivation and glycerol accumulation in *S. cerevisiae*, much like fludioxonil, then addition of exogenous glycerol may increase NaD1's toxic effect on *S. cerevisiae*. It would also be interesting to see how deletion of *Scfus3* in diploid *S. cerevisiae* cells, which do not mate, affects NaD1 activity. Lastly, it would be beneficial to test a mutant with deletion of *Sckss1*, the MAPK of the invasive growth pathway, as the ScKss1 pathway shares ScSte7, ScSte11, ScSho1 and ScMsb2 with the ScHog1 and ScFus3 pathways, and deletion of all of these components rendered cells less sensitive to NaD1 treatment.

6.3.6 Hog1 activation by NaD1 in other pathogens

Although deletion of CaHog1 in *C. albicans* increased the sensitivity to NaD1, the same deletion in the model organism *S. cerevisiae* slightly increased resistance. For Hog1 to be a viable target to increase NaD1's efficacy, it is essential that deletion of Hog1 in other fungal pathogens causes NaD1 sensitivity. Hog1 deletions in a variety of fungal pathogens of both plants and humans should be tested for sensitivity to NaD1. This would then permit disruption of Hog1, potentially through the use of an inhibitor, to increase antifungal

activity against a broad spectrum of pathogens. The potential use of a Hog1 inhibitor is discussed further in Section 6.3.8.

6.3.7 Stress pathway activation by other AMPs

Considering plant defensins activate different stress signalling pathways, it would be interesting to observe how *C. albicans* responds to other antimicrobial peptides, including CP29, Bac2a, bactenecin and BMAP-28 (Section 2.1). In doing so, we will gather more information about their mechanisms of action and will be able to make more informed decisions about AMPs that are likely to work in synergy. A fluorescent reporter system for Hog1 and Mkc1 activation, essentially as described in McClean et al. (2007), would be a more rapid system for screening peptides. McClean and co-workers (2007) used a *S. cerevisiae* fluorescent reporter system to investigate cross-talk between the HOG and mating pathways. Construction of these reporter systems involves replacing a stress induced gene with a fluorescent marker downstream of the native promoter (Figure 6.1). An example is the gene *CaSTL1*, which encodes a glycerol transporter that is induced by osmotic stress through activation of CaHog1 (Kayingo et al., 2009). Hog1 activation would drive transcription from the *STL1* promoter and cause expression of the fluorescent molecule, which could be monitored by fluorescence microscopy or flow cytometry. This would allow high throughput screening (particularly using flow cytometry) to define the stress signalling pathways that are activated in *C. albicans* by these peptides. Choosing genes that are specifically expressed after osmotic or oxidative stress would allow assessment of whether an antifungal peptide causes oxidative or osmotic stress.

6.3.8 NaD2's mechanism of action

While NaD1 activates only CaHog1, both CaHog1 and CaMkc1 are involved in tolerance to NaD2. Further investigation of NaD2, focusing on alterations or targets in the cell wall, could give valuable information about its mechanism of action. In doing so, this may prove the hypothesis that stress signalling pathways can quickly narrow down possibilities for a peptide's antifungal mechanism.

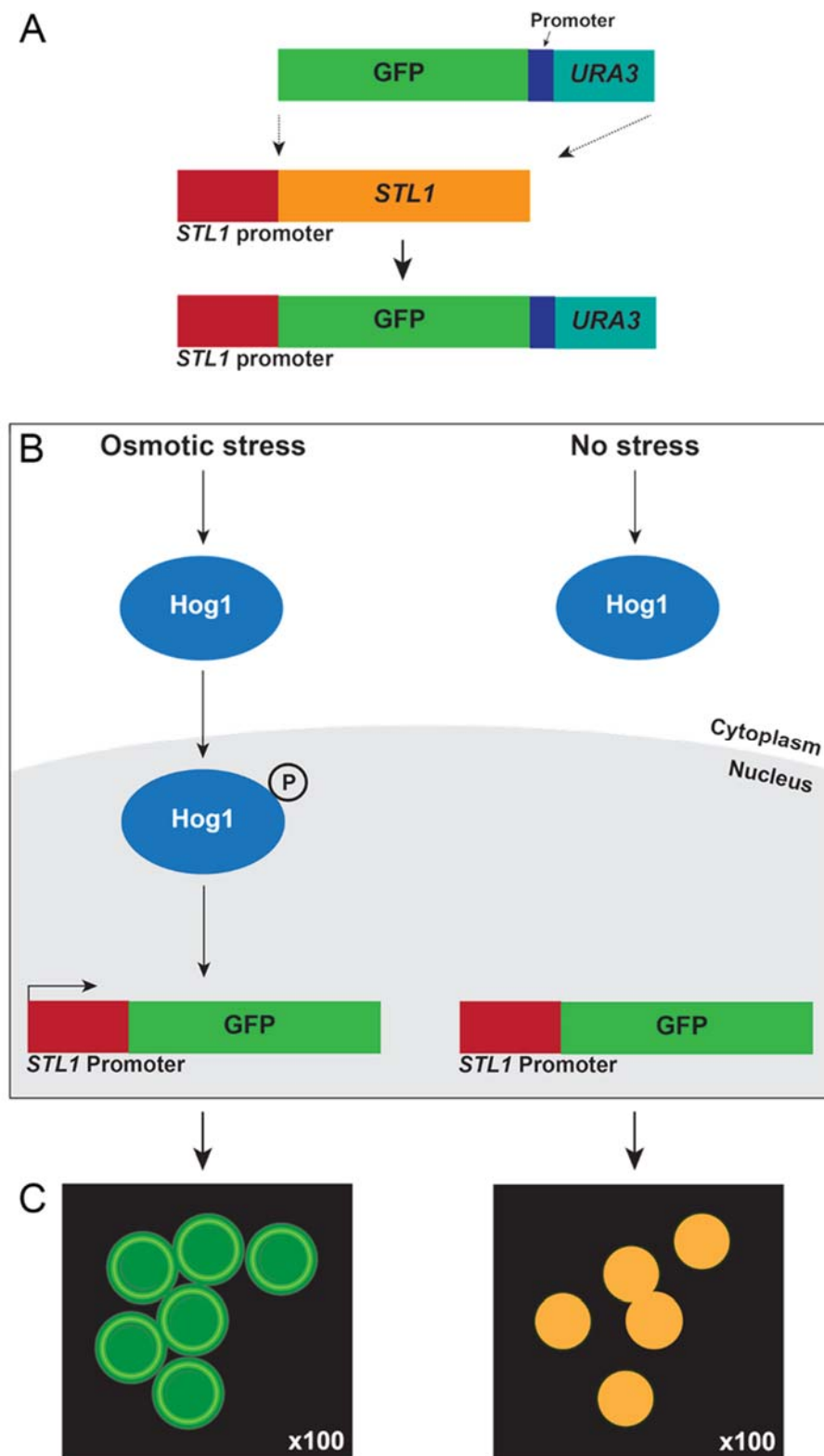


Figure 6.1 Reporter system for Hog1 activation

(A) A Hog1 activated gene (*STL1* in this example) can be replaced by DNA which encodes for a fluorescent molecule (in this case GFP) downstream of the native promoter. A *URA3* marker (and a constitutive promoter) is also included for selection of transformed colonies. (B) Upon osmotic stress Hog1 activation would drive expression from the *STL1* promoter, resulting in GFP expression. In the absence of stress, no GFP would be expressed. (C) GFP fluorescence could be monitored in cells using fluorescence microscopy.

6.3.9 Inhibitors of stress signalling pathways

In this thesis I showed that NaD1 and NaD2 act in synergy with the signalling inhibitors FK506 and cercosporamide. However, further investigation is required to determine the molecular basis of this synergy and whether stress signalling inhibitors can be used to increase the efficacy of antifungal peptides. The use of stress signalling inhibitors in antifungal therapy may be a challenge given the sequence conservation between fungal and mammalian MAPKs and kinases. For example, Hog1 is an ortholog of the human p38 MAPK, with 51% identity between Hog1 and one of the four p38 MAPKs (p38 α) (Dinér et al., 2011; Han et al., 1994).

For a Hog1 inhibitor to be used in combination with an antifungal molecule in the treatment of human disease, it would need to be specific for Hog1 and have no effect on p38 signalling. Recently, an inhibitor of Hog1 has been designed, based on an inhibitor of p38. Signalling through p38 α and p38 β is inhibited by the drug SB203580 (Cuenda & Rousseau, 2007; Dinér et al., 2011). However, this compound does not inhibit Hog1 in yeast because the inhibitor does not accumulate in yeast cells. The new inhibitor based on SB203580, 4-(1-benzyl-4-phenyl-1H-1,2,3-triazol-5-yl)-*N*-isopropylpyridin-2-amine, enters yeast cells and selectively inhibits Hog1 (Blomqvist et al., 2014; Dinér et al., 2011). This inhibitor could potentially be used as a therapeutic in combination with antifungal molecules that activate Hog1 signalling. However, the ability of this compound to inhibit activation of the p38 MAPK has not been studied.

Many of the current inhibitors of the cell wall integrity pathway and calcineurin signalling are also not appropriate for treatment of fungal disease in humans, due to their effect on human signalling pathways. For example, treatment of a *Cryptococcus* infection in rabbits with the calcineurin inhibitor FK506 exacerbates the infection, as the immunosuppressive effects of FK506 outweighed its toxic effect against yeast (Odom et al., 1997). Likewise, cercosporamide, a CWI pathway inhibitor, also inhibits human protein kinase C, MAPK-interacting kinases (Mnk) and several other kinases (Konicek et al., 2011; Sussman et al., 2004).

However, an FK506 variant was discovered that does not suppress the human immune system, while remaining toxic to *Cryptococcus* (Odom et al., 1997). More recently, Juvvadi and colleagues (2013) reported that *A. fumigatus* calcineurin has a 14 residue region which is specific to filamentous fungi and absent in mammals. This region may be a suitable target for future calcineurin inhibitors specific to filamentous fungi.

6.4 In summary

Fungal disease is an increasing problem in agriculture and human health. With the emergence of resistance to chemical fungicides, novel treatment strategies are sought for fungal infections. The use of antimicrobial peptides is one such strategy. In this thesis I focused on the plant defensin NaD1. I showed that NaD1 has antifungal activity against pathogens that infect humans and that NaD1 acts in synergy with other AMPs and proteinase inhibitors against these human pathogens. I also showed that NaD1 probably transits the plasma membrane by endocytosis, whereupon the peptide induces production of reactive oxygen species. Lastly, I showed that *C. albicans* adapts to NaD1 exposure by activation of the HOG stress signalling pathway and that different plant defensins activate different stress response pathways. The plant defensin NaD1 could potentially be used for therapeutic purposes and Hog1 may be viable target to increase the efficacy of NaD1 against fungal pathogens.

Appendix

AI Hayes et al. (2013)

Hayes BME, Bleackley MR, Wiltshire JL, Anderson MA, Traven A, van der Weerden NL (2013) Identification and mechanism of action of the plant defensin NaD1 as a new member of the antifungal drug arsenal against *Candida albicans*. *Antimicrob Agents Chemother* **57**: 3667-3675

Due to copyright, this article has been excluded from this version of the thesis.

AII Amino acid dropout media recipes

Amino acid dropout media (1 L) requires:

200 mL 5× Amino acid dropout mix

200 mL 5× yeast nitrogen base

100 mL 10× glucose

500 mL water or 2% agar (for plates)

Table A.1 Amino acid dropout mix recipes

5x Amino acid dropout mix	- trp (mg/500 mL)	- ura (mg/500 mL)	- arg (mg/500 mL)	- his (mg/500 mL)
Adenine	25	25	25	25
Arginine	125	125		125
Aspartic acid	200	200	200	200
Histidine	50	50	50	
Isoleucine	125	125	125	125
Leucine	250	250	250	250
Lysine	125	125	125	125
Methionine	50	50	50	50
Phenylalanine	125	125	125	125
Threonine	250	250	250	250
Tryptophan		125	125	125
Tyrosine	125	125	125	125
Uracil	50		50	50
Valine	350	350	350	350


```

      10      20      30      40      50      60
Pbs2      MVEDKDIDLNINNLKIHDAPTRTPPVSLPPALPTPPTPSGILLNTTMOAKLMAFQQORSK
Pbs2-3 Fw1 MVEDKDIDLNINNLKIHDAPTRTPPVSLPPALPTPPTPSGILLNTTMOAKLMAFQQORSK
Pbs2-3 Fw2
Pbs2-3 Fw3
Pbs2-3 Fw4
Pbs2-3 Rv

      70      80      90      100     110     120
Pbs2      AAAAAAAAAASVSSSSSGTQASSSSISASTSESSVSTIPANINRTVSGKKKPKPNLKLSDL
Pbs2-3 Fw1 AAAAAAAAAASVSSSSSGTQASSSSISASTSESSVSTIPANINRTVSGKKKPKPNLKLSDL
Pbs2-3 Fw2
Pbs2-3 Fw3
Pbs2-3 Fw4
Pbs2-3 Rv

      130     140     150     160     170     180
Pbs2      PLSRNNLHRSNTSADSSVTTPEADTPTGKISNEPQPQGLFANYSDYVDIKSGQLNFAG
Pbs2-3 Fw1 PLSRNNLHRSNTSADSSVTTPEADTPTGKISNEPQPQGLFANYSDYVDIKSGQLNFAG
Pbs2-3 Fw2      NTSADSSVTTPEADTPTGKISNEPQPQGLFANYSDYVDIKSGQLNFAG
Pbs2-3 Fw3
Pbs2-3 Fw4
Pbs2-3 Rv

      190     200     210     220     230     240
Pbs2      KASLHSGIDFLSGSSFRVSLDEFEYLEELGRGNYGSVLKVLHKPTGVLMAMKEVRLELD
Pbs2-3 Fw1 KASLHSGIDFLSGSSFRVSLDEFEYLEELGRGNYGSVLKVLHKPTGVLMAMKEVRLELD
Pbs2-3 Fw2 KASLHSGIDFLSGSSFRVSLDEFEYLEELGRGNYGSVLKVLHKPTGVLMAMKEVRLELD
Pbs2-3 Fw3
Pbs2-3 Fw4
Pbs2-3 Rv      VLKVLHKPTGVLMAMKEVRLELD

      250     260     270     280     290     300
Pbs2      ENKFTQILMELDI LHKCDSPYIVDFYGAFFVEGAVYMCIEYMDGGS LDRI FGNDVGVKDE
Pbs2-3 Fw1 ENKFTQILMELDI LHKCDSPYIVDFYGAFFVEGAVYMCIEYMDGGS LDRI FGNDVGVKDE
Pbs2-3 Fw2 ENKFTQILMELDI LHKCDSPYIVDFYGAFFVEGAVYMCIEYMDGGS LDRI FGNDVGVKDE
Pbs2-3 Fw3
Pbs2-3 Fw4
Pbs2-3 Rv ENKFTQILMELDI LHKCDSPYIVDFYGAFFVEGAVYMCIEYMDGGS LDRI FGNDVGVKDE

      310     320     330     340     350     360
Pbs2      YELAYITESVILGLKELKDKHNI IHRDVKPTNILVNTQGKVKLCDFGVSGNLVASLAKTN
Pbs2-3 Fw1 YELAYITESV
Pbs2-3 Fw2 YELAYITESVILGLKELKDKHNI IHRDVKPTNILVNTQGKVKLCDFGVSGNLVASLAKTN
Pbs2-3 Fw3      LAYITESVILGLKELKDKHNI IHRDVKPTNILVNTQGKVKLCDFGVSGNLVASLAKTN
Pbs2-3 Fw4
Pbs2-3 Rv YELAYITESVILGLKELKDKHNI IHRDVKPTNILVNTQGKVKLCDFGVSGNLVASLAKTN

      370     380     390     400     410     420
Pbs2      IGCQSYMAPERINTMRPDDATYSVQSDVWSLGLTILELAVGHYPYPAETYDNIFSQLSAI
Pbs2-3 Fw1 IGCQSYMAPERINTMRPDDATYSVQSDVWSLGLTILELAVGHYPYPAETYDNIFSQLSAI
Pbs2-3 Fw2 IGCQSYMAPERINTMRPDDATYSVQSDVWSLGLTILELAVGHYPYPAETYDNIFSQLSAI
Pbs2-3 Fw3 IGCQSYMAPERINTMRPDDATYSVQSDVWSLGLTILELAVGHYPYPAETYDNIFSQLSAI
Pbs2-3 Fw4
Pbs2-3 Rv IGCQSYMAPERINTMRPDDATYSVQSDVWSLGLTILELAVGHYPYPAETYDNIFSQLSAI

```

```

          430      440      450      460      470      480
Pbs2      VDGEPPKLYPKVYSKEAQIFVKSLAKNPDLRPSYAALLNPNWLIKNRGKETNLAQTVKD
Pbs2-3 Fw1
Pbs2-3 Fw2 VDGEPPKLYPKVYSKEAQIFVKSLAKNPDLRPSYAALLNPNWLIKNRGKET
Pbs2-3 Fw3 VDGEPPKLYPKVYSKEAQIFVKSLAKNPDLRPSYAALLNPNWLIKNRGKETNLAQTVKD
Pbs2-3 Fw4                                     NRGKETNLAQTVKD
Pbs2-3 Rv  VDGEPPKLYPKVYSKEAQIFVKSLAKNPDLRPSYAALLNPNWLIKNRGKETNLAQTVKD

          490      500      510      520      530      540
Pbs2      RVEETIAKLEKNKSVSRNSMKNKSAAAVPPPRNVESVQSLLRNKVKAPALHRGGLOKVNRS
Pbs2-3 Fw1
Pbs2-3 Fw2 RVEETIAKLEKNKSVSRNSMKNKSAAAVPPPRNVESVQSLLRNKVKAPALHRGGLOKVNRS
Pbs2-3 Fw3 RVEETIAKLEKNKSVSRNSMKNKSAAAVPPPRNVESVQSLLRNKVKAPALHRGGLOKVNRS
Pbs2-3 Fw4 RVEETIAKLEKNKSVSRNSMKNKSAAAVPPPRNVESVQSLLRNKVKAPALHRGGLOKVNRS
Pbs2-3 Rv  RVEETIAKLEKNKSVSRNSMKNKSAAAVPPPRNVESVQSLLRNKVKAPALHRGGLOKVNRS

          ....|.
Pbs2      FLNNH*
Pbs2-3 Fw1
Pbs2-3 Fw2
Pbs2-3 Fw3 FLNNH*
Pbs2-3 Fw4 FLNNH*
Pbs2-3 Rv  FLNNH*

```

Figure A.2 Sequencing of pDDB78-PBS2 (PBS2-3)

To check for successful insertion of *PBS2* into the pDDB78 vector, PBS2-3 was sequenced using four forward primers and one reverse primer. This sequencing confirmed the *PBS2* gene was present without any mutations. Sequences were aligned using BioEdit (version 7.0.9.0) (Hall, 1999).

References

- Aerts AM, Bammens L, Govaert G, Carmona-Gutierrez D, Madeo F, Cammue BP, Thevissen K (2011) The antifungal plant defensin HsAFP1 from *Heuchera sanguinea* induces apoptosis in *Candida albicans*. *Front Microbiol* **2**: 1-9
- Aerts AM, Carmona-Gutierrez D, Lefevre S, Govaert G, Francois IE, Madeo F, Santos R, Cammue BP, Thevissen K (2009) The antifungal plant defensin RsAFP2 from radish induces apoptosis in a metacaspase independent way in *Candida albicans*. *FEBS Lett* **583**: 2513-2516
- Aerts AM, Francois IE, E.M.K M, Li Q-T, Cammue BP, Thevissen K (2007) The antifungal activity of RsAFP2, a plant defensin from *Raphanus sativus*, involves the induction of reactive oxygen species in *Candida albicans*. *J Mol Microbiol Biotechnol* **13**: 243-247
- Aerts AM, Francois IEJA, Cammue BPA, Thevissen K (2008) The mode of antifungal action of plant, insect and human defensins. *Cell Mol Life Sci* **65**: 2069-2079
- Alarco A, Raymond M (1999) The bZip transcription factor Cap1p is involved in multidrug resistance and oxidative stress response in *Candida albicans*. *J Bacteriol* **181**: 700 - 708
- Alekseeva L, Huet D, Femenia F, Mouyna I, Abdelouahab M, Cagna A, Guerrier D, Tichanne-Seltzer V, Baeza-Squiban A, Chermette R, Latge JP, Berkova N (2009) Inducible expression of beta defensins by human respiratory epithelial cells exposed to *Aspergillus fumigatus* organisms. *BMC Microbiol* **9**: 33
- Alonso-Monge R, Navarro-García F, Román E, Negredo AI, Eisman B, Nombela C, Pla J (2003) The Hog1 mitogen-activated protein kinase is essential in the oxidative stress response and chlamyospore formation in *Candida albicans*. *Eukaryot Cell* **2**: 351-361
- Anderson M, Heath R, McKenna J, Van der Weerden N (2009) Antifungal Methods. *Patent Application US 2009/0197809 A1*
- Aouida M, Texeira MR, Thevelein JM, Poulin R, Ramotar D (2013) Agp2, a member of the yeast amino acid permease family, positively regulates polyamine transport at the transcriptional level. *PLoS ONE* **8**: e65717
- Apodaca G (2001) Endocytic traffic in polarized epithelial cells: Role of the actin and microtubule cytoskeleton. *Traffic* **2**: 149-159
- Argimon S, Fanning S, Blankenship JR, Mitchell AP (2011) Interaction between the *Candida albicans* high-osmolarity glycerol (HOG) pathway and the response to human b-Defensins 2 and 3. *Eukaryot Cell* **10**: 272-275
- Ascenzi P, Bocedi A, Bolognesi M, Spallarossa A, Coletta M, Cristofaro R, Menegatti E (2003) The bovine basic pancreatic trypsin inhibitor (kunitz inhibitor): A milestone protein. *Curr Prot Pept Sci* **4**: 231-251

- Ayscough KR, Stryker J, Pokala N, Sanders M, Crews P, Drubin DG (1997) High rates of actin filament turnover in budding yeast and roles for actin in establishment and maintenance of cell polarity revealed using the actin inhibitor latrunculin-A. *J Cell Biol* **137**: 399-416
- Bader T, Bodendorfer B, Schröppel K, Morschhäuser J (2003) Calcineurin is essential for virulence in *Candida albicans*. *Infect Immun* **71**: 5344-5354
- Badrane H, Cheng S, Nguyen MH, Jia HY, Zhang Z, Weisner N, Clancy CJ (2005) *Candida albicans* IRS4 contributes to hyphal formation and virulence after the initial stages of disseminated candidiasis. *Microbiol* **151**: 2923-2931
- Baker RT, Catanzariti AM, Karunasekara Y, Soboleva TA, Sharwood R, Whitney S, Board PG (2005) Using deubiquitylating enzymes as research tools. In *Methods Enzymol*, Raymond JD (ed), Vol. 398, pp 540-554. Academic Press
- Balandin M, Royo J, Gomez E, Muniz LM, Molina A, Hueros G (2005) A protective role for the embryo surrounding region of the maize endosperm, as evidenced by the characterisation of ZmESR-6, a defensin gene specifically expressed in this region. *Plant Mol Biol* **58**: 269-282
- Bartnicki-Garcia S (1968) Cell wall chemistry, morphogenesis, and taxonomy of fungi. *Annu Rev Microbiol* **22**: 87-108
- Belenky P, Camacho D, Collins James J (2013) Fungicidal drugs induce a common oxidative-damage cellular death pathway. *Cell Rep* **3**: 350-358
- Belenky P, Collins JJ (2011) Antioxidant strategies to tolerate antibiotics. *Science* **334**: 915-916
- Bénédicti H, Raths S, Crausaz F, Riezman H (1994) The *END3* gene encodes a protein that is required for the internalization step of endocytosis and for actin cytoskeleton organization in yeast. *Mol Biol Cell* **5**: 1023-1037
- Benincasa M, Scocchi M, Pacor S, Tossi A, Nobili D, Basaglia G, Busetto M, Gennaro R (2006) Fungicidal activity of five cathelicidin peptides against clinically isolated yeasts. *J Antimicrob Chemother* **58**: 950-959
- Berman J, Sudbery PE (2002) *Candida albicans*: A molecular revolution built on lessons from budding yeast. *Nat Rev Genet* **3**: 918-932
- Biss M, Hanna MD, Xiao W (2014) Isolation of yeast nucleic acids. In *Yeast Protocols*, Xiao W (ed), Third edn, pp 15-21. Springer New York
- Blankenship JR, Fanning S, Hamaker JJ, Mitchell AP (2010) An extensive circuitry for cell wall regulation in *Candida albicans*. *PLoS Pathog* **6**: e1000752
- Bleackley MR, Hayes BM, Parisi K, Saiyed T, Traven A, Potter ID, van der Weerden NL, Anderson MA (2014a) Bovine pancreatic trypsin inhibitor is a new antifungal peptide that inhibits cellular magnesium uptake. *Mol Microbiol* **92**: 1188-1197

- Bleackley MR, Wiltshire JL, Perrine-Walker F, Vasa S, Burns RL, van der Weerden NL, Anderson MA (2014b) Agp2p, the plasma membrane transregulator of polyamine uptake, regulates the antifungal activities of the plant defensin NaD1 and other cationic peptides. *Antimicrob Agents Chemother* **58**: 2688-2698
- Blomqvist CH, Dinér P, Grøtli M, Goksör M, Adiels CB (2014) A single-cell study of a highly effective Hog1 inhibitor for in situ yeast cell manipulation. *Micromachines* **5**: 81-96
- Boettner DR, Chi RJ, Lemmon SK (2012) Lessons from yeast for clathrin-mediated endocytosis. *Nat Cell Biol* **14**: 2-10
- Bonifacino JS, Rojas R (2006) Retrograde transport from endosomes to the trans-Golgi network. *Nat Rev Mol Cell Biol* **7**: 568-579
- Bose I, Reese AJ, Ory JJ, Janbon G, Doering TL (2003) A yeast under cover: the capsule of *Cryptococcus neoformans*. *Eukaryot Cell* **2**: 655-663
- Bowman SM, Free SJ (2006) The structure and synthesis of the fungal cell wall. *Bioessays* **28**: 799-808
- Brandenburg L-O, Merres J, Albrecht L-J, Varoga D, Pufe T (2012) Antimicrobial peptides: multifunctional drugs for different applications. *Polymers* **4**: 539-560
- Broekaert WF, Terras FRG, Cammue BPA, Vanderleyden J (1990) An automated quantitative assay for fungal growth inhibition. *Fems Microbiol Lett* **69**: 55-59
- Brown GD, Denning DW, Gow NAR, Levitz SM, Netea MG, White TC (2012) Hidden killers: Human fungal infections. *Sci Transl Med* **4**: 165rv113
- Butts A, Krysan DJ (2012) Antifungal drug discovery: something old and something new. *PLoS Pathog* **8**: e1002870
- Catanzariti A-M, Soboleva TA, Jans DA, Board PG, Baker RT (2004) An efficient system for high-level expression and easy purification of authentic recombinant proteins. *Protein Sci* **13**: 1331-1339
- Chauhan N, Inglis D, Roman E, Pla J, Li D, Calera J, Calderone R (2003) *Candida albicans* response regulator gene SSK1 regulates a subset of genes whose functions are associated with cell wall biosynthesis and adaptation to oxidative stress. *Eukaryot Cell* **2**: 1018 - 1024
- Cheetham J, Smith DA, da Silva Dantas A, Doris KS, Patterson MJ, Bruce CR, Quinn J (2007) A single MAPKKK regulates the Hog1 MAPK pathway in the pathogenic fungus *Candida albicans*. *Mol Biol Cell* **18**: 4603-4614
- Childs AC, Mehta DJ, Gerner EW (2003) Polyamine-dependent gene expression. *Cell Mol Life Sci* **60**: 1394-1406
- Conner SD, Schmid SL (2003) Regulated portals of entry into the cell. *Nature* **422**: 37-44
- Correia I, Pla J (2010) MAPK cell-cycle regulation in *Saccharomyces cerevisiae* and *Candida albicans*. *Future Microbiol* **5**: 1125-1141

- Cruz MC, Goldstein AL, Blankenship JR, Del Poeta M, Davis D, Cardenas ME, Perfect JR, McCusker JH, Heitman J (2002) Calcineurin is essential for survival during membrane stress in *Candida albicans*. *EMBO J* **21**: 546-559
- Cuenda A, Rousseau S (2007) p38 MAP-Kinases pathway regulation, function and role in human diseases. *BBA Mol Cell Res* **1773**: 1358-1375
- Cuesta-Marbán Á, Botet J, Czyz O, Cacharro LM, Gajate C, Hornillos V, Delgado J, Zhang H, Amat-Guerri F, Acuña AU, McMaster CR, Revuelta JL, Zarembeg V, Mollinedo F (2013) Drug uptake, lipid rafts, and vesicle trafficking modulate resistance to an anticancer lysophosphatidylcholine analogue in yeast. *J Biol Chem* **288**: 8405-8418
- Cullen PJ, Sabbagh W, Graham E, Irick MM, van Olden EK, Neal C, Delrow J, Bardwell L, Sprague GF (2004) A signaling mucin at the head of the Cdc42- and MAPK-dependent filamentous growth pathway in yeast. *Genes Dev* **18**: 1695-1708
- Davis D, Edwards JE, Mitchell AP, Ibrahim AS (2000) *Candida albicans* RIM101 pH response pathway is required for host-pathogen interactions. *Infect Immun* **68**: 5953-5959
- Davis DA, Bruno VM, Loza L, Filler SG, Mitchell AP (2002) *Candida albicans* Mds3p, a conserved regulator of pH responses and virulence identified through insertional mutagenesis. *Genetics* **162**: 1573-1581
- De Samblanx GW, Goderis IJ, Thevissen K, Raemaekers R, Fant F, Borremans F, Acland DP, Osborn RW, Patel S, Broekaert WF (1997) Mutational analysis of a plant defensin from radish (*Raphanus sativas* L.) reveals two adjacent sites important for antifungal activity. *J Biol Chem* **272**: 1171-1179
- de Zélicourt A, Letousey P, Thoiron S, Campion C, Simoneau P, Elmorjani K, Marion D, Simier P, Delavault P (2007) Ha-DEF1, a sunflower defensin, induces cell death in Orobanche parasitic plants. *Planta* **226**: 591-600
- Del Poeta M, Cruz MC, Cardenas ME, Perfect JR, Heitman J (2000) Synergistic antifungal activities of bafilomycin A1, fluconazole, and the pneumocandin MK-0991/caspofungin acetate (L-743,873) with calcineurin inhibitors FK506 and L-685,818 against *Cryptococcus neoformans*. *Antimicrob Agents Chemother* **44**: 739-746
- Den Hertog A, van Marle J, van Veen H, van't Hof W, Bolscher J, Veerman E, Nieuw Amerongen A (2005) Candidacidal effects of two antimicrobial peptides: histatin 5 causes small membrane defects, but LL-37 causes massive disruption of the cell membrane. *Biochem J* **388**: 689-695
- Deshayes S, Morris MC, Divita G, Heitz F (2005) Cell-penetrating peptides: tools for intracellular delivery of therapeutics. *Cell Mol Life Sci* **62**: 1839-1849
- Diné P, Veide Vilg J, Kjellén J, Migdal I, Andersson T, Gebbia M, Giaever G, Nislow C, Hohmann S, Wysocki R, Tamás MJ, Grøtli M (2011) Design, synthesis, and characterization of a highly effective Hog1 inhibitor: A powerful tool for analyzing MAP kinase signaling in yeast. *PLoS ONE* **6**: e20012

- Doherty GJ, McMahon HT (2009) Mechanisms of endocytosis. *Annu Rev Biochem* **78**: 857-902
- Dong J, Vylkova S, Li XS, Edgerton M (2003) Calcium blocks fungicidal activity of human salivary histatin 5 through disruption of binding with *Candida albicans*. *J Dent Res* **82**: 748-752
- Dracatos PM, van der Weerden NL, Carroll KT, Johnson ED, Plummer KM, Anderson MA (2013) Inhibition of cereal rust fungi by both class I and II defensins derived from the flowers of *Nicotiana glauca*. *Mol Plant Pathol* **15**: 67-79
- Dutta D, Donaldson JG (2012) Search for inhibitors of endocytosis: Intended specificity and unintended consequences. *Cell Logist* **2**: 203-208
- Edgerton M, Koshlukova SE, Lo TE, Chrzan BG, Straubinger RM, Raj PA (1998) Candidacidal activity of salivary histatins. *J Biol Chem* **273**: 20438-20447
- el Baya A, Linnemann R, vonOlleschikElbheim L, Robenek H, Schmidt MA (1997) Endocytosis and retrograde transport of pertussis toxin to the Golgi complex as a prerequisite for cellular intoxication. *Eur J Cell Biol* **73**: 40-48
- Eliopoulos GM, Perea S, Patterson TF (2002) Antifungal resistance in pathogenic fungi. *Clin Infect Dis* **35**: 1073-1080
- Enjalbert B, Nantel A, Whiteway M (2003) Stress-induced gene expression in *Candida albicans*: Absence of a general stress response. *Mol Biol Cell* **14**: 1460-1467
- Enjalbert B, Smith DA, Cornell MJ, Alam I, Nicholls S, Brown AJP, Quinn J (2006) Role of Hog-1 stress-activated protein kinase in the global transcriptional response to stress in the fungal pathogen *Candida albicans*. *Mol Biol Cell* **17**: 1018-1032
- Enloe B, Diamond A, Mitchell AP (2000) A single-transformation gene function test in diploid *Candida albicans*. *J Bacteriol* **182**: 5730-5736
- Fahrner RL, Dieckmann T, Harwig SS, Lehrer RI, Eisenberg D, Feigon J (1996) Solution structure of protegrin-1, a broad-spectrum antimicrobial peptide from porcine leukocytes. *Chem Biol* **3**: 543-550
- Feng Z, Jiang B, Chandra J, Ghannoum M, Nelson S, Weinberg A (2005) Human beta-defensins: differential activity against Candidal species and regulation by *Candida albicans*. *J Dent Res* **84**: 445-450
- Fisher MC, Henk DA, Briggs CJ, Brownstein JS, Madoff LC, McCraw SL, Gurr SJ (2012) Emerging fungal threats to animal, plant and ecosystem health. *Nature* **484**: 186-194
- Fox JL (2013) Antimicrobial peptides stage a comeback. *Nat Biotech* **31**: 379-382
- Friedrich CL, Moyles D, Beveridge TJ, Hancock RE (2000) Antibacterial action of structurally diverse cationic peptides on gram-positive bacteria. *Antimicrob Agents Chemother* **44**: 2086-2092

- Gagny B, Wiederkehr A, Dumoulin P, Winsor B, Riezman H, Haguenaer-Tsapis R (2000) A novel EH domain protein of *Saccharomyces cerevisiae*, Ede1p, involved in endocytosis. *J Cell Sci* **113**: 3309-3319
- Galletta BJ, Mooren OL, Cooper JA (2010) Actin dynamics and endocytosis in yeast and mammals. *Curr Opin Biotechnol* **21**: 604-610
- Ganz T (2003) Defensins: antimicrobial peptides of innate immunity. *Nat Rev Immunol* **3**: 710-720
- Gao AG, Hakimi SM, Mittanck CA, Wu Y, Woerner BM, Stark DM, Shah DM, Liang J, Rommens CM (2000) Fungal pathogen protection in potato by expression of a plant defensin peptide. *Nat Biotechnol* **18**: 1307-1310
- Garcia-Olmedo F, Molina A, Alamillo JM, Rodriguez-Palenzuela P (1998) Plant defense peptides. *Bipolymers* **47**: 479-491
- Gaspar YM, McKenna JA, McGinness BS, Hinch J, Poon S, Connelly AA, Anderson MA, Heath RL (2014) Field resistance to *Fusarium oxysporum* and *Verticillium dahliae* in transgenic cotton expressing the plant defensin NaD1. *J Exp Bot* **65**: 1541-1550
- Geli MI, Riezman H (1998) Endocytic internalization in yeast and animal cells: similar and different. *J Cell Sci* **111**: 1031-1037
- Gonçalves S, Teixeira A, Abade J, de Medeiros LN, Kurtenbach E, Santos NC (2012) Evaluation of the membrane lipid selectivity of the pea defensin Psd1. *BBA Biomembranes* **1818**: 1420-1426
- Griffioen G, Thevelein J (2002) Molecular mechanisms controlling the localisation of protein kinase A. *Curr Genet* **41**: 199-207
- Gyurko C, Lendenmann U, Troxler RF, Oppenheim FG (2000) *Candida albicans* mutants deficient in respiration are resistant to the small cationic salivary antimicrobial peptide histatin 5. *Antimicrob Agents Chemother* **44**: 348-354
- Hall TA (1999) BioEdit: a user-friendly biological sequence alignment editor and analysis program for Windows 95/98/NT. *Nucl Acids Symp Ser* **41**: 95-98
- Hamm HE, Gilchrist A (1996) Heterotrimeric G proteins. *Curr Opin Cell Biol* **8**: 189-196
- Han J, Lee JD, Bibbs L, Ulevitch RJ (1994) A MAP kinase targeted by endotoxin and hyperosmolarity in mammalian cells. *Science* **265**: 808-811
- Hayes BME, Anderson MA, Traven A, van der Weerden NL, Bleackley MR (2014) Activation of stress signalling pathways enhances tolerance of fungi to chemical fungicides and antifungal proteins. *Cell Mol Life Sci* **71**: 2651-2666
- Hayes BME, Bleackley MR, Wiltshire JL, Anderson MA, Traven A, van der Weerden NL (2013) Identification and mechanism of action of the plant defensin NaD1 as a new member of the antifungal drug arsenal against *Candida albicans*. *Antimicrob Agents Chemother* **57**: 3667-3675

- Heitz F, Morris MC, Divita G (2009) Twenty years of cell-penetrating peptides: from molecular mechanisms to therapeutics. *Br J Pharmacol* **157**: 195-206
- Helmerhorst EJ, Breeuwer P, van't Hof W, Walgreen-Weterings E, Oomen LC, Veerman EC, Amerongen AV, Abee T (1999) The cellular target of histatin 5 on *Candida albicans* is the energized mitochondrion. *J Biol Chem* **274**: 7286-7291
- Hemsley A, Arnheim N, Toney MD, Cortopassi G, Galas DJ (1989) A simple method for site-directed mutagenesis using the polymerase chain reaction. *Nucleic Acids Res* **17**: 6545-6551
- Henne William M, Buchkovich Nicholas J, Emr Scott D (2011) The ESCRT pathway. *Dev Cell* **21**: 77-91
- Herce HD, Garcia AE (2007) Molecular dynamics simulations suggest a mechanism for translocation of the HIV-1 TAT peptide across lipid membranes. *Proc Natl Acad Sci* **104**: 20805-20810
- Hernday AD, Noble SM, Mitrovich QM, Johnson AD (2010) Genetics and molecular biology in *Candida albicans*. In *Methods Enzymol*, Jonathan W, Christine G, Gerald RF (eds), Vol. Volume 470, 31, pp 737-758. Academic Press
- Hersen P, McClean MN, Mahadevan L, Ramanathan S (2008) Signal processing by the HOG MAP kinase pathway. *Proc Natl Acad Sci* **105**: 7165-7170
- Heytler PG, Prichard WW (1962) A new class of uncoupling agents -- Carbonyl cyanide phenylhydrazones. *Biochem Biophys Res Commun* **7**: 272-275
- Horak CE, Snyder M (2002) ChIP-chip: a genomic approach for identifying transcription factor binding sites. *Methods Enzymol* **350**: 469-483
- Idnurm A, Bahn YS, Nielsen K, Lin XR, Fraser JA, Heitman J (2005) Deciphering the model pathogenic fungus *Cryptococcus neoformans*. *Nat Rev Microbiol* **3**: 753-764
- Igarashi K, Kashiwagi K (1999) Polyamine transport in bacteria and yeast. *Biochem J* **344**: 633-642
- Igarashi K, Kashiwagi K (2010) Modulation of cellular function by polyamines. *Int J Biochem Cell Biol* **42**: 39-51
- Invitrogen (2010) Pichia Expression Kit For Expression of Recombinant Proteins in *Pichia pastoris*.
- Ishikawa H, Bae S, Katayama I (2009) Human beta-defensin-2 expression by keratinocytes is induced by co-culture with *Trichophyton rubrum* through toll-like receptors 2 and 4. *Open Dermatol J* **3**: 81-85
- Jackson CL, Casanova JE (2000) Turning on ARF: the Sec7 family of guanine-nucleotide-exchange factors. *Trends Cell Biol* **10**: 60-67
- Jang WS, Bajwa JS, Sun JN, Edgerton M (2010) Salivary histatin 5 internalization by translocation, but not endocytosis, is required for fungicidal activity in *Candida albicans*. *Mol Microbiol* **77**: 354-370

- Janssen BJC, Schirra HJ, Lay FT, Anderson MA, Craik DJ (2003) Structure of *Petunia hybrida* defensin 1, a novel plant defensin with five disulfide bonds. *Biochemistry-Ur* **42**: 8214-8222
- Johansson J, Gudmundsson GH, Rottenberg MnE, Berndt KD, Agerberth B (1998) Conformation-dependent antibacterial activity of the naturally occurring human peptide LL-37. *J Biol Chem* **273**: 3718-3724
- Johnson DS, Mortazavi A, Myers RM, Wold B (2007) Genome-wide mapping of in vivo protein-DNA interactions. *Science* **316**: 1497-1502
- Juvvadi PR, Gehrke C, Fortwendel JR, Lamoth F, Soderblom EJ, Cook EC, Hast MA, Asfaw YG, Moseley MA, Creamer TP, Steinbach WJ (2013) Phosphorylation of calcineurin at a novel serine-proline rich region orchestrates hyphal growth and virulence in *Aspergillus fumigatus*. *PLoS Pathog* **9**: e1003564
- Kaksonen M, Toret CP, Drubin DG (2005) A modular design for the clathrin- and actin-mediated endocytosis machinery. *Cell* **123**: 305-320
- Kaksonen M, Toret CP, Drubin DG (2006) Harnessing actin dynamics for clathrin-mediated endocytosis. *Nat Rev Mol Cell Biol* **7**: 404-414
- Kaslow HR, Burns DL (1992) Pertussis toxin and target eukaryotic cells: binding, entry, and activation. *FASEB J* **6**: 2684-2690
- Katada T (2012) The inhibitory G protein G_i identified as pertussis toxin-catalyzed ADP-ribosylation. *Biol Pharm Bull* **35**: 2103-2111
- Kaur J, Sagaram US, Shah D (2011) Can plant defensins be used to engineer durable commercially useful fungal resistance in crop plants? *Fungal Biol Rev* **25**: 128-135
- Kayingo G, Martins A, Andrie R, Neves L, Lucas C, Wong B (2009) A permease encoded by *STL1* is required for active glycerol uptake by *Candida albicans*. *Microbiol* **155**: 1547-1557
- Kelly J, Rowan R, McCann M, Kavanagh K (2009) Exposure to caspofungin activates Cap and Hog pathways in *Candida albicans*. *Med Mycol* **47**: 697-706
- Kojima K, Bahn Y-S, Heitman J (2006) Calcineurin, Mpk1 and Hog1 MAPK pathways independently control fludioxonil antifungal sensitivity in *Cryptococcus neoformans*. *Microbiol* **152**: 591-604
- Konicek BW, Stephens JR, McNulty AM, Robichaud N, Peery RB, Dumstorf CA, Dowless MS, Iversen PW, Parsons S, Ellis KE, McCann DJ, Pelletier J, Furic L, Yingling JM, Stancato LF, Sonenberg N, Graff JR (2011) Therapeutic inhibition of MAP kinase interacting kinase blocks eukaryotic initiation factor 4E phosphorylation and suppresses outgrowth of experimental lung metastases. *Cancer Res* **71**: 1849-1857
- Koselj-Kajtina M, Kandus A, Rott T, Zver S, Zupan I, Koselj M, Bren A (2001) *Aspergillus* infection in immunocompromised patients. *Transplant Proc* **33**: 2176-2178

- Koshlukova SE, Lloyd TL, Araujo MWB, Edgerton M (1999) Salivary histatin 5 induces non-lytic release of ATP from *Candida albicans* leading to cell death. *J Biol Chem* **274**: 18872-18879
- Kubler E, Riezman H (1993) Actin and fimbrin are required for the internalization step of endocytosis in yeast. *EMBO J* **12**: 2855-2862
- Kumar R, Chadha S, Saraswat D, Bajwa JS, Li RA, Conti HR, Edgerton M (2011) Histatin 5 uptake by *Candida albicans* utilizes polyamine transporters Dur3 and Dur31 proteins. *J Biol Chem* **286**: 43748-43758
- LaFayette SL, Collins C, Zaas AK, Schell WA, Betancourt-Quiroz M, Gunatilaka AAL, Perfect JR, Cowen LE (2010) PKC signaling regulates drug resistance of the fungal pathogen *Candida albicans* via circuitry comprised of Mkc1, calcineurin, and Hsp90. *PLoS Pathog* **6**: e1001069
- Latge JP, Calderone R (2002) Host-microbe interactions: fungi invasive human fungal opportunistic infections. *Curr Opin Microbiol* **5**: 355-358
- Lay F, Poon S, McKenna J, Connelly A, Barbeta B, McGinness B, Fox J, Daly N, Craik D, Heath R, Anderson M (2014) The C-terminal propeptide of a plant defensin confers cytoprotective and subcellular targeting functions. *BMC Plant Biol* **14**: 41
- Lay FT, Anderson MA (2005) Defensins - components of the innate immune system in plants. *Curr Prot Pep Sci* **6**: 85-101
- Lay FT, Brugliera F, Anderson MA (2003a) Isolation and properties of floral defensins from ornamental tobacco and petunia. *J Plant Physiol* **131**: 1283-1293
- Lay FT, Schirra HJ, Scanlon MJ, Anderson MA, Craik DJ (2003b) The three-dimensional solution structure of NaD1, a new floral defensin from *Nicotiana glauca* and its application to homology model of crop defense protein alfAFP. *J Mol Biol* **325**: 175-188
- Levin DE (2011) Regulation of cell wall biogenesis in *Saccharomyces cerevisiae*: The cell wall integrity signaling pathway. *Genetics* **189**: 1145-1175
- Li XS, Reddy MS, Baev D, Edgerton M (2003) *Candida albicans* Ssa1/2p is the cell envelope binding protein for human salivary histatin 5. *J Biol Chem* **278**: 28553-28561
- Lin KF, Lee TR, Tsai PH, Hsu MP, Chen CS, Lyu PC (2007) Structure-based protein engineering for alpha-amylase inhibitory activity of plant defensin. *Proteins* **68**: 530-540
- Lindgren M, Langel Ü (2011) Classes and prediction of cell-penetrating peptides. In *Cell-Penetrating Peptides*, Langel Ü (ed), Vol. 683, 1, pp 3-19. Humana Press
- Lindgren ME, Hällbrink MM, Elmquist AM, Langel U (2004) Passage of cell-penetrating peptides across a human epithelial cell layer in vitro. *Biochem J* **377**: 69-76

- Lippincott-Schwartz J, Yuan L, Tipper C, Amherdt M, Orci L, Klausner RD (1991) Brefeldin A's effects on endosomes, lysosomes, and the TGN suggest a general mechanism for regulating organelle structure and membrane traffic. *Cell* **67**: 601-616
- Lobo DS, Pereira IB, Fragel-Madeira L, Medeiros LN, Cabral LM, Faria J, Bellio M, Campos RC, Linden R, Kurtenbach E (2007) Antifungal *Pisum sativum* defensin 1 interacts with *Neurospora crassa* cyclin F related to the cell cycle. *Biochemistry-Us* **46**: 987-996
- Locht C, Coutte L, Mielcarek N (2011) The ins and outs of pertussis toxin. *Febs J* **278**: 4668-4682
- Lupetti A, Danesi R, Wout JWvt, Dissel JTv, Senesi S, Nibbering PH (2002) Antimicrobial peptides: therapeutic potential for the treatment of *Candida* infections. *Expert Opin Investig Drugs* **11**: 309-318
- Maeda T, Takekawa M, Saito H (1995) Activation of yeast PBS2 MAPKK by MAPKKs or by binding of an SH3-containing osmosensor. *Science* **269**: 554-558
- Maeda T, Wurgler-Murphy S, Saito H (1994) A two-component system that regulates an osmosensing MAP kinase cascade in yeast. *Nature* **369**: 242 - 245
- Maisetta G, Di Luca M, Esin S, Florio W, Brancatisano FL, Bottai D, Campa M, Batoni G (2008) Evaluation of the inhibitory effects of human serum components on bactericidal activity of human beta defensin 3. *Peptides* **29**: 1-6
- Matteoni R, Kreis TE (1987) Translocation and clustering of endosomes and lysosomes depends on microtubules. *J Biol Chem* **105**: 1253-1265
- Mavrianos J, Desai C, Chauhan N (2014) Two-component histidine phosphotransfer protein Ypd1 is not essential for viability in *Candida albicans*. *Eukaryot Cell* **13**: 452-460
- McClellan MN, Mody A, Broach JR, Ramanathan S (2007) Cross-talk and decision making in MAP kinase pathways. *Nat Genet* **39**: 409-414
- McKenna JA (2012) *In planta* activity of the antifungal defensin NaD1 and molecules that act in synergy with NaD1. Doctor of Philosophy Thesis, School of Botany, The University of Melbourne, Melbourne
- Menzin J, Meyers JL, Friedman M, Perfect JR, Langston AA, Danna RP, Papadopoulos G (2009) Mortality, length of hospitalization, and costs associated with invasive fungal infections in high-risk patients. *Am J Health Syst Pharm* **66**: 1711-1717
- Milligan SB, Gasser CS (1995) Nature and regulation of pistil-expressed genes in tomato. *Plant Mol Biol* **28**: 691-711
- Miyajima I, Nakafuku M, Nakayama N, Brenner C, Miyajima A, Kaibuchi K, Arai K-i, Kaziro Y, Matsumoto K (1987) GPA1, a haploid-specific essential gene, encodes a yeast homolog of mammalian G protein which may be involved in mating factor signal transduction. *Cell* **50**: 1011-1019

- Mohr FC, Fewtrell C (1987) The relative contributions of extracellular and intracellular calcium to secretion from tumor mast cells. Multiple effects of the proton ionophore carbonyl cyanide m-chlorophenylhydrazone. *J Biol Chem* **262**: 10638-10643
- Monge RA, Román E, Nombela C, Pla J (2006) The MAP kinase signal transduction network in *Candida albicans*. *Microbiol* **152**: 905-912
- Morales-Johansson H, Jenoe P, Cooke FT, Hall MN (2004) Negative regulation of phosphatidylinositol 4,5-bisphosphate levels by the INP51-associated proteins TAX4 and IRS4. *J Biol Chem* **279**: 39604-39610
- Muñoz A, Chu M, Marris PI, Sagaram US, Kaur J, Shah DM, Read ND (2014) Specific domains of plant defensins differentially disrupt colony initiation, cell fusion and calcium homeostasis in *Neurospora crassa*. *Mol Microbiol*
- Nakafuku M, Obara T, Kaibuchi K, Miyajima I, Miyajima A, Itoh H, Nakamura S, Arai K, Matsumoto K, Kaziro Y (1988) Isolation of a second yeast *Saccharomyces cerevisiae* gene (GPA2) coding for guanine nucleotide-binding regulatory protein: studies on its structure and possible functions. *Proc Natl Acad Sci* **85**: 1374-1378
- Nanni V, Schumacher J, Giacomelli L, Brazzale D, Sbolci L, Moser C, Tudzynski P, Baraldi E (2013) VvAMP2, a grapevine flower-specific defensin capable of inhibiting *Botrytis cinerea* growth: insights into its mode of action. *Plant Pathol*
- Navarro-García F, Eisman B, Fiuza SM, Nombela C, Pla J (2005) The MAP kinase Mkc1p is activated under different stress conditions in *Candida albicans*. *Microbiol* **151**: 2737-2749
- Nebenführ A, Ritzenthaler C, Robinson DG (2002) Brefeldin A: deciphering an enigmatic inhibitor of secretion. *Plant Physiol* **130**: 1102-1108
- Nett JE, Lepak AJ, Marchillo K, Andes DR (2009) Time course global gene expression analysis of an in vivo *Candida* biofilm. *J Infect Dis* **200**: 307-313
- Nobile C, Mitchell A (2009) Large-scale gene disruption using the UAU1 cassette. In *Candida albicans*, Cihlar R, Calderone R (eds), Vol. 499, 17, pp 175-194. Humana Press
- Nobile CJ, Mitchell AP (2005) Regulation of cell-surface genes and biofilm formation by the *C. albicans* transcription factor Bcr1p. *Curr Biol* **15**: 1150-1155
- Norice CT, Smith FJ, Solis N, Filler SG, Mitchell AP (2007) Requirement for *Candida albicans* Sun41 in biofilm formation and virulence. *Eukaryot Cell* **6**: 2046-2055
- O'Rourke SM, Herskowitz I (2002) A third osmosensing branch in *Saccharomyces cerevisiae* requires the Msb2 protein and functions in parallel with the Sho1 branch. *Molecular and Cellular Biology* **22**: 4739-4749
- O'Rourke SM, Herskowitz I (2004) Unique and redundant roles for HOG MAPK pathway components as revealed by whole-genome expression analysis. *Mol Biol Cell* **15**: 532-542

- Oberparleiter C, Kaiserer L, Haas H, Ladurner P, Andratsch M, Marx F (2003) Active internalization of the *Penicillium chrysogenum* antifungal protein PAF in sensitive Aspergilli. *Antimicrob Agents Chemother* **47**: 3598-3601
- Odom A, Del Poeta M, Perfect J, Heitman J (1997) The immunosuppressant FK506 and its nonimmunosuppressive analog L-685,818 are toxic to *Cryptococcus neoformans* by inhibition of a common target protein. *Antimicrob Agents Chemother* **41**: 156-161
- Okamoto T, Tanida T, Wei B, Ueta E, Yamamoto T, Osaki T (2004) Regulation of fungal infection by a combination of amphotericin B and peptide 2, a lactoferrin peptide that activates neutrophils. *Clin Diagn Lab Immunol* **11**: 1111-1119
- Onyewu C, Blankenship JR, Del Poeta M, Heitman J (2003) Ergosterol biosynthesis inhibitors become fungicidal when combined with calcineurin inhibitors against *Candida albicans*, *Candida glabrata*, and *Candida krusei*. *Antimicrob Agents Chemother* **47**: 956-964
- Oppenheirn FG, Xu T, McMillian FM, Levitzli SM, Diamondl RD, Offner GD, Troxler RF (1988) Histatins, a novel family of histidine-rich proteins in human parotid secretion. *J Biol Chem* **263**: 7472-7477
- Ordonez SR, Amarullah IH, Wubbolts RW, Veldhuizen EJA, Haagsman HP (2014) Fungicidal mechanisms of cathelicidins LL-37 and CATH-2 revealed by live-cell imaging. *Antimicrob Agents Chemother* **58**: 2240-2248
- Palm-Apergi C, Lorents A, Padari K, Pooga M, Hällbrink M (2009) The membrane repair response masks membrane disturbances caused by cell-penetrating peptide uptake. *FASEB J* **23**: 214-223
- Pasupuleti M, Schmidtchen A, Malmsten M (2012) Antimicrobial peptides: key components of the innate immune system. *Crit Rev Biotech* **32**: 143-171
- Patterson TF (2005) Advances and challenges in management of invasive mycoses. *Lancet* **366**: 1013-1025
- Patton JL, Lester RL (1991) The phosphoinositol sphingolipids of *Saccharomyces cerevisiae* are highly localized in the plasma membrane. *J Bacteriol* **173**: 3101-3108
- Perinpanayagam HER, VanWuyckhuysen BC, Ji ZS, Tabak LA (1995) Characterization of low-molecular-weight peptides in human parotid saliva. *J Dent Res* **74**: 345-350
- Perlin DS (2011) Current perspectives on echinocandin class drugs. *Future Microbiol* **6**: 441-457
- Peters BM, Shirtliff ME, Jabra-Rizk MA (2010) Antimicrobial peptides: Primeval molecules or future drugs? *PLoS Pathog* **6**: e1001067
- Pooga M, Kut C, Kihlmark M, Hallbrink M, Fernaeus S, Raid R, Land T, Hallberg E, Bartfai T, Langel Ü (2001) Cellular translocation of proteins by transportan. *FASEB J* **15**: 1451-1453

- Poon IKH, Baxter AA, Lay F, Mills GD, Adda CG, Payne JAE, Phan TK, Ryan GF, White JA, Veneer PK, Van Der Weerden N, Anderson M, Kvensakul M, Hulett MD (2014) Phosphoinositide-mediated oligomerization of a defensin induces cell lysis. *Elife* **3**
- Posas F, Wurgler-Murphy SM, Maeda T, Witten EA, Thai TC, Saito H (1996) Yeast HOG1 MAP kinase cascade is regulated by a multistep phosphorelay mechanism in the SLN1–YPD1–SSK1 “two-component” osmosensor. *Cell* **86**: 865-875
- Puri S, Edgerton M (2014) How does it kill - Understanding the candidacidal mechanism of salivary Histatin 5. *Eukaryot Cell* **13**: 958-964
- Qi M, Elion EA (2005) MAP kinase pathways. *J Cell Sci* **118**: 3569-3572
- Qiagen (2003) The QIAexpressionist: a handbook for high level expression and purification of 6*His-tagged proteins.
- Ramamoorthy V, Cahoon EB, Li J, Thokala M, Minto RE, Shah DM (2007a) Glucosylceramide synthase is essential for alfalfa defensin-mediated growth inhibition but not for pathogenicity of *Fusarium graminearum*. *Mol Microbiol* **66**: 771-786
- Ramamoorthy V, Zhao X, Snyder AK, Xu J-R, Shah DM (2007b) Two mitogen-activated protein kinase signalling cascades mediate basal resistance to antifungal plant defensins in *Fusarium graminearum*. *Cell Microbiol* **9**: 1491-1506
- Ramanathan B, Davis EG, Ross CR, Blecha F (2002) Cathelicidins: microbicidal activity, mechanisms of action, and roles in innate immunity. *Microbes Infect* **4**: 361-372
- Raths S, Rohrer J, Crausaz F, Riezman H (1993) *end3* and *end4*: two mutants defective in receptor-mediated and fluid-phase endocytosis in *Saccharomyces cerevisiae*. *J Cell Biol* **120**: 55-65
- Richer DL (1987) Synergism—a patent view. *Pestic Sci* **19**: 309-315
- Rieg G, Fu Y, Ibrahim AS, Zhou X, Filler SG, Edwards JE (1999) Unanticipated heterogeneity in growth rate and virulence among *Candida albicans* AAF1 null mutants. *Infect Immun* **67**: 3193-3198
- Riezman H (1993) Yeast endocytosis. *Trends Cell Biol* **3**: 273-277
- Robson GD, Wiebe MG, Trinci APJ (1991) Involvement of Ca²⁺ in the regulation of hyphal extension and branching in *Fusarium graminearum* A 3/5. *Exp Mycol* **15**: 263-272
- Román E, Cottier F, Ernst JF, Pla J (2009) Msb2 signaling mucin controls activation of Cek1 mitogen-activated protein kinase in *Candida albicans*. *Eukaryot Cell* **8**: 1235-1249
- Román E, Nombela C, Pla J (2005) The Sho1 adaptor protein links oxidative stress to morphogenesis and cell wall biosynthesis in the fungal pathogen *Candida albicans*. *Mol Cell Biol* **25**: 10611-10627

- Sabatini LM, Azen EA (1989) Histatins, a family of salivary histidine-rich proteins, are encoded by at least two loci (HIS1 and HIS2). *Biochem Biophys Res Commun* **160**: 495-502
- Sagaram US, El-Mounadi K, Buchko GW, Berg HR, Kaur J, Pandurangi RS, Smith TJ, Shah DM (2013) Structural and functional studies of a phosphatidic acid-binding antifungal plant defensin MtDef4: Identification of an RGFRRR motif governing fungal cell entry. *PLoS ONE* **8**: e82485
- Sagaram US, Pandurangi R, Kaur J, Smith TJ, Shah DM (2011) Structure-activity determinants in antifungal plant defensins MsDef1 and MtDef4 with different modes of action against *Fusarium graminearum*. *PLoS ONE* **6**: e18550
- Saito H (2010) Regulation of cross-talk in yeast MAPK signaling pathways. *Curr Opin Microbiol* **13**: 677-683
- Saksena S, Sun J, Chu T, Emr SD (2007) ESCRTing proteins in the endocytic pathway. *Trends Biochem Sci* **32**: 561-573
- Sandvig K, Grimmer S, Lauvrak S, Torgersen M, Skretting G, van Deurs B, Iversen T (2002) Pathways followed by ricin and Shiga toxin into cells. *Histochem Cell Biol* **117**: 131-141
- Sanglard D (2002) Resistance of human fungal pathogens to antifungal drugs. *Curr Opin Microbiol* **5**: 379-385
- Sawai MV, Jia HP, Liu L, Aseyev V, Wiencek JM, McCray PB, Ganz T, Kearney WR, Tack BF (2001) The NMR structure of human beta-defensin-2 reveals a novel alpha-helical segment. *Biochem* **40**: 3810-3816
- Scales SJ, Gomez M, Kreis TE (2000) Coat proteins regulating membrane traffic. In *Int Rev Cytol*, Kwang WJ (ed), Vol. 195, pp 67-144. Academic Press
- Schindelin J, Arganda-Carreras I, Frise E, Kaynig V, Longair M, Pietzsch T, Preibisch S, Rueden C, Saalfeld S, Schmid B, Tinevez J-Y, White DJ, Hartenstein V, Eliceiri K, Tomancak P, Cardona A (2012) Fiji: an open-source platform for biological-image analysis. *Nat Meth* **9**: 676-682
- Schmid SL, Smythe E (1991) Stage-specific assays for coated pit formation and coated vesicle budding in vitro. *J Cell Biol* **114**: 869-880
- Schröder J-M, Harder J (1999) Human beta-defensin-2. *Int J Biochem Cell Biol* **31**: 645-651
- Scocchi M, Skerlavaj B, Romeo D, Gennaro R (1992) Proteolytic cleavage by neutrophil elastase converts inactive storage proforms to antibacterial bactenecins. *Eur J Biochem* **209**: 589-595
- Sever S, Damke H, Schmid SL (2000) Dynamin:Gtp controls the formation of constricted coated pits, the rate limiting step in clathrin-mediated endocytosis. *J Cell Biol* **150**: 1137-1148

- Shih SC, Katzmann DJ, Schnell JD, Sutanto M, Emr SD, Hicke L (2002) Epsins and Vps27p/Hrs contain ubiquitin-binding domains that function in receptor endocytosis. *Nat Cell Biol* **4**: 389-393
- Silveira LA, Wong DH, Masiarz FR, Schekman R (1990) Yeast clathrin has a distinctive light chain that is important for cell growth. *J Cell Biol* **111**: 1437-1449
- Singh KK (2000) The *Saccharomyces cerevisiae* sln1p-ssk1p two-component system mediates response to oxidative stress and in an oxidant-specific fashion. *Free Radic Biol Med* **29**: 1043-1050
- Singh SD, Robbins N, Zaas AK, Schell WA, Perfect JR, Cowen LE (2009) Hsp90 governs echinocandin resistance in the pathogenic yeast *Candida albicans* via calcineurin. *PLoS Pathog* **5**: e1000532
- Skerlavaj B, Gennaro R, Bagella L, Merluzzi L, Risso A, Zanetti M (1996) Biological characterization of two novel cathelicidin-derived peptides and identification of structural requirements for their antimicrobial and cell lytic activities. *J Biol Chem* **271**: 28375-28381
- Smet KD, Contreras R (2005) Human antimicrobial peptides: defensins, cathelicidins and histatins. *Biotechnol Lett* **27**: 1337-1347
- Smith DA, Morgan BA, Quinn J (2010) Stress signalling to fungal stress-activated protein kinase pathways. *Fems Microbiol Lett* **306**: 1-8
- Sol A, Skvirsky Y, Nashef R, Zelentsova K, Burstyn-cohen T, Blotnick E, Muhlrad A, Bachrach G (2014) Actin enables the antimicrobial action of LL-37 in the presence of microbial proteases. *J Biol Chem*
- Spelbrink RG, Dilmac N, Allen A, Smith TJ, Shah DM, Hockerman GH (2004) Differential antifungal and calcium channel-blocking activity among structurally related plant defensins. *Plant Physiol* **135**: 2055-2067
- Stevens J, Dunse K, Fox J, Evans S, Anderson M (2012) Biotechnological approaches for the control of insect pests in crop plants. In *Pesticides - Advances in Chemical and Botanical Pesticides*, pp 269-308. Rijeka: InTech
- Strange RN, Scott PR (2005) Plant disease: A threat to global food security. *Annu Rev Phytopathol* **43**: 83-116
- Sussman A, Huss K, Chio L-C, Heidler S, Shaw M, Ma D, Zhu G, Campbell RM, Park T-S, Kulanthaivel P, Scott JE, Carpenter JW, Strege MA, Belvo MD, Swartling JR, Fischl A, Yeh W-K, Shih C, Ye XS (2004) Discovery of cercosporamide, a known antifungal natural product, as a selective Pkc1 kinase inhibitor through high-throughput screening. *Eukaryot Cell* **3**: 932-943
- Tamaki H (2007) Glucose-stimulated cAMP-protein kinase a pathway in yeast *Saccharomyces cerevisiae*. *J Biosci Bioeng* **104**: 245-250
- Tamamura H, Ikoma R, Niwa M, Funakoshi S, Murakami T, Fujii N (1993) Antimicrobial activity and conformation of tachyplesin I and its analogs. *Chem Pharm Bull* **41**: 978-980

- Tanaka K, Tatebayashi K, Nishimura A, Yamamoto K, Yang H-Y, Saito H (2014) Yeast osmosensors Hkr1 and Msb2 activate the Hog1 MAPK cascade by different mechanisms. *Sci Signal* **7**: ra21
- Tatebayashi K, Tanaka K, Yang H-Y, Yamamoto K, Matsushita Y, Tomida T, Imai M, Saito H (2007) Transmembrane mucins Hkr1 and Msb2 are putative osmosensors in the SHO1 branch of yeast HOG pathway. *EMBO J* **26**: 3521-3533
- Tati S, Jang WS, Li R, Kumar R, Puri S, Edgerton M (2013) Histatin 5 resistance of *Candida glabrata* can be reversed by insertion of *Candida albicans* polyamine transporter-encoding genes *DUR3* and *DUR31*. *PLoS ONE* **8**: e61480
- Terras FR, Schoofs HM, De Bolle MF, Van Leuven F, Rees SB, Vanderleyden J, Cammue BP, Broekaert WF (1992) Analysis of two novel classes of plant antifungal proteins from radish (*Raphanus sativus* L.) seeds. *J Biol Chem* **267**: 15301-15309
- Terras FRG, Eggermont K, Kovaleva V, Raikhel NV, Osborn RW, Kester A, Rees SB, Torrekem S, Van Leuven F, Vanderleyden J, Cammue BPA, Broekaert WF (1995) Small cysteine-rich antifungal proteins from radish: Their role in host defense. *Plant Cell* **7**: 573-588
- Theis T, Stahl U (2004) Antifungal proteins: targets, mechanisms and prospective applications. *Cell Mol Life Sci* **61**: 437-455
- Thevissen K, de Mello Tavares P, Xu D, Blankenship J, Vandenbosch D, Idkowiak-Baldys J, Govaert G, Bink A, Rozental S, de Groot PW, Davis TR, Kumamoto CA, Vargas G, Nimrichter L, Coenye T, Mitchell A, Roemer T, Hannun YA, Cammue BP (2012) The plant defensin RsAFP2 induces cell wall stress, septin mislocalization and accumulation of ceramides in *Candida albicans*. *Mol Microbiol* **84**: 166-180
- Thevissen K, Ghazi A, De Samblanz GW, Brownlee C, Osborn RW, Broekaert WF (1996) Fungal Membrane Responses Induced by Plant Defensins and Thionins. *J Biol Chem* **271**: 15018-15025
- Thevissen K, Osborn RW, Acland DP, Broekaert WF (2000) Specific binding sites for an antifungal plant defensin from Dahlia (*Dahlia merckii*) on fungal cells are required for antifungal activity. *Mol Plant Microbe Interact* **13**: 54-61
- Thevissen K, Terras FR, Broekaert WF (1999) Permeabilization of fungal membranes by plant defensins inhibits fungal growth. *Appl Environ Microbiol* **65**: 5451-5458
- Thevissen K, Warnecke DC, Francois IEJA, Leipelt M, Heinz E, Ott C, Zahringer U, Thomma BPHJ, Ferket KKA, Cammue BPA (2004) Defensins from insects and plants interact with fungal glucosylceramides. *J Biol Chem* **279**: 3900-3905
- Thomma BPHJ, Cammue BPA, Thevissen K (2002) Plant defensins. *Planta* **216**: 193-202
- Troxler RF, Offner GD, Xu T, Vanderspek JC, Oppenheim FG (1990) Structural relationship between human salivary histatins. *J Dent Res* **9**: 2-6
- van der Weerden N, Anderson MA (2012a) Modified plant defensins useful as anti-pathogenic agents. *Patent Application WO 2012/106759*

- van der Weerden N, Bleackley M, Anderson M (2013) Properties and mechanisms of action of naturally occurring antifungal peptides. *Cell Mol Life Sci* **70**: 3545-3570
- van der Weerden NL (2007) Investigating the molecular mechanism of a defensin from the flowers of *Nicotiana glauca*. Doctor of Philosophy Thesis, Biochemistry, La Trobe University, Melbourne
- van der Weerden NL, Anderson MA (2012b) Plant defensins: common fold, multiple functions. *Fungal Biol Rev*
- van der Weerden NL, Hancock REW, Anderson MA (2010) Permeabilization of fungal hyphae by the plant defensin NaD1 occurs through a cell wall-dependent process. *J Biol Chem* **285**: 37513-37520
- van der Weerden NL, Lay FT, Anderson MA (2008) The plant defensin, NaD1, enters the cytoplasm of *Fusarium oxysporum* hyphae. *J Biol Chem* **283**: 14445-14452
- Vercauteren D, Vandenbroucke RE, Jones AT, Rejman J, Demeester J, De Smedt SC, Sanders NN, Braeckmans K (2010) The use of inhibitors to study endocytic pathways of gene carriers: Optimization and pitfalls. *Mol Ther* **18**: 561-569
- Versele M, Lemaire K, Thevelein JM (2001) Sex and sugar in yeast: two distinct GPCR systems. *EMBO Rep* **2**: 574-579
- Vriens K, Cammue B, Thevissen K (2014) Antifungal plant defensins: Mechanisms of action and production. *Molecules* **19**: 12280-12303
- Vylkova S, Jang WS, Li W, Nayyar N, Edgerton M (2007) Histatin 5 initiates osmotic stress response in *Candida albicans* via activation of the Hog1 mitogen-activated protein kinase pathway. *Eukaryot Cell* **6**: 1876-1888
- Walker LA, Munro CA, de Bruijn I, Lenardon MD, McKinnon A, Gow NAR (2008) Stimulation of chitin synthesis rescues *Candida albicans* from echinocandins. *PLoS Pathog* **4**: e1000040
- Walling LL (2009) Chapter 13 adaptive defense responses to pathogens and insects. In *Adv Bot Res*, Loon LCV (ed), Vol. 51, pp 551-612. Academic Press
- Wang G (2008) Structures of human host defense cathelicidin LL-37 and its smallest antimicrobial peptide KR-12 in lipid micelles. *J Biol Chem* **283**: 32637-32643
- Wang G, Li X, Wang Z (2009a) APD2: the updated antimicrobial peptide database and its application in peptide design. *Nucleic Acids Res* **37**: D933-937
- Wang Z, Gerstein M, Snyder M (2009b) RNA-Seq: a revolutionary tool for transcriptomics. *Nat Rev Genet* **10**: 57-63
- Wanke B, Lazéra MdS, Nucci M (2000) Fungal infections in the immunocompromised host. *Clin Haematol* **95**: 153-158

- Wesp A, Hicke L, Palecek J, Lombardi R, Aust T, Munn AL, Riezman H (1997) End4p/Sla2p interacts with actin-associated proteins for endocytosis in *Saccharomyces cerevisiae*. *Mol Biol Cell* **8**: 2291-2306
- Wiesner J, Vilcinskas A (2010) Antimicrobial peptides: The ancient arm of the human immune system. *Virulence* **1**: 440-464
- Wolfe BL, Trejo J (2007) Clathrin-dependent mechanisms of G protein-coupled receptor endocytosis. *Traffic* **8**: 462-470
- Wong-Beringer A, Kriengkauykiat J (2003) Systemic antifungal therapy: New options, new challenges. *Pharmacotherapy* **23**: 1441-1462
- Wood SA, Park JE, Brown WJ (1991) Brefeldin A causes a microtubule-mediated fusion of the trans-Golgi network and early endosomes. *Cell* **67**: 591-600
- Wu M, Hancock REW (1999a) Improved derivatives of bactenecin, a cyclic dodecameric antimicrobial cationic peptide. *Antimicrob Agents Chemother* **43**: 1274-1276
- Wu M, Hancock REW (1999b) Interaction of the cyclic antimicrobial cationic peptide bactenecin with the outer and cytoplasmic membrane. *J Biol Chem* **274**: 29-35
- Xu D, Jiang B, Ketela T, Lemieux S, Veillette K, Martel N, Davison J, Sillaots S, Trosok S, Bachewich C, Bussey H, Youngman P, Roemer T (2007) Genome-wide fitness test and mechanism-of-action studies of inhibitory compounds in *Candida albicans*. *PLoS Pathog* **3**: e92
- Xu T, Levitz SM, Diamond RD, Oppenheim FG (1991) Anticandidal activity of major human salivary histatins. *Infect Immun* **59**: 2549-2554
- Xu Y, Barbieri JT (1995) Pertussis toxin-mediated ADP-ribosylation of target proteins in Chinese hamster ovary cells involves a vesicle trafficking mechanism. *Infect Immun* **63**: 825-832
- Yaakov G, Bell M, Hohmann S, Engelberg D (2003) Combination of two activating mutations in one HOG1 gene forms hyperactive enzymes that induce growth arrest. *Mol Cell Biol* **23**: 4826-4840
- Yun D-J, Ibeas JI, Lee H, Coca MA, Narasimhan ML, Uesono Y, Hasegawa PM, Pardo JM, Bressan RA (1998) Osmotin, a plant antifungal protein, subverts signal transduction to enhance fungal cell susceptibility. *Mol Cell* **1**: 807-817
- Zanetti M (2004) Cathelicidins, multifunctional peptides of the innate immunity. *J Leukoc Biol* **75**: 39-48
- Zanetti M, Litteri L, Griffiths G, Gennaro R, Romeo D (1991) Stimulus-induced maturation of probactenecins, precursors of neutrophil antimicrobial polypeptides. *J Immunol* **146**: 4295-4300
- Zaslhoff M (2002) Antimicrobial peptides of multicellular organisms. *Nature* **415**: 389-395

Zhang Y, Lamm R, Pillonel C, Lam S, Xu J-R (2002) Osmoregulation and fungicide resistance: the *Neurospora crassa* os-2 gene encodes a HOG1 mitogen-activated protein kinase homologue. *Appl Environ Microbiol* **68**: 532-538